



TECHNICAL NOTE

D-1972

HEAT TRANSFER WITH LAMINAR FLOW IN CONCENTRIC ANNULI
WITH CONSTANT AND VARIABLE WALL TEMPERATURE
WITH HEAT FLUX

By R. E. Lundberg, W. C. Reynolds,
and W. M. Kays

Prepared under Grant NsG-52-60 by
STANFORD UNIVERSITY
Stanford, California
for

NATIONAL AERONAUTICS AND SPACE ADMINISTRATION
WASHINGTON

August 1963

CASE FILE COPY

TECHNICAL NOTE D-1972

HEAT TRANSFER WITH LAMINAR FLOW IN CONCENTRIC ANNULI WITH
CONSTANT AND VARIABLE WALL TEMPERATURE AND HEAT FLUX

By R. E. Lundberg, W. C. Reynolds,
and W. M. Kays

SUMMARY

The general problem of heat transfer in a concentric annulus with hydrodynamically fully established laminar flow is considered. Under the assumptions that the fluid in the annulus is incompressible, has constant properties, and that internal viscous generation is negligible, the differential equation for the temperature field is solved for certain special or fundamental boundary conditions. These fundamental solutions can be superposed to satisfy any general axially symmetric boundary conditions.

The fundamental boundary conditions fall into four basic categories. The fluid has initially a uniform zero temperature; at some plane normal to the annular axis, $x = 0$, one of the following occurs:

1. The temperature on one wall is increased to unity, the other wall is maintained at zero;
2. The heat flux on one wall is increased to a constant, the other wall is insulated;
3. The temperature on one wall is increased to unity, the other wall is insulated;
4. The heat flux on one wall is increased to a constant, the other wall is maintained at zero temperature.

Since each of these four cases is applied to both the inner and the outer walls of the annulus eight separate solutions to the energy equation are generated. From the fundamental solutions dimensionless wall temperatures, wall heat fluxes, and mean temperatures are defined and evaluated. The use of these quantities in solving problems of simple superposition is described and illustrated.

These fundamental solutions are obtained for values of the ratio of the inner to the outer radius, r^* , of 0.02, 0.05, 0.1, 0.25, and 0.5. These values together with existing results for r^* of unity (the parallel plane channel) are presented in tabular and graphical form to facilitate interpolation so that problems in virtually any annular geometry can be solved.

The solutions to the differential equation are obtained by the method of separation of variables. The wall boundary conditions are reduced to a homogeneous form by subtracting from the desired solutions the fully developed solutions, i.e., the solutions valid as the axial coordinate, x , tends to infinity. The eigenvalues, eigenfunctions, and expansion coefficients arising in the resulting Sturm-Liouville equation are obtained through a direct numerical integration facilitated by a convergent iteration method for obtaining the eigenvalues. The eigenvalues and relevant combinations of the expansion coefficients and the eigenfunctions are presented in tabular and graphical form for the previous values of r^* and for $r^* = 0$ (the circular tube). These quantities enable the consideration of continuous axial variation of boundary conditions via the Stieltjes integral.

An apparatus for the experimental study of heat transfer to air with constant (but arbitrary level) heat flux at either or both of the boundary walls is described. The apparatus enables the direct experimental determination of the fundamental solutions satisfying boundary condition 2 above, and superpositions thereof.

A comparison of these experimentally determined values with those predicted by the theory is presented and exhibits the very good agreement between them.

TABLE OF CONTENTS

Summary	i
Index to the Figures	v
Index to the Tables	xii
Nomenclature	xv
I. Introduction	1
I.A The Problem	1
I.B. Method of Solution	2
I.C. Objective	14
I.D. Summary	14
I.E. Conclusions	15
II. The Fundamental Solutions	17
II.A Previous Studies	17
II.B. The Hydrodynamic Problem	19
II.C The Energy Equation	21
II.D Asymptotic (large \bar{x}) Values of the Fundamental Solutions, Homogenization of the Boundary Conditions	22
II.E Limiting (small \bar{x}) Leveque Approximations to the Fundamental Solutions	43
II.F Solution of the Energy Equation	54
II.G Behavior of the Solutions as λ becomes Large	60
II.H Solution of the Sturm-Liouville Equation	83
II.I The Fundamental Solutions	99

III. Experimental Work	130
III.A Description of Apparatus	130
III.B Comparison of Experimental and Theoretical Values	147
Appendices	149
Appendix A Correction for the Tube Wall Temperature due to Internal Generation	149
Appendix B Heat Leak Determination for the Outer Tube	152
Appendix C The Effect of Radiation Interchange between the Two Surfaces	157
Appendix D Experimental Uncertainty	160
Appendix E Details of the Numerical Solution	163
Appendix F Derivation of the Expansion Coefficients	170
Appendix G Examples of Superposition of the Fundamental Solutions	177
References	192

INDEX TO THE FIGURES

FIG. I.A.1	Coordinate System in a Concentric Annulus	1
FIG. I.B.1	The Fundamental Solutions of the First Kind, Temperature Step at the Inner Wall	4
FIG. I.B.2	The Fundamental Solutions of the Second Kind, Inner Wall Heated	5
FIG. I.B.3	The Fundamental Solutions of the Third Kind, Temperature Step at the Inner Wall	6
FIG. I.B.4	The Fundamental Solutions of the Fourth Kind, Inner Wall Heated	7
FIG. I.B.5	Illustration of an Arbitrary Wall Temperature Distribution	13
FIG. II.B.1	Friction Factor for Fully Developed Laminar Flow in a Concentric Annulus	20
FIG. II.D.1	Asymptotic (Large \bar{x}) Values of the Fundamental Solutions of the First Kind $\Phi_{ii}^{(1)}{}_{fd}$ and $\Phi_{oo}^{(1)}{}_{fd}$ vs r^*	36
FIG. II.D.2	Asymptotic (Large \bar{x}) Values of the Fundamental Solutions of the First Kind $\theta_{mo}^{(1)}{}_{fd}$ and $\theta_{mi}^{(1)}{}_{fd}$ vs r^*	36
FIG. II.D.3	Asymptotic (Large \bar{x}) Values of the Fundamental Solutions of the First Kind $Nu_{ii}^{(1)}{}_{fd}$ and $Nu_{oo}^{(1)}{}_{fd}$ vs r^*	37
FIG. II.D.4	Asymptotic (Large \bar{x}) Values of the Fundamental Solutions of the Second Kind $Nu_{ii}^{(2)}{}_{fd}$ and $Nu_{oo}^{(2)}{}_{fd}$ vs r^*	37

FIG. II.D.5	Asymptotic (Large \bar{x}) Values of the Fundamental Solutions of the Second Kind $(\theta_{oo}^{(2)} - \theta_{mo}^{(2)})_{fd}$ and $(\theta_{ii}^{(2)} - \theta_{mi}^{(2)})_{fd}$ vs r^*	38
FIG. II.D.6	Asymptotic (Large \bar{x}) Values of the Fundamental Solutions of the Second Kind - $(\theta_{io}^{(2)} - \theta_{mo}^{(2)})_{fd}$ and - $(\theta_{oi}^{(2)} - \theta_{mi}^{(2)})_{fd}$ vs r^*	38
FIG. II.D.7	Asymptotic (Large \bar{x}) Values of the Fundamental Solutions of the Fourth Kind $(\theta_{oo}^{(4)})_{fd}$ and $(\theta_{ii}^{(4)})_{fd}$ vs r^*	39
FIG. II.D.8	Asymptotic (Large \bar{x}) Values of the Fundamental Solutions of the Fourth Kind - $\phi_{io}^{(4)}_{fd}$ and - $\phi_{oi}^{(4)}_{fd}$ vs r^*	39
FIG. II.D.9	Asymptotic (Large \bar{x}) Values of the Fundamental Solutions of the Fourth Kind $\theta_{mo}^{(4)}_{fd}$ and $\theta_{mi}^{(4)}_{fd}$ vs r^*	40
FIG. II.D.10	Asymptotic (Large \bar{x}) Values of the Fundamental Solutions of the Fourth Kind $Nu_{ii}^{(4)}_{fd}$ and $Nu_{oo}^{(4)}_{fd}$ vs r^*	40
FIG. II.D.11	Fully Developed Temperature Profile for a Fundamental Solution of the First Kind	41
FIG. II.D.12	Fully Developed Temperature Profile for a Fundamental Solution of the Second Kind	41
FIG. II.D.13	Fully Developed Temperature Profile for a Fundamental Solution of the Third Kind	42

FIG. II.D.14	Fully Developed Temperature Profile for a Fundamental Solution of the Fourth Kind	42
FIG. II.E.1	Constants in the Limiting (Small \bar{x}) Approximations to the Fundamental Solutions $c_{ii}^{(1)} = c_{ii}^{(3)}$ and $c_{oo}^{(1)} = c_{oo}^{(3)}$ vs r^*	53
FIG. II.E.2	Constants in the Limiting (Small \bar{x}) Approximations to the Fundamental Solutions $c_{oo}^{(2)} = c_{oo}^{(4)}$ and $c_{ii}^{(2)} = c_{ii}^{(4)}$ vs r^*	53
FIG. II.G.1	Constants in the Asymptotic (Large λ) Solutions γ vs r^*	82
FIG. II.G.2	Constants in the Asymptotic (Large λ) Solutions π/γ vs r^*	82
FIG. II.H.1	Eigenvalues for the Fundamental Solutions of the First Kind $(\lambda_n)^1$ vs r^*	89
FIG. II.H.2	Eigenvalues for the Fundamental Solutions of the Second Kind $(\lambda_n)^2$ vs r^*	89
FIG. II.H.3	Eigenvalues for the Fundamental Solutions of the Third and Fourth Kind $(\lambda_n)_1^3 = (\lambda_n)_0^4$ vs r^*	90
FIG. II.H.4	Eigenvalues for the Fundamental Solutions of the Third and Fourth Kinds $(\lambda_n)_0^3 = (\lambda_n)_1^4$ vs r^*	90
FIG. II.H.5	Functions in the Fundamental Solutions of the First Kind $-2(1 - r^*)(C_n)_1^{(1)} R_n^1(r^*)$ vs r^*	91
FIG. II.H.6	Functions in the Fundamental Solutions of the First Kind $(-1)^n 2(1 - r^*)(C_n)_1^{(1)} R_n^1(1)$ vs r^*	91

FIG. II.H.7	Functions in the Fundamental Solutions of the First Kind - $(-1)^n 2(1-r^*)(C_n)_o^{(1)} R_n'(r^*)$ vs r^*	92
FIG. II.H.8	Functions in the Fundamental Solutions of the First Kind $2(1 - r^*)(C_n)_o^{(1)} R_n'(1)$ vs r^*	92
FIG. II.H.9	Functions in the Fundamental Solutions of the Second Kind - $(C_n)_i^{(2)} R_n(r^*)$ vs r^*	93
FIG. II.H.10	Functions in the Fundamental Solutions of the Second Kind - $(-1)^n (C_n)_i^{(2)} R_n(1)$ vs r^*	93
FIG. II.H.11	Functions in the Fundamental Solutions of the Second Kind - $(-1)^n (C_n)_o^{(2)} R_n(r^*)$ vs r^*	94
FIG. II.H.12	Functions in the Fundamental Solutions of the Second Kind - $(C_n)_o^{(2)} R_n(1)$ vs r^*	94
FIG. II.H.13	Functions in the Fundamental Solutions of the Third Kind - $2(1 - r^*)(C_n)_i^{(3)} R_n'(r^*)$ vs r^*	95
FIG. II.H.14	Functions in the Fundamental Solutions of the Third Kind - $(-1)^n (C_n)_i^{(3)} R_n(1)$ vs r^*	95
FIG. II.H.15	Functions in the Fundamental Solutions of the Third Kind - $(-1)^n (C_n)_o^{(3)} R_n(r^*)$ vs r^*	96
FIG. II.H.16	Functions in the Fundamental Solutions of the Third Kind $2(1 - r^*)(C_n)_o^{(3)} R_n'(1)$ vs r^*	96
FIG. II.H.17	Functions in the Fundamental Solutions of the Fourth Kind - $(C_n)_i^{(4)} R_n(r^*)$ vs r^*	97

FIG. II.H.18	Functions in the Fundamental Solutions of the Fourth Kind $(-1)^n 2(1 - r^*)(C_n)_1^{(4)} R_n^!(1)$ vs r^*	97
FIG. II.H.19	Functions in the Fundamental Solutions of the Fourth Kind $- (-1)^n 2(1 - r^*)(C_n)_o^{(4)} R_n^!(r^*)$ vs r^*	98
FIG. II.H.20	Functions in the Fundamental Solutions of the Fourth Kind $- (C_n)_o^{(4)} R_n(1)$ vs r^*	98
FIG. II.I.1	The Fundamental Solutions of the First Kind $\Phi_{ii}^{(1)}$ vs \bar{x}	118
FIG. II.I.2	The Fundamental Solutions of the First Kind $\Phi_{oo}^{(1)}$ vs \bar{x}	119
FIG. II.I.3	The Fundamental Solutions of the First Kind $- \Phi_{io}^{(1)}$ and $- \Phi_{oi}^{(1)}$ vs \bar{x}	120
FIG. II.I.4	The Fundamental Solutions of the First Kind $\theta_{mi}^{(1)}$ and $\theta_{mo}^{(1)}$ vs \bar{x}	121
FIG. II.I.5	The Fundamental Solutions of the Second Kind $(\theta_{ii}^{(2)} - \theta_{mi}^{(2)})$ and $(\theta_{oo}^{(2)} - \theta_{mo}^{(2)})$ vs \bar{x}	122
FIG. II.I.6	The Fundamental Solutions of the Second Kind $- (\theta_{oi}^{(2)} - \theta_{mi}^{(2)})$ and $- (\theta_{io}^{(2)} - \theta_{mo}^{(2)})$ vs \bar{x}	123
FIG. II.I.7	The Fundamental Solutions of the Third Kind $\Phi_{ii}^{(3)}$ and $\Phi_{oo}^{(3)}$ vs \bar{x}	124

FIG. II.I.8	The Fundamental Solutions of the Third Kind $\theta_{oi}^{(3)}$ and $\theta_{io}^{(3)}$ vs \bar{x}	125
FIG. II.I.9	The Fundamental Solutions of the Third Kind $\theta_{mi}^{(3)}$ and $\theta_{mo}^{(3)}$ vs \bar{x}	126
FIG. II.I.10	The Fundamental Solutions of the Fourth Kind $\theta_{ii}^{(4)}$ and $\theta_{oo}^{(4)}$ vs \bar{x}	127
FIG. II.I.11	The Fundamental Solutions of the Fourth Kind - $\phi_{oi}^{(4)}$ and - $\phi_{io}^{(4)}$ vs \bar{x}	128
FIG. II.I.12	The Fundamental Solutions of the Fourth Kind $\theta_{mi}^{(4)}$ and $\theta_{mo}^{(4)}$ vs \bar{x}	129
FIG.III.A.1	Entrance Nozzle Velocity Traverses	133
FIG.III.A.2	Power Supply and Instrumentation Circuit	137
FIG.III.A.3	Assembly Details	138
FIG.III.A.4	Air Metering System	139
FIG.III.A.5	Outer Tube Thermocouple Locations	140
FIG.III.A.6	Core Tube Thermocouple Locations	141
FIG.III.A.7	Core Tube Construction	142
FIG.III.A.8	Thermocouple Selector System	143
FIG.III.A.9	Thermocouple Circuit	144
FIG.III.A.10	Inconel Tubes used in the Test Section	145
FIG.III.A.11	Test Assembly, Exit End	145

FIG.III.A.12	Power Supply and Instrumentation	146
FIG.III.B.1	A Comparison of Experimental and Theoretical Results, Inner Wall Heated	148
FIG.III.B.2	A Comparison of Experimental and Theoretical Results, Outer Wall Heated	148
FIG. A.1	Coordinate System used in the Calculation of the Wall Tempera- ture Correction Factor	149
FIG. B.1	Idealized System Used in the Determination of the Outer Tube Heat Leak	153
FIG. B.2	A Comparison of Measured and Calculated Tube Wall Temperatures During the Determination of the Heat Leak	156
FIG. E.1	Interval Numbering System Used in the Numerical Integration	164
FIG. G.1	Inner Wall Heat Flux Used in Example 1	180
FIG. G.2	Wall and Mean Temperatures in Example 1	181
FIG. G.3	Outer Wall Heat Flux in Example 1	181
FIG. G.4	Wall Heat Fluxes for Run G.1	186
FIG. G.5	A Comparison of Measured and Predicted Wall Temperatures for Run G.1	187
FIG. G.6	Wall Heat Fluxes in Run G.2	188
FIG. G.7	A Comparison of Measured and Predicted Wall Temperatures in Run G.2	18
FIG. G.8	The Fundamental Solutions of the Second Kind $r^* = 0.375$	190
FIG. G.9	The Fundamental Solutions of the Second Kind $r^* = 0.375$	191

INDEX TO THE TABLES

Table II.D.1	Asymptotic (Large \bar{x}) Values of the Fundamental Solutions of the First Kind	35
Table II.D.2	Asymptotic (Large \bar{x}) Values of the Fundamental Solutions of the Second Kind	35
Table II.D.3	Asymptotic (Large \bar{x}) Values of the Fundamental Solutions of the Fourth Kind	35
Table II.E.1	Constants in the Limiting (Small \bar{x}) Approximations to the Fundamental Solutions	52
Table II.G.1	Asymptotic Values of the Functions in the Fundamental Solutions of the First Kind	80
Table II.G.2	Asymptotic Values of the Functions in the Fundamental Solutions of the Second Kind	80
Table II.G.3	Asymptotic Values of the Functions in the Fundamental Solutions of the Third Kind	80
Table II.G.4	Asymptotic Values of the Functions in the Fundamental Solutions of the Fourth Kind	80
Table II.G.5	Constants in the Asymptotic (Large λ) Solutions	81
Table II.H.1	Functions in the Fundamental Solutions of the First Kind	87
Table II.H.2	Functions in the Fundamental Solutions of the Second Kind	87
Table II.H.3	Functions in the Fundamental Solutions of the Third and Fourth Kinds	88
Table II.H.4	Functions in the Fundamental Solutions of the Third and Fourth Kinds	88

Table II.I.1	The Fundamental Solutions of the First Kind, Temperature Step at the Inner Wall	110
Table II.I.2	The Fundamental Solutions of the First Kind, Temperature Step at the Outer Wall	111
Table II.I.3	The Fundamental Solutions of the Second Kind, Inner Wall Heated	112
Table II.I.4	The Fundamental Solutions of the Second Kind, Outer Wall Heated	113
Table II.I.5	The Fundamental Solutions of the Third Kind, Temperature Step at the Inner Wall	114
Table II.I.6	The Fundamental Solutions of the Third Kind, Temperature Step at the Outer Wall	115
Table II.I.7	The Fundamental Solutions of the Fourth Kind, Inner Wall Heated	116
Table II.I.8	The Fundamental Solutions of the Fourth Kind, Outer Wall Heated	117

NOMENCLATURE

English letter symbols

A	heat transfer area
A_c	cross section area
a	constant in the similarity solutions, $a = E_1/3$ or $E_0/3$
$A_{n,m}$	constants in a series solution
B	$B = (r^{*2} - 1)/\ln r^*$
C_n	constants in the eigenvalue problem
$C_{jj}^{(k)}$	constants in the Leveque solutions
C_t	tube circumference
c_p	specific heat at constant pressure
D_h	hydraulic diameter, $D_h = 2(r_o - r_i)$
E_1	$E_1 = N[(B/r^*) - 2r^*]$
E_0	$E_0 = N(2 - B)$
F_e	radiation view factor
$F_j^{(k)}(r)$	initial condition in the orthogonal expansion
f	friction factor
$f(p)$	functions in the similarity solutions
G, H	arbitrary constants
$g(\bar{r})$	function in the WKBJ solutions
h	convection conductance
h_L	heat leak coefficient
K_L	power lead heat leak coefficient
K_n	normalizing constant in the iteration scheme

k	thermal conductivity
M	$M = 1 + r^{*2} - B$
m	$m = \sqrt{h_L C_t / k A_c}$
N	$N = 1/2M(1 - r^*)^2$
n	normal distance into the fluid from the wall
Nu	Nusselt number, $Nu = hD_h/k$
P	pressure
Pr	Prandtl number, $Pr = c_p \mu / k$
p	similarity parameter, $p = (\bar{r} - r^*)/\bar{x}^{1/3}$, or $p = (1 - \bar{r})/\bar{x}^{1/3}$
p	position index in the numerical integration procedure
q	heat rate BTU/hr
q"	heat flux BTU/hr-ft ²
q'''	heat generation rate BTU/hr-ft ³
Re	Reynolds number, $Re = U_m \rho D_h / \mu$
$R_n(\bar{r})$	eigenfunction
r	radius, radial coordinate
\bar{r}	$\bar{r} = r/r_o$
r^*	$r^* = r_i/r_o$
T	absolute temperature, °R
t	temperature, °F
\bar{t}	$\bar{t} = t - t_a$
U	velocity
\bar{U}	$\bar{U} = U/U_m$
w	mass flow rate

$w(\bar{r})$	weight function in the Sturm-Liouville system, $w(\bar{r}) = N(\bar{r} - \bar{r}^3 + B\bar{r} \ln \bar{r})$
$X(\bar{x})$	function used in the separation of variables $X(\bar{x}) = Ce^{-\lambda^2 \bar{x}}$
x	axial coordinate
x_0	axial coordinate at the step change in boundary conditions ($x_0 = 0$ in the fundamental solutions)
\bar{x}	$\bar{x} = (x/D_h)/(\text{RePr})$
z	$z = \bar{r} - r^*$

Greek letter symbols

α	thermal diffusivity, $= k/c_p$
γ	$\gamma = \int_{r^*}^1 \sqrt{N(1 - \bar{r}^2 + B \ln \bar{r})} d\bar{r}$
Δ	increment or difference
ϵ	gray body emmissivity
ϵ_H	eddy diffusivity for heat
ξ	$\xi = \lambda_n^{2/3} \xi$ in the WKBJ solutions
η	$\eta = \lambda_n^{2/3} z$
$\theta_j^{(k)}(\bar{r}, \bar{x})$	non-dimensional temperature
$\bar{\theta}_j^{(k)}(\bar{r}, \bar{x})$	$\bar{\theta}_j^{(k)}(\bar{r}, \bar{x}) = \theta_j^{(k)}(\bar{r}, \bar{x}) - \theta_j^{(k)}(\bar{r})$) _{fd}
$\theta_{jj}^{(k)}, \theta_{lj}^{(k)}$	non-dimensional wall temperatures in the fundamental solutions
$\theta_{mj}^{(k)}$	non-dimensional mean temperatures

λ	constant in the differential equation
λ_n	eigenvalue
μ	absolute viscosity
ξ	axial coordinate in the superposition problems
ξ_n	value of the axial coordinate at which the n th discontinuity in wall boundary conditions occurs
ξ	$\xi = (1 - \bar{r})$ in the WKBJ solutions
ρ	mass density
σ	Stefan-Boltzman constant, $0.173 \cdot 10^{-8}$ BTU/hr-ft ² - °R ⁴
σ	dummy variable
τ	shearing stress
$\Phi_{jj}^{(k)}, \Phi_{lj}^{(k)}$	non-dimensional heat fluxes in the fundamental solutions
ϕ	phase shift in the WKBJ solutions

Subscripts

a	ambient conditions
fd	fully developed
i	inner wall
k	iteration index
m	mixed mean
n,m	eigenvalue and summation indices
o	outer wall
r	via radiation
0,1,2, ..	defined where used

Superscripts

(k)	refers to the fundamental solution of the k th kind
'	denotes differentiation with respect to the independent variable

I. INTRODUCTION

I. A. The Problem

Geometrically an annulus is a region bounded both internally and externally by cylindrical surfaces. Complete geometric specification of the annulus requires not only the size of one of the tubes but the ratio of the radii and some knowledge of the orientation of the axes of the two tubes. In the concentric annulus the axes are coincident. Figure I.A.1 illustrates a concentric annular passage and defines the coordinate system which will be used in describing it. The radial coordinate, r , is measured from the

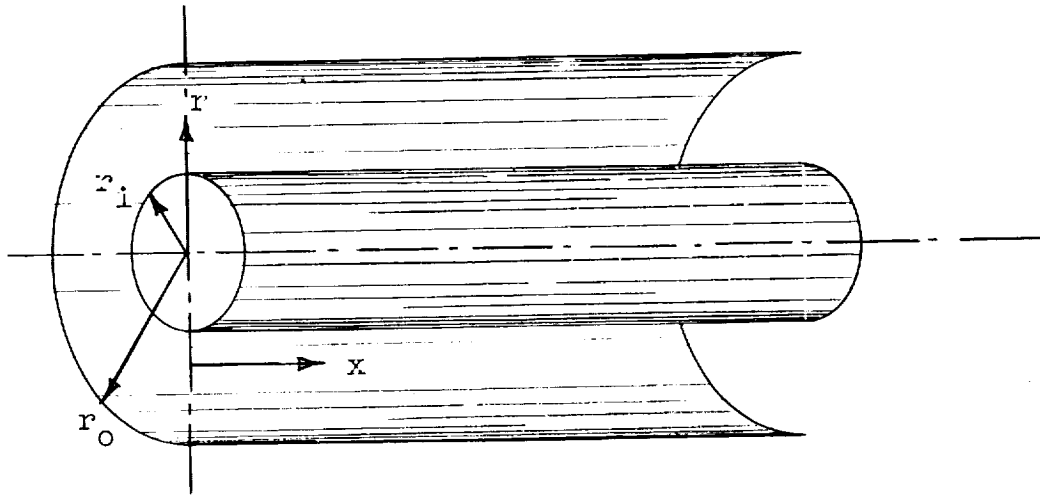


FIG. I.A.1.

common axis, the axial distance, x , is measured from an arbitrary reference plane normal to the tube axes. The concentric annular passage is a natural generalization of the circular tube and encompasses both the tube and the parallel plane channel as limiting geometries as the ratio of the inner radius to the outer radius, r^* , varies between the limits zero and one.

As a fundamental internal flow geometry the annulus is frequently used in a situation where heat is transferred to or from the contained fluid. An annulus is a simple form

for a two fluid heat exchanger and a water or steam jacket around a pipe has been used for years as a method of heating or cooling the central fluid. An annular coolant passage surrounding a central fuel element has been used as a core configuration for a nuclear reactor.

Since there are two distinct boundary surfaces annular heat transfer is inherently asymmetric, i.e., heat can be transferred at either the inner or the outer surfaces or both. In practice some heat transfer usually does occur at both boundaries even though it may be unwanted heat leakage through an insulating blanket or result from radiation from one surface to the other. Further, the temperature and/or the heat flux at either surface may vary both peripherally and axially in an arbitrary manner.

The possible asymmetry in heating conditions and the relative geometric complexity combine to create a large number of heat transfer problems in annular passages which are of significant interest.

I. B. Method of Solution

In order to formulate a systematic approach to the solution of problems in annular heat transfer we will restrict our considerations somewhat. Let us consider heat transfer in a concentric annular passage where the flow is hydrodynamically fully established and the temperature field is axially symmetric.

The problems which might possibly be of interest here can be defined by various conditions at the boundary surfaces. These are:

1. Temperature arbitrarily specified on both surfaces,
2. Heat flux arbitrarily specified on both surfaces,
3. Heat flux arbitrarily specified on one surface and temperature arbitrarily specified on the other,

4. Heat flux specified over a portion of one or both surfaces and temperature specified over another portion.

If we assume that the fluid is incompressible, has constant properties, and that axial conduction can be neglected, then the equation of the temperature field for laminar flow and no energy generated internally is

$$\frac{\partial^2 t}{\partial r^2} + \frac{1}{r} \frac{\partial t}{\partial r} = \frac{U(r)}{\alpha} \frac{\partial t}{\partial x} \quad (\text{I.B.1})$$

Since the energy equation is linear, any linear combination of solutions is again a solution. It may then, be possible to develop certain special or fundamental solutions to Eq. (I.B.1) satisfying particular boundary conditions which can be combined to satisfy the more general boundary conditions 1 through 4 above.

For fully established, incompressible, turbulent flow, one can define an eddy conductivity, and the energy equation becomes

$$\frac{\partial}{\partial r} \left[r (\epsilon_H + \alpha) \frac{\partial t}{\partial r} \right] = r U(r) \frac{\partial t}{\partial x} \quad (\text{I.B.2})$$

Then if ϵ_H is independent of the temperature, the equation is still linear and all of the superposition techniques will be valid. Our consideration of the fundamental solutions is not restricted to laminar flow, in fact, Eq. (I.B.2) can be considered as including the case of laminar flow when $\epsilon_H = 0$.

1. The fundamental solutions of the first kind

Consider the case where the fluid is flowing with a constant temperature t_e . At the station $x = x_o$, the temperature on wall j (where $j = 1$ or 0 corresponding to the inner or the outer walls respectively) is increased to t_j

and remains at that value for all $x > x_0$ while the opposite wall is maintained at t_e .

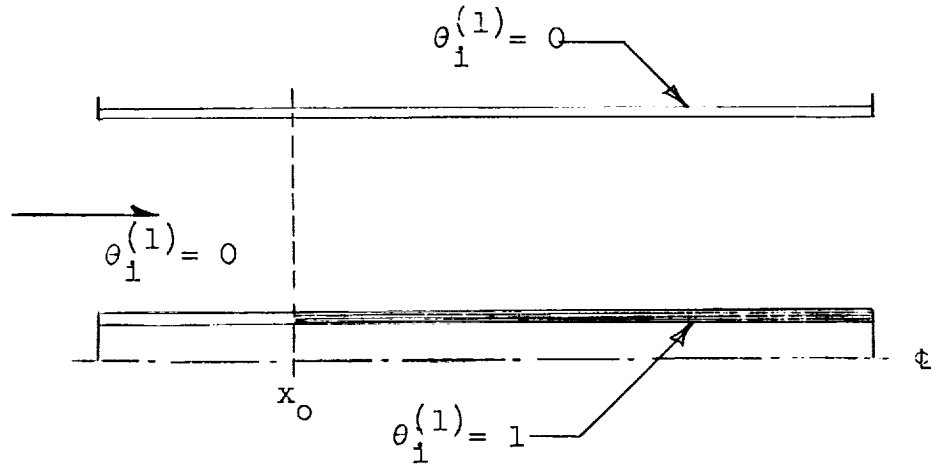


FIG. I.B.1: The fundamental solutions of the first kind, temperature step at the inner wall.

If we let

$$\theta_j^{(1)} = \frac{t - t_e}{t_j - t_e} \quad (\text{I.B.3})$$

where t is a solution to the energy equation satisfying the boundary conditions indicated above, then $\theta_j^{(1)}$ will be a solution of the energy equation satisfying the boundary conditions

$$\begin{aligned} \theta_j^{(1)} &= 1 \text{ on wall } j, \\ &= 0 \text{ on the opposite wall for } x \geq x_0, \end{aligned} \quad (\text{I.B.4})$$

and $\theta_j^{(1)} = 0$ for all $r \neq r_j$ at $x = x_0$

2. The fundamental solutions of the second kind

Consider the case where the fluid again has the initial temperature t_e , and at $x = x_0$ the heat flux on wall j is increased to q_j'' , while the opposite wall is insulated.

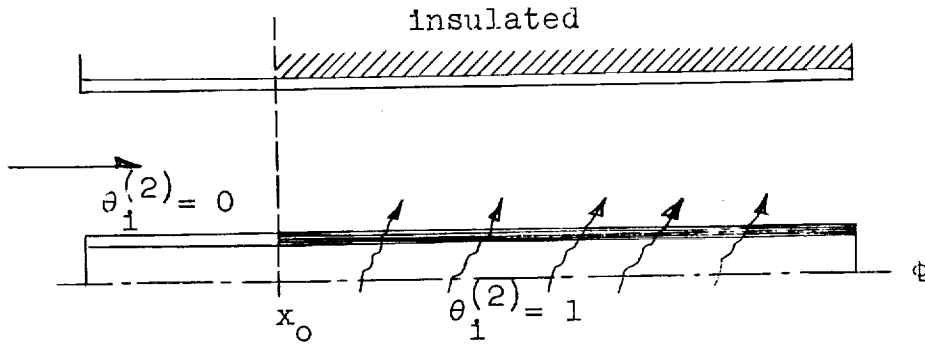


FIG. I.B.2: The fundamental solutions of the second kind, inner wall heated.

Let

$$\theta_j^{(2)} = \frac{t - t_e}{q_j'' D_h / k} \quad (\text{I.B.5})$$

where $D_h = 2(r_o - r_i)$, is the hydraulic diameter, and k is the fluid thermal conductivity. $\theta_j^{(2)}$ will be a solution of the energy equation satisfying the boundary conditions

$$\begin{aligned} \phi_j^{(2)} &= - D_h \frac{\partial \theta_j^{(2)}}{\partial n} = 1 \text{ on wall } j \\ &= 0 \text{ on the opposite wall for } x \geq x_0 \end{aligned}$$

$$\text{and } \theta_j^{(2)} = 0 \text{ for all } r \neq r_j \text{ at } x = x_0 \quad (\text{I.B.6})$$

Here n is the direction normal to the wall, measured as positive into the fluid.

3. The fundametal solutions of the third kind

At $x = x_0$ wall j is increased to t_j while the opposite wall is insulated.

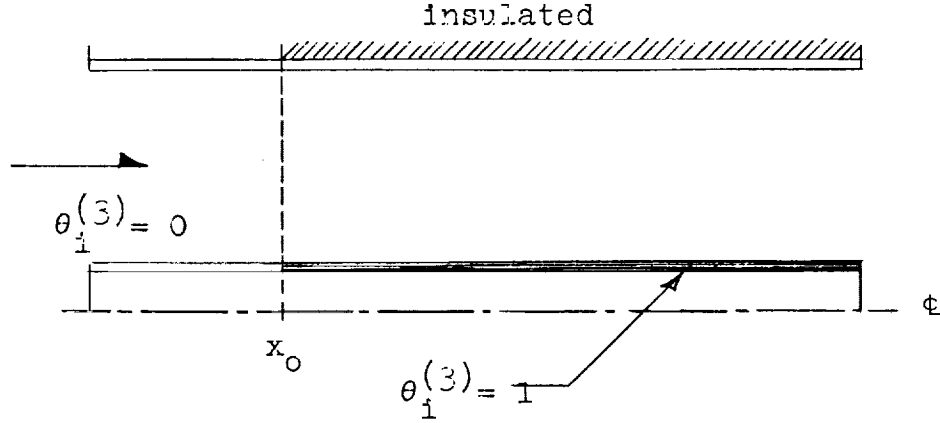


FIG. I.B.3: The fundamental solutions of the third kind, temperature step at the inner wall.

Let

$$\theta_j^{(3)} = \frac{t - t_e}{t_j - t_e} \quad (\text{I.B.7})$$

$\theta_j^{(3)}$ will be a solution to the energy equation satisfying the boundary conditions

$$\begin{aligned} \theta_j^{(3)} &= 1 \text{ on wall } j, \\ \Phi_j^{(3)} = -D_h \frac{\partial \theta_j^{(3)}}{\partial n} &= 0 \text{ on the opposite wall for } x \geq x_0, \end{aligned}$$

$$\text{and } \theta_j^{(3)} = 0 \text{ for all } r \neq r_j \text{ at } x \leq x_0 \quad (\text{I.B.8})$$

4. The fundamental solutions of the fourth kind

At $x = x_0$ wall j has the applied heat flux q_j'' while the opposite wall is maintained at the upstream temperature t_e .

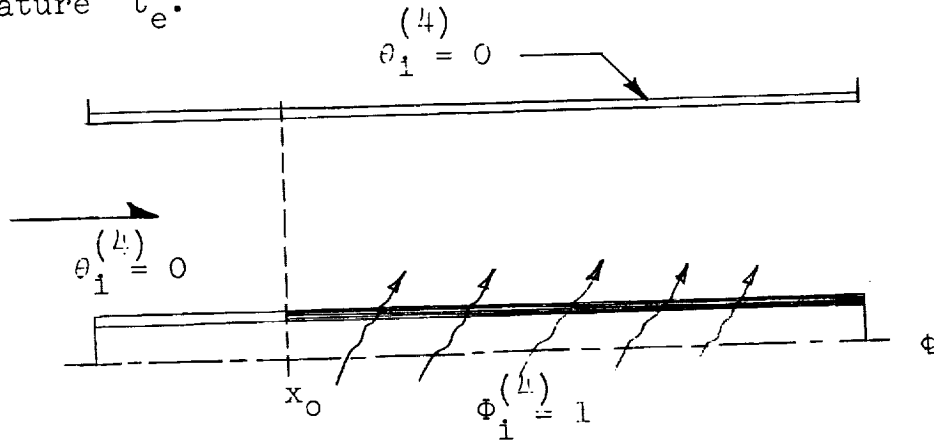


FIG. I.B.4: The fundamental solutions of the fourth kind, inner wall heated.

Let

$$\theta_j^{(4)} = \frac{t - t_e}{q_j'' D_h / k} \quad (\text{I.B.9})$$

$\theta_j^{(4)}$ will be a solution of the energy equation satisfying the boundary conditions

$$\Phi_j^{(4)} = - D_h \frac{\partial \theta_j^{(4)}}{2n} = 1 \text{ on wall } j,$$

$$\theta_j^{(4)} = 0 \text{ on the opposite wall for } x \geq x_0,$$

$$\text{and } \theta_j^{(4)} = 0 \text{ for all } r \neq r_j \text{ at } x \leq x_0 \quad (\text{I.B.10})$$

It is obvious from the defining equations that the fundamental solutions, $\theta_j^{(k)}$, are, in fact, dimensionless temperatures. Similarly the $\Phi_j^{(k)}$ can be considered as

dimensionless heat fluxes.

These four fundamental solutions can be superposed to form solutions satisfying the more general boundary conditions.

The engineer is frequently not concerned with the details of the fluid temperature field but only with the temperatures and the heat fluxes at the boundary walls and their relationship to the mixed mean fluid temperature. It will be convenient to introduce a generalized notation for the fundamental solutions. The general non-dimensional wall temperature for any fundamental case, k , has the form $\theta_{\ell j}^{(k)}$

where

$\ell = 1$ or 0 , referring to the wall at which the temperature is evaluated;

$j = 1$ or 0 , referring to the wall at which the non-zero boundary condition is applied.

Similarly the general non-dimensional wall flux has the form $\Phi_{\ell j}^{(k)}$ where the subscripts have the same meaning as before. The general mixed-mean (or cup mixing) temperature is denoted as $\theta_{mj}^{(k)}$ where $j = 1$ or 0 referring to the wall with the non-zero boundary condition. By definition

$$\theta_{mj}^{(k)} = \frac{1}{A U_m} \int_A U \theta_j^{(k)} dA$$

or

$$\theta_{mj}^{(k)}(x) = \frac{1}{\pi (r_0^2 - r_1^2) U_m} \int_{r_1}^{r_0} U(r) \theta_j^{(k)}(r, x) 2\pi r dr$$

.... (I.B.11)

where U_m is the bulk mean fluid velocity.

We will, then, be principally concerned with constructing the functions giving the wall temperatures and heat fluxes, and the mean temperature in non-dimensional form for the various boundary conditions. We may summarize the principal functions of interest for each of the fundamental cases as follows:

(1) First kind

We seek

$$\begin{array}{ccc} \theta_{mi}^{(1)} & \Phi_{ii}^{(1)} & \Phi_{oi}^{(1)} \\ \theta_{mo}^{(1)} & \Phi_{oo}^{(1)} & \Phi_{io}^{(1)} \end{array}$$

From the boundary conditions

$$\begin{array}{l} \theta_{ii}^{(1)} = \theta_{oo}^{(1)} = 1 \\ \text{and} \quad \theta_{io}^{(1)} = \theta_{oi}^{(1)} = 0 \end{array}$$

(2) Second kind

We seek

$$\begin{array}{ccc} \theta_{mi}^{(2)} & \theta_{ii}^{(2)} & \theta_{oi}^{(2)} \\ \theta_{mo}^{(2)} & \theta_{oo}^{(2)} & \theta_{io}^{(2)} \end{array}$$

From the boundary conditions

$$\begin{array}{l} \Phi_{ii}^{(2)} = \Phi_{oo}^{(2)} = 1 \\ \text{and} \quad \Phi_{oi}^{(2)} = \Phi_{io}^{(2)} = 0 \end{array}$$

(3) Third kind

We seek

$$\begin{array}{ccc} \theta_{mi}^{(3)} & \theta_{oi}^{(3)} & \Phi_{ii}^{(3)} \\ \theta_{mo}^{(3)} & \theta_{io}^{(3)} & \Phi_{oo}^{(3)} \end{array}$$

From the boundary conditions

$$\theta_{11}^{(3)} = \theta_{00}^{(3)} = 1$$

$$\Phi_{01}^{(3)} = \Phi_{10}^{(3)} = 0$$

(4) Fourth kind

We seek $\theta_{m1}^{(4)} \quad \theta_{11}^{(4)} \quad \Phi_{01}^{(4)}$

$$\theta_{m0}^{(4)} \quad \theta_{00}^{(4)} \quad \Phi_{10}^{(4)}$$

From the boundary conditions

$$\Phi_{11}^{(4)} = \Phi_{00}^{(4)} = 1$$

$$\theta_{01}^{(4)} = \theta_{10}^{(4)} = 0$$

To illustrate the use of the method of superposition and the utility of the pertinent non-dimensional functions let us consider as examples special cases of the arbitrary boundary conditions.

1. Constant but unequal wall temperatures

We have the boundary conditions that for $x \geq x_0$

$$t = t_0 \quad \text{on the outer wall,}$$

$$t = t_1 \quad \text{on the inner wall, and}$$

$t = t_e$ for all r at $x < x_0$. It can be seen from the boundary conditions (I.B.4) that if we let

$$t = t_0 \theta_0^{(1)} + t_1 \theta_1^{(1)} + t_e \tag{I.B.12}$$

t will be a solution to the energy equation satisfying the desired boundary conditions. Since the wall temperatures

are prescribed we are principally interested in the heating rates at the walls and the axial variation of the mean temperature. By manipulation of (I.B.12) we can obtain

$$q''_i = \frac{k}{D_h} [t_i \phi_{ii}^{(1)} + t_o \phi_{io}^{(1)}] \quad (\text{I.B.13})$$

and

$$q''_o = \frac{k}{D_h} [t_i \phi_{oi}^{(1)} + t_o \phi_{oo}^{(1)}] \quad (\text{I.B.14})$$

Because of the linearity of Eq. (I.B.11) we have

$$t_m = t_i \theta_{mi}^{(1)} + t_o \theta_{mo}^{(1)} + t_e \quad (\text{I.B.15})$$

2. Constant but unequal wall heat fluxes

If we specify

$$q'' = q''_i \quad \text{on the inner wall,}$$

$q'' = q''_o$ on the outer wall, for $x \geq x_o$ and $t = t_e$ for all r when $x \leq x_o$, then we can see from (I.B.6) that

$$t = \frac{D_h}{k} [q''_i \theta_i^{(2)} + q''_o \theta_o^{(2)}] + t_e \quad (\text{I.B.16})$$

is a solution of the energy equation satisfying the appropriate boundary conditions. Further we find

$$t_m = \frac{D_h}{k} [q''_i \theta_{mi}^{(2)} + q''_o \theta_{mo}^{(2)}] + t_e \quad (\text{I.B.17})$$

$$t_i = \frac{D_h}{k} [q''_i \theta_{ii}^{(2)} + q''_o \theta_{io}^{(2)}] + t_e \quad (\text{I.B.18})$$

$$t_o = \frac{D_h}{k} [q''_i \theta_{oi}^{(2)} + q''_o \theta_{oo}^{(2)}] + t_e \quad (\text{I.B.19})$$

3. Constant heat flux on one wall and constant temperature on the other

Let $t = t_a$ on wall a ,

$q'' = q''_b$ on wall b , for $x \geq x_o$ and

$t = t_e$ for all r when $x \leq x_o$. Combining the mixed cases we see that

$$t = t_a \theta_a^{(3)} + \frac{D_h}{k} q''_b \theta_b^{(4)} + t_e \quad (\text{I.B.20})$$

is a solution satisfying the correct boundary conditions, the other quantities follow as before.

Then if the $\phi_{lj}^{(k)}$, $\theta_{lj}^{(k)}$, and the $\theta_{mj}^{(k)}$, were available as functions of the axial coordinate, x , for the particular annulus of interest, the heat fluxes or temperatures at the walls and the mean temperature at any axial location could be computed readily by a simple linear combination of the appropriate values.

We would like to generalize these simpler considerations to the case of arbitrary axial variation of the wall boundary conditions. Consider the wall temperature variation shown in Fig. I.B.5. One might visualize this shape as being constructed from a large number of steps of infinitesimal height. Summing up the contributions of these steps and passing to the limit, the solution of the energy equation satisfying this boundary condition may be written in the form of a Stieltjes integral.

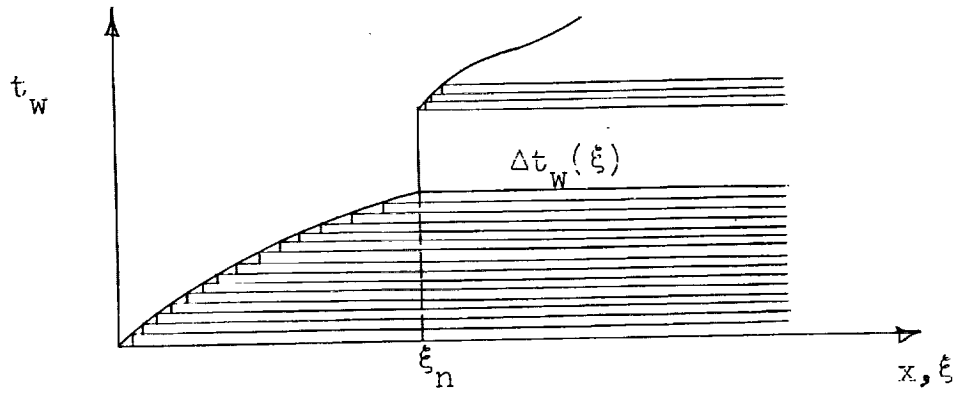


FIG. I.B.5

$$t(r, x) = \int_{\xi=0}^{\xi=x} \theta_j^{(1)}(r, x-\xi) \left(\frac{dt_w(\xi)}{d\xi} \right) d\xi \quad (\text{I.B.21})$$

The integral is evaluated by using $dt_w/d\xi$ wherever $t_w(\xi)$ is continuous and adding $\theta_j^{(1)}(r, x-\xi_n) \Delta t_w(\xi_n)$ to the expression for $t(r, x)$ for $x > \xi_n$. For a more detailed discussion of this superposition method see Klein and Tribus²², or Reynolds et al.¹⁶

Using (I.B.21) we can write for the cases of arbitrary wall temperature and heat flux the following equations:

$$t(r, x) = \int_{\xi=0}^{\xi=x} \theta_j^{(1)}(r, x-\xi) \left(\frac{dt_i(\xi)}{d\xi} \right) d\xi + \int_{\xi=0}^{\xi=x} \theta_o^{(1)}(r, x-\xi) \left(\frac{dt_o(\xi)}{d\xi} \right) d\xi \quad (\text{I.B.22})$$

$$t(r, x) = \frac{D_h}{k} \int_{\xi=0}^{\xi=x} \theta_1^{(2)}(r, x-\xi) \left(\frac{dq_1''(\xi)}{d\xi} \right) d\xi + \frac{D_h}{k} \int_{\xi=0}^{\xi=x} \theta_o^{(2)}(r, x-\xi) \left(\frac{dq_1''(\xi)}{d\xi} \right) d\xi \quad (\text{I.B.23})$$

The mixed cases follow in an analogous manner. Since the integrations are performed on the variable ξ , manipulations with respect to the radial coordinate r can be performed on the integrating kernels and the wall temperatures and heat fluxes together with the mixed-mean temperatures are immediately obvious.

While the evaluation of the integral expressions for the arbitrary boundary conditions is considerably more difficult than the linear superposition of the previous examples, if we are provided with the fundamental solutions in sufficient detail, it can certainly be carried out.

I.C. Objective

The objective herein is to obtain the fundamental solutions for the situation where the fluid in the annulus has constant properties, is in fully established laminar flow, and the effects of internal energy generation and axial conduction are negligible.

The fundamental solutions are sought in two ways; first, by solving (I.B.1) subject to each of the fundamental boundary conditions, and second, for the fundamental solutions of the second kind, through experimental measurement.

In order to provide a complete description of laminar flow heat transfer in annuli these solutions are sought for a sufficient number of specific values of the radius ratio, r^* , to encompass most practical sizes.

I.D. Summary

The methods described in sections II.A through II.H provide analytical expressions for the fundamental solutions and the numerical values necessary to evaluate these expressions.

The values of the related non-dimensional quantities are presented in section II.I as functions of the axial distance parameter

$$\bar{x} = \frac{x/D_h}{\text{RePr}} ,$$

for various values of the ratio of the radii, r^* . To facilitate interpolation on r^* , the values of all the fundamental solutions obtained by McCuen¹¹ for the parallel plane channel are presented.

A comparison of the fundamental solutions of the second kind with experimental values obtained as described in section III.A is presented in section III.B.

Numerical examples of the use of the fundamental solutions in problems of superposition are considered in Appendix G.

I.E. Conclusions

The values for the fundamental solutions which are presented provide a method for solving laminar flow heat transfer problems in annuli which is, essentially, complete. That is, values are provided for all \bar{x} for enough values of r^* to enable the consideration of virtually any annular geometry.

There are two effects which influence the departure of the behavior of the solutions from the simple, fully established (constant film coefficient) situation. These are:

1. The effect of axial variation of boundary conditions;
2. The effect of heating asymmetry, i.e., the influence of the boundary condition at the opposite wall.

The axial effects will be significant near any discontinuities of boundary conditions or if the continuous variation is rapid. The asymmetric effects will predominate in long tubes and will be larger for a greater degree of asymmetry.

For cases of simple superposition like the examples on pages 10 to 12, probable criteria for the influence of these two effects can be presented as follows.

For $\bar{x} < 0.01$, the axial effects will predominate, for $\bar{x} > 0.1$, the asymmetric effects will predominate, and for $0.01 < \bar{x} < 0.1$, the effects will be comparable.

The good agreement obtained between the predictions of the theory and the measured values indicates the validity of the assumptions for fluids of Prandtl numbers near unity.

II THE FUNDAMENTAL SOLUTIONS

II. A. Previous Studies

Laminar flow heat transfer for the cases which represent the limiting forms of the annulus (i.e., the circular tube and the parallel plane channel) ~~has~~ received considerable attention.

Heat transfer to a fluid in laminar flow in a circular tube with constant wall temperature is the classical Graetz⁵ problem. The original work by Graetz and the extension of it by Sellars, Tribus and Klein¹⁹ comprise a relatively complete solution corresponding to the limiting geometry for the fundamental solution of the third kind. Sellars et al also work out the case where the heat flux at the wall is constant by an inversion method. A direct solution for the fundamental solution of the second kind was obtained by Siegel, Sparrow and Hallman²⁰. The fundamental cases, one and four, have no counterpart for flow in a circular tube.

For laminar flow in a parallel plane channel all of fundamental cases have significance although they are symmetric (i.e., $\theta_{ii}^{(k)} = \theta_{oo}^{(k)}$). All of the cases have received some analytical attention. Perhaps the greatest effort has been for the case of constant and equal temperatures at the duct walls (sometimes called the Purday¹⁵ problem). More recently Cess and Schaffer have published solutions for cases one and two (Refs. 2 and 3). Case three has been considered by Schenke¹⁸. McCuen¹¹ has reduced all of the available solutions to a form consistent with the definitions given in section I.B and has completed the solutions of the third and fourth kind.

The principal technique employed in obtaining these cases is that which Graetz used, solution of the energy equation by separation of variables. This method expresses the solution for the temperature field as an infinite series,

the terms of which are products of an exponential involving the axial coordinate x , the eigenfunctions of the resulting Sturm-Liouville equation, and a coefficient resulting from an orthogonal expansion of the initial condition. This approach has two main disadvantages:

1. Near the step change in boundary conditions ($x \rightarrow 0$) the infinite series converges rather slowly necessitating a large number of terms,
2. The eigenfunctions corresponding to the higher modes of the Sturm-Liouville equation are difficult to calculate directly.

To avoid the series solution Leveque⁹ used the fact that very near the step change in boundary conditions the temperature signal has affected the fluid only in the immediate vicinity of the wall. He was able to obtain a similarity solution for the temperature field which becomes exact as x approaches zero. Sellars et al have applied the WKBJ approximation to the Sturm-Liouville system to provide an asymptotic form for the higher modes and to a large extent have circumvented the difficulty associated with that calculation.

For true annular flow very few of the problems have received much attention. Jakob and Rees⁶ obtained the temperature distribution valid as x tends to infinity for the fundamental solution of the second kind. Singh²¹ proposed a method for solution for a more general form of Eq. I.B.1 which includes the effects of axial conduction and viscous generation. This method involves the expression of the eigenfunctions as a series of Bessel functions satisfying the boundary conditions. Murakawa^{12, 13} has presented an integral equation formulation for the solution of the first kind and a series solution approach to the same problem including the more difficult case where arbitrary peripheral variations are allowed. Murakawa does not carry his solutions to the point of numerical computation.

II.B The Hydrodynamic Problem

The velocity profile for fully established laminar flow in a concentric annulus with constant fluid properties was first presented by Lamb⁸. If we let

$$\bar{r} = r/r_o \quad \bar{U} = U/U_m \quad \text{and} \quad r^* = r_1/r_o$$

where U_m , the bulk mean velocity is given by

$$U_m = \frac{2}{r_o^2 - r_1^2} \int_{r_1}^{r_o} U(r) r \, dr \quad (\text{II.B.1})$$

Then we may write

$$\bar{U} = \frac{2}{M} (1 - \bar{r}^2 + B \ln \bar{r}) \quad (\text{II.B.2})$$

where

$$B = (r^{*2} - 1)/\ln r^* \quad \text{and} \quad M = 1 + r^{*2} - B$$

The friction factor f is defined by

$$f = \frac{\tau_1 r_1 + \tau_o r_o}{r_1 + r_o} / \frac{1}{2} \rho U_m^2 \quad (\text{II.B.3})$$

where τ_1 and τ_o are the stresses exerted by the boundary walls on the fluid at the inner and the outer surfaces respectively. The friction factor is related to the axial pressure gradient by

$$-\frac{dP}{dx} = \frac{4f}{D_h} \rho \frac{U_m^2}{2} \quad (\text{II.B.4})$$

From the definition of the shear stress in laminar flow and Eq. (II.B.2) we can obtain

$$f = \frac{16}{Re} \frac{(1 - r^*)^2}{M} \quad (\text{II.B.5})$$

When $r^* = 0$, the friction factor becomes $16/Re$, the value for the circular tube. At $r^* = 1$ successive application of L'Hospital's rule yields $f = 24/Re$, the friction factor for flow between parallel planes. Figure II.B.1 presents $f \cdot Re$ as a function of the radius ratio r^* .

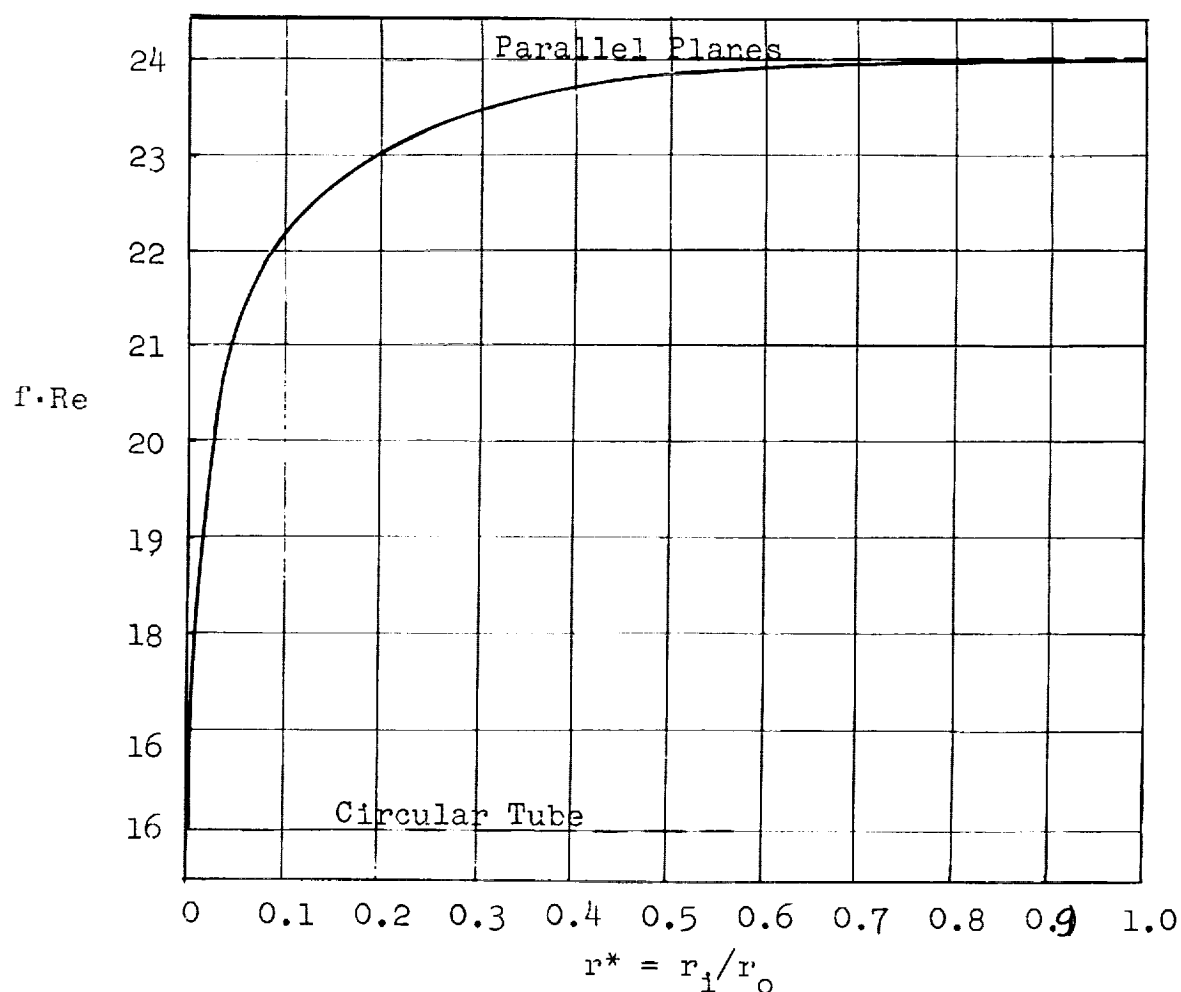


FIG. II.B.1 Friction factor for fully-developed laminar flow in a concentric annulus

II. C. The Energy Equation

Let us introduce the non-dimensional variables

$$\bar{r} = r/r_0, \quad r^* = r_1/r_0 \quad \bar{x} = \frac{x/D_h}{\text{RePr}}$$

where

$$D_h = 2(r_0 - r_1)$$

into Eq. (I.B.1). The velocity distribution, $U(r)$, is given by (II.B.2). By virtue of the defining relationships we have

$$\frac{\partial^2 \theta_j^{(k)}}{\partial \bar{r}^2} + \frac{1}{\bar{r}} \frac{\partial \theta_j^{(k)}}{\partial \bar{r}} = \frac{(1 - \bar{r}^2 + B \ln \bar{r})}{2M (1 - r^*)} \frac{\partial \theta_j^{(k)}}{\partial \bar{x}} \quad (\text{II.C.1})$$

where, as before

$$B = \frac{r^{*2} - 1}{\ln r^*} \quad \text{and} \quad M = 1 + r^* - B$$

This is the differential equation which the fundamental solutions must satisfy.

II.D. Asymptotic (large \bar{x}) Values of the Fundamental Solutions, Homogenization of the Boundary Conditions

We will seek solutions to Eq. (II.C.1) by the method of separation of variables. This method results in expression of the solution as an infinite series. In order to satisfy the initial condition we will need to express a function (representing the temperature distribution at $\bar{x} = 0$) as an infinite series of the orthogonal eigenfunctions. The resulting Sturm-Liouville equation will generate such a set only if the dependent variable satisfies general homogeneous boundary conditions. We note, however, that the boundary conditions specified for the fundamental solutions (I.B.4, I.B.6, I.B.8, I.B.10) are inhomogeneous. We shall resort to the method of Siegel, Sparrow, and Hallman²⁰. If we let

$$\bar{\theta}_j^{(k)} = \theta_j^{(k)} - \theta_j^{(k)}{}_{fd} \quad (\text{II.D.1})$$

where $\theta_j^{(k)}{}_{fd}$ is the "fully developed" temperature profile, that is, the asymptotic value of $\theta_j^{(k)}$ as \bar{x} tends to infinity, then the $\bar{\theta}_j^{(k)}$ will satisfy homogeneous boundary conditions.

1. The fundamental solutions of the first kind

We have defined $\theta_j^{(1)}$ as solutions to Eq. (II.C.1) satisfying the boundary conditions:

$$\begin{aligned} \theta_j^{(1)} &= 1 \text{ on wall } j \\ &= 0 \text{ on the opposite wall, for all } \bar{x} > 0 \\ \text{and } \theta_j^{(1)} &= 0 \text{ for all } \bar{r} \text{ at } \bar{x} \leq 0. \end{aligned}$$

As \bar{x} approaches infinity we see that, because the two walls are at different temperatures, whatever heat crosses wall 1 must cross wall 0 and hence $\partial\theta_j^{(1)}/\partial\bar{x} \rightarrow 0$. Then Eq. (II.C.1) reduces to

$$\frac{\partial^2 \theta_j^{(1)}}{\partial \bar{r}^2} + \frac{1}{\bar{r}} \frac{\partial \theta_j^{(1)}}{\partial \bar{r}} = 0 \quad (\text{II.D.2})$$

so that

$$\theta_j^{(1)}|_{fd} = G_1 \ln \bar{r} + H_1 \quad (\text{II.D.3})$$

Evaluating G_1 and H_1 by the boundary conditions, we obtain

$$\theta_1^{(1)}|_{fd} = \frac{\ln \bar{r}}{\ln r^*} \quad (\text{II.D.4})$$

and

$$\theta_0^{(1)}|_{fd} = 1 - \frac{\ln \bar{r}}{\ln r^*} \quad (\text{II.D.5})$$

Now if we let $\bar{\theta}_j^{(1)} = \theta_j^{(1)} - \theta_j^{(1)}|_{fd}$ we see that $\bar{\theta}_j^{(1)}$ is a solution to equation (II.C.1) and has homogeneous boundary conditions at $r = r^*$ and 1. That is, $\bar{\theta}_1^{(1)}(\bar{r}, \bar{x})$ satisfies Eq. (II.C.1) and the boundary conditions

$$\bar{\theta}_1^{(1)}(1, \bar{x}) = 0$$

$$\bar{\theta}_1^{(1)}(\bar{r}, 0) = - \frac{\ln \bar{r}}{\ln r^*}$$

$$\bar{\theta}_1^{(1)}(r^*, \bar{x}) = 0$$

Similarly $\bar{\theta}_0^{(1)}(\bar{r}, \bar{x})$ satisfies Eq. (II.C.1) and the boundary conditions

$$\begin{aligned}\bar{\theta}_0^{(1)}(1, \bar{x}) &= 0 \\ \bar{\theta}_0^{(1)}(r^*, \bar{x}) &= 0\end{aligned}\quad \bar{\theta}_0^{(1)}(\bar{r}, 0) = \frac{\ln \bar{r}}{\ln r^*} - 1$$

The asymptotic values of the $\Phi_j^{(1)}$ can be obtained from Eqs. (II.D.4) and (II.D.5).

$$\Phi_{11}^{(1)}{}_{fd} = - \frac{2}{r^*} \frac{(1 - r^*)}{\ln r^*} \quad (\text{II.D.6})$$

$$\Phi_{01}^{(1)}{}_{fd} = \frac{2(1 - r^*)}{\ln r^*} \quad (\text{II.D.7})$$

$$\Phi_{00}^{(1)}{}_{fd} = - \frac{2(1 - r^*)}{\ln r^*} \quad (\text{II.D.8})$$

$$\Phi_{10}^{(1)}{}_{fd} = \frac{2(1 - r^*)}{r^* \ln r^*} \quad (\text{II.D.9})$$

We may determine the asymptotic values of $\theta_{m1}^{(1)}$ and $\theta_{m1}^{(1)}$ as follows.

$$\theta_{mj}^{(k)} = \frac{2}{[1 - (r^*)^2]} \int_{r^*}^1 \theta_j^{(k)} \bar{U} \bar{r} d\bar{r} \quad (\text{II.D.10})$$

Substituting, successively, Eqs. (II.D.4) and (II.D.5) into the above and carrying out the integration yields

$$\theta_{m1}^{(1)}{}_{fd} = \frac{4}{M \ln r^*} \left[\frac{B}{4} - \frac{3}{16} - \frac{7}{16} (r^*)^2 + \frac{(r^*)^4}{4B} \right] \quad \dots (\text{II.D.11})$$

$$\theta_{mo}^{(1)} \big|_{fd} = 1 - \frac{4}{M \ln r^*} \left[\frac{B}{4} - \frac{3}{16} - \frac{7}{16} (r^*)^2 + \frac{(r^*)^4}{4B} \right] \quad (\text{II.D.12})$$

Recalling the definition of Nusselt number, this can be related to the fundamental solutions as follows.

$$Nu_{lj}^{(k)} = \frac{h D_h}{k} = \frac{\phi_j^{(k)}}{[\theta_{lj}^{(k)} - \theta_{mj}^{(k)}]} \quad (\text{II.D.13})$$

Then we can obtain

$$Nu_{11}^{(1)} \big|_{fd} = \frac{M(1 - r^*)}{r^* [\frac{B}{2} - \frac{7}{8} - \frac{3}{8} (r^*)^2 + \frac{1}{2B}]} = Nu_{10}^{(1)} \big|_{fd} \quad (\text{II.D.14})$$

$$Nu_{00}^{(1)} \big|_{fd} = \frac{M(1 - r^*)}{[\frac{3}{8} + \frac{7}{8} (r^*)^2 - \frac{B}{2} - \frac{(r^*)^4}{2B}]} = Nu_{01}^{(1)} \big|_{fd} \quad (\text{II.D.15})$$

2. The fundamental solutions of the second kind

We have defined $\theta_j^{(2)}$ as solutions to Eq. (II.C.1) satisfying the boundary conditions:

$$\phi_j^{(2)} = -D_h \frac{\partial \theta_j^{(2)}}{\partial n} = 1 \text{ on wall } j,$$

$$= 0 \text{ on the opposite wall, for all } \bar{x}$$

$$\text{and } \theta_j^{(2)} = 0 \text{ for all } \bar{r} \text{ at } \bar{x} \leq 0.$$

As \bar{x} approaches infinity $\partial \theta_j^{(2)} / \partial \bar{x}$ becomes constant and is equal to $\partial \theta_{mj}^{(2)} / \partial \bar{x}$. Then Eq. (II.C.1) becomes

$$\frac{\partial^2 \theta_j^{(2)}}{\partial \bar{r}^2} + \frac{1}{\bar{r}} \frac{\partial \theta_j^{(2)}}{\partial \bar{r}} = \left(\frac{\partial \theta_{mj}^{(2)}}{\partial \bar{x}} \right) \frac{(1 - \bar{r}^2 + B \ln \bar{r})}{2M (1 - r^*)^2} \quad (\text{II.D.16})$$

Equation (II.D.16) may be integrated directly to yield

$$\theta_j^{(2)} \big|_{fd} = \left(\frac{\partial \theta_{mj}^{(2)}}{\partial \bar{x}} \right) \frac{1}{2M(1 - r^*)^2} \left[\frac{(1 - B)}{4} \bar{r}^2 - \frac{\bar{r}^4}{16} + \frac{B\bar{r}^2}{4} \ln \bar{r} \right] + G_2 \ln \bar{r} + H_2 \quad (\text{II.D.17})$$

as the general form of the asymptotic value of the fundamental solution of the second kind. From the concept of $\theta_j^{(k)}$ as a non-dimensional temperature we can evaluate $\partial \theta_{mj}^{(2)} / \partial \bar{x}$ from energy considerations. We have

$$\frac{\partial \theta_{m1}^{(2)}}{\partial \bar{x}} = \frac{4r^*}{(1 + r^*)} \quad (\text{II.D.18})$$

and

$$\frac{\partial \theta_{mo}^{(2)}}{\partial \bar{x}} = \frac{4}{(1 + r^*)} \quad (\text{II.D.19})$$

from which we can obtain

$$\theta_{m1}^{(2)} = \frac{4r^*}{(1 + r^*)} \bar{x} \quad (\text{II.D.20})$$

and

$$\theta_{mo}^{(2)} = \frac{4}{(1 + r^*)} \bar{x} \quad (\text{II.D.21})$$

Using Eqs. (II.D.17) and (II.D.18) together with the appropriate boundary conditions

$$\begin{aligned} \theta_{11}^{(2)} \big|_{fd} = & \frac{r^*}{(1+r^*)} \frac{1}{M(1-r^*)^2} \left[\frac{(1-B)}{2} (\bar{r}^2 - \ln \bar{r}) \right. \\ & \left. - \frac{\bar{r}^4}{8} + \frac{B}{2} \bar{r}^2 \ln \bar{r} - \frac{(r^*)^2 M}{2} + \frac{(1 + \ln r^*)}{2} - \frac{(r^*)^4}{8} \right] + \theta_{11}^{(2)} \\ & \dots \quad (II.D.22) \end{aligned}$$

Here $\theta_{11}^{(2)}$ is still unknown but it can be evaluated by noticing that $\theta_{11}^{(2)} - \theta_{m1}^{(2)}$ is a function of r^* only as \bar{x} gets large. Using Eq. (II.D.10) we can obtain

$$\begin{aligned} \theta_{11}^{(2)} - \theta_{m1}^{(2)} \big|_{fd} = & \frac{r^*}{(1+r^*)} \frac{1}{M^2(1-r^*)^2} \left\{ - \left[\frac{73}{48} - \frac{31}{18} B + \frac{11}{16} B^2 - \frac{1}{2B} \right] \right. \\ & \left. - \left[\frac{25}{48} - \frac{2}{9} B - \frac{5}{16} B^2 \right] (r^*)^2 - \left[\frac{19}{36} B - \frac{11}{48} \right] (r^*)^4 + \frac{11}{48} (r^*)^6 \right\} \\ & \dots \quad (II.D.23) \end{aligned}$$

Using Eqs. (II.D.17) and (II.D.19) we can obtain a similar expression for $\theta_o^{(2)} \big|_{fd}$

$$\begin{aligned} \theta_o^{(2)} \big|_{fd} = & \frac{1}{(1+r^*)} \frac{1}{M(1-r^*)^2} \left\{ \frac{(1-B)}{2} (\bar{r}^2 - 1) - \frac{(\bar{r}^4 - 1)}{8} \right. \\ & \left. + \frac{B \bar{r}^2}{2} \ln \bar{r} - \frac{(r^*)^2}{2} [(r^*)^2 - B] \ln \bar{r} \right\} + \theta_{oo}^{(2)} \\ & \dots \quad (II.D.24) \end{aligned}$$

As before $\theta_{oo}^{(2)}$ can be evaluated from (II.D.24) and (II.D.10).

$$\begin{aligned} \theta_{oo}^{(2)} - \theta_{mo}^{(2)} \Big|_{fd} = & \frac{1}{(1+r^*) M^2 (1-r^*)^2} \left\{ \left[\frac{11}{48} - \frac{19}{36} B + \frac{5}{16} B^2 \right] \right. \\ & + \left[\frac{11}{48} + \frac{2B}{9} - \frac{11}{16} B^2 \right] (r^*)^2 - \left[\frac{25}{48} - \frac{31}{18} B \right] (r^*)^4 - \frac{73}{48} (r^*)^6 \\ & \left. + \frac{(r^*)^8}{2B} \right\} \end{aligned} \quad (II.D.25)$$

Now if we let $\bar{\theta}_j^{(2)} = \theta_j^{(2)} - \theta_j^{(2)} \Big|_{fd}$ we see that $\bar{\theta}_j^{(2)}$ is a solution to Eq. (II.C.1) and has homogeneous boundary conditions at $r = r^*$ and 1. Explicitly, $\bar{\theta}_1^{(2)}(\bar{r}, \bar{x})$ satisfies Eq. (II.C.1) and the boundary conditions

$$\frac{\partial \bar{\theta}_1^{(2)}}{\partial \bar{r}} = 0 \quad \text{at } \bar{r} = r^* \text{ and } 1, \quad \text{for all } \bar{x}, \text{ and}$$

$$\begin{aligned} \bar{\theta}_1^{(2)}(\bar{r}, 0) = & - \frac{r^*}{(1+r^*) M (1-r^*)^2} \left[\frac{(1-B)}{2} (\bar{r}^2 - \ln \bar{r}) \right. \\ & - \frac{\bar{r}^4}{8} + \frac{B}{2} \bar{r}^2 \ln \bar{r} - \frac{(r^*)^2 M}{2} + \frac{(1 + \ln r^*)}{2} - \frac{(r^*)^4}{8} \Big] \\ & - (\theta_{11}^{(2)} - \theta_{m1}^{(2)})_{fd} \end{aligned}$$

and $\bar{\theta}_0^{(2)}(\bar{r}, \bar{x})$ satisfies Eq. (II.C.1) and the boundary conditions

$$\frac{\partial \bar{\theta}_0^{(2)}}{\partial \bar{r}} = 0 \quad \text{at } \bar{r} = r^* \text{ and } 1, \quad \text{for all } \bar{x} \text{ and}$$

$$\begin{aligned}
\bar{\theta}_o^{(2)}(\bar{r}, o) &= \frac{1}{(1 + r^*) M(1 - r^*)} \left\{ \frac{(1 - B)}{2} (\bar{r}^2 - 1) - \frac{(\bar{r}^4 - 1)}{8} \right. \\
&\quad \left. + \frac{B}{2} \bar{r}^2 \ln \bar{r} - \frac{(r^*)^2}{2} [(r^*)^2 - B] \ln \bar{r} \right\} \\
&\quad - (\theta_{oo}^{(2)} - \theta_{mo}^{(2)})_{fd}
\end{aligned}$$

Using Eqs. (II.D.22) and (II.D.23) we can obtain the asymptotic expression for

$$\begin{aligned}
\theta_{oi}^{(2)} - \theta_{mi}^{(2)} \Big|_{fd} &= - \frac{r^*}{(1 + r^*) M^2(1 - r^*)} \\
&\quad \left\{ \left[\frac{55}{48} - \frac{11}{9} B + \frac{11}{16} B^2 - \frac{1}{2B} \right] \right. \\
&\quad + \left[\frac{25}{48} - \frac{2}{9} B - \frac{5}{16} B^2 + \frac{M}{2} \right] (r^*)^2 \\
&\quad + \left[\frac{19}{36} B - \frac{17}{48} \right] (r^*)^4 - \frac{11}{48} (r^*)^6 \\
&\quad \left. - \frac{(1 + \ln r^*)}{2} \right\} \tag{II.D.26}
\end{aligned}$$

and similarly from (II.D.24) and (II.D.25) we get

$$\begin{aligned}
\theta_{io}^{(2)} - \theta_{mo}^{(2)} \Big|_{fd} = & - \frac{1}{(1 + r^*) M^2 (1 - r^*)^2} \left\{ \left[\frac{7}{48} + \frac{B}{36} - \frac{5}{16} B^2 \right] \right. \\
& + \left[\frac{13}{48} + \frac{5}{18} B + \frac{11}{16} B^2 \right] (r^*)^2 \\
& + \left[\frac{17}{48} - \frac{31}{18} B \right] (r^*)^4 + \frac{73}{48} (r^*)^6 - \frac{(r^*)^8}{2B} \\
& \left. + \frac{(r^*)^4}{2} \ln r^* \right\} \quad (II.D.27)
\end{aligned}$$

Because of the specified boundary conditions we see that $Nu_{oi}^{(2)} = Nu_{io}^{(2)} = 0$, and

$$Nu_{ii}^{(2)} = \frac{1}{\theta_{ii}^{(2)} - \theta_{mi}^{(2)}} \quad (II.D.28)$$

$$Nu_{oo}^{(2)} = \frac{1}{\theta_{oo}^{(2)} - \theta_{mo}^{(2)}} \quad (II.D.29)$$

3. The fundamental solutions of the third kind

We have defined $\theta_j^{(3)}$ as solutions to Eq. (II.C.1) satisfying the boundary conditions

$$\theta_j^{(3)} = 1 \quad \text{on wall } j$$

$$\Phi_j^{(3)} = -D_h \partial \theta_j^{(3)} / \partial n = 0 \quad \text{on the opposite wall, for all } \bar{x} > 0$$

and $\theta_j^{(3)} = 0$ for all \bar{r} when $\bar{x} \leq 0$.

As \bar{x} approaches infinity the temperature of the fluid tends toward a constant equal to that of wall j . Hence

$$\theta_i^{(3)}|_{fd} = \theta_{ii}^{(3)}|_{fd} = \theta_{oi}^{(3)}|_{fd} = \theta_{mi}^{(3)}|_{fd} = 1 \quad (\text{II.D.30})$$

$$\Phi_{ii}^{(3)}|_{fd} = \Phi_{oi}^{(3)}|_{fd} = 0 \quad (\text{II.D.31})$$

and

$$\theta_o^{(3)}|_{fd} = \theta_{oo}^{(3)}|_{fd} = \theta_{io}^{(3)}|_{fd} = \theta_{mo}^{(3)}|_{fd} = 1 \quad (\text{II.D.32})$$

$$\Phi_{oo}^{(3)}|_{fd} = \Phi_{io}^{(3)}|_{fd} = 0 \quad (\text{II.D.33})$$

Now if we let $\bar{\theta}_j^{(3)} = \theta_j^{(3)} - \theta_j^{(3)}|_{fd}$ we see that $\bar{\theta}_j^{(3)}$ satisfies Eq.(II.C.1) and has homogeneous boundary conditions at $r = r^*$ and 1. Explicitly $\bar{\theta}_i^{(3)}(\bar{r}, \bar{x})$ satisfies Eq.(II.C.1) and the boundary conditions

$$\bar{\theta}_i^{(3)}(r^*, \bar{x}) = 0$$

$$\bar{\theta}_i^{(3)}(1, \bar{x}) = 0 \quad \text{and} \quad \bar{\theta}_i^{(3)}(\bar{r}, 0) = -1$$

and $\bar{\theta}_o^{(3)}(\bar{r}, \bar{x})$ satisfies Eq. (II.C.1) and the boundary conditions

$$\bar{\theta}_0^{(3)}(1, \bar{x}) = 0$$

$$\bar{\Phi}_0^{(3)}(r^*, \bar{x}) = 0 \quad \text{and} \quad \bar{\theta}_0^{(3)}(\bar{r}, 0) = -1$$

The limiting Nusselt numbers reduce to an indeterminate form and cannot be evaluated from these considerations.

4. The fundamental solutions of the fourth kind

We have defined the $\theta_j^{(4)}$ as solutions to Eq. (II.C.1) satisfying the boundary conditions

$$\Phi_j^{(4)} = -D_h \frac{\partial \theta_j^{(4)}}{\partial n} = 1 \text{ on wall } j$$

$$\theta_j^{(4)} = 0 \text{ on the opposite wall for all } \bar{x} > 0$$

$$\text{and } \theta_j^{(4)} = 0 \text{ for all } \bar{r} \text{ when } \bar{x} \leq 0$$

As \bar{x} approaches infinity the heat passing through wall 1 must also pass wall 0 and $\partial \theta_j^{(4)} / \partial \bar{x} \rightarrow 0$. Then $\theta_j^{(4)}$ will satisfy equation (II.D.2) and

$$\theta_j^{(4)}|_{fd} = G_4 \ln \bar{r} + H_4 \quad (\text{II.D.34})$$

By application of the appropriate boundary conditions one obtains

$$\theta_1^{(4)}|_{fd} = \frac{r^*}{2(1 - r^*)} \ln \bar{r} \quad (\text{II.D.35})$$

and

$$\theta_0^{(4)}|_{fd} = \frac{1}{2(1 - r^*)} \ln \left(\frac{\bar{r}}{r^*} \right) \quad (\text{II.D.36})$$

Now if we let $\bar{\theta}_j^{(4)} = \theta_j^{(4)} - \theta_j^{(4)}_{fd}$ we see that $\bar{\theta}_j^{(4)}$ satisfies Eq. (II.C.1) and has homogeneous boundary conditions at $r = r^*$ and 1. That is $\bar{\theta}_1^{(4)}(\bar{r}, \bar{x})$ satisfies Eq. (II.C.1) and the boundary conditions

$$\bar{\Phi}_1^{(4)}(r^*, \bar{x}) = 0$$

$$\bar{\theta}_1^{(4)}(1, \bar{x}) = 0, \quad \bar{\theta}_1^{(4)}(\bar{r}, 0) = \frac{r^*}{2(1 - r^*)} \ln \bar{r}$$

and $\bar{\theta}_0^{(4)}(\bar{r}, \bar{x})$ satisfies Eq. (II.C.1) and the boundary conditions

$$\bar{\Phi}_0^{(4)}(1, \bar{x}) = 0$$

$$\bar{\theta}_0^{(4)}(r^*, \bar{x}) = 0 \quad \text{and} \quad \bar{\theta}_0^{(4)}(\bar{r}, 0) = -\frac{1}{2(1 - r^*)} \ln \left(\frac{\bar{r}}{r^*} \right)$$

Then as before

$$\theta_{11}^{(4)}_{fd} = \frac{-r^* \ln r^*}{2(1 - r^*)} \quad (\text{II.D.37})$$

$$\Phi_{01}^{(4)}_{fd} = -r^* \quad (\text{II.D.38})$$

$$\theta_{00}^{(4)}_{fd} = -\frac{\ln r^*}{2(1 - r^*)} \quad (\text{II.D.39})$$

and

$$\Phi_{10}^{(4)}_{fd} = -\frac{1}{r^*} \quad (\text{II.D.40})$$

Further

$$\theta_{m1}^{(4)}_{fd} = \frac{2r^*}{M(1 - r^*)} \left[\frac{3}{16} + \frac{7}{16} (r^*) - \frac{B}{4} - \frac{(r^*)^4}{4B} \right] \quad (\text{II.D.41})$$

$$\theta_{mo}^{(4)} \big|_{fd} = \frac{2}{M(1 - r^*)} \left[\frac{B}{4} - \frac{3}{16} - \frac{7}{16} (r^*)^2 + \frac{(r^*)^4}{4B} \right] - \frac{\ln r^*}{2(1 - r^*)} \quad \dots \quad (II.D.42)$$

We may also determine the limiting Nusselt numbers

$$Nu_{ii}^{(4)} \big|_{fd} = \frac{M(1 - r^*)}{r^* \left[\frac{B}{2} - \frac{7}{8} - \frac{3}{8}(r^*)^2 + \frac{1}{2B} \right]} = Nu_{io}^{(4)} \big|_{fd} \quad (II.D.43)$$

$$Nu_{oo}^{(4)} \big|_{fd} = \frac{M(1 - r^*)}{\left[\frac{3}{8} + \frac{7}{8}(r^*)^2 - \frac{B}{2} - \frac{(r^*)^4}{2B} \right]} = Nu_{oi}^{(4)} \big|_{fd} \quad (II.D.44)$$

The large \bar{x} values of the various non-dimensional quantities are given, as functions of r^* , in tables II.D.1 to II.D.3 and in Figs. II.D.1 to II.D.10.

The nature of many of the algebraic expressions is such that when $r^* \rightarrow 1$, they present an indeterminate form. At $r^* = 1$, this can be avoided either by using L'Hospital's rule or by transforming Eq.(I.B.1) to rectangular coordinates and generating the solutions to the transformed equation. For r^* near unity, however, the evaluation of many of the preceding forms involves the differences of nearly equal quantities with a resulting loss of accuracy. This is reflected in the tables by the presentation of only three significant figures for $r^* = 0.9$ ($r^* = 0.8$ and 0.9 for the second kind).

Examples of the fully-developed temperature profiles are given in Figs. II.D.11 to II.D.14.

TABLE II.D.1						
ASYMPTOTIC (LARGE \bar{X}) VALUES OF THE FUNDAMENTAL SOLUTIONS OF THE FIRST KIND						
r^*	$\phi_{11}^{(1)} = -\phi_{10}^{(1)}$	$\phi_{00}^{(1)} = -\phi_{01}^{(1)}$	$\theta_{m1}^{(1)}$	$\theta_{m0}^{(1)}$	$Nu_{11}^{(1)} = Nu_{10}^{(1)}$	$Nu_{00}^{(1)} = Nu_{01}^{(1)}$
0	∞	0	0	1	∞	2.66667
0.02	25.0510	0.501020	0.169969	0.830031	30.1808	2.94772
0.04	14.9120	0.596482	0.198875	0.801125	18.6139	2.99928
0.05	12.6847	0.634236	0.210090	0.789910	16.0584	3.01887
0.06	11.1371	0.668228	0.220072	0.779928	14.3042	3.03640
0.08	9.10607	0.728486	0.237760	0.762240	11.9465	3.06395
0.10	7.81730	0.781730	0.252556	0.747444	10.4587	3.09528
0.20	4.97068	0.994136	0.309374	0.690626	7.19736	3.21338
0.25	3.32809	1.08202	0.331197	0.668803	6.47139	3.26700
0.30	3.87606	1.16282	0.350455	0.649545	5.96629	3.31803
0.40	3.27407	1.30963	0.382846	0.617155	5.30510	3.42077
0.50	2.88539	1.44270	0.409987	0.590013	4.89038	3.51888
0.60	2.61015	1.56609	0.432800	0.567200	4.60183	3.61851
0.70	2.40315	1.68220	0.452770	0.547230	4.38978	3.71536
0.80	2.24071	1.79257	0.470300	0.529700	4.23014	3.81154
0.90	2.11	1.90	0.486	0.514	4.11	3.91
1.0	2.00000	2.00000	0.500000	0.500000	4.00000	4.00000

TABLE II.D.2						
ASYMPTOTIC (LARGE \bar{X}) VALUES OF THE FUNDAMENTAL SOLUTIONS OF THE SECOND KIND						
r^*	$(\theta_{11}^{(2)} - \theta_{m1}^{(2)})$	$(\theta_{01}^{(2)} - \theta_{m1}^{(2)})$	$(\theta_{00}^{(2)} - \theta_{m0}^{(2)})$	$(\theta_{10}^{(2)} - \theta_{m0}^{(2)})$	$Nu_{11}^{(2)}$	$Nu_{00}^{(2)}$
0	0	0	0.229167	-0.145833	∞	4.36364
0.2	0.0305763	-0.00255890	0.211227	-0.127945	32.7051	4.73424
0.04	0.0487585	-0.00496488	0.209292	-0.124122	20.5092	4.77802
0.05	0.0561442	-0.00612838	0.208582	-0.122567	17.8113	4.79198
0.06	0.0627609	-0.00726861	0.208193	-0.121143	15.9335	4.80322
0.08	0.0742498	-0.00948471	0.207439	-0.118559	13.4681	4.82070
0.10	0.0839928	-0.0116214	0.206859	-0.116214	11.9058	4.83421
0.20	0.117662	-0.0212779	0.204809	-0.106390	8.49892	4.88259
0.25	0.128974	-0.0255187	0.203884	-0.102207	7.75348	4.90475
0.30	0.138099	-0.0295091	0.203222	-0.0983635	7.24116	4.92801
0.40	0.151899	-0.0365981	0.200836	-0.0914955	6.58331	4.97918
0.50	0.161785	-0.0427568	0.198549	-0.0855135	6.18102	5.03655
0.60	0.169154	-0.0481504	0.196108	-0.0802490	5.91176	5.09922
0.70	0.174759	-0.0529590	0.193554	-0.0755920	5.72215	5.16653
0.80	0.179	-0.0570	0.191	-0.0717	5.58	5.24
0.90	0.183	-0.0609	0.188	-0.0677	5.47	5.31
1.0	0.185714	-0.0642857	0.185714	-0.0642857	5.38461	5.38461

TABLE II.D.3								
ASYMPTOTIC (LARGE \bar{X}) VALUES OF THE FUNDAMENTAL SOLUTIONS OF THE FOURTH KIND								
r^*	$\theta_{11}^{(4)}$	$\phi_{01}^{(4)}$	$\theta_{00}^{(4)}$	$\phi_{10}^{(4)}$	$\theta_{m1}^{(4)}$	$\theta_{m0}^{(4)}$	$Nu_{11}^{(4)} = Nu_{10}^{(4)}$	$Nu_{00}^{(4)} = Nu_{01}^{(4)}$
0	0	0	∞	∞	0	∞	∞	2.66667
0.02	0.039919	-0.02	1.99593	-50.0000	0.006785	1.65669	30.1808	2.94772
0.04	0.067060	-0.04	1.67650	-25.00000	0.013337	1.34309	18.6139	2.99928
0.05	0.078835	-0.05	1.57670	-20.00000	0.016563	1.24545	16.0584	3.01887
0.06	0.089670	-0.06	1.49650	-16.66667	0.019760	1.16716	14.3042	3.03640
0.08	0.109817	-0.08	1.37271	-12.50000	0.026110	1.04663	11.9465	3.06395
0.10	0.127921	-0.10	1.27921	-10.00000	0.032307	0.956141	10.4587	3.09528
0.20	0.201180	-0.20	1.00590	-5.00000	0.062240	0.694700	7.19736	3.21338
0.25	0.231049	-0.25	0.924196	-4.00000	0.076523	0.618104	6.47139	3.26700
0.30	0.257994	-0.30	0.859979	-3.33333	0.090385	0.558695	5.96629	3.31803
0.40	0.305430	-0.40	0.763576	-2.50000	0.116933	0.471244	5.30510	3.42077
0.50	0.346574	-0.50	0.693147	-2.00000	0.142091	0.408966	4.89038	3.51888
0.60	0.383119	-0.60	0.638532	-1.66667	0.165814	0.362175	4.60183	3.61851
0.70	0.416209	-0.70	0.594584	-1.42857	0.188407	0.325431	4.38978	3.71536
0.80	0.446287	-0.80	0.557859	-1.25000	0.209889	0.295499	4.23014	3.81154
0.90	0.474	-0.90	0.527	-1.11	0.230	0.272	4.11	3.91
1.0	0.500000	-1.00	0.500000	-1.00000	0.250000	0.250000	4.00000	4.00000

ASYMPTOTIC (LARGE \bar{x}) VALUES OF THE
FUNDAMENTAL SOLUTIONS OF THE FIRST KIND

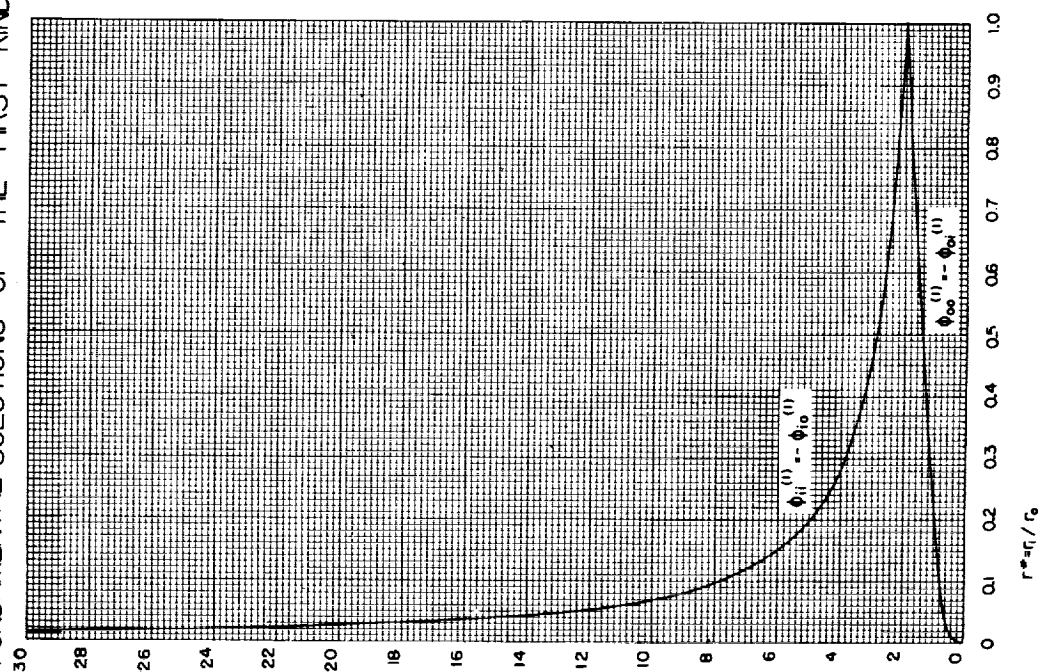


FIGURE II.D. 1

ASYMPTOTIC (LARGE \bar{x}) VALUES OF THE
FUNDAMENTAL SOLUTIONS OF THE FIRST KIND

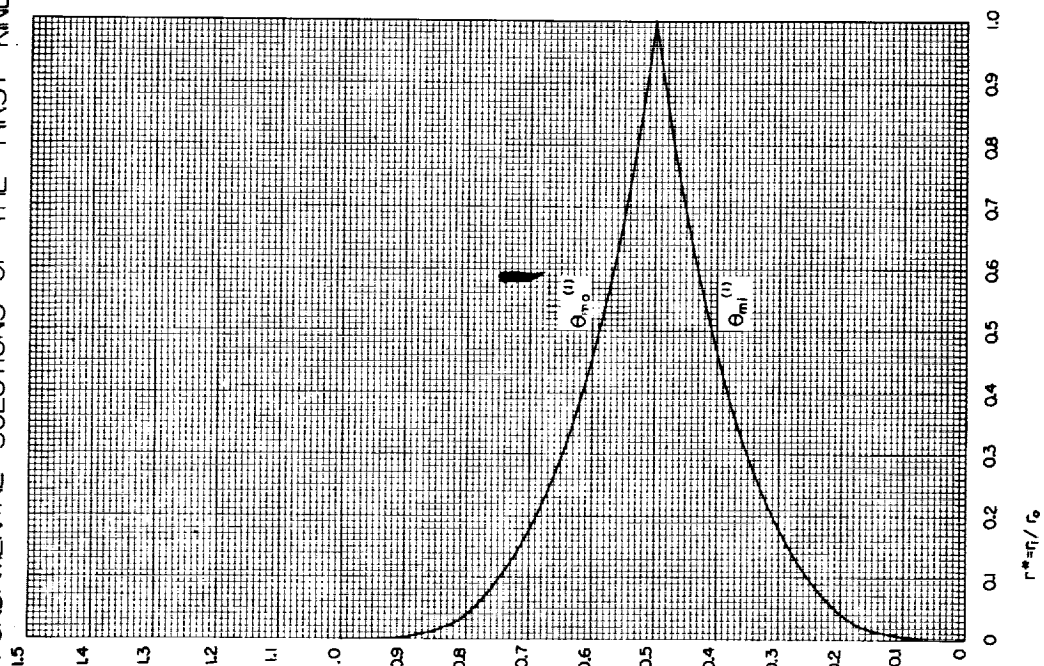


FIGURE II.D. 2

ASYMPTOTIC (LARGE \bar{x}) VALUES OF THE
FUNDAMENTAL SOLUTIONS OF THE FIRST KIND

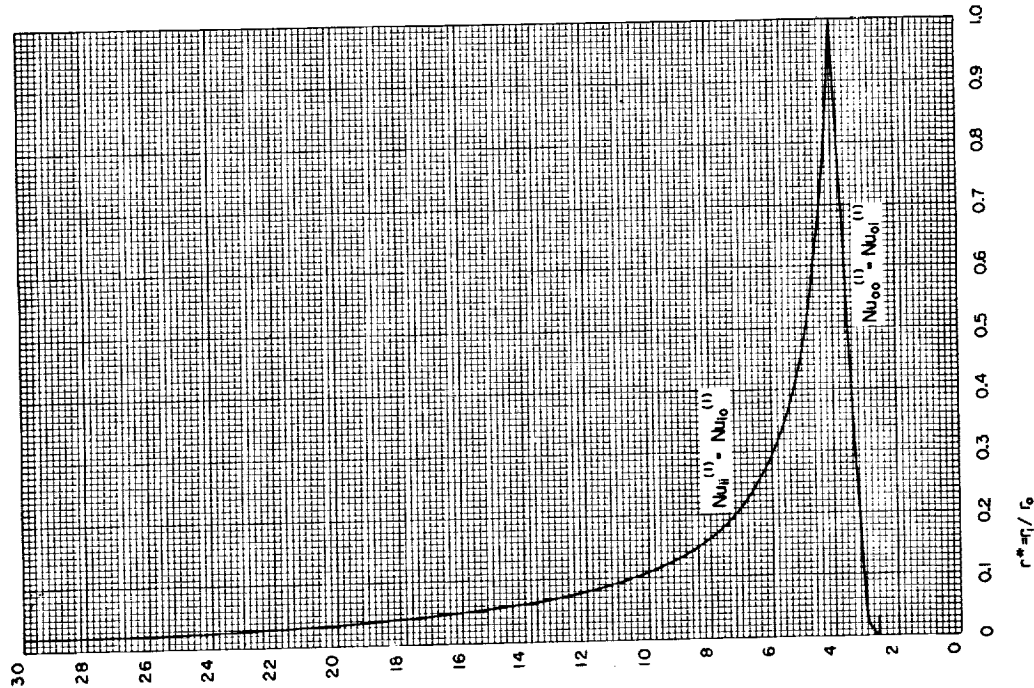


FIGURE II. D. 3

ASYMPTOTIC (LARGE \bar{x}) VALUES OF THE
FUNDAMENTAL SOLUTIONS OF THE SECOND KIND

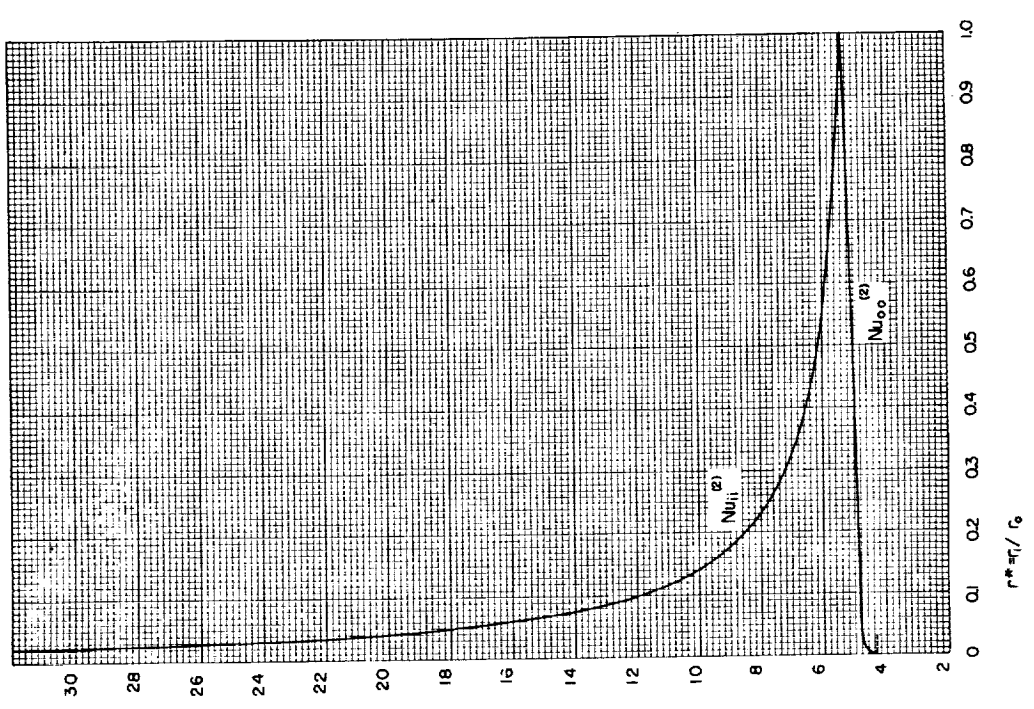


FIGURE II. D. 4

ASYMPTOTIC (LARGE \bar{x}) VALUES OF THE
FUNDAMENTAL SOLUTIONS OF THE SECOND KIND

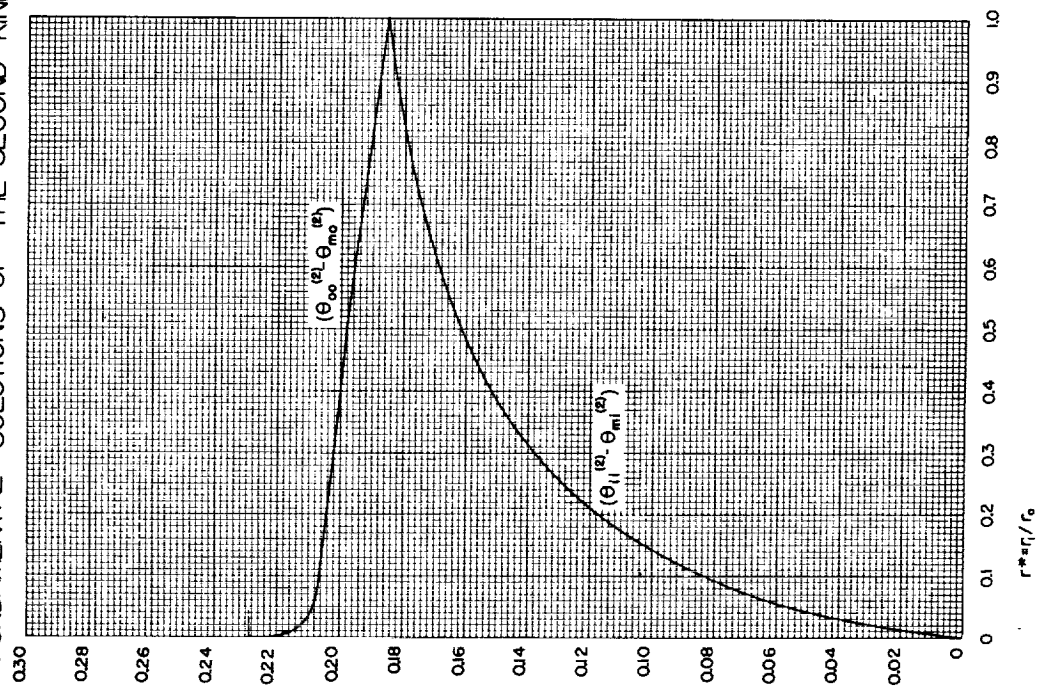


FIGURE II. D. 5

ASYMPTOTIC (LARGE \bar{x}) VALUES OF THE
FUNDAMENTAL SOLUTIONS OF THE SECOND KIND

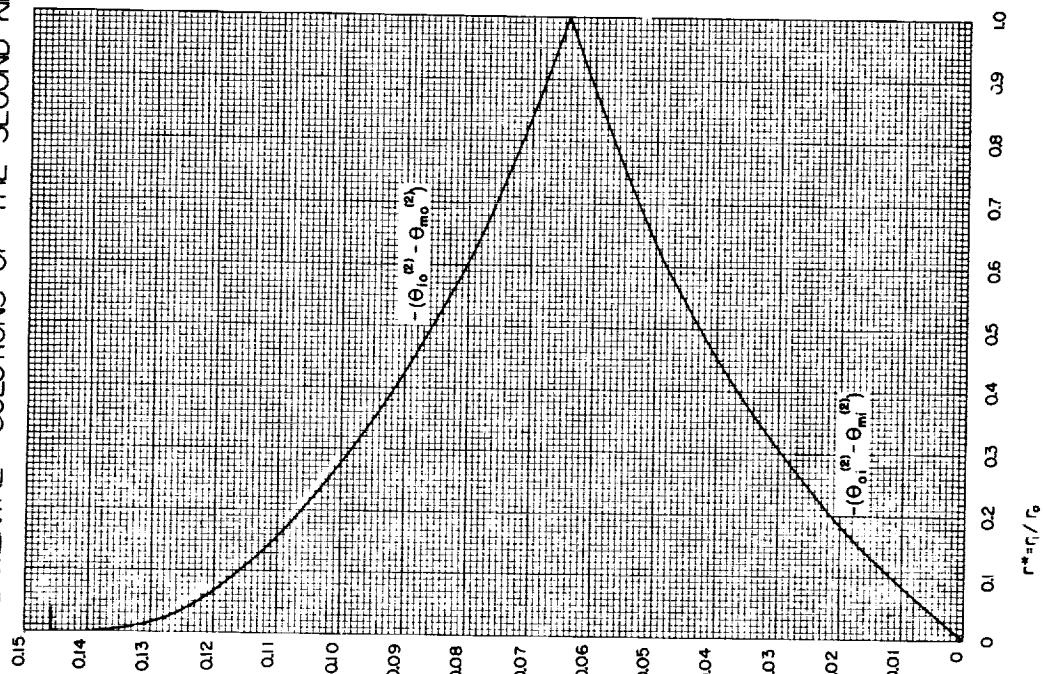


FIGURE II. D. 6

ASYMPTOTIC (LARGE \bar{x}) VALUES OF THE
FUNDAMENTAL SOLUTIONS OF THE FOURTH KIND

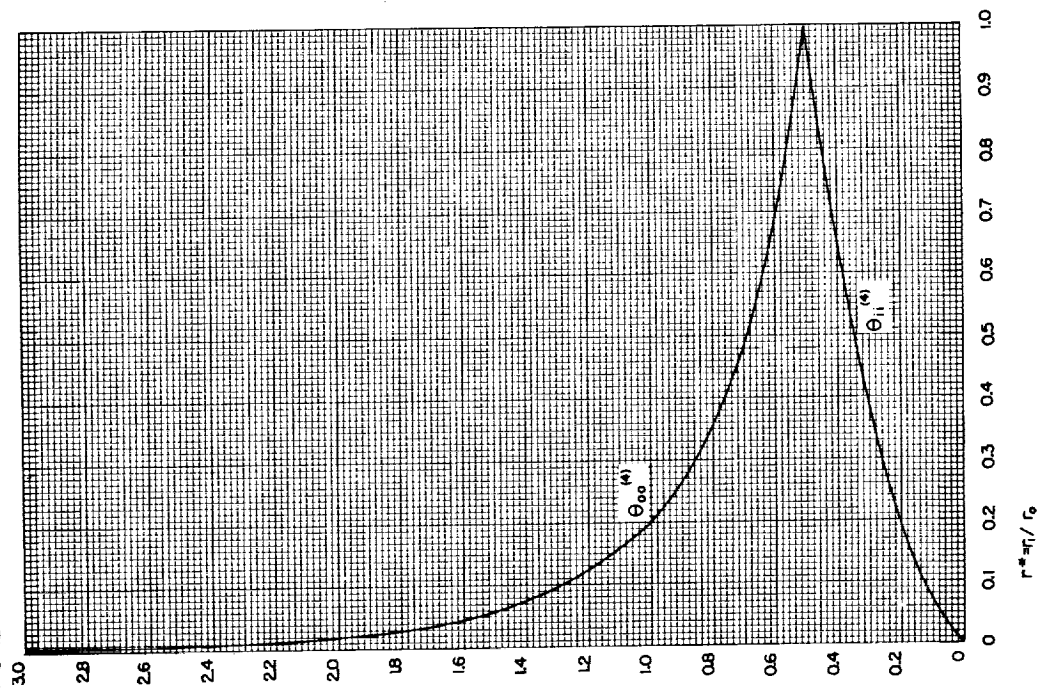


FIGURE II. D. 7

ASYMPTOTIC (LARGE \bar{x}) VALUES OF THE
FUNDAMENTAL SOLUTIONS OF THE FOURTH KIND

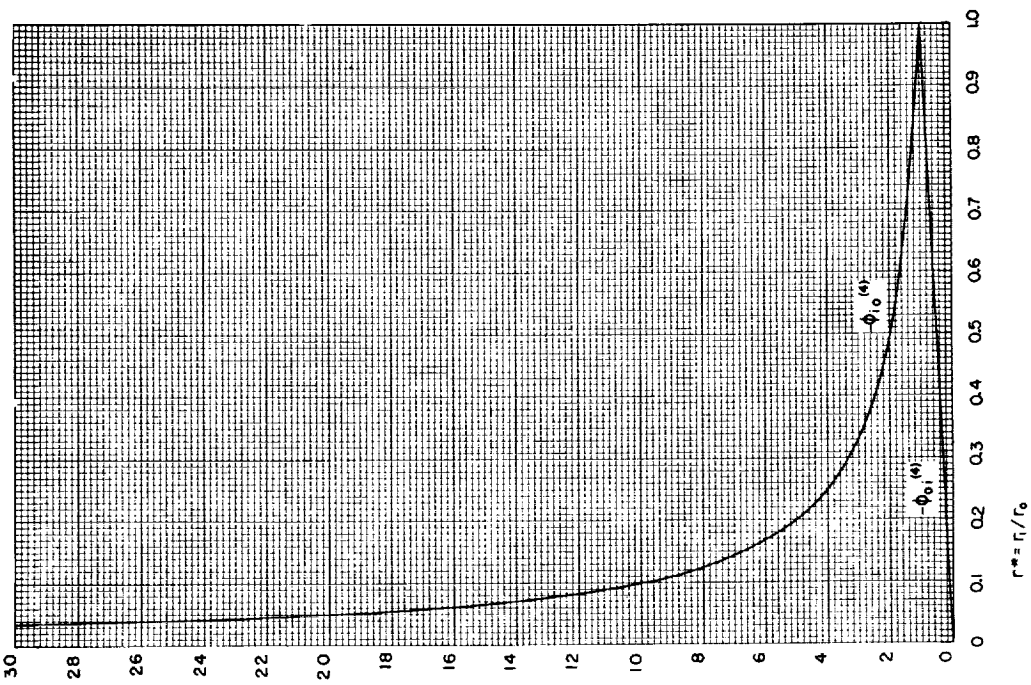


FIGURE II. D. 8

ASYMPTOTIC (LARGE \bar{x}) VALUES OF THE
FUNDAMENTAL SOLUTIONS OF THE FOURTH KIND

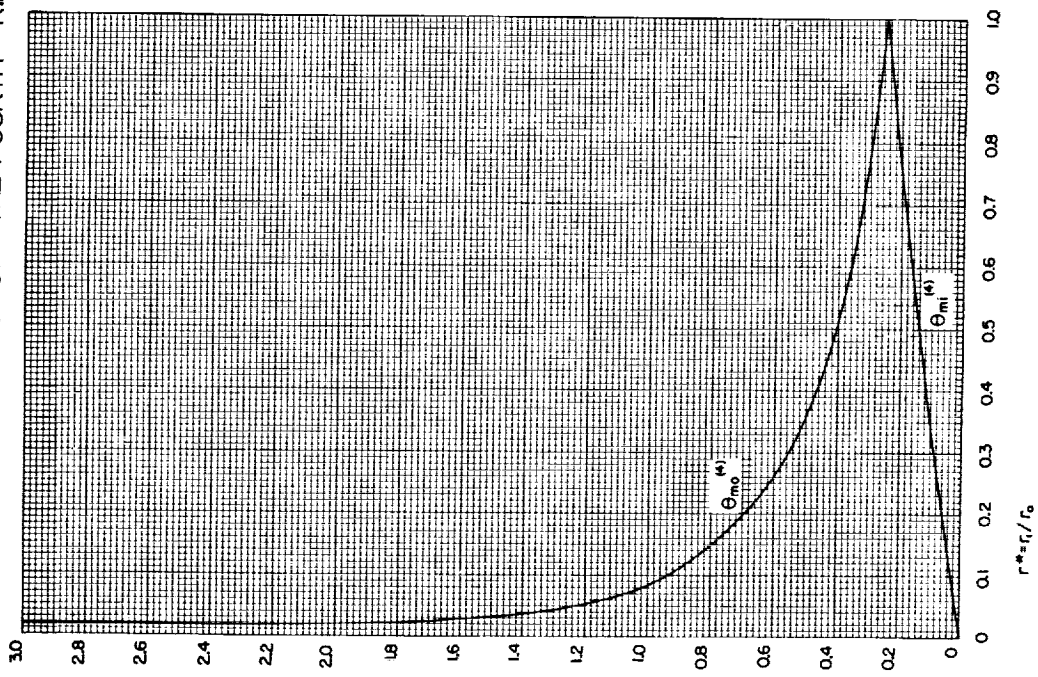


FIGURE II. D. 9

ASYMPTOTIC (LARGE \bar{x}) VALUES OF THE
FUNDAMENTAL SOLUTIONS OF THE FOURTH KIND

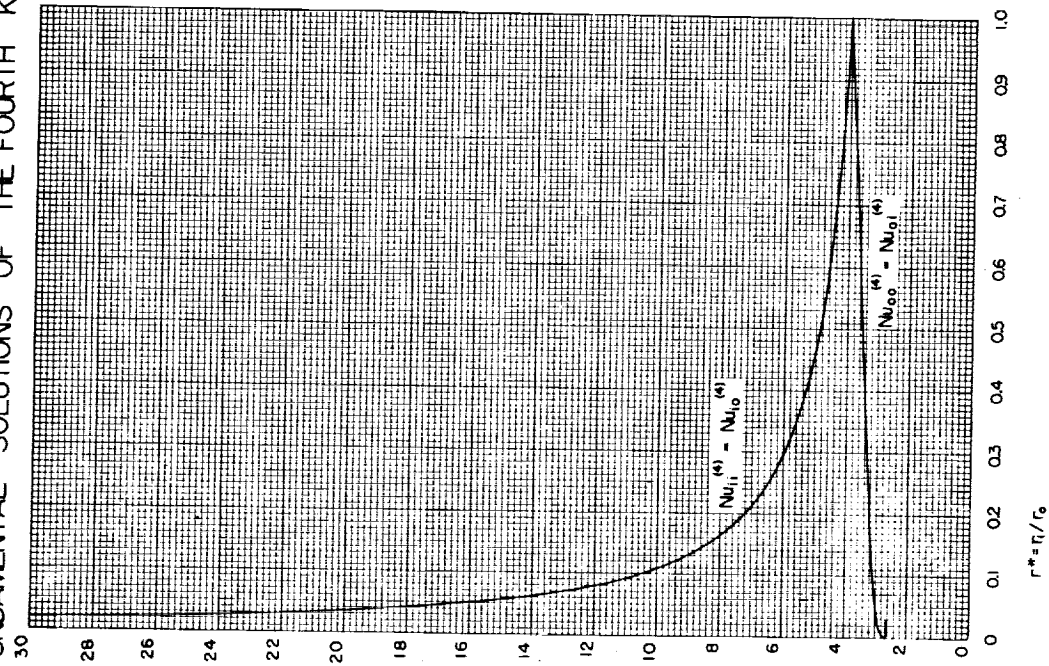
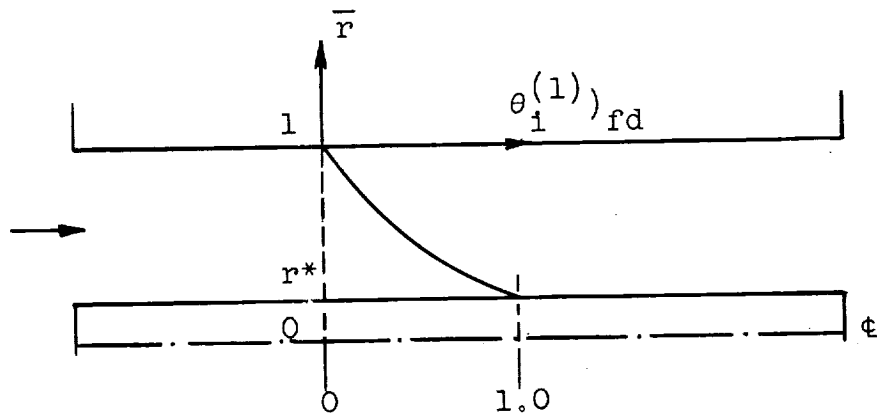
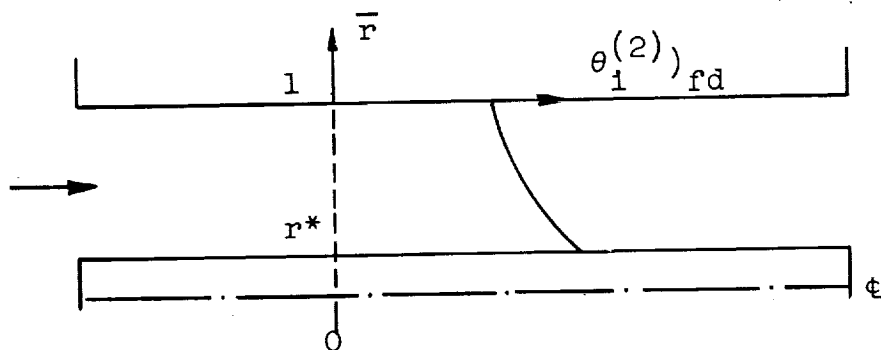


FIGURE II. D. 10



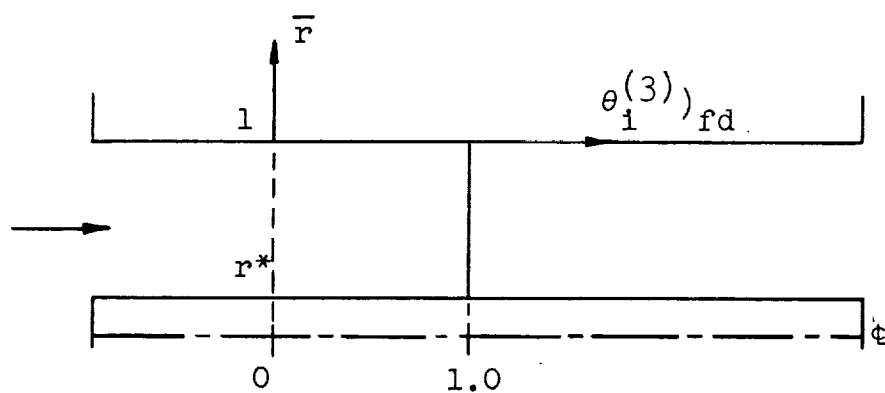
Fully developed temperature profile for a
fundamental solution of the first kind

FIG. II. D. 11



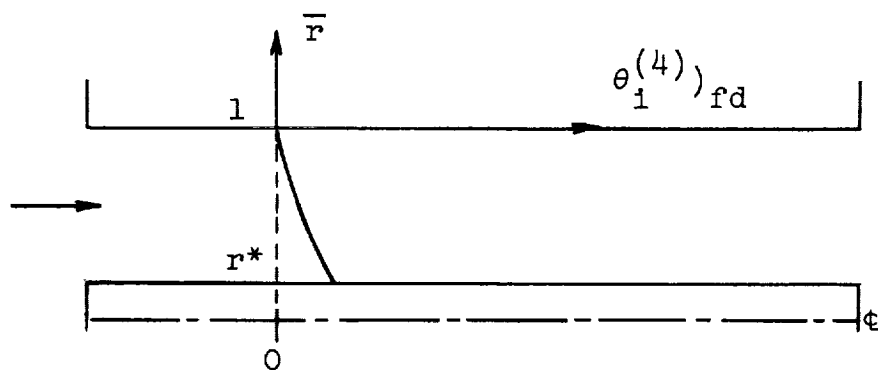
Fully developed temperature profile for a
fundamental solution of the second kind

FIG. II.D.12



Fully developed temperature profile for a
fundamental solution of the third kind

FIG. II.D.13



Fully developed temperature profile for a
fundamental solution of the fourth kind

FIG. II.D.14

II. E. Limiting (small \bar{x}) Leveque Approximations to the Fundamental Solutions

We seek a solution of (I.B.1) valid near the step change in boundary conditions which accompanies the fundamental solutions. Following the scheme of Leveque⁹ we will replace the expression for the velocity by a linear profile having the same slope at the wall. Differentiating (II.B.2) we have

$$\left. \frac{\partial U}{\partial r} \right|_{r=r_1} = \frac{2U_m}{r_o M} \left(\frac{B}{r^*} - 2r^* \right) \quad (\text{II.E.1})$$

and

$$\left. \frac{\partial U}{\partial r} \right|_{r=r_o} = \frac{2U_m}{r_o M} (B - 2) \quad (\text{II.E.2})$$

Accordingly let us use as the velocity near the inner wall

$$U_1 = \frac{2U_m}{M} \left(\frac{B}{r^*} - 2r^* \right) (\bar{r} - r^*) \quad (\text{II.E.3})$$

and near the outer wall

$$U_o = \frac{2U_m}{M} (B - 2) (\bar{r} - 1) \quad (\text{II.E.4})$$

Consider first the solutions where the step change in boundary conditions occurs at the inner wall. Substituting (II.E.3) into (I.B.1) and transforming to the non-dimensional variables, \bar{r} and \bar{x} we have

$$\frac{\partial^2 \theta}{\partial \bar{r}^2} + \frac{1}{\bar{r}} \frac{\partial \theta}{\partial \bar{r}} = E_1 (\bar{r} - r^*) \frac{\partial \theta}{\partial \bar{x}} \quad (\text{II.E.5})$$

where $E_1 = N(B/r^* - 2r^*)$

and $N = 1/2 M(1 - r^*)^2$

as the equation which the fundamental solutions must satisfy near the step change in boundary conditions.

This equation, and the analagous one obtained by using (II.E.4) in (I.B.1) near the outer wall, will be valid only for \bar{x} sufficiently close to the step change in boundary conditions ($\bar{x} = 0$) so that in the radial distance for which the temperature deviates from the initial condition, $\theta = 0$, the velocity profile is closely approximated by (II.E.3) or (II.E.4).

1. The fundamental solutions of the first and third kind

Since the temperature signal only affects the fluid in the immediate vicinity of the inner wall, the boundary condition on the outer wall is immaterial and a step change in wall temperature provides the small \bar{x} approximations to the solutions of the first and third kinds. Further for the region close to the wall the effect of curvature is slight and the term $\frac{1}{\bar{r}} \frac{\partial \theta}{\partial \bar{r}}$ can be neglected and Eq. (II.E.5) becomes

$$\frac{\partial^2 \theta}{\partial \bar{r}^2} = E_1 (\bar{r} - r^*) \frac{\partial \theta}{\partial \bar{x}} \quad (\text{II.E.6})$$

We now seek a similarity solution of the form

$$\theta = f(p) \quad \text{where} \quad p = \frac{(\bar{r} - r^*)}{\bar{x}^{\frac{1}{3}}}$$

Substitution into (II.E.6) yields the ordinary differential equation

$$f'' + a p^2 f' = 0 \quad (\text{II.E.7})$$

where $a = E_1/3$

The boundary conditions in terms of $f(p)$ become

$$f = 1 \quad \text{at } p = 0$$

$$f = 0 \quad \text{as } p \rightarrow \infty$$

The solution to (II.E.7) is

$$f = G_1 \int e^{-\frac{ap^3}{3}} dp + H_1 \quad (\text{II.E.8})$$

Applying the boundary conditions we obtain

$$G_1 = \frac{-1}{\int_0^\infty e^{-\frac{ap^3}{3}} dp} \quad (\text{II.E.9})$$

and

$$H_1 = 1 - [G_1 \int e^{-\frac{ap^3}{3}} dp]_{p=0} \quad (\text{II.E.10})$$

We need to evaluate

$$\int_0^\infty e^{-\frac{ap^3}{3}} dp = \frac{1}{\sqrt[3]{a/3}} \int_0^\infty e^{-\sigma^3} d\sigma$$

but

$$\int_0^\infty e^{-\sigma^3} d\sigma = \left(\frac{1}{3}\right)! = 0.89298$$

Then

$$G_1 = -1.1198 \sqrt[3]{a/3} \quad (\text{II.E.11})$$

Now we can write

$$\theta_1^{(k)}(\bar{r}, \bar{x}) = 1 - 1.1198 \int_0^{\left[\frac{(\bar{r} - r^*)}{\sqrt[3]{3\bar{x}/a}} \right]} e^{-\sigma^3} d\sigma \quad (\text{II.E.12})$$

for $k = 1$ or 3 .

We are interested in the value of $\Phi_{11}^{(k)}$. From the definition of Φ we get

$$\Phi_{11}^{(k)} = -2(1 - r^*) \frac{\partial \theta}{\partial \sigma} \Big|_{\sigma=0} \frac{\partial \sigma}{\partial \bar{r}} \quad (\text{II.E.13})$$

Then from (II.E.12)

$$\Phi_{11}^{(k)} = 2.2396(1 - r^*) \left[\frac{\frac{B}{r^*} - 2r^*}{18(1 - r^*)^2 M} \right]^{1/3} (\bar{x})^{-1/3} \dots \quad (\text{II.E.14})$$

for $k = 1$ or 3 .

The variation of mean temperature can be deduced from energy considerations. We have

$$\frac{\partial \theta_{m1}^{(k)}}{\partial \bar{x}} = \frac{4r^*}{1 + r^*} \Phi_{11}^{(k)} \quad (\text{II.E.15})$$

from which

$$\theta_{m1}^{(k)} = \left(\frac{6r^*}{1+r^*} \right) 2.2396(1 - r^*) \left[\frac{\frac{B}{r^*} - 2r^*}{18(1 - r^*)^2 M} \right]^{1/3} \bar{x}^{2/3} \dots (II.E.16)$$

for $k = 1$ or 3 .

2. The fundamental solutions of the second and fourth kinds

Again since the temperature change is not felt at the outer wall, a step change in Φ provides the approximation to the solutions of the second and fourth kinds.

Because the derivative at the wall must be independent of \bar{x} , let us seek a similarity solution of the form $\theta = \xi^n f(p)$, where $p = (\bar{r} - r^*)/\bar{x}^n$, and $\xi = \bar{x}$. Equation (II.E.5) becomes

$$f''(p) + n E_1 \bar{x}^{(3n-1)} p^2 f'(p) - n E_1 \bar{x}^{(3n-1)} p f(p) = 0$$

If n is chosen as $1/3$, \bar{x} vanishes and we have

$$f''(p) + a p^2 f'(p) - a p f(p) = 0 \quad (II.E.17)$$

where $a = E_1/3$.

The solution to Eq. (II.E.17) is

$$f(p) = G_2 p \int \frac{e^{-\frac{ap^3}{3}}}{p^2} dp + H_2 p \quad (II.E.18)$$

Then

$$\theta = \bar{x}^{\frac{1}{3}} \left[G_2 p \int \frac{e^{-\frac{ap^3}{3}}}{p^2} dp + H_2 p \right]$$

or, integrating by parts

$$\theta = \bar{x}^{\frac{1}{3}} \left[H_2 p - G_2 e^{-\frac{ap^3}{3}} - G_2 p \int a p e^{-\frac{ap^3}{3}} dp \right] \dots (II.E.19)$$

The boundary conditions to be applied are

$$\theta = 0 \text{ when } \bar{x} \rightarrow 0 \text{ (} p \rightarrow \infty \text{),}$$

and

$$\left. \frac{\partial \theta}{\partial \bar{r}} \right)_{\bar{r}=r^*} = - \frac{1}{2(1 - r^*)}$$

We see that

$$\left. \frac{\partial \theta}{\partial \bar{r}} \right)_{\bar{r}=r^*} = \bar{x}^{\frac{1}{3}} f'(p) \Big|_{p=0} \left(\frac{\partial p}{\partial \bar{r}} = f'(p) \right)_{p=0} \quad (II.E.20)$$

From (II.E.19) we obtain

$$f'(p) \Big|_{p=0} = \left[H_2 - G_2 \int a p e^{-\frac{ap^3}{3}} dp \right]_{p=0}$$

The integral on the right vanishes which can be seen by

expanding the exponential in a series and integrating term by term. Then

$$H_2 = - \frac{1}{2(1 - r^*)} \quad (\text{II.E.21})$$

The remaining boundary condition demands that

$$0 = (\bar{r} - r^*) \left[- \frac{1}{2(1 - r^*)} - G_2 \left(\int_0^\infty a p e^{-\frac{ap^3}{3}} dp \right)_{p=0} \right] \quad \dots \quad (\text{II.E.22})$$

Since $(\bar{r} - r^*) \neq 0$, the bracketed term must vanish. We have already seen that the integral in (II.E.22) vanishes at $p = 0$, so we may write

$$\left(a \int_0^\infty p e^{-\frac{ap^3}{3}} dp \right)_{p=0} = a \int_0^\infty p e^{-\frac{ap^3}{3}} dp = \frac{a^{\frac{1}{3}} 3^{\frac{2}{3}}}{2} \left(\frac{2}{3} \right) !$$

From this

$$G_2 = \frac{-0.36925}{(1 - r^*) \sqrt[3]{a/3}} \quad (\text{II.E.23})$$

and

$$\theta_1^{(k)}(\bar{r}, \bar{x}) = (\bar{x})^{\frac{1}{3}} \left[\frac{0.36925}{(1 - r^*) \sqrt[3]{a/3}} \left(e^{-\frac{ap^3}{3}} + p \int_0^\infty a p e^{-\frac{ap^3}{3}} dp \right) - \frac{p}{2(1 - r^*)} \right] \quad (\text{II.E.24})$$

for $k = 2$ or 4 .

We are interested in the value at the heated wall.

$$\theta_{ii}^{(k)} = \frac{0.36925}{(1 - r^*)} \left[\frac{\frac{B}{r^*} - 2r^*}{18(1 - r^*)^2 M} \right]^{-\frac{1}{3}} \bar{x}^{\frac{1}{3}} \quad (\text{II.E.25})$$

for $k = 2$ or 4 .

If the step change in boundary conditions occurs at the outer wall, U is given by Eq. (II.E.4) and Eq. (II.E.6) becomes

$$\frac{\partial^2 \theta}{\partial \bar{r}^2} = E_o (\bar{r} - 1) \frac{\partial \theta}{\partial \bar{x}}$$

where $E_o = N(B - 2)$.

If we now define $p = (\bar{r} - 1)/\bar{x}^{\frac{1}{3}}$, Eqs. (II.E.7) and (II.E.17) result where $a = E_o/3$. Then, with the exception of the expression for the mean temperature in cases 1 and 3, the only difference is in the factor a , and we have

$$\Phi_{oo}^{(k)} = - 2.2396(1 - r^*) \left[\frac{B - 2}{18(1 - r^*)^2 M} \right]^{\frac{1}{3}} \bar{x}^{-\frac{1}{3}} \quad (\text{II.E.26})$$

and

$$\theta_{mo}^{(k)} = - \left(\frac{6}{1 + r^*} \right) 2.2396(1 - r^*) \left[\frac{B - 2}{18(1 - r^*)^2 M} \right]^{\frac{1}{3}} \bar{x}^{\frac{2}{3}} \quad \dots \quad (\text{II.E.27})$$

for $k = 1$ or 3 .

Further

$$\theta_{oo}^{(k)} = - \frac{0.36925}{(1 - r^*)} \left[\frac{B - 2}{18(1 - r^*)^2 M} \right]^{-\frac{1}{3}} \bar{x}^{\frac{1}{3}} \quad (\text{II.E.28})$$

for $k = 2$ or 4 .

All of these equations have the form of a constant multiplied by a power of \bar{x} . Table II.E.1 presents these constants for various values of r^* . They are given graphically in Figs. II.E.1 and II.E.2. The symbols used are as follows.

$$\phi_{jj}^{(k)} = c_{jj}^{(k)} \bar{x}^{-\frac{1}{3}}$$

$$\theta_{mj}^{(k)} = c_{mj}^{(k)} \bar{x}^{\frac{2}{3}} \quad \text{for } j = 1 \text{ or } 0, \quad k = 1 \text{ and } 3$$

and

$$\theta_{jj}^{(k)} = c_{jj}^{(k)} \bar{x}^{\frac{1}{3}} \quad \text{for } j = 1 \text{ or } 0, \quad k = 2 \text{ and } 4.$$

CONSTANTS IN THE LIMITING (SMALL \bar{x}) APPROXIMATIONS
TO THE FUNDAMENTAL SOLUTIONS

$r^* \quad c_{ii}^{(1)} = c_{ii}^{(3)}$	$c_{oo}^{(1)} = c_{oo}^{(3)}$	$c_{mi}^{(1)} = c_{mi}^{(3)}$	$c_{mo}^{(1)} = c_{mo}^{(3)}$	$c_{ii}^{(2)} = c_{ii}^{(4)}$	$c_{oo}^{(2)} = c_{oo}^{(4)}$
0	∞	0	6.4602	0	0.76808
0.02	2.1862	0.25720	6.6301	0.37826	0.73371
0.04	1.8804	0.43394	6.5475	0.43978	0.72868
0.05	1.7954	0.51296	6.5065	0.46059	0.72627
0.06	1.7351	0.58964	6.4602	0.47661	0.72457
0.08	1.6455	0.73133	6.3663	0.50255	0.72166
0.10	1.5833	0.86362	6.2708	0.52230	0.71934
0.20	1.42718	1.4272	5.8227	0.57944	0.71013
0.30	1.3589	1.8816	5.4236	0.60857	0.70374
0.40	1.3194	2.2618	5.0822	0.62679	0.69738
0.50	1.29314	2.5863	4.7775	0.63950	0.69239
0.60	1.2743	2.8672	4.5113	0.64895	0.68741
0.70	1.2602	3.1134	4.2741	0.65620	0.68284
0.80	1.2492	3.3312	4.0617	0.66202	0.67869
0.90	1.24	3.41	3.88	0.667	0.675
1.0	1.2334	3.7003	3.7003	0.67097	0.67097

TABLE II.E.1

CONSTANTS IN THE LIMITING (SMALL \bar{x})
APPROXIMATIONS TO THE FUNDAMENTAL SOLUTIONS

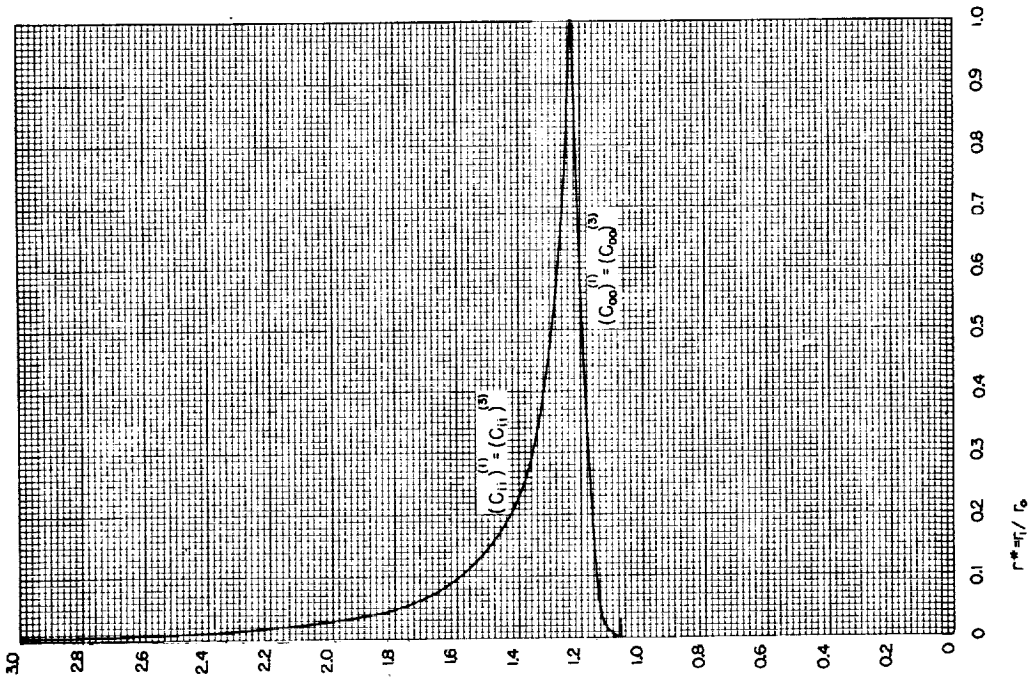


FIGURE II.E.1

CONSTANTS IN THE LIMITING (SMALL \bar{x})
APPROXIMATIONS TO THE FUNDAMENTAL SOLUTIONS

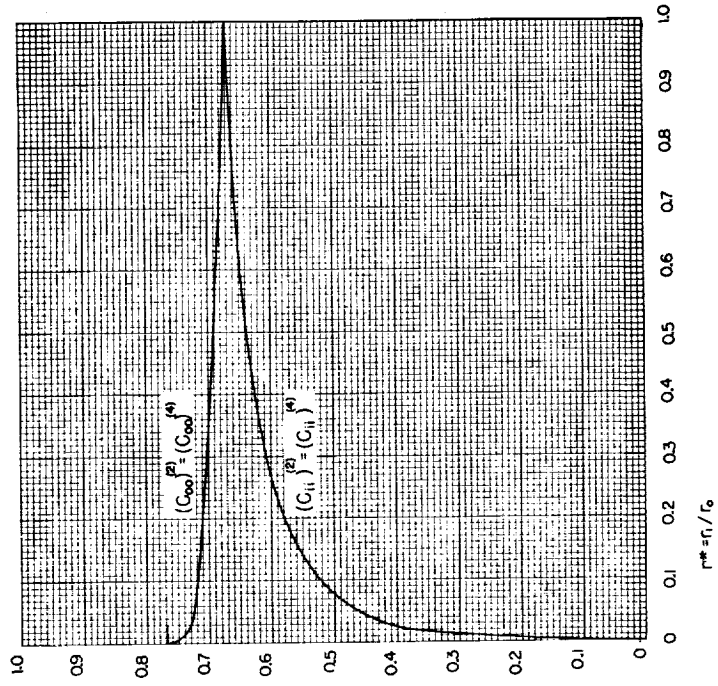


FIGURE II.E.2

II. F. Solution of the Energy Equation

The $\bar{\theta}_j^{(k)}$ will be solutions to Eq. (II.C.1) satisfying the homogeneous boundary conditions as outlined in section II.D. Omitting the sub- and super-scripts for brevity, let us assume that $\bar{\theta} = R(\bar{r})X(\bar{x})$, where $R(\bar{r})$ and $X(\bar{x})$ are functions only of \bar{r} and \bar{x} respectively. Then by the method of separation of variables we obtain the two ordinary differential equations

$$X' + \lambda^2 X = 0 \quad (\text{II.F.1})$$

and

$$R'' + \frac{1}{\bar{r}} R' + \lambda^2 N(1 - \bar{r}^2 + B \ln \bar{r})R = 0 \quad (\text{II.F.2})$$

where

$$N = 1/2 M(1 - r^*)^2$$

Equation (II.F.1) yields

$$X(\bar{x}) = C e^{-\lambda^2 \bar{x}} \quad (\text{II.F.3})$$

where C is an arbitrary constant. Equation (II.F.2) is of the Sturm-Liouville type* and will, in general, give rise to an infinite set of eigenvalues λ_n , $n = 0, 1, 2, \dots$, and corresponding eigenfunctions R_n , $n = 0, 1, 2, \dots$. It can be shown that these functions $R_n(\bar{r})$ form an orthogonal set with respect to the weight function

$$w(\bar{r}) = N(\bar{r} - \bar{r}^3 + B\bar{r} \ln \bar{r}) \quad (\text{II.F.4})$$

that is
$$\int_{r^*}^1 w(\bar{r}) R_n(\bar{r}) R_m(\bar{r}) d\bar{r} = 0 \text{ if } n \neq m \quad (\text{II.F.5})$$

* A comprehensive discussion of Sturm-Liouville theory may be found in Ref.(4).

Further, this orthogonal set is complete so that we may express an arbitrary function (having proper smoothness conditions) as an infinite series of the eigenfunctions as follows:

$$F(\bar{r}) = \sum_{n=0}^{\infty} C_n R_n(\bar{r}) \quad (\text{II.F.6})$$

where

$$C_n = \frac{\int_{r^*}^1 w(\bar{r}) F(\bar{r}) R_n(\bar{r}) d\bar{r}}{\int_{r^*}^1 w(\bar{r}) R_n^2(\bar{r}) d\bar{r}} \quad (\text{II.F.7})$$

In view of this we can write the desired solution as

$$\bar{\theta}(\bar{r}, \bar{x}) = \sum_{n=0}^{\infty} C_n R_n(\bar{r}) e^{-\lambda_n^2 \bar{x}} \quad (\text{II.F.8})$$

with the λ_n and the C_n so chosen as to satisfy the appropriate boundary and initial conditions. We are now able to determine the boundary conditions in terms of Eq.(II.F.2) and to write an explicit expression for (II.F.7) for the various fundamental cases.

1. The first kind

The boundary conditions for this case require that for both $\bar{\theta}_1^{(1)}$ and $\bar{\theta}_0^{(1)}$,

$$R_n^{(1)}(r^*) = R_n^{(1)}(1) = 0 \quad (\text{II.F.9})$$

In essence this is the equation of the eigenvalues. The values of the parameter λ^2 in Eq. (II.F.2) must be chosen such that the solutions generated satisfy the condition

(II.F.9) above. We see then that $(\lambda_n)_1^{(1)} = (\lambda_n)_0^{(1)}$. The coefficients, C_n , in Eq. (II.F.8) can be obtained from (II.F.7) with $F(r) = \bar{\theta}_j^{(1)}(\bar{r}, 0)$. With some manipulation of the differential equation (II.F.2) we can obtain*

$$(C_n)_1^{(1)} = \frac{-2r^* \left(\frac{\partial R_n}{\partial \bar{r}} \right)_{\bar{r}=r^*}}{\lambda_n \left[\left(\frac{\partial R_n}{\partial \bar{r}} \right) \left(\frac{\partial R_n}{\partial \lambda_n} \right)_{\bar{r}=1} - r^* \left(\frac{\partial R_n}{\partial \bar{r}} \right) \left(\frac{\partial R_n}{\partial \lambda_n} \right)_{\bar{r}=r^*} \right]} \quad (\text{II.F.10})$$

and

$$(C_n)_0^{(1)} = \frac{2 \left(\frac{\partial R_n}{\partial \bar{r}} \right)_{\bar{r}=1}}{\lambda_n \left[\left(\frac{\partial R_n}{\partial \bar{r}} \right) \left(\frac{\partial R_n}{\partial \lambda_n} \right)_{\bar{r}=1} - r^* \left(\frac{\partial R_n}{\partial \bar{r}} \right) \left(\frac{\partial R_n}{\partial \lambda_n} \right)_{\bar{r}=r^*} \right]} \quad \dots \quad (\text{II.F.11})$$

2. The second kind

The boundary conditions require that for both $\bar{\theta}_1^{(2)}$ and $\bar{\theta}_0^{(2)}$

$$\left(\frac{\partial R_n}{\partial \bar{r}} \right)_{\bar{r}=r^*} = \left(\frac{\partial R_n}{\partial \bar{r}} \right)_{\bar{r}=1} = 0 \quad (\text{II.F.12})$$

Note that $(\lambda_n)_1^{(2)} = (\lambda_n)_0^{(2)}$. Again the coefficients are evaluated from (II.F.7) and may be written as

* See appendix F. Note that $\left(\frac{\partial R_n}{\partial \lambda_n} \right)$ is used to indicate $\left(\frac{\partial R_n}{\partial \lambda} \right)_{\lambda=\lambda_n}$

$$(C_n)_i^{(2)} = \frac{-\frac{r^*}{(1-r^*)} R_n(r^*)}{\lambda_n \left[R_n(r^*) r^* \frac{\partial}{\partial \bar{r}} \left(\frac{\partial R_n}{\partial \lambda_n} \right)_{\bar{r}=r^*} - R_n(1) \frac{\partial}{\partial \bar{r}} \left(\frac{\partial R_n}{\partial \lambda_n} \right)_{\bar{r}=1} \right]}$$

.... (II.F.13)

and

$$(C_n)_o^{(2)} = \frac{-\frac{1}{(1-r^*)} R_n(r^*)}{\lambda_n \left[R_n(r^*) r^* \frac{\partial}{\partial \bar{r}} \left(\frac{\partial R_n}{\partial \lambda_n} \right)_{\bar{r}=r^*} - R_n(1) \frac{\partial}{\partial \bar{r}} \left(\frac{\partial R_n}{\partial \lambda_n} \right)_{\bar{r}=1} \right]}$$

.... (II.F.14)

3. The third kind

Here the boundary conditions on the eigenfunctions are not symmetric so we must consider separately the cases where the temperature step is applied at the inner or the outer walls.

For $\bar{\theta}_i^{(3)}$ we have

$$R_n(r^*) = \frac{\partial R_n}{\partial \bar{r}} \Big|_{\bar{r}=1} = 0 \quad (\text{II.F.15})$$

and

$$(C_n)_i^{(3)} = \frac{2r^* \left(\frac{\partial R_n}{\partial \bar{r}} \right)_{\bar{r}=r^*}}{\lambda_n \left[R_n(1) \frac{\partial}{\partial \bar{r}} \left(\frac{\partial R_n}{\partial \lambda_n} \right)_{\bar{r}=1} + r^* \left(\frac{\partial R_n}{\partial \lambda_n} \right) \left(\frac{\partial R_n}{\partial \bar{r}} \right)_{\bar{r}=r^*} \right]}$$

.... (II.F.16)

For $\bar{\theta}_0^{(3)}$ we have

$$\left(\frac{\partial R_n}{\partial \bar{r}} \right)_{\bar{r}=r^*} = R_n(1) = 0 \quad (\text{II.F.17})$$

and

$$(c_n)_0^{(3)} = \frac{2 \left(\frac{\partial R_n}{\partial \bar{r}} \right)_{\bar{r}=1}}{\lambda_n \left[R_n(r^*) r^* \frac{\partial}{\partial \bar{r}} \left(\frac{\partial R_n}{\partial \lambda_n} \right)_{\bar{r}=r^*} + \left(\frac{\partial R_n}{\partial \lambda_n} \right) \left(\frac{\partial R_n}{\partial \bar{r}} \right)_{\bar{r}=1} \right]} \quad \dots \quad (\text{II.F.18})$$

Note that here $(\lambda_n)_1^{(3)} \neq (\lambda_n)_0^{(3)}$.

4. The fourth kind

For $\bar{\theta}_1^{(4)}$ we have

$$\left(\frac{\partial R_n}{\partial \bar{r}} \right)_{\bar{r}=r^*} = R_n(1) = 0 \quad (\text{II.F.19})$$

and

$$(c_n)_1^{(4)} = \frac{- \frac{r^*}{(1-r^*)} R_n(r^*)}{\lambda_n \left[R_n(r^*) r^* \frac{\partial}{\partial \bar{r}} \left(\frac{\partial R_n}{\partial \lambda_n} \right)_{\bar{r}=r^*} + \left(\frac{\partial R_n}{\partial \lambda_n} \right) \left(\frac{\partial R_n}{\partial \bar{r}} \right)_{\bar{r}=1} \right]} \quad \dots \quad (\text{II.F.20})$$

since (II.F.19) is identical with (II.F.17) we will have

$$(\lambda_n)_1^{(4)} = (\lambda_n)_0^{(3)}$$

For $\bar{\theta}_o^{(4)}$ we have

$$R_n(r^*) = \frac{\partial R_n}{\partial \bar{r}} \Big|_{\bar{r}=1} = 0 \quad (\text{II.F.21})$$

and

$$(c_n)_o^{(4)} = \frac{R_n(1)}{(1-r^*)} \lambda_n \left[R_n(1) \frac{\partial}{\partial \bar{r}} \left(\frac{\partial R_n}{\partial \lambda_n} \right) \Big|_{\bar{r}=1} + r^* \left(\frac{\partial R_n}{\partial \lambda_n} \right) \left(\frac{\partial R_n}{\partial \bar{r}} \right) \Big|_{\bar{r}=r^*} \right] \dots \quad (\text{II.F.22})$$

Note that

$$(\lambda_n)_o^{(4)} = (\lambda_n)_1^{(3)}$$

II. G. Behavior of the Solutions as Lambda Becomes Large.

We would like to examine the behavior of the solutions to (II.F.2) as λ_n becomes large. Following the method of Sellars, Tribus and Klein¹⁹, let us develop the so-called WKBJ*approximation to the solution of (II.F.2). If we let

$$R_n = e^{g(\bar{r})}$$

we find that $g(\bar{r})$ must be a solution to

$$g''(\bar{r}) + (g'(\bar{r}))^2 + \frac{g'(\bar{r})}{\bar{r}} + \lambda_n^2 N(1 - \bar{r}^2 + B \ln \bar{r}) = 0 \quad \dots(\text{II.G.1})$$

An asymptotic solution is sought in the form

$$g = \lambda g_0 + g_1 + \lambda^{-1} g_2 + \dots \quad (\text{II.G.2})$$

Substituting (II.G.2) into (II.G.1) and observing that to satisfy the equation for all values of λ_n , the coefficient of each power of λ_n must vanish, we can obtain

$$g'_0 = \pm 1 \sqrt{N(1 - \bar{r}^2 + B \ln \bar{r})} \quad (\text{II.G.3})$$

and

$$g_1 = - \ln \sqrt{g'_0 \bar{r}} \quad (\text{II.G.4})$$

Since λ_n is large, the remaining terms in (II.G.2) are neglected. From (II.G.3) and (II.G.4) we may write

* After Wentzel, Kramers, Brillouin, and Jefferies.

$$R_n(\bar{r}) = \left[G e^{+i\lambda \int_{\bar{r}}^{\bar{r}} \sqrt{N(1-\bar{r}^2 + B \ln \bar{r})} d\bar{r}} + H e^{-i\lambda \int_{\bar{r}}^{\bar{r}} \sqrt{N(1-\bar{r}^2 + B \ln \bar{r})} d\bar{r}} \right] / \sqrt{\bar{r}} [N(1-\bar{r}^2 + B \ln \bar{r})]^{1/4} \quad (\text{II.G.5})$$

This is the WKBJ approximation. Equation (II.G.5) must be patched unto the regular solution of (II.F.2) near the boundary walls. Equation (II.G.5) can be put into a somewhat more useful form for our purposes which is

$$R_n(\bar{r}) = \frac{G_o \cos \left[\lambda \int_{r^*}^{\bar{r}} \sqrt{N(1-\bar{r}^2 + B \ln \bar{r})} d\bar{r} - \phi \right]}{\sqrt{\bar{r}} [N(1-\bar{r}^2 + B \ln \bar{r})]^{1/4}} \quad (\text{II.G.6})$$

Near the inner wall, $\bar{r} \rightarrow r^*$. Let $\bar{r} = r^* + z$ and $(1 - \bar{r}^2 + B \ln \bar{r}) = 1 - r^{*2} - 2r^*z - z^2 + r^* - 1 + \frac{Bz}{r^*}$

Since z is small we neglect terms of higher than first order and

$$(1 - \bar{r}^2 + B \ln \bar{r}) \rightarrow -z \left(\frac{B}{r^*} - 2r^* \right) \text{ as } z \rightarrow 0$$

Equation (II.F.2) becomes

$$R_n'' + \frac{1}{\bar{r}} R_n' + \lambda_n^2 E_1 z R_n = 0$$

where

$$E_1 = N(B/r^* - 2r^*)$$

Let $\eta = \lambda_n^{2/3} z$, then we have

$$\frac{d^2 R_n}{d\eta^2} + \frac{1}{\lambda_n^{2/3}(r^* + \eta/\lambda_n^{2/3})} \frac{dR_n}{d\eta} + E_1 \eta R_n = 0 \quad (\text{II.G.7a})$$

which, if λ_n is large, becomes

$$\frac{d^2 R_n}{d\eta^2} + E_1 \eta R_n = 0 \quad (\text{II.G.7b})$$

Equation (II.G.7b) is a form of Bessel's equation and has the solution

$$R_n = G_1 \eta^{1/2} J_{1/3}\left(\frac{2\sqrt{E_1}}{3} \eta^{3/2}\right) + H_1 \eta^{1/2} J_{-1/3}\left(\frac{2\sqrt{E_1}}{3} \eta^{3/2}\right) \dots \quad (\text{II.G.8})$$

We desire Eq.(II.G.6) to correspond to Eq.(II.G.8) as $r \rightarrow r^*$. Observe that for this condition the integral appearing in (II.G.6) becomes

$$\int_0^z \sqrt{E_1} \sigma^{1/2} d\sigma = \frac{2}{3} \sqrt{E_1} z^{3/2}, \text{ and } \sqrt{r} \rightarrow \sqrt{r^*}$$

Using this we have

$$R_n \xrightarrow{r \rightarrow r^*} = \frac{G_0 \cos[2/3 \sqrt{E_1} \lambda_n z^{3/2} - \phi]}{\sqrt{r^*} E_1^{1/4} z^{1/4}} \quad (\text{II.G.9})$$

For large η , Eq. (II.G.8) can be written

$$R_n = \left[\frac{1}{\frac{\pi}{3} \lambda_n^{1/6}} \right] \left\{ G_1 \cos \left[\frac{2\sqrt{E_1}}{3} \lambda_n z^{3/2} - \frac{5\pi}{12} \right] + H_1 \cos \left[\frac{2\sqrt{E_1}}{3} \lambda_n z^{3/2} - \frac{\pi}{12} \right] \right\} / E_1^{1/4} z^{1/4} \quad (\text{II.G.10})$$

If G_0 is taken as

$$G_0 = \sqrt{r^*} / \sqrt{\frac{\pi}{3}} \lambda_n^{1/6} \quad (\text{II.G.11})$$

then Eqs. (II.G.9) and (II.G.10) are identical in form. Expanding the cosine of the difference of angles occurring in (II.G.9) and (II.G.10) one obtains as the equations for the coefficients

$$G_1 \cos(5\pi/12) + H_1 \cos(\pi/12) = \cos\phi \quad (\text{II.G.12})$$

$$G_1 \sin(5\pi/12) + H_1 \sin(\pi/12) = \sin\phi \quad (\text{II.G.13})$$

Since ϕ is, as yet, an unknown quantity, (II.G.12) and (II.G.13) are insufficient to define completely G_1 and H_1 , and we need to apply the appropriate boundary conditions. Let us reserve this to a later time and continue the general development.

Near the outer wall, $\bar{r} \rightarrow 1$. Let $\bar{r} = 1 - \xi$ and

$$(1 - \bar{r}^2 + \beta \ln \bar{r}) \rightarrow \xi(2 - \beta)$$

Let $\xi = \lambda_n^{2/3} \xi$, then for large λ Eq.(II.F.2) can be

reduced to

$$\frac{d^2 R_n}{d \zeta^2} + E_0 \zeta R_n = 0 \quad (\text{II.G.14})$$

where

$$E_0 = N(2 - B)$$

Equation (II.G.14) has the solution

$$R_n = G_2 \zeta^{1/2} J_{1/3} \left(\frac{2\sqrt{E_0}}{3} \zeta^{3/2} \right) + H_2 \zeta^{1/2} J_{-1/3} \left(\frac{2\sqrt{E_0}}{3} \zeta^{3/2} \right) \dots \quad (\text{II.G.15})$$

Here we desire (II.G.15) to correspond to (II.G.6) as $\bar{r} \rightarrow 1$. For this condition the integral appearing in (II.G.6) becomes

$$\int_{r^*}^1 \sqrt{N(1 - \bar{r}^2 + B \ln \bar{r})} d\bar{r} - \int_0^{\xi} \sqrt{E_0} \sigma^{1/2} d\sigma = \gamma - \frac{2}{3} \sqrt{E_0} \xi^{3/2}$$

where

$$\gamma = \int_{r^*}^1 \sqrt{N(1 - \bar{r}^2 + B \ln \bar{r})} d\bar{r} \quad (\text{II.G.16})$$

Using this we have

$$R_n = \frac{\sqrt{r^*} \cos \left[\frac{2}{3} \sqrt{E_0} \lambda_n \xi^{3/2} - \gamma \lambda_n + \phi \right]}{\sqrt{\frac{\pi}{3}} \lambda_n^{1/6} E_0^{1/4} \xi^{1/4}} \quad (\text{II.G.17})$$

For large ξ Eq.(II.G.15) may be written

$$R_n = \left[\frac{1}{\frac{\pi}{3} \lambda_n^{1/6}} \right] \left\{ G_2 \cos \left[\frac{2\sqrt{E_0}}{3} \lambda_n \xi^{3/2} - \frac{5\pi}{12} \right] + H_2 \cos \left[\frac{2\sqrt{E_0}}{3} \lambda_n \xi^{3/2} - \frac{\pi}{12} \right] \right\} / E_0^{1/4} \xi^{1/4} \quad (\text{II.G.18})$$

An appropriate choice of G_2 and H_2 would make (II.G.17) and (II.G.18) identical. As before, we obtain as the equations of the coefficients

$$G_2 \cos(5\pi/12) + H_2 \cos(\pi/12) = r^* \cos(\gamma \lambda_n - \phi) \quad (\text{II.G.19})$$

$$G_2 \sin(5\pi/12) + H_2 \sin(\pi/12) = r^* \sin(\gamma \lambda_n - \phi) \quad (\text{II.G.20})$$

To complete this analysis we must apply the specific boundary conditions for the various fundamental cases.

1. The fundamental solutions of the first kind

For this case the boundary conditions are given by (II.F.9). In Eq. (II.G.8), as $\eta \rightarrow 0$, the term $\eta^{1/2} J_{-1/3}(\frac{2\sqrt{E_1}}{3} \eta^{3/2})$ does not vanish but approaches a constant. Then in order to satisfy the inner wall boundary condition H_1 must equal zero. From (II.G.12) and (II.G.13) we see that this demands that

$$\sin\phi \cos(5\pi/12) - \cos\phi \sin(5\pi/12) = 0$$

or

$$\sin(\phi - 5\pi/12) = 0 \quad (\text{II.G.21})$$

(II.G.21) will be satisfied if

$$\phi = \frac{5\pi}{12} \pm n\pi, \quad n = 0, 1, 2, \dots \quad (\text{II.G.22})$$

There is no loss of generality if n is taken to be zero.
Further

$$G_1 = 1 \quad (\text{II.G.23})$$

Then, near the inner wall, we have

$$R_n = \lambda_n^{1/3} z^{1/2} J_{1/3}\left(\frac{2\sqrt{E_1}}{3} \lambda_n z^{3/2}\right) \quad (\text{II.G.24})$$

At the outer wall we must insist that H_2 vanish,
hence

$$\sin(\gamma \lambda_n - \phi - 5\pi/12) = 0 \quad (\text{II.G.25})$$

(II.G.25) will be satisfied if

$$\lambda_n = \left(n + \frac{5}{6}\right) \frac{\pi}{\gamma}, \quad n = 0, 1, 2, \dots \quad (\text{II.G.26})$$

where

$$\gamma = \int_{r^*}^1 \sqrt{N(1 - \bar{r}^2 + B \ln \bar{r})} d\bar{r}$$

This is the equation for the eigenvalues as n becomes large. Further

$$G_2 = (-1)^n \sqrt{r^*} \quad (\text{II.G.27})$$

Then for \bar{r} close to unity we have

$$R_n = (-1)^n \sqrt{r^*} \lambda_n^{1/3} \xi^{1/2} J_{1/3} \left(\frac{2\sqrt{E_0}}{3} \lambda_n \xi^{3/2} \right) \quad (\text{II.G.28})$$

We still need the expansion coefficients given by (II.F.10) and (II.F.11). Differentiating (II.G.24) we have

$$\begin{aligned} \frac{\partial R_n}{\partial \bar{r}} \Big|_{\bar{r}=r^*} &= \lambda_n^{1/3} \frac{J_{1/3} \left(\frac{2\sqrt{E_1}}{3} \lambda_n z^{3/2} \right)}{z^{1/2}} - \sqrt{E_1} \lambda_n z J_{4/3} \left(\frac{2\sqrt{E_1}}{3} \lambda_n z^{3/2} \right) \\ &\dots \quad (\text{II.G.29}) \end{aligned}$$

When $z \rightarrow 0$, $z J_{4/3} \rightarrow 0$, then

$$\frac{\partial R_n}{\partial \bar{r}} \Big|_{\bar{r}=r^*} = \frac{\lambda_n^{2/3} (E_1)^{1/6}}{3^{1/3} \Gamma(4/3)} \quad (\text{II.G.30})$$

From (II.G.24) we see that at $\bar{r} = r^*$, R_n vanishes for any value of λ , therefore

$$\left(\frac{\partial R_n}{\partial \lambda_n} \right)_{\bar{r}=r^*} = 0 \quad (\text{II.G.31})$$

Differentiating (II.G.28) we have (since $\frac{\partial}{\partial \bar{r}} = - \frac{\partial}{\partial \xi}$)

$$\left. \frac{\partial R_n}{\partial r} \right|_{r=1} = (-1)^{n+1} \sqrt{r^*} \lambda_n^{1/3} \left[\frac{J_{1/3} \left(\frac{2\sqrt{E_0}}{3} \lambda_n \xi^{3/2} \right)}{\xi^{1/2}} - \sqrt{E_0} \lambda_n \xi J_{4/3} \left(\frac{2\sqrt{E_0}}{3} \lambda_n \xi^{3/2} \right) \right] \quad (\text{II.G.32})$$

As ξ approaches zero this becomes

$$\left. \frac{\partial R_n}{\partial r} \right|_{r=1} = \frac{(-1)^{n+1} \sqrt{r^*} \lambda_n^{2/3} (E_0)^{1/6}}{3^{1/3} \Gamma(4/3)} \quad (\text{II.G.33})$$

At the outer wall R_n vanishes but only at $\lambda = \lambda_n$, therefore we must retain both terms of (II.G.15) in computing $(\partial R_n / \partial \lambda_n)$

$$\begin{aligned} \frac{\partial R_n}{\partial \lambda_n} &= G_2 \frac{\partial}{\partial \lambda_n} [\xi^{1/2} J_{1/3}] + H_2 \frac{\partial}{\partial \lambda_n} [\xi^{1/2} J_{-1/3}] \\ &+ \frac{\partial G_2}{\partial \lambda_n} [\xi^{1/2} J_{1/3}] + \frac{\partial H_2}{\partial \lambda_n} [\xi^{1/2} J_{-1/3}] \end{aligned}$$

As $\xi \rightarrow 0$ the first three terms above vanish but since

$$H_2 = \frac{\sqrt{r^*} \sin(\gamma \lambda_n - \phi - 5\pi/12)}{\sin(-\pi/3)}$$

then

$$\frac{\partial H_2}{\partial \lambda_n} = \frac{\sqrt{r^*} \gamma (-1)^{n+1}}{\sqrt{3/2}} \quad (\text{II.G.34})$$

and

$$\frac{\partial R_n}{\partial \lambda_n} \bigg|_{\bar{r}=1} = \frac{(-1)^{n+1} 2\sqrt{r^*} \gamma}{3^{1/6} (E_0)^{1/6} \Gamma(2/3)} \quad (\text{II.G.35})$$

Now we have

$$(c_n)_1^{(1)} = - \frac{(E_1)^{1/6} 3^{1/6} \Gamma(2/3)}{\gamma \lambda_n} \quad (\text{II.G.36})$$

Similarly

$$(c_n)_0^{(1)} = - \frac{(-1)^n 3^{1/6} (E_0)^{1/6} \Gamma(2/3)}{\sqrt{r^*} \gamma \lambda_n} \quad (\text{II.G.37})$$

2. The fundamental solutions of the second kind

We must apply the boundary conditions given by (II.F.12) Differentiating (II.G.8) we have

$$\frac{\partial R_n}{\partial \bar{r}} = \frac{\lambda^{2/3} G_1}{2 \eta^{1/2}} J_{1/3} \left(\frac{2\sqrt{E_1}}{3} \eta^{3/2} \right) - \lambda^{2/3} H_1 J_{2/3} \left(\frac{2\sqrt{E_1}}{3} \eta^{3/2} \right) \dots (\text{II.G.38})$$

In order for this to vanish as $\eta \rightarrow 0$ ($\bar{r} \rightarrow r^*$), G_1 must be zero, then from (II.G.12) and (II.G.13) we have

$$\sin (\pi/12 - \phi) = 0$$

$$\phi = \frac{\pi}{12} \pm n\pi, \quad n = 0, 1, 2 \dots \quad (\text{II.G.39})$$

Again n may be taken as zero. We find that

$$H_1 = 1 \quad (\text{II.G.40})$$

We have a similar condition at the outer wall resulting in

$$\sin(\pi/12 - \gamma \lambda_n + \phi) = 0$$

$$\lambda_n = (n + \frac{1}{6}) \pi/\gamma, \quad n = 0, 1, 2, \dots \quad (\text{II.G.41})$$

This is the equation for the eigenvalues as n becomes large. Then, as before,

$$H_2 = (-1)^n \sqrt{r^*} \quad (\text{II.G.42})$$

For \bar{r} near r^* the solution becomes

$$R_n = \lambda_n^{1/3} z^{1/2} J_{-1/3} \left(\frac{2\sqrt{E_1}}{3} \lambda_n z^{3/2} \right) \quad (\text{II.G.43})$$

and for \bar{r} near 1 the solution is

$$R_n = (-1)^n \sqrt{r^*} \lambda_n^{1/3} \xi^{1/2} J_{-1/3} \left(\frac{2\sqrt{E_1}}{3} \lambda_n \xi^{3/2} \right) \quad (\text{II.G.44})$$

We will need to get $\partial/\partial\bar{r} (\partial R_n/\partial\lambda_n)$ near both walls. Differentiating (II.G.43) we have

$$\begin{aligned} \frac{\partial}{\partial\bar{r}} \left(\frac{\partial R_n}{\partial\lambda_n} \right)_{\bar{r} \rightarrow r^*} &= - \lambda_n^{1/3} \frac{2}{3} \sqrt{E_1} \left[2z J_{2/3} \left(\frac{2\sqrt{E_1}}{3} \lambda_n z^{3/2} \right) \right. \\ &\quad \left. + z^2 J'_{2/3} \left(\frac{2\sqrt{E_1}}{3} \lambda_n z^{3/2} \right) \right] \quad (\text{II.G.45}) \end{aligned}$$

As $z \rightarrow 0$ ($\bar{r} \rightarrow r^*$), Eq. (II.G.45) vanishes. Near the outer

wall we can see in an analogous manner that there is no contribution from the term involving $J_{-1/3}$, but recall that

$$G_2 = \frac{\sqrt{r^*} \sin(\pi/12 - \gamma \lambda_n + \phi)}{\sin(-\pi/3)} \quad (\text{II.G.46})$$

Then

$$\frac{\partial G_2}{\partial \lambda_n} = (-1)^n \gamma \frac{\sqrt{r^*}}{\sqrt{3}} \quad (\text{II.G.47})$$

Now

$$\frac{\partial}{\partial \bar{r}} \left(\frac{\partial R_n}{\partial \lambda_n} \right) = (-1)^n \gamma \sqrt{r^*} \frac{2}{3} \frac{\partial}{\partial \bar{r}} \left[\xi^{1/2} J_{1/3} \left(\frac{2\sqrt{E_o}}{3} \xi^{3/2} \right) \right]$$

As $\xi \rightarrow 0$ we have

$$\frac{\partial}{\partial \bar{r}} \left(\frac{\partial R_n}{\partial \lambda_n} \right)_{\bar{r}=1} = \frac{(-1)^{n+1} \gamma \sqrt{r^*} E_o^{1/6} \lambda_n^{2/3}}{3^{5/6} \Gamma(4/3)} \quad (\text{II.G.48})$$

We also need the ordinates at the boundary walls.

$$R_n(r^*) = \frac{3^{1/3}}{(E_1)^{1/6} \Gamma(2/3)} \quad (\text{II.G.49})$$

$$R_n(1) = \frac{(-1)^n \sqrt{r^*} 3^{1/3}}{(E_o)^{1/6} \Gamma(2/3)} \quad (\text{II.G.50})$$

Using (II.F.13) and (II.F.14) we may write

$$(c_n)_1^{(2)} = - \frac{3^{5/6} \Gamma(4/3)}{2(1-r^*)(E_1)^{1/6} \gamma \lambda_n^{5/3}} \quad (\text{II.G.51})$$

$$(c_n)_0^{(2)} = - \frac{(-1)^n 3^{5/6} \Gamma(4/3)}{2(1-r^*) \sqrt{r^*}(E_0)^{1/6} \gamma \lambda_n^{5/3}} \quad (\text{II.G.52})$$

3. The fundamental solution of the third kind

For $\bar{\theta}_1^{(3)}$ we have the boundary conditions (II.F.15).
The condition at the inner wall yields

$$\phi = \frac{5\pi}{12} \pm n\pi, \quad n = 0, 1, 2, \dots \quad (\text{II.G.53})$$

If we set n equal to 0, we get

$$R_{n \rightarrow r^*} = \lambda_n^{1/3} z^{1/2} J_{1/3}\left(\frac{2\sqrt{E_1}}{3} \lambda_n z^{3/2}\right) \quad (\text{II.G.54})$$

At the outer wall, by differentiating (II.G.15), we have

$$\sin\left(\frac{\pi}{12} - \gamma \lambda_n + \phi\right) = 0$$

$$\lambda_n = \left(n + \frac{1}{2}\right) \frac{\pi}{\gamma} \quad (\text{II.G.55})$$

This is the equation for the eigenvalues as n becomes

large. For \bar{r} near 1 we have

$$R_n \xrightarrow{\bar{r} \rightarrow 1} = (-1) \sqrt{r^*} \lambda_n^{1/3} \xi^{1/2} J_{-1/3} \left(\frac{2\sqrt{E_0}}{3} \lambda_n \xi^{3/2} \right) \dots \quad (\text{II.G.56})$$

The derivative at the inner wall is given by (II.G.30), the ordinate at the outer wall by (II.G.50). We may use (II.F.16) to write

$$(C_n)_1^{(3)} = - \frac{(E_1)^{1/6} \Gamma(2/3) 3^{1/6}}{\gamma \lambda_n} \quad (\text{II.G.57})$$

For $\bar{\theta}_0^{(3)}$ we use (II.F.17). At the inner wall we obtain

$$\phi = \pi/12 \quad (\text{II.G.58})$$

and

$$R_n \xrightarrow{\bar{r} \rightarrow r^*} = \lambda_n^{1/3} z^{1/2} J_{-1/3} \left(\frac{2\sqrt{E_1}}{3} \lambda_n z^{3/2} \right) \quad (\text{II.G.59})$$

At the outer wall we must have

$$\sin(\gamma \lambda_n - \phi - 5\pi/12) = 0$$

or

$$\lambda_n = (n + \frac{1}{2}) \frac{\pi}{\gamma} \quad (\text{II.G.60})$$

This is the equation of the eigenvalues as n becomes large.
We now have

$$R_n \xrightarrow{r \rightarrow 1} = (-1)^n \sqrt{r^*} \lambda_n^{1/3} \xi^{1/2} J_{1/3} \left(\frac{2\sqrt{E_0}}{3} \lambda_n \xi^{3/2} \right) \quad (\text{II.G.61})$$

The ordinate at the inner wall is given by (II.G.49),
the derivative at the outer wall by (II.G.33). Then

$$(c_n)_o^{(3)} = - \frac{(-1)^n 3^{1/6} (E_0)^{1/6} \Gamma(2/3)}{\sqrt{r^*} \gamma \lambda_n} \quad (\text{II.G.62})$$

4. The fundamental solutions of the fourth kind

For the $\bar{\theta}_1^{(4)}$ we have the boundary conditions (II.F.19).
Since (II.F.19) corresponds to (II.F.17) we will have

$$\lambda_n = (n + \frac{1}{2}) \frac{\pi}{\gamma} \quad (\text{II.G.63})$$

as the equation of the eigenvalues with (II.G.49) and (II.G.33)
giving the inner wall ordinate and the outer wall derivative
respectively. Then

$$(c_n)_1^{(4)} = - \frac{3^{5/6} \Gamma(4/3)}{2(1 - r^*) (E_1)^{1/6} \gamma \lambda_n^{5/3}} \quad (\text{II.G.64})$$

For the $\bar{\theta}_o^{(4)}$, (II.F.21) must be applied, but this
corresponds to (II.F.15). We will therefore have

$$\lambda_n = (n + \frac{1}{2}) \frac{\pi}{\gamma} \quad (\text{II.G.65})$$

as n becomes large. The derivative at the inner wall and the ordinate at the outer wall will be given by (II.G.30) and (II.G.50). Then

$$(C_n)_o^{(4)} = - \frac{(-1)^n 3^{5/6} \Gamma(4/3)}{2(1-r^*) \sqrt{r^*} (E_o)^{1/6} \gamma \lambda_n^{5/3}} \quad (\text{II.G.66})$$

In practice there will be certain combinations of the expansion coefficients and the ordinates or derivatives at the boundary wall which contribute to the wall θ 's and ϕ 's comprising the kernel conditions.

$$2(1-r^*)(C_n)_i^{(1)} \frac{\partial R_n^{(1)}}{\partial r} (r^*) = \frac{2(1-r^*)(E_i)^{1/3} \Gamma(2/3)}{3^{1/6} \Gamma(4/3) \gamma} \lambda_n^{-1/3} \dots (\text{II.G.67})$$

$$2(1-r^*)(C_n)_i^{(1)} \frac{\partial R_n^{(1)}}{\partial r} (1) = \frac{2(1-r^*)(-1)^n (E_i)^{1/6} (E_o)^{1/6} \Gamma(2/3) \sqrt{r^*}}{3^{1/6} \Gamma(4/3) \gamma} \lambda_n^{-1/3} \dots (\text{II.G.68})$$

$$2(1-r^*)(C_n)_o^{(1)} \frac{\partial R_n^{(1)}}{\partial r} (r^*) =$$

$$\frac{2(1-r^*)(-1)^n (E_i)^{1/6} (E_o)^{1/6} \Gamma(2/3)}{3^{1/6} \Gamma(4/3) \gamma \sqrt{r^*}} \lambda_n^{-1/3} \quad (\text{II.G.69})$$

$$2(1 - r^*)(c_n)_o^{(1)} \frac{\partial R_n^{(1)}}{\partial \bar{r}} (1) = \frac{2(1-r^*)(E_o)^{1/3} \Gamma(2/3)}{3^{1/6} \Gamma(4/3) \gamma} \lambda_n^{-1/3}$$

.... (II.G.70)

$$(c_n)_1^{(2)} R_n^{(2)}(r^*) = - \frac{3^{1/6} \Gamma(4/3)}{2(1-r^*)(E_1)^{1/3} \Gamma(2/3) \gamma} \lambda_n^{-5/3}$$

.... (II.G.71)

$$(c_n)_1^{(2)} R_n^{(2)}(1) = - \frac{(-1)^n 3^{7/6} \sqrt{r^*} \Gamma(4/3)}{2(1-r^*)(E_1)^{1/6} (E_o)^{1/6} \Gamma(2/3) \gamma} \lambda_n^{-5/3}$$

.... (II.G.72)

$$(c_n)_o^{(2)} R_n^{(2)}(r^*) = - \frac{(-1)^n 3^{7/6} \Gamma(4/3)}{2(1-r^*) \sqrt{r^*} (E_o)^{1/6} (E_1)^{1/6} \Gamma(2/3) \gamma} \lambda_n^{-5/3}$$

.... (II.G.73)

$$(c_n)_o^{(2)} R_n^{(1)} = - \frac{3^{7/6} \Gamma(4/3)}{2(1-r^*)(E_o)^{1/3} \Gamma(2/3) \gamma} \lambda_n^{-5/3} \quad (\text{II.G.74})$$

$$2(1-r^*)(c_n)_1^{(3)} \frac{\partial R_n^{(3)}}{\partial \bar{r}} (r^*) = - \frac{2(1-r^*)(E_1)^{1/3} \Gamma(2/3)}{3^{1/6} \Gamma(4/3) \gamma} \lambda_n^{-1/3}$$

.... (II.G.75)

$$(c_n)_1^{(3)} R_n^{(3)}(1) = - \frac{(-1)^n \sqrt{r^*} (E_1)^{1/6} \sqrt{3}}{(E_o)^{1/6} \gamma} \lambda_n^{-1} \quad (\text{II.G.76})$$

$$(C_n)_o^{(3)} R_n^{(3)}(r^*) = - \frac{(-1)^n (E_o)^{1/6} \sqrt{3}}{\sqrt{r^*} (E_1)^{1/6} \gamma} \lambda_n^{-1} \quad (\text{II.G.77})$$

$$2(1-r^*)(C_n)_o^{(3)} \frac{\partial R_n}{\partial \bar{r}}(1) = \frac{2(1-r^*)(E_o)^{1/3} \Gamma(2/3)}{3^{1/6} \Gamma(4/3) \gamma} \lambda_n^{-1/3}$$

.... (II.G.78)

$$(C_n)_i^{(4)} R_n^{(4)}(r^*) = - \frac{3^{7/6} \Gamma(4/3)}{2(1-r^*)(E_1)^{1/3} \Gamma(2/3) \gamma} \lambda_n^{-5/3}$$

.... (II.G.79)

$$2(1-r^*)(C_n)_i^{(4)} \frac{\partial R_n}{\partial \bar{r}}(1) = \frac{(-1)^n 3^{1/2} \sqrt{r^*} (E_o)^{1/6}}{(E_1)^{1/6} \gamma} \lambda_n^{-1}$$

.... (II.G.80)

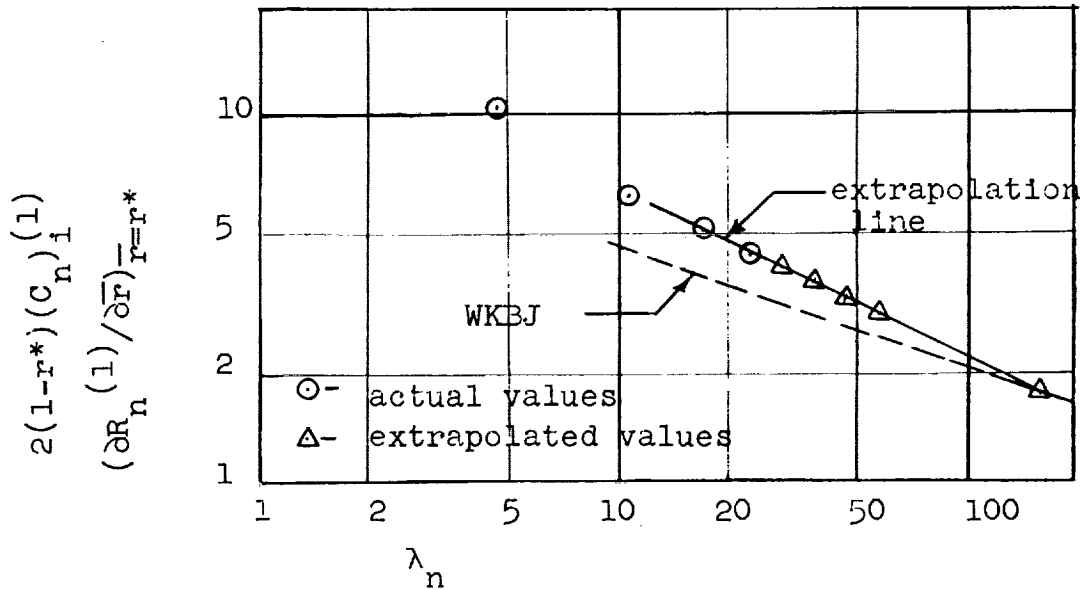
$$2(1-r^*)(C_n)_i^{(4)} \frac{\partial R_n}{\partial \bar{r}}(r^*) = - \frac{(-1)^n 3^{1/2} (E_1)^{1/6}}{\sqrt{r^*} (E_o)^{1/6} \gamma} \lambda_n^{-1}$$

.... (II.G.81)

$$(C_n)_o^{(4)} R_n^{(4)}(1) = - \frac{3^{7/6} \Gamma(4/3)}{2(1-r^*)(E_o)^{1/3} \Gamma(2/3) \gamma} \lambda_n^{-5/3}$$

.... (II.G.82)

Near the inner wall Eq.(II.G.7b) is taken as an approximation to the actual equation as λ_n becomes large. It is apparent from (II.G.7a) that if r^* is small, λ_n must be very large in order to make (II.G.7b) a reasonable approximation to the actual equation. A comparison of the eigenvalues predicted by this method and those obtained from the actual solution (see section II.H) shows very good agreement for all $n \geq 4$, even if r^* is zero. The forms (II.G.67) through (II.G.82), however, provide some difficulty, particularly those evaluated at the inner wall, or where the non-zero boundary condition is applied at the inner wall. For $r^* \leq 0.1$, λ_4 is not sufficiently large to remove the effect of the first derivative term in (II.G.7a). When λ_n becomes very large then (II.G.7a) approaches (II.G.7b) but for small r^* this value may be so large as to lie outside the range of practical interest. What is needed is an approximation for the next succeeding constants. Below is a logarithmic plot of the quantity $2(1-r^*)(C_{n1})^{(1)}(\partial R_n^{(1)}/\partial r)_{r=r^*}$ as a function of λ_n , together with the line representing the approximate expression (II.G.67), for $r^* = 0.02$



Since the constants for $n = 1, 2$, and 3 lie on a nearly straight line an extrapolation line is constructed to pass through the last two. Then the values of the eigenconstants are taken as ordinates on this line at the values of λ_n given by the asymptotic expression. Eventually (i.e. for λ_n large enough) the WKBJ expression should become valid, and it is used for the region beyond the intersection of the extrapolation line and the line corresponding to (II.G.67). Both the WKBJ approximation and the extrapolation line have the form $K \lambda_n^{-S}$ for all cases. Tables II.G.1 through II.G.4 give the values of the constant K for the WKBJ approximation and K and S from the extrapolation lines for all of the fundamental cases. It can be seen that for $r^* \geq 0.25$ the WKBJ approximation provides an adequate expression for the eigenconstants.

These considerations apply to the absolute values of the pertinent functions. The assignment of the correct algebraic sign in any case can be made from the expressions (II.G.67) to (II.G.82).

Values of the quantities γ and π/γ are given in Table II.G.5 and in Figures II.G.1 and II.G.2.

TABLE II.G.1												
ASYMPTOTIC VALUES OF THE FUNCTIONS IN THE FUNDAMENTAL SOLUTIONS OF THE FIRST KIND												
r*	$2(1-r^*)(C_n)_1 R_n'(r^*)$			$2(1-r^*)(C_n)_1 R_n'(1)$			$2(1-r^*)(C_n)_0 R_n'(r^*)$			$2(1-r^*)(C_n)_0 R_n'(1)$		
	K	K	S	K	K	S	K	K	S	K	K	S
	WKBJ	GRAPH		WKBJ	GRAPH		WKBJ	GRAPH		WKBJ	GRAPH	
0	∞			0			∞			4.5477		
0.02	9.9307	20.2	0.490	1.0086	1.515	0.427	50.429	73.1	0.420	5.1213	5.40	0.348
0.05	8.3218	11.62	0.408	1.4810	1.805	0.378	29.619	37.8	0.396	5.2708	5.43	0.340
0.1	7.4489	9.17	0.392	2.0072	2.08	0.335	20.072	22.9	0.368	5.4090	5.44	0.334
0.2	6.8213			2.7560			13.780			5.5669		
0.25	6.6623	6.77	0.336	3.0596	3.07	0.334	12.238	12.9	0.347	5.6201	5.63	0.334
0.3	6.5495			3.3372			11.124			5.6682		
0.4	6.3898			3.8306			9.5766			5.7422		
0.5	6.2813	6.28	0.334	4.2690	4.29	0.334	8.5380	8.58	0.334	5.8028	5.85	0.334
0.6	6.2019			4.6674			7.7790			5.8542		
0.7	6.1398			5.0355			7.1934			5.8998		
0.8	6.0908			5.3804			6.7256			5.9408		
1.0	6.0368			6.0368			6.0368			6.0368		

TABLE II.G.2												
ASYMPTOTIC VALUES OF THE FUNCTIONS IN THE FUNDAMENTAL SOLUTIONS OF THE SECOND KIND												
r*	$(C_n)_1 R_n(r^*)$			$(C_n)_1 R_n(1)$			$(C_n)_0 R_n(r^*)$			$(C_n)_0 R_n(1)$		
	K	K	S	K	K	S	K	K	S	K	K	S
	WKBJ	GRAPH		WKBJ	GRAPH		WKBJ	GRAPH		WKBJ	GRAPH	
0	0			0			∞			2.1389		
0.02	1.1336	0.0714	1.162	0.2325	0.0677	1.462	11.163	3.020	1.423	2.1389	2.78	1.71
0.05	1.4039	0.2065	1.280	0.3947	0.198	1.54	7.8994	3.86	1.535	2.2166	2.72	1.70
0.1	1.6198	0.533	1.442	0.6012	0.394	1.582	6.0112	3.94	1.582	2.2307	2.54	1.68
0.2	1.8261			0.90404			4.5202			2.2379		
0.25	1.8863	1.122	1.542	1.0270	0.863	1.622	4.1080	4.00	1.66	2.2360	2.51	1.68
0.3	1.9335			1.1384			3.7947			2.2341		
0.4	2.0010			1.3351			3.3378			2.2267		
0.5	2.0478	1.78	1.625	1.5065	1.46	1.645	3.0130	3.13	1.66	2.2166	2.45	1.68
0.6	2.0819			1.6599			2.7665			2.2055		
0.7	2.1080			1.7992			2.5703			2.1938		
0.8	2.1280			1.9271			2.4089			2.1816		
1.0	2.1483			2.1483			2.1483			2.1483		

TABLE II.G.3												
ASYMPTOTIC VALUES OF THE FUNCTIONS IN THE FUNDAMENTAL SOLUTIONS OF THE THIRD KIND												
r*	$2(1-r^*)(C_n)_1 R_n'(r^*)$			$(C_n)_1 R_n(1)$			$(C_n)_0 R_n(r^*)$			$2(1-r^*)(C_n)_0 R_n'(1)$		
	K	K	S	K	K	S	K	K	S	K	K	S
	WKBJ	GRAPH		WKBJ	GRAPH		WKBJ	GRAPH		WKBJ	GRAPH	
0	∞			0			∞			4.5477		
0.02	9.9307	12.40	0.520	0.66073	1.21	1.142	17.039	4.38	0.758	5.1213	5.09	0.329
0.05	8.3218	12.12	0.428	0.96037	1.480	1.105	12.166	4.72	0.813	5.2708	5.26	0.333
0.10	7.4489	9.84	0.406	1.2890	1.773	1.080	9.3602	4.91	0.859	5.4090		
0.2	6.8213			1.7473			7.1298			5.5669		
0.25	6.6623	7.13	0.350	1.9298	2.190	1.021	6.5120	5.33	0.960	5.6201		
0.3	6.5495			2.0950			6.0444			5.6682		
0.4	6.3898			2.3855			5.3599			5.7422		
0.5	6.2813	6.37	0.338	2.6384	2.86	1.012	4.8751	4.60	0.983	5.8028		
0.6	6.2019			2.8648			4.5071			5.8542		
0.7	6.1398			3.0703			4.2154			5.8998		
0.8	6.0908			3.2601			3.9755			5.9408		
1.0	6.0368			3.6013			3.6013			6.0368		

TABLE II.G.4												
ASYMPTOTIC VALUES OF THE FUNCTIONS IN THE FUNDAMENTAL SOLUTIONS OF THE FOURTH KIND												
r*	$(C_n)_1 R_n(r^*)$			$2(1-r^*)(C_n)_1 R_n'(1)$			$2(1-r^*)(C_n)_0 R_n'(r^*)$			$(C_n)_0 R_n(1)$		
	K	K	S	K	K	S	K	K	S	K	K	S
	WKBJ	GRAPH		WKBJ	GRAPH		WKBJ	GRAPH		WKBJ	GRAPH	
0	0			0			∞			2.1389		
0.02	1.1336	0.0709	1.170	0.34078	0.0825	0.740	33.037	65.1	1.17	2.1983	3.70	1.80
0.05	1.4039	0.2065	1.282	0.60830	0.221	0.788	19.207	27.6	1.082	2.2166	3.27	1.76
0.10	1.6198	0.417	1.359	0.93602	0.458	0.836	12.890	17.3	1.07	2.2307	2.99	1.73
0.2	1.8261			1.4260			8.7365			2.2379		
0.25	1.8863	0.976	1.495	1.6280	1.241	0.939	7.7192	9.70	1.059	2.2360	2.63	1.69
0.3	1.9335			1.8133			6.9833			2.2341		
0.4	2.0010			2.1440			5.9638			2.2267		
0.5	2.0478	1.820	1.635	2.4376	2.30	0.986	5.2768	5.80	1.017	2.2166	2.52	1.68
0.6	2.0819			2.7043			4.7747			2.2055		
0.7	2.1080			2.9508			4.3861			2.1938		
0.8	2.1280			3.1804			4.0751			2.1816		
1.0	2.1483			3.6013			3.6013			2.1483		

CONSTANTS IN THE ASYMPTOTIC (LARGE λ) SOLUTIONS

r^*	γ	π/γ
0.0	0.555360	5.65685
0.01	0.522132	6.01685
0.02	0.516231	6.08584
0.03	0.512245	6.13298
0.04	0.509194	6.16973
0.05	0.506718	6.19988
0.06	0.504635	6.22547
0.07	0.502843	6.24766
0.08	0.501275	6.26720
0.09	0.499884	6.28464
0.10	0.498638	6.30034
0.20	0.490731	6.40186
0.30	0.486729	6.45450
0.40	0.484388	6.48569
0.50	0.482937	6.50518
0.60	0.482022	6.51752
0.70	0.481453	6.52523
0.80	0.481118	6.52977
1.00	0.480956	6.53197

Table II.G.5

CONSTANTS IN THE ASYMPTOTIC
(LARGE λ) SOLUTIONS

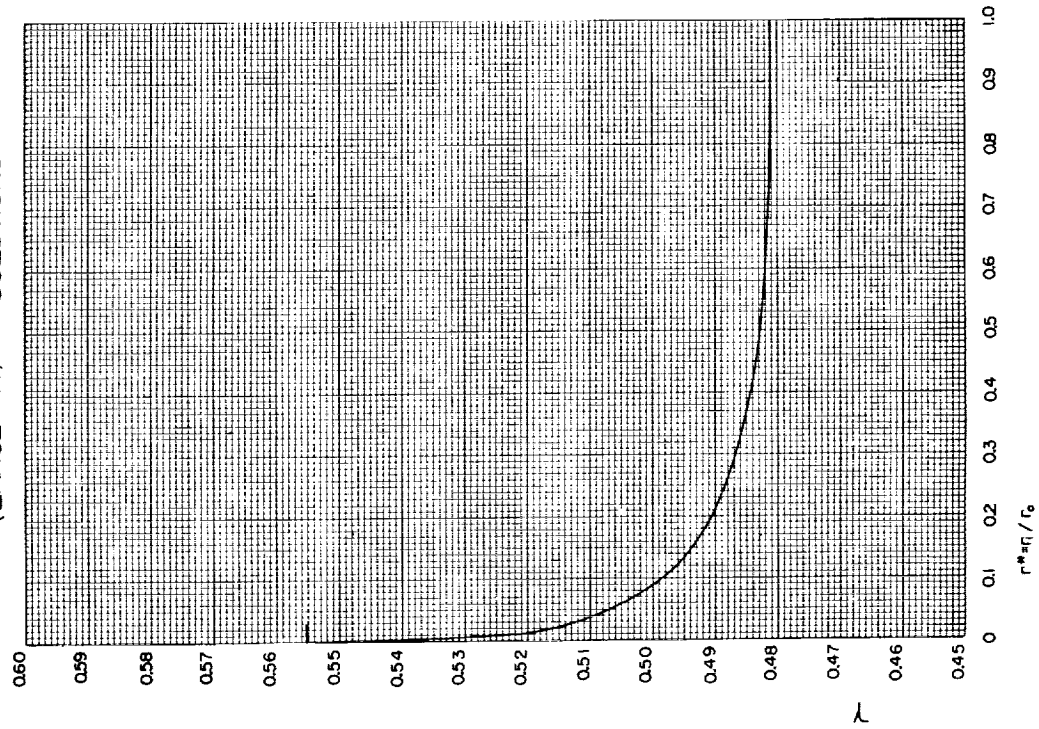


FIGURE II. G. 1

CONSTANTS IN THE ASYMPTOTIC
(LARGE λ) SOLUTIONS

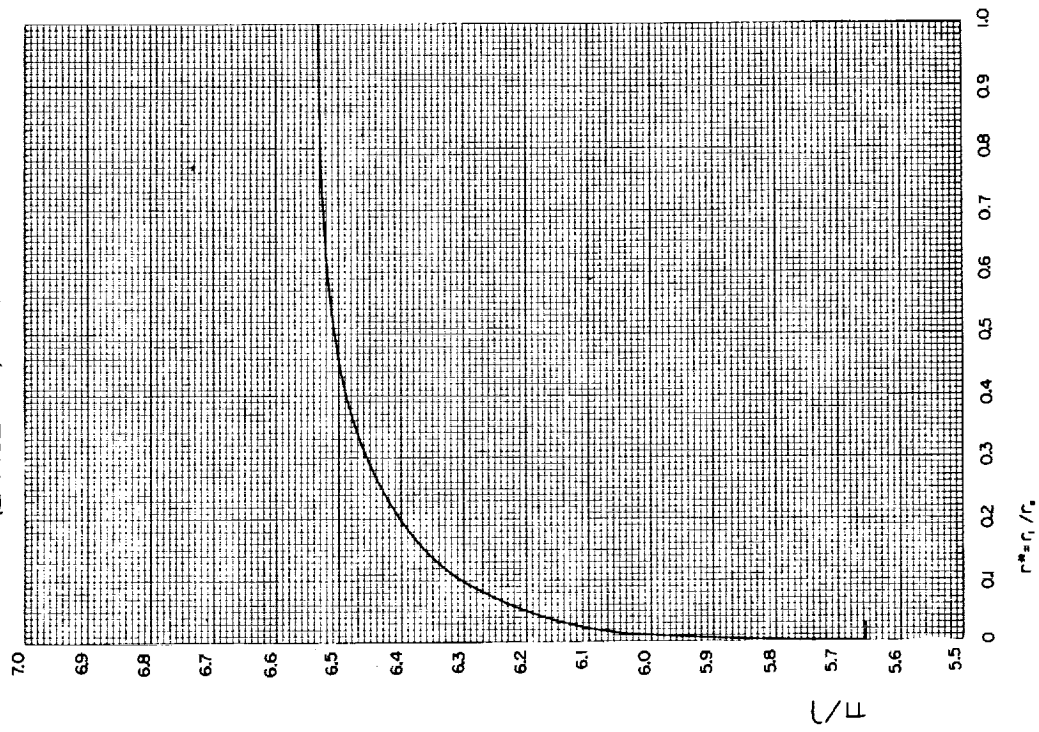


FIGURE II. G. 2

II. H. Solution of the Sturm-Liouville Equation

The method used by Graetz and most of the other workers to generate solutions to the counterpart of equation (II.F.2), for the particular geometry which they considered, was the series solution technique of Frobenius. This method assumes a solution of the form

$$R_n(\bar{r}) = \sum_{m=0}^{\infty} A_{n,m} \bar{r}^{m+c}$$

and by substitution into the differential equation attempts to formulate a recurrence relation among the $A_{n,m}$. The principal drawback, for these simpler cases, is the difficulty with the higher modes of the equation. The $A_{n,m}$ involve the eigenvalues λ_n , and the equation for the λ_n is the condition that the series or its derivative vanishes at one of the boundaries. For the higher modes of the equation, the $A_{n,m}$ grow very large before diminishing, and the summing of the series to zero involves the differences of large numbers with the result that if accuracy is desired many digits must be carried in the computation.

For equation (II.F.2) the difficulty is further compounded by the appearance of the logarithm of the independent variable, \bar{r} , as a coefficient. To a certain extent this difficulty can be circumvented by expanding the solution about the point $\bar{r} = 1$, but the resulting recurrence relation among the $A_{n,m}$ is a many term relationship. In fact, the coefficient $A_{n,m}$ is an explicit function of all the preceding $A_{n,k}$, $k = 0, 1, 2, \dots, m-1$, which makes practical computation of the solution, at best, difficult.

These difficulties are largely eliminated by the iterative method of Berry and de Prima¹. This method may be essentially summarized as follows:

If $(\lambda_n^2)_k$ is the kth approximation to the desired value, λ_n^2 , and $(R_n(\bar{r}))_k$ is a solution to equation (II.F.2) with $\lambda^2 = (\lambda_n^2)_k$ such that $(R_n)_k$ satisfies the requisite boundary condition only at $\bar{r} = r^*$; and if

$$\int_{r^*}^1 w(\bar{r})(R_n(\bar{r}))_k^2 d\bar{r} = 1 \quad (\text{II.H.1})$$

then the next approximation is given by

$$(\lambda_n^2)_{k+1} = (\lambda_n^2)_k \pm (R_n(1))_k (R'_n(1))_k \quad (\text{II.H.2})$$

This sequence of approximations converges monotonically to λ_n^2 . In (II.H.2) the plus (+) sign is associated with the condition of zero derivative desired at the outer wall ($\bar{r} = 1$), and the minus (-) sign with zero ordinate at $\bar{r} = 1$.

Computationally, the method consists of assuming a value for the slope or the ordinate at $\bar{r} = r^*$, (whichever is not specified as zero by the boundary condition) and integrating equation (II.F.2) numerically. The inner wall value is adjusted to satisfy (II.H.1), then the assumed value of λ_n^2 is corrected by (II.H.2) and the process is repeated. The logarithmic term in the differential equation does not pose any fundamental difficulty with this method, in fact, $w(\bar{r})$ need not be an explicit algebraic form at all so that this method can readily be applied to these same problems in turbulent flow.

The computation of these solutions has been performed on the Burroughs 220 Electronic Digital Computer at the Stanford computation center. The nature of the computation is such that the values of the expansion coefficients are obtained directly from (II.F.7) using a simple numerical integration. The condition (II.H.1) makes the denominator of (II.F.7) always equal to unity. Details of the computational procedure are contained in appendix E.

The eigenvalues and the pertinent combinations of constants are given in tables II.H.1 to II.H.4. The same quantities are presented in graphical form in figures II.H.1 to II.H.20 to facilitate interpolation for the intermediate values of radius ratio.

The values for parallel planes ($r^* = 1$) were provided by McCuen¹¹, those for the circular tube ($r^* = 0$) are from Lipkis¹⁰ and Siegel, Sparrow, and Hallman²⁰.

For the two limiting geometries, the tube and the parallel plane channel, the constant N (which is a function of r^*) has the values $1/2$ and $3/32$ respectively if \bar{x} and \bar{r} are defined in the manner used here. It seems customary* to absorb that constant into the eigenvalue resulting in values which are somewhat different than those reported here. The practice would produce some difficulty for the case at hand since $N \rightarrow \infty$ as $r^* \rightarrow 1$, which would result in λ becoming very large. To preserve the continuity of the eigenvalues as $r^* \rightarrow 1$ this constant is excluded from λ . To transform the previously reported eigenvalues for the tube and the parallel plane channel into the values reported here requires multiplication by $\sqrt{2}$ and $\sqrt{32/3}$ respectively.

An analogous difficulty arises in regard to those functions which involve the derivatives at the walls.

$$C_n \frac{\partial R_n}{\partial \bar{r}} \rightarrow \infty \quad \text{as} \quad r^* \rightarrow 1$$

but the product

$$2(1 - r^*) C_n \frac{\partial R_n}{\partial \bar{r}}$$

* C.f. Sellars, et. al.¹⁹

remains finite. Further, it is this second form which is desired in computing the Φ 's since this is equivalent to

$$D_h C_n \frac{\partial R_n}{\partial r}$$

All the functions involving the derivatives are reported in the above form.

TABLE II.H.1

FUNCTIONS IN THE FUNDAMENTAL SOLUTIONS OF THE FIRST KIND

r^*	n	$(\lambda_n)^{(1)}$	$(\lambda_n^2)^{(1)}$	$2(1-r^*)$ $\cdot (c_n)_1^{(1)} R_n'(r^*)$	$2(1-r^*)$ $\cdot (c_n)_1^{(1)} R_n'(1)$	$2(1-r^*)$ $\cdot (c_n)_0^{(1)} R_n'(r^*)$	$2(1-r^*)$ $\cdot (c_n)_0^{(1)} R_n'(1)$
0.02	0	4.74805	22.5440	-10.2263	+0.80760	-40.2547	+3.17904
	1	10.8763	118.294	-6.39215	-0.549498	+27.3773	+2.35347
	2	16.9948	228.824	-5.06568	+0.452437	-22.5521	+2.01421
	3	23.1043	533.810	-4.35330	-0.397809	+19.8221	+1.81137
0.05	0	4.93941	24.3978	-6.69710	+1.03835	-20.7790	+3.22168
	1	11.1805	125.003	-4.45700	-0.730683	+14.6215	+2.39706
	2	17.4093	303.085	-3.64722	+0.611777	-12.2431	+2.05363
	3	23.6290	538.332	-3.20042	-0.543755	+10.8819	+1.84885
0.1	0	5.10557	26.0669	-5.17154	+1.29745	-12.9769	+3.25568
	1	11.4367	130.799	-3.61850	-0.938758	+9.38927	+2.43589
	2	17.7580	315.346	-3.02917	+0.795670	-7.95812	+2.09036
	3	24.0720	579.459	-2.69415	-0.712271	+7.12413	+1.88347
0.25	0	5.32304	28.3348	-4.05663	+1.82903	-7.31778	+3.29990
	1	11.7580	138.252	-3.00828	-1.37025	+5.48090	+2.49651
	2	18.1952	331.065	-2.51348	+1.17600	-4.70388	+2.14955
	3	24.6305	606.663	-2.31513	-1.05935	+4.23720	+1.93866
0.5	0	5.44515	29.6562	-3.63663	+2.46559	-4.93127	+3.34333
	1	11.9303	142.332	-2.77072	-1.88131	+3.76263	+2.55482
	2	18.4308	339.693	-2.38880	+1.62265	-3.24530	+2.20445
	3	24.9339	621.698	-2.15661	-1.46516	+2.93030	+1.99079
1.0	0	5.49209	30.1630	-3.43234	+3.43234	-3.43234	+3.43234
	1	11.9937	143.848	-2.60888	-2.60888	+2.60888	+2.60888
	2	18.5177	342.906	-2.27786	+2.27786	-2.27786	+2.27786
	3	25.0463	627.316	-2.05809	-2.05809	+2.05809	+2.05809

TABLE II.H.2

FUNCTIONS IN THE FUNDAMENTAL SOLUTIONS OF THE SECOND KIND

r^*	n	$(\lambda_n)^{(2)}$	$(\lambda_n^2)^{(2)}$	$(c_n)_1^{(2)} R_n(r^*)$	$(c_n)_1^{(2)} R_n(1)$	$(c_n)_0^{(2)} R_n(r^*)$	$(c_n)_0^{(2)} R_n(1)$
0	1	7.16654	51.3593	0	0	+0.201742	-0.099361
	2	12.9508	167.724	0	0	-0.087555	-0.034629
	3	18.6636	348.329	0	0	+0.052797	-0.018261
	4	24.3532	593.080	0	0	-0.03664	-0.011507
0.01	1	7.50711	56.3567	-0.00347335	+0.00179521	+0.179521	-0.092786
	2	13.6217	185.551	-0.00178909	-0.00075895	-0.075893	-0.032195
0.02	1	7.53889	56.8349	-0.00665350	+0.0035018	+0.175092	-0.092151
	2	13.7049	187.825	-0.0033414	-0.0014612	-0.073059	-0.031922
	3	19.8078	393.348	-0.0021827	+0.0008562	+0.042809	-0.016792
	4	25.8930	670.448	-0.001603	-0.0005839	-0.029010	-0.010558
0.035	1	7.55723	57.1117	-0.0110611	+0.0059587	+0.170252	-0.091716
0.05	1	7.56239	57.1897	-0.0151141	+0.0083162	+0.166324	-0.091516
	2	13.8132	190.803	-0.0071613	-0.0033617	-0.067237	-0.031563
	3	20.0134	400.537	-0.0044722	+0.0019246	+0.038488	-0.016563
	4	26.2024	686.569	-0.0031492	-0.0012802	-0.025607	-0.010409
0.075	1	7.55942	57.1448	-0.0212168	+0.0120597	+0.160796	-0.091397
0.1	1	7.55041	57.0087	-0.0266349	+0.0156020	+0.156018	-0.091391
	2	13.8836	192.753	-0.0117253	-0.0060579	-0.060580	-0.031299
	3	20.1791	407.198	-0.0069693	+0.0033763	+0.033790	-0.016369
	4	26.4683	700.572	-0.0047401	-0.0022056	-0.022058	-0.010263
	5	32.7568	1073.01	-0.0034799	+0.0015744	+0.015740	-0.007122
	6	39.0459	1524.58	-0.0026878	-0.0011910	-0.011912	-0.005278
0.175	1	7.51572	56.4860	-0.0397586	+0.0252307	+0.144177	-0.091494
0.25	1	7.48406	56.0112	-0.049403	+0.033643	+0.134564	-0.091451
	2	13.9539	194.710	-0.019141	-0.012135	-0.048534	-0.030769
	3	20.3940	415.917	-0.010610	+0.006510	+0.026042	-0.015979
	4	26.8276	719.722	-0.006890	-0.004146	-0.016590	-0.009983
0.375	1	7.44514	55.4301	-0.060955	+0.045580	+0.121550	-0.090891
0.5	1	7.42034	55.0615	-0.068661	+0.055527	+0.111053	-0.089811
	2	13.9888	195.686	-0.024215	-0.018997	-0.037994	-0.029807
	3	20.5195	421.048	-0.012888	+0.009971	+0.019945	-0.015431
	4	27.0385	731.082	-0.008178	-0.006276	-0.012553	-0.009633
0.7	1	7.39945	54.7518	-0.076527	+0.068417	+0.097750	-0.087391
1.0	1	7.39139	54.6329	-0.083014	+0.083014	-0.083014	-0.083014
	2	14.0023	196.064	-0.027778	-0.027778	+0.027778	-0.027778
	3	20.5686	423.067	-0.014468	+0.014468	-0.014468	-0.014468
	4	27.1205	735.519	-0.008670	-0.008670	+0.008670	-0.008670

TABLE II.H.3							
FUNCTIONS IN THE FUNDAMENTAL SOLUTIONS OF THE THIRD AND FOURTH KINDS							
r^*	n	$(\lambda_n)^{(3)} - (\lambda_n)^{(4)}$	(λ_n^2)	$2(1 - r^*)$ $\cdot (C_n)^{(3)}_{R_n(r^*)}$	$(C_n)^{(3)}_{R_n(1)}$	$2(1 - r^*)$ $\cdot (C_n)^{(4)}_{R_n(r^*)}$	$(C_n)^{(4)}_{R_n(1)}$
0.02	0	1.52956	2.53626	-31.7792	-1.07360	-53.5098	-1.80732
	1	8.45591	71.5024	-7.59043	+0.108022	+5.36368	-0.076332
	2	14.7044	216.219	-5.52771	-0.056343	-2.81542	-0.028697
	3	20.8730	435.682	-4.60870	+0.037862	+1.87650	-0.015416
0.05	0	1.82368	3.32580	-17.1123	-1.09236	-21.8599	-1.39542
	1	8.73469	76.2948	-5.17349	+0.136946	+2.73988	-0.072526
	2	15.0887	227.668	-3.93218	-0.073469	-1.47056	-0.027476
	3	21.3656	456.490	-3.36102	+0.050123	+1.00256	-0.014951
0.1	0	2.05027	4.20362	-11.2121	-1.11276	-11.1298	-1.10459
	1	8.97827	80.6094	-4.12691	+0.168675	+1.68692	-0.068948
	2	15.4168	237.678	-3.23924	-0.092579	-0.924952	-0.026464
	3	21.7847	474.573	-2.81551	+0.063855	+0.638696	-0.014486
0.25	0	2.42830	5.89665	-6.98949	-1.15233	-4.60952	-0.759954
	1	9.31079	86.6908	-3.35613	+0.230576	+0.922335	-0.063367
	2	15.8447	251.055	-2.72768	-0.130316	-0.521331	-0.024907
	3	22.3254	498.423	-2.40759	+0.090973	+0.363942	-0.013752
0.5	0	2.76602	7.65088	-5.30242	-1.19491	-2.38986	-0.538562
	1	9.53544	90.9247	-3.04516	+0.297663	+0.595329	-0.058182
	2	16.1056	259.389	-2.51847	-0.171774	-0.343531	-0.023431
	3	22.6421	512.665	-2.23664	+0.120832	+0.241646	-0.013055
1.0	0	3.11796	9.72165	-4.35312	-1.24842	-1.248436	-0.358038
	1	9.71413	94.3647	-2.854332	+0.383198	+0.393268	-0.051454
	2	16.2682	264.654	-2.387368	-0.226323	-0.226400	-0.021463
	3	22.8118	520.379	-2.127292	+0.160551	+0.160704	-0.012129

TABLE II.H.4							
FUNCTIONS IN THE FUNDAMENTAL SOLUTIONS OF THE THIRD AND FOURTH KINDS							
r^*	n	$(\lambda_n)^{(4)} - (\lambda_n)^{(3)}$	(λ_n^2)	$2(c - r^*)$ $\cdot (C_n)^{(4)}_{R_n(r^*)}$	$(C_n)^{(4)}_{R_n(1)}$	$2(1 - r^*)$ $\cdot (C_n)^{(3)}_{R_n(r^*)}$	$(C_n)^{(3)}_{R_n(1)}$
0	0	3.824549	14.62718	0	0	-1.46622	+2.99516
	1	9.445581	89.21900	0	0	+0.80248	+2.17696
	2	15.09444	227.8421	0	0	-0.58709	+1.85152
	3	20.74805	430.4816	0	0	+0.47490	+1.66072
0.02	0	3.95731	15.6603	-0.0127464	+0.0289949	-1.44975	+3.29778
	1	9.94704	98.9435	-0.0047162	-0.0150085	+0.750414	+2.38808
	2	15.9795	255.346	-0.0027714	+0.0106132	-0.530669	+2.03225
	3	22.0248	485.094	-0.0019160	-0.0083610	+0.418050	+1.82426
0.05	0	3.93106	15.4532	-0.0305157	+0.0716530	-1.43305	+3.36492
	1	9.99141	99.8283	-0.0104624	-0.0357396	+0.714786	+2.44169
	2	16.1156	259.711	-0.0058357	+0.0246326	-0.492656	+2.07949
	3	22.2616	495.518	-0.0038742	-0.0190190	+0.380383	+1.86734
0.1	0	3.86760	14.9583	-0.057923	+0.141044	-1.41047	+3.43456
	1	9.99430	99.8861	-0.017888	-0.066845	+0.668553	+2.49829
	2	16.2096	262.750	-0.009377	+0.044671	-0.446729	+2.12819
	3	22.4544	504.200	-0.005966	-0.033772	+0.337525	+1.91074
0.25	0	3.68006	13.5428	-0.128700	+0.340089	-1.36035	+3.59471
	1	9.93693	98.7426	-0.031544	-0.143358	+0.573406	+2.60594
	2	16.3028	265.783	-0.014912	+0.090833	-0.363314	+2.21309
	3	22.6973	515.170	-0.008924	-0.066513	+0.266097	+1.98324
0.5	0	3.43679	11.8115	-0.221934	+0.653514	-1.30702	+3.84871
	1	9.84575	96.9388	-0.042427	-0.240047	+0.480096	+2.71634
	2	16.3249	266.502	-0.018654	+0.146212	-0.292413	+2.29196
	3	22.8169	520.611	-0.010781	-0.105092	+0.210151	+2.04857
1.0	0	3.11796	9.72165	-0.358038	+1.248436	-1.24842	+4.35312
	1	9.71413	94.3647	-0.051454	-0.393268	+0.383198	+2.854322
	2	16.2682	264.654	-0.021463	+0.226400	-0.226323	+2.387368
	3	22.8118	520.379	-0.012129	-0.160704	+0.160551	+2.127292

EIGENVALUES FOR THE FUNDAMENTAL SOLUTIONS OF THE SECOND KIND

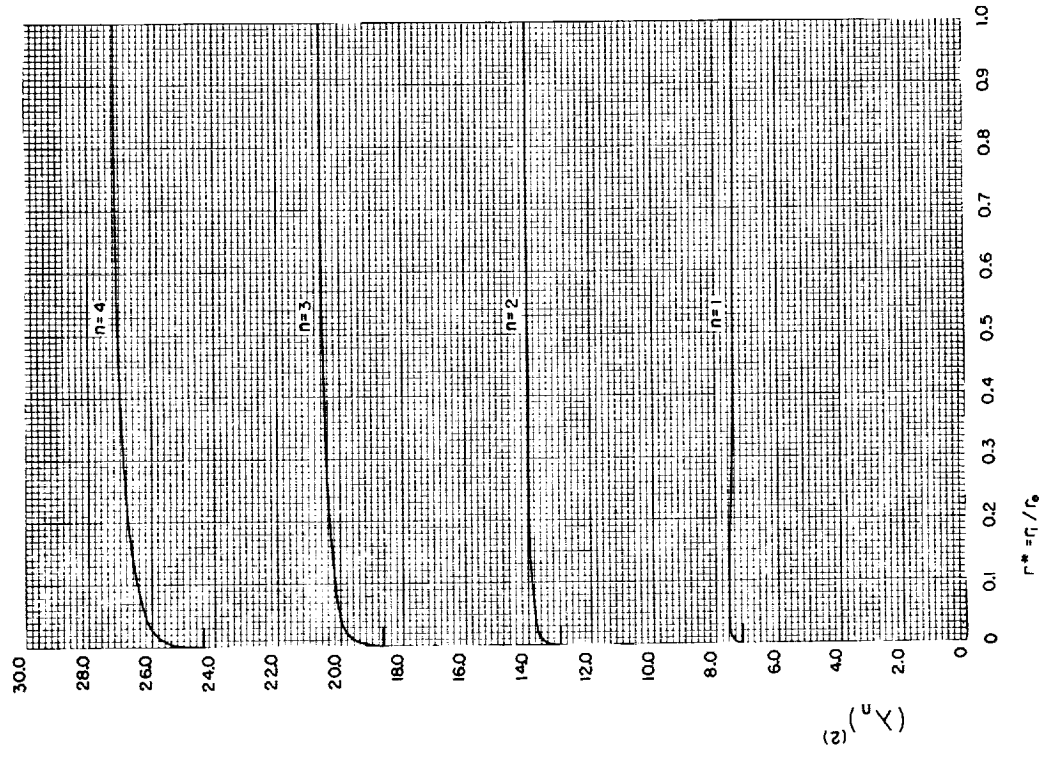


FIGURE II. H. 2

EIGENVALUES FOR THE FUNDAMENTAL SOLUTIONS OF THE FIRST KIND

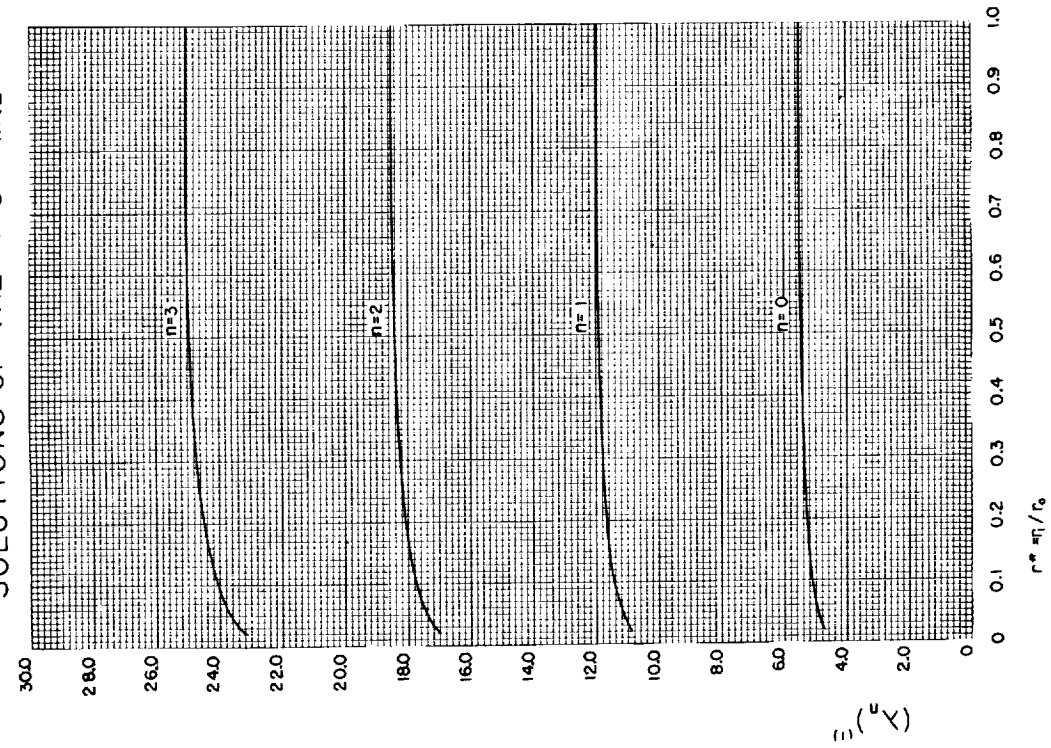


FIGURE II. H. 1

EIGENVALUES FOR THE FUNDAMENTAL
SOLUTIONS OF THE THIRD AND FOURTH KINDS

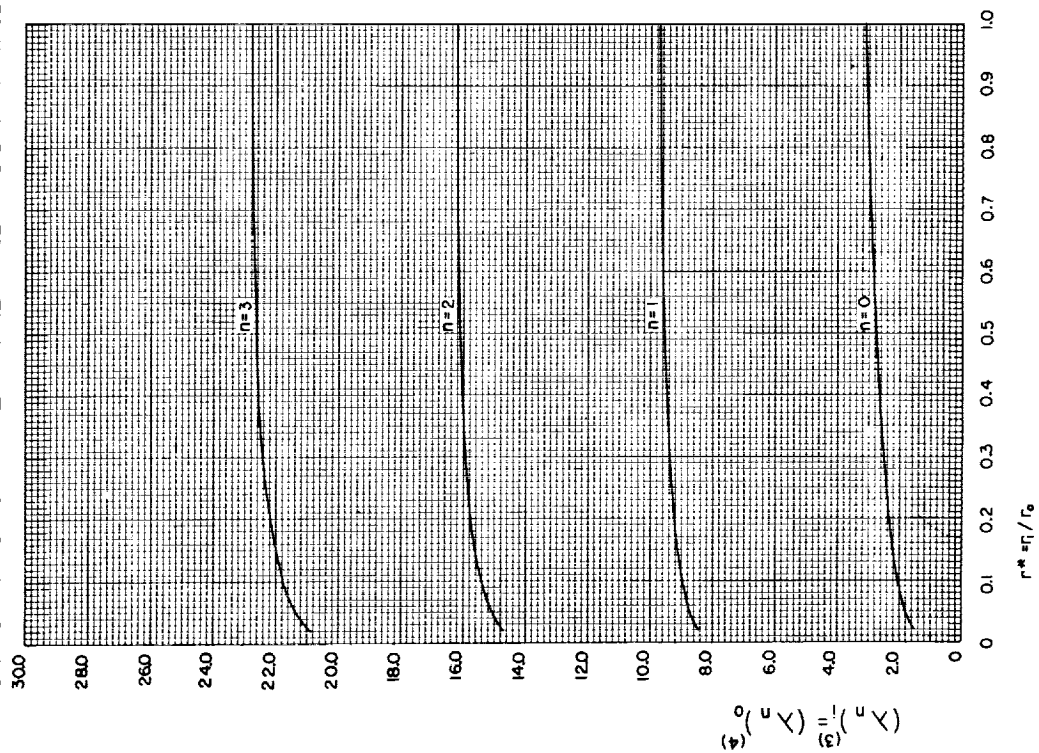


FIGURE II. H. 3

EIGENVALUES FOR THE FUNDAMENTAL
SOLUTIONS OF THE THIRD AND FOURTH KINDS

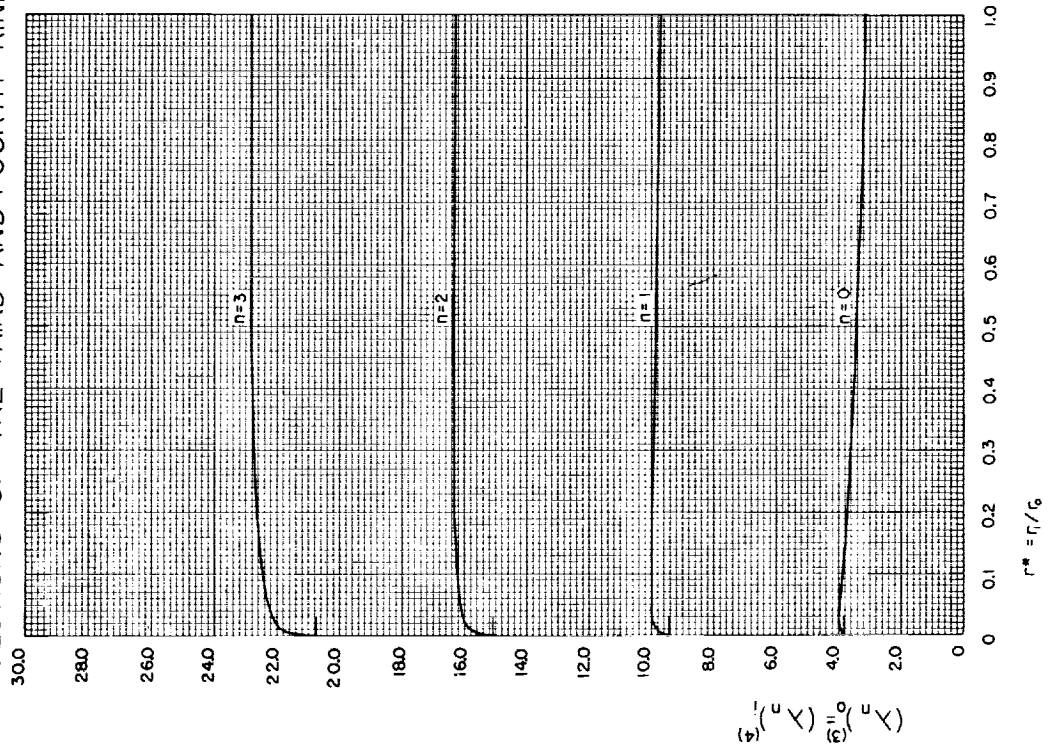


FIGURE II. H. 4

FUNCTIONS IN THE FUNDAMENTAL
SOLUTIONS OF THE FIRST KIND

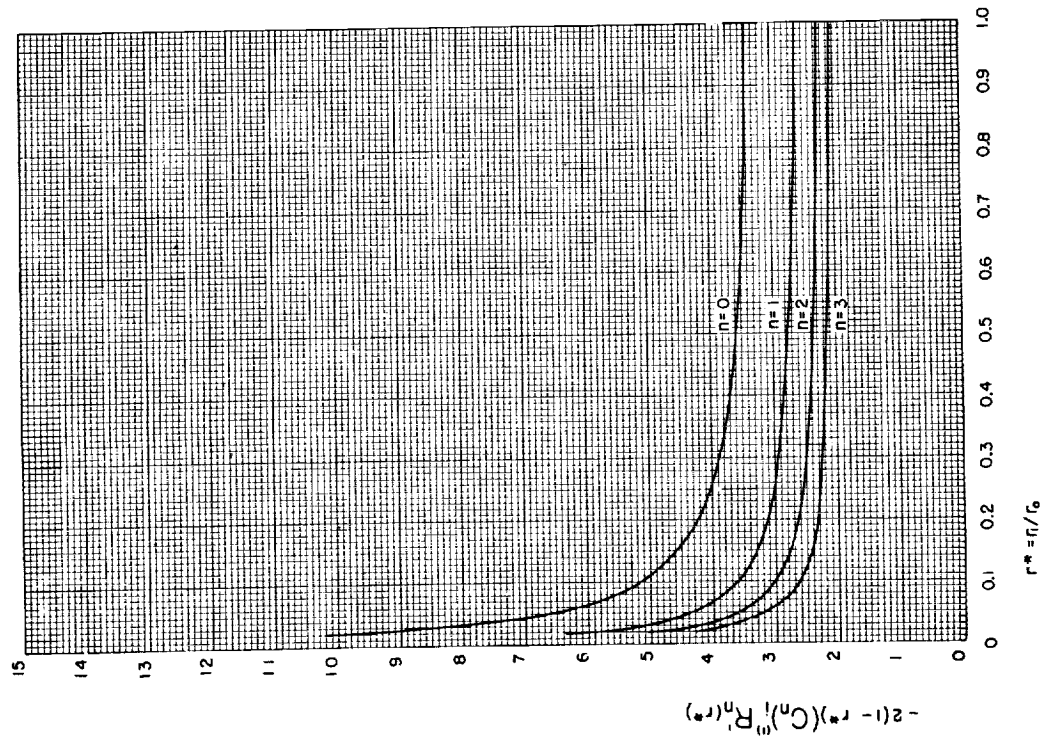


FIGURE II. H. 5

FUNCTIONS IN THE FUNDAMENTAL
SOLUTIONS OF THE FIRST KIND

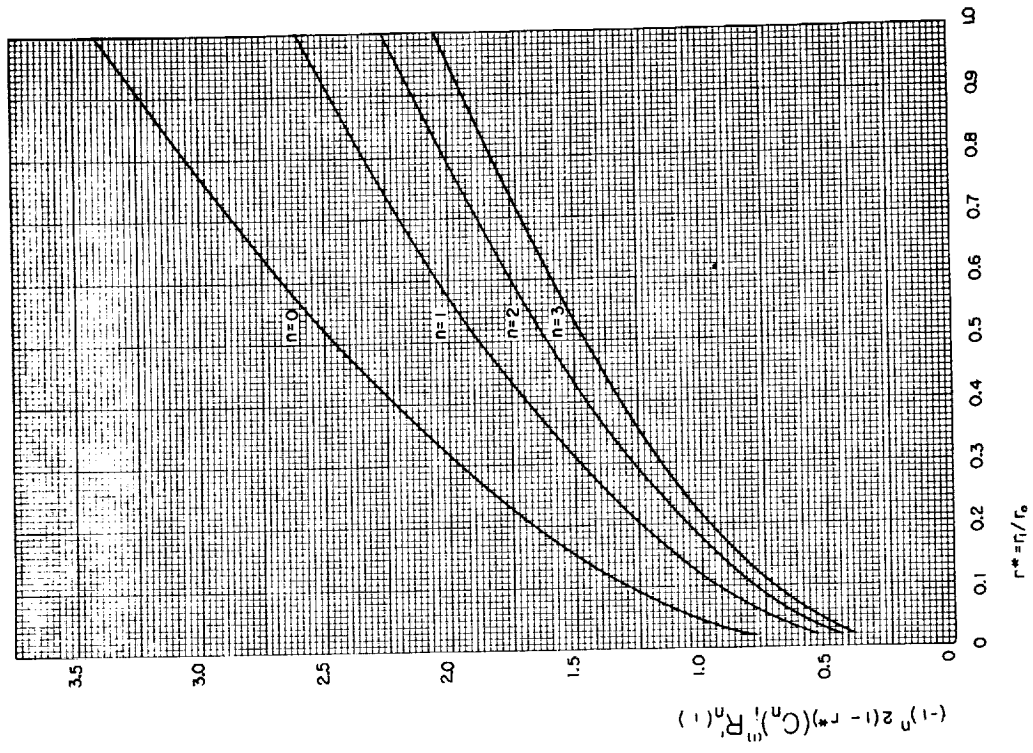


FIGURE II. H. 6

FUNCTIONS IN THE FUNDAMENTAL
SOLUTIONS OF THE FIRST KIND

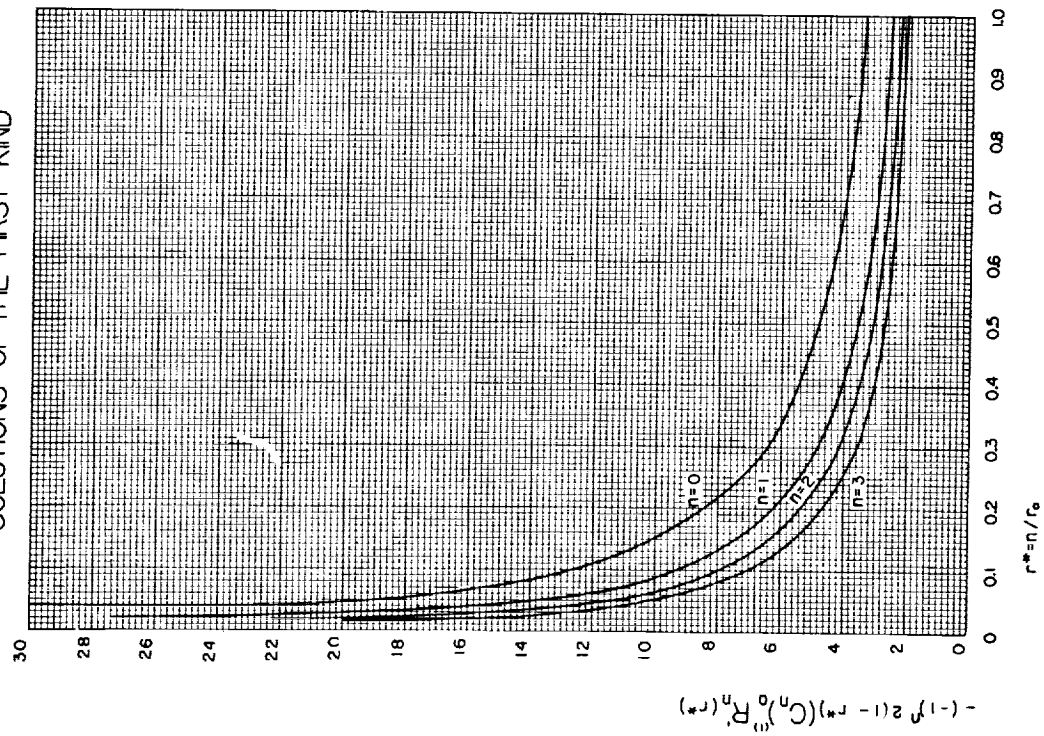


FIGURE II. H. 7

FUNCTIONS IN THE FUNDAMENTAL
SOLUTIONS OF THE FIRST KIND

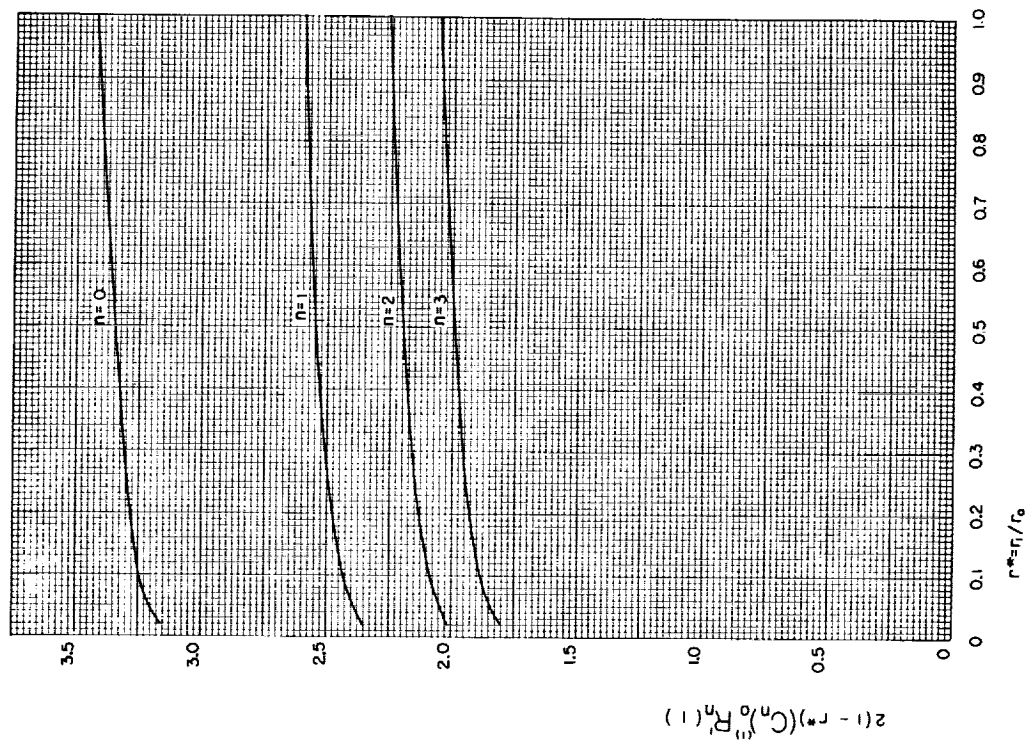


FIGURE II. H. 8

FUNCTIONS IN THE FUNDAMENTAL
SOLUTIONS OF THE SECOND KIND

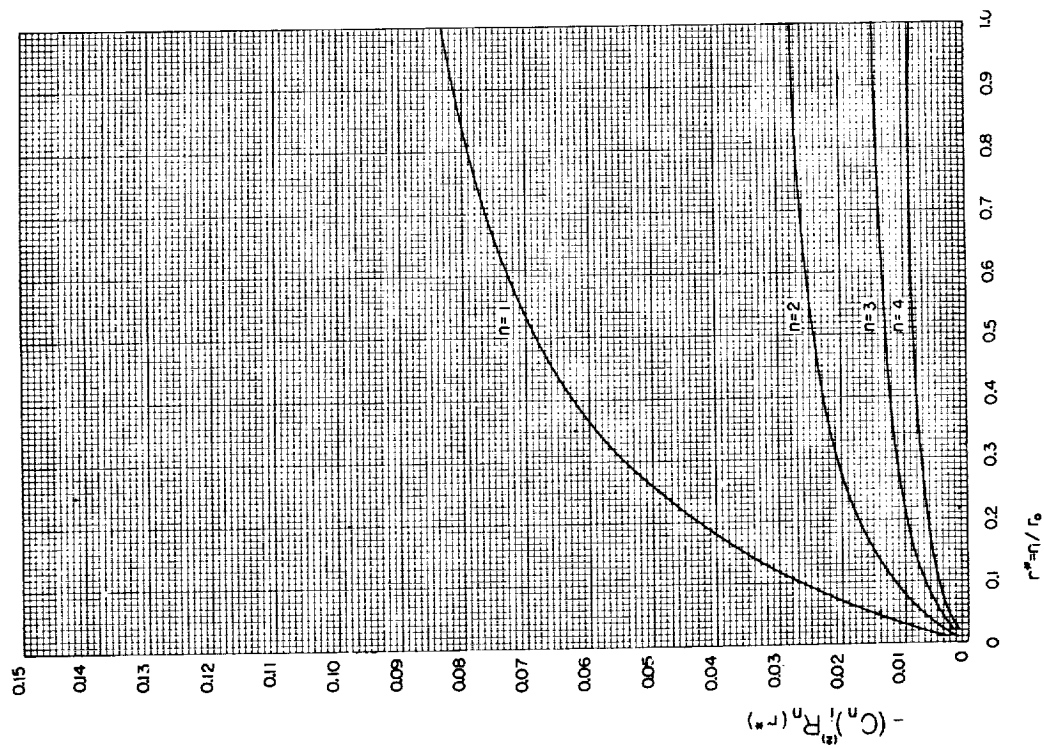


FIGURE II. H. 9

FUNCTIONS IN THE FUNDAMENTAL
SOLUTIONS OF THE SECOND KIND

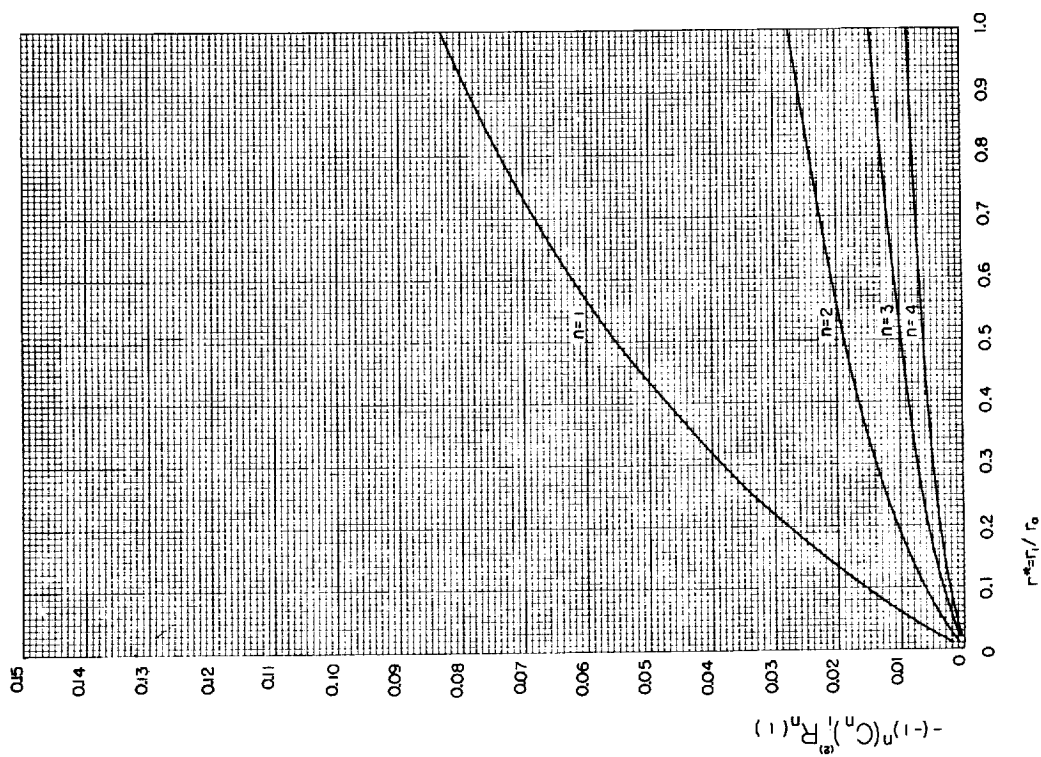


FIGURE II. H. 10

FUNCTIONS IN THE FUNDAMENTAL
SOLUTIONS OF THE SECOND KIND

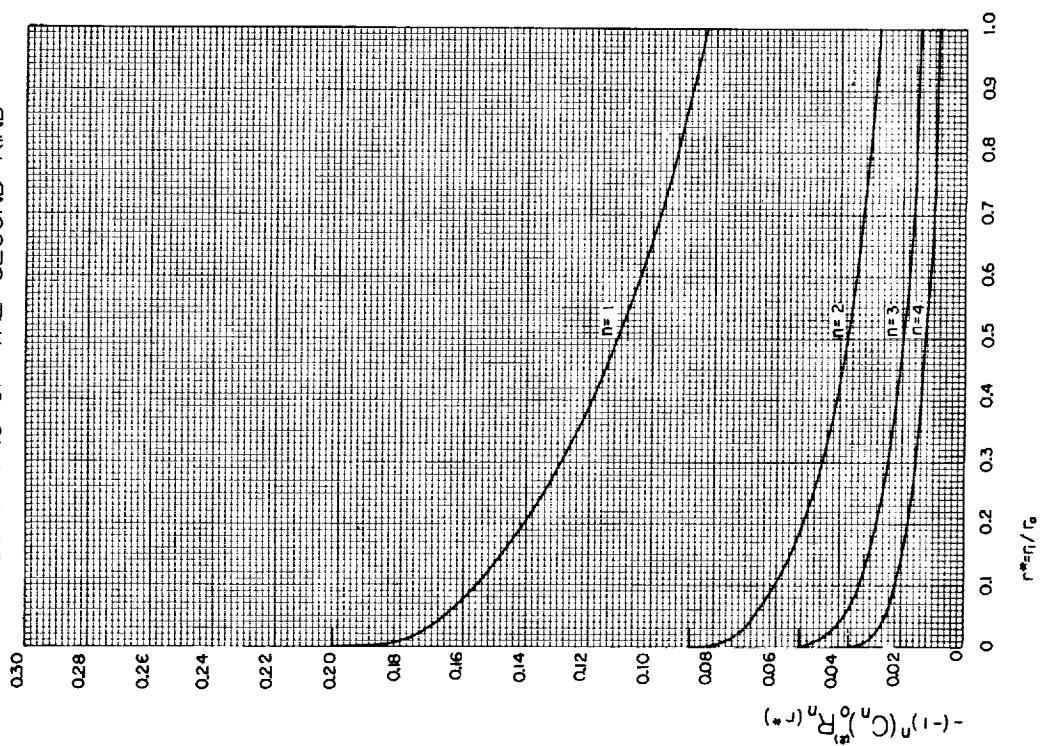


FIGURE II. H. 1.1

FUNCTIONS IN THE FUNDAMENTAL
SOLUTIONS OF THE SECOND KIND

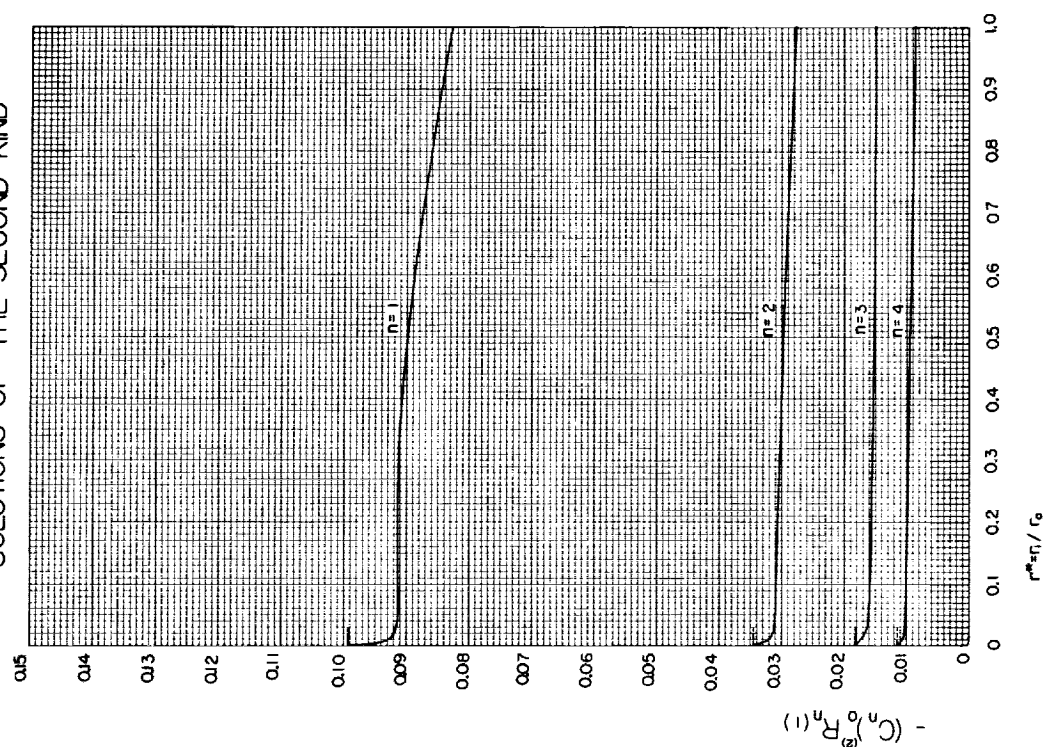


FIGURE II. H. 1.2

FUNCTIONS IN THE FUNDAMENTAL
SOLUTIONS OF THE THIRD KIND

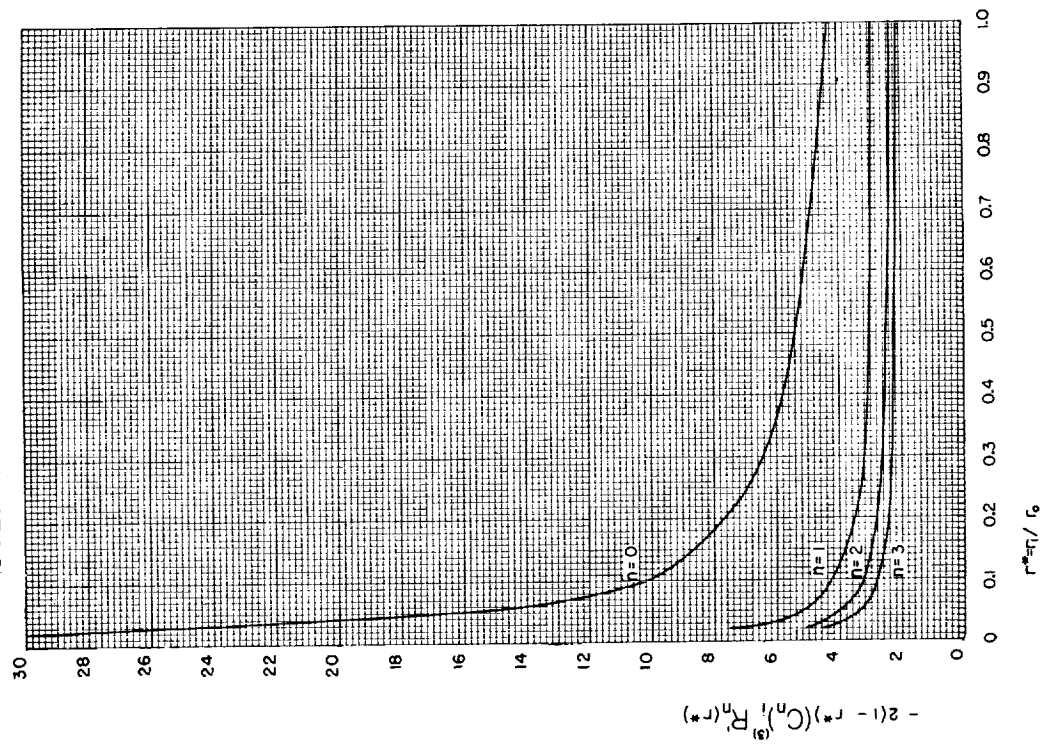


FIGURE II H.13

FUNCTIONS IN THE FUNDAMENTAL
SOLUTIONS OF THE THIRD KIND

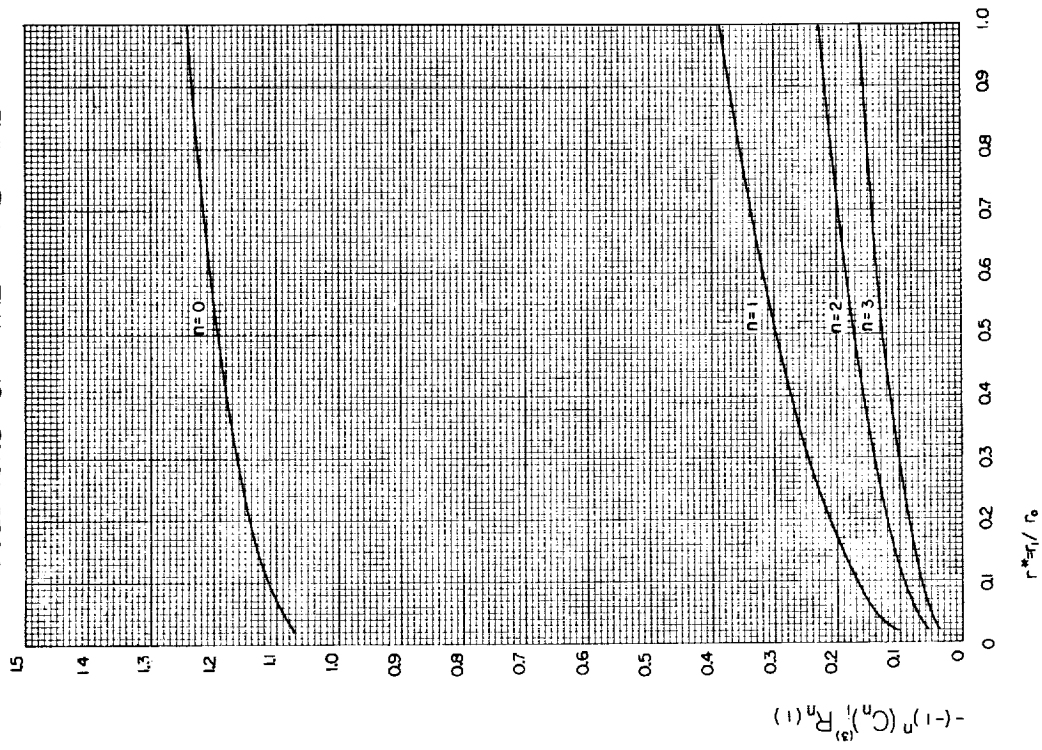


FIGURE II H.14

FUNCTIONS IN THE FUNDAMENTAL
SOLUTIONS OF THE THIRD KIND

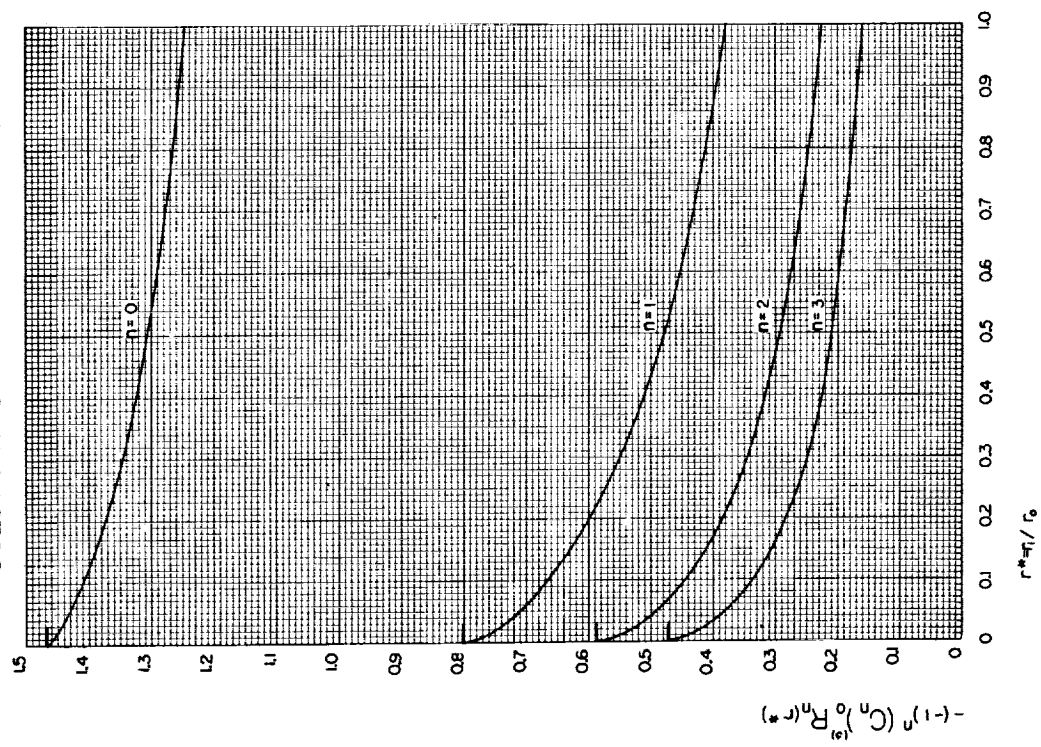


FIGURE II H. 15

FUNCTIONS IN THE FUNDAMENTAL
SOLUTIONS OF THE THIRD KIND

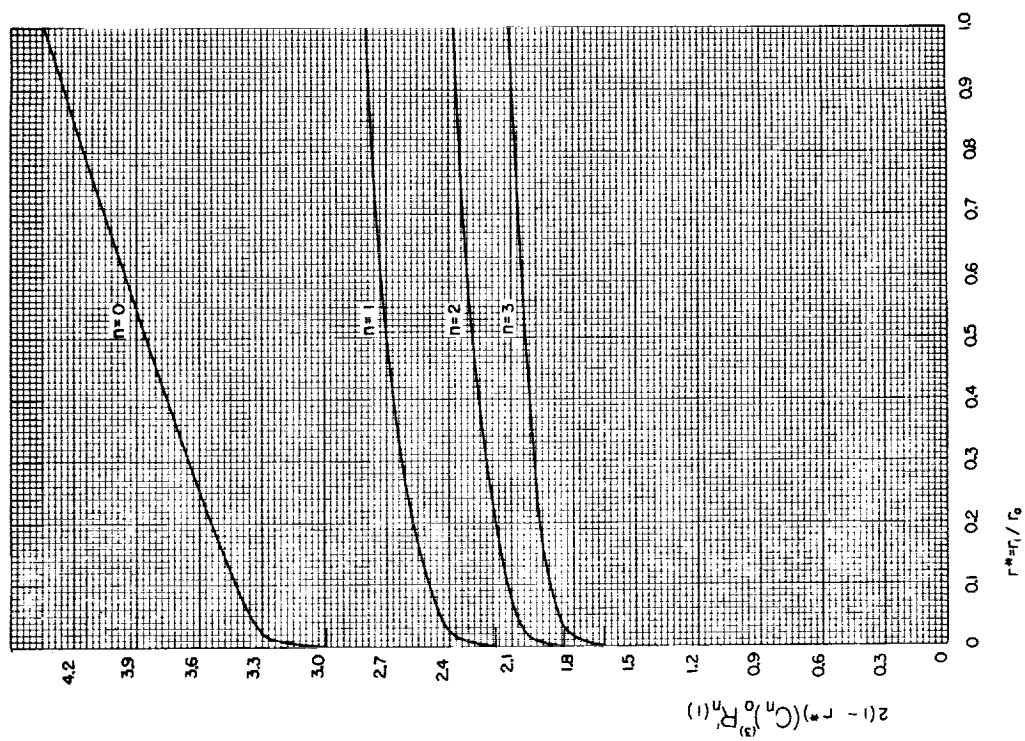


FIGURE II H. 16

FUNCTIONS IN THE FUNDAMENTAL
SOLUTIONS OF THE FOURTH KIND

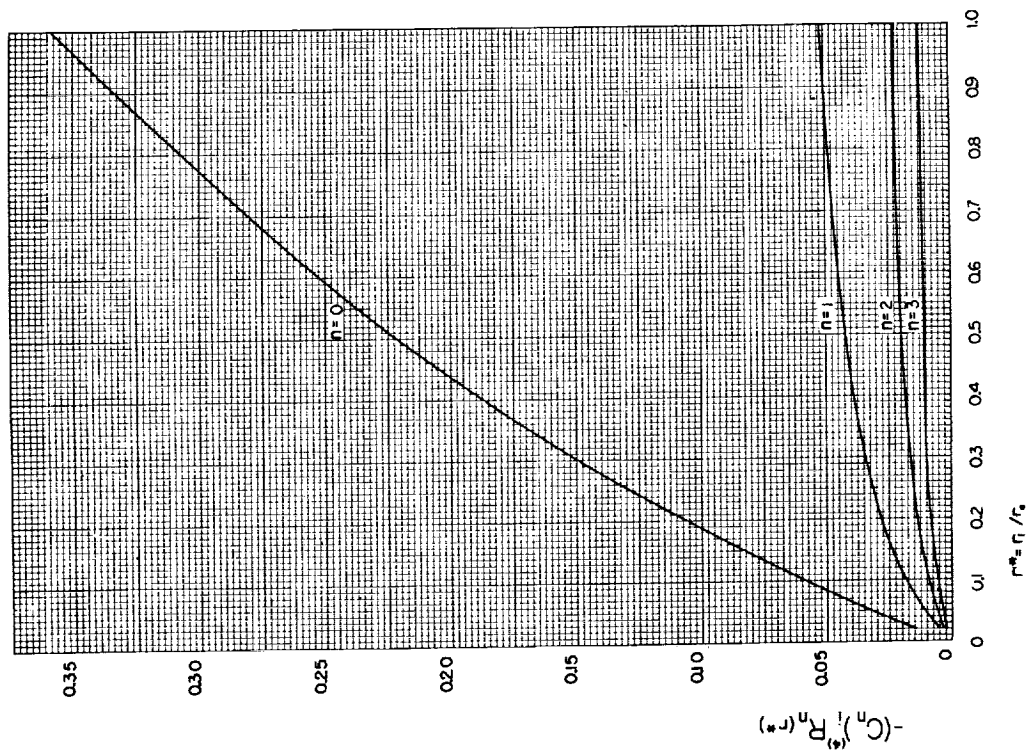


FIGURE II. H. 17

FUNCTIONS IN THE FUNDAMENTAL
SOLUTIONS OF THE FOURTH KIND

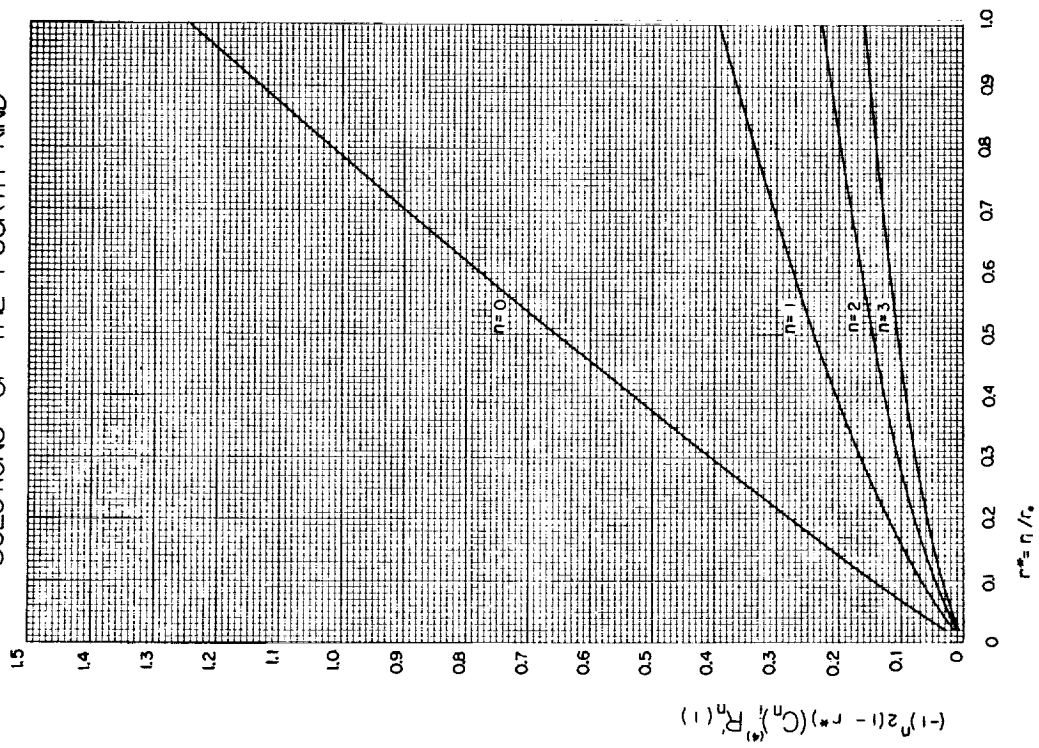


FIGURE II. H. 18

FUNCTIONS IN THE FUNDAMENTAL
SOLUTIONS OF THE FOURTH KIND

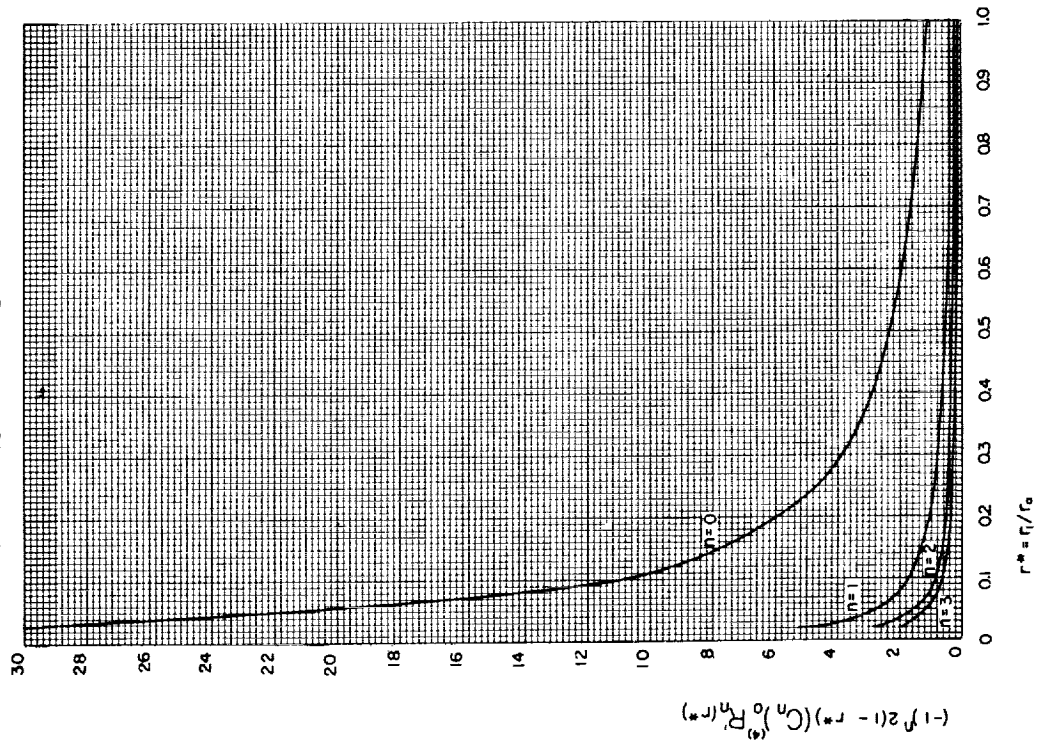


FIGURE II. H. 19

FUNCTIONS IN THE FUNDAMENTAL
SOLUTIONS OF THE FOURTH KIND

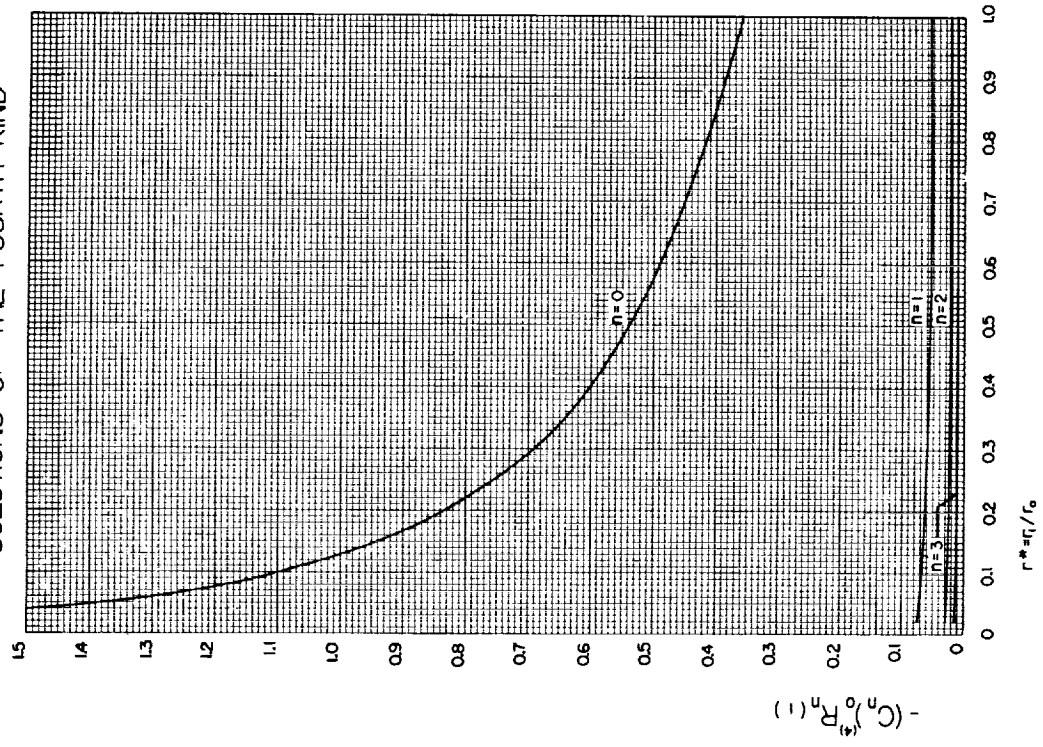


FIGURE II. H. 20

II. I. The Fundamental Solutions

We are now prepared to construct the various fundamental solutions using the relationship

$$\theta_j^{(k)} = \bar{\theta}_j^{(k)} + \theta_j^{(k)} \Big|_{fd} \quad (II.I.1)$$

and the series solution for $\bar{\theta}_j^{(k)}$, (II.F.8). The fully developed solutions are taken from section II.D.

The pertinent non-dimensional quantities (as outlined in section I.B) may be readily obtained from (II.I.1) and the defining equations. Let us formulate some general relationships of interest before turning to the specific cases

$$\Phi_{1j}^{(k)}(x) = -2(1 - r^*) \left(\frac{\partial \theta_j^{(k)}}{\partial \bar{r}} \right)_{\bar{r}=r^*} \quad (II.I.2)$$

$$\Phi_{oj}^{(k)}(x) = 2(1 - r^*) \left(\frac{\partial \theta_j^{(k)}}{\partial \bar{r}} \right)_{\bar{r}=1} \quad (II.I.3)$$

The $\theta_{mj}^{(k)}$ may be obtained from (I.B.11) or, since $\theta_{mj}^{(k)} = 0$ at $\bar{x} = 0$, from consideration of an energy balance on the flowing fluid. We see that

$$\frac{\partial \theta_{mj}^{(k)}}{\partial \bar{x}} = \frac{4}{1 + r^*} (r^* \Phi_{1j}^{(k)}(\bar{x}) + \Phi_{oj}^{(k)}(x)) \quad (II.I.4)$$

or

$$\theta_{mj}^{(k)}(\bar{x}) = \left(\frac{4}{1 + r^*} \right) \int_0^{\bar{x}} (r^* \Phi_{1j}^{(k)}(\bar{x}) + \Phi_{oj}^{(k)}(\bar{x})) d\bar{x} \quad (II.I.5)$$

The conventional treatment of problems of this sort generally involves the Nusselt Modulus. It is related to the θ 's and the Φ 's by

$$Nu_{lj}^{(k)} = \frac{\Phi_{lj}^{(k)}}{[\theta_{lj}^{(k)} - \theta_{mj}^{(k)}]} \quad (II.I.6)$$

1. The first kind

$$\theta_i^{(1)}(\bar{r}, \bar{x}) = \frac{\ln \bar{r}}{\ln r^*} + \sum_{n=0}^{\infty} (C_n)_i^{(1)} R_n^{(1)}(\bar{r}) e^{-(\lambda_n^2)^{(1)} \bar{x}} \quad \dots (II.I.7)$$

$$\begin{aligned} \Phi_{i1}^{(1)}(\bar{x}) &= \Phi_{i1}^{(1)}_{fd} \\ &- \sum_{n=0}^{\infty} 2(1 - r^*) (C_n)_i^{(1)} \left(\frac{dR_n^{(1)}}{d\bar{r}} \right)_{\bar{r}=r^*} e^{-(\lambda_n^2)^{(1)} \bar{x}} \end{aligned} \quad \dots (II.I.8)$$

$$\begin{aligned} \Phi_{o1}^{(1)}(\bar{x}) &= \Phi_{o1}^{(1)}_{fd} \\ &+ \sum_{n=0}^{\infty} 2(1 - r^*) (C_n)_i^{(1)} \left(\frac{dR_n^{(1)}}{d\bar{r}} \right)_{\bar{r}=1} e^{-(\lambda_n^2)^{(1)} \bar{x}} \end{aligned} \quad \dots (II.I.9)$$

$$\begin{aligned} \theta_{m1}^{(1)}(\bar{x}) &= \theta_{m1}^{(1)}_{fd} + \frac{4}{(1 + r^*)} \sum_{n=0}^{\infty} 2(1 - r^*) (C_n)_i^{(1)} \\ &\left[r^* \left(\frac{dR_n^{(1)}}{d\bar{r}} \right)_{\bar{r}=r^*} - \left(\frac{dR_n^{(1)}}{d\bar{r}} \right)_{\bar{r}=1} \right] \frac{e^{-(\lambda_n^2)^{(1)} \bar{x}}}{(\lambda_n^2)^{(1)}} \end{aligned} \quad (II.I.10)$$

$$Nu_{i1}^{(1)}(\bar{x}) = \frac{\Phi_{i1}^{(1)}(\bar{x})}{1 - \theta_{m1}^{(1)}(\bar{x})} \quad (II.I.11)$$

$$\text{Nu}_{o1}^{(1)}(\bar{x}) = \frac{\Phi_{o1}^{(1)}(\bar{x})}{-\theta_{m1}^{(1)}(\bar{x})} \quad (\text{II.I.12})$$

$$\theta_{11}^{(1)}(\bar{x}) = 1.0 \quad (\text{II.I.13})$$

$$\theta_{o1}^{(1)}(\bar{x}) = 0.0 \quad (\text{II.I.14})$$

$$\theta_o^{(1)}(\bar{r}, \bar{x}) = 1 - \frac{\ell n \bar{r}}{\ell n r^*} + \sum_{n=0}^{\infty} (C_n)_o^{(1)} R_n^{(1)}(\bar{r}) e^{-(\lambda_n^2)^{(1)} \bar{x}} \dots (\text{II.I.15})$$

$$\Phi_{oo}^{(1)}(\bar{x}) = \Phi_{oo}^{(1)} \Big|_{fd} + \sum_{n=0}^{\infty} 2(1 - r^*) (C_n)_o^{(1)} \left(\frac{dR_n^{(1)}}{d\bar{r}} \right)_{\bar{r}=1} e^{-(\lambda_n^2)^{(1)} \bar{x}} \quad (\text{II.I.16})$$

$$\Phi_{1o}^{(1)}(\bar{x}) = \Phi_{1o}^{(1)} \Big|_{fd} - \sum_{n=0}^{\infty} 2(1 - r^*) (C_n)_o^{(1)} \left(\frac{dR_n^{(1)}}{d\bar{r}} \right)_{\bar{r}=r^*} e^{-(\lambda_n^2)^{(1)} \bar{x}} \quad (\text{II.I.17})$$

$$\theta_{mo}^{(1)}(\bar{x}) = \theta_{mo}^{(1)} \Big|_{fd} + \frac{4}{(1 + r^*)} \sum_{n=0}^{\infty} 2(1 - r^*) (C_n)_o^{(1)} \left[r^* \left(\frac{dR_n^{(1)}}{d\bar{r}} \right)_{\bar{r}=r^*} - \left(\frac{dR_n^{(1)}}{d\bar{r}} \right)_{\bar{r}=1} \right] \frac{e^{-(\lambda_n^2)^{(1)} \bar{x}}}{(\lambda_n^2)^{(1)}} \quad (\text{II.I.18})$$

$$\text{Nu}_{00}^{(1)}(\bar{x}) = \frac{\Phi_{00}^{(1)}(\bar{x})}{1 - \theta_{m0}^{(1)}(\bar{x})} \quad (\text{II.I.19})$$

$$\text{Nu}_{10}^{(1)}(\bar{x}) = \frac{\Phi_{10}^{(1)}(\bar{x})}{-\theta_{m0}^{(1)}(\bar{x})} \quad (\text{II.I.20})$$

$$\theta_{00}^{(1)}(\bar{x}) = 1.0 \quad (\text{II.I.21})$$

$$\theta_{10}^{(1)}(\bar{x}) = 0.0 \quad (\text{II.I.22})$$

2. The second kind

$$\begin{aligned} \theta_1^{(2)}(\bar{r}, \bar{x}) = & \frac{r^*}{(1 + r^*)M(1 - r^*)^2} \left[\frac{(1 - B)}{2} (\bar{r}^2 - \ln \bar{r}) \right. \\ & - \frac{\bar{r}^4}{8} + \frac{Br^2}{2} \ln \bar{r} - \frac{(r^*)^2 M}{2} + \frac{(1 + \ln r^*)}{2} \\ & \left. - \frac{(r^*)^4}{8} \right] + (\theta_{11}^{(2)} - \theta_{m1}^{(2)})_{fd} + \frac{4r^*}{1 + r^*} \bar{x} \\ & + \sum_{n=1}^{\infty} (C_n)_1^{(2)} R_n^{(2)}(\bar{r}) e^{-(\lambda_n^2)^{(2)} \bar{x}} \end{aligned} \quad (\text{II.I.23})$$

$$\begin{aligned} \theta_{11}^{(2)}(\bar{x}) = & (\theta_{11}^{(2)} - \theta_{m1}^{(2)})_{fd} + \frac{4r^*}{1 + r^*} \bar{x} \\ & + \sum_{n=1}^{\infty} (C_n)_1^{(2)} R_n^{(2)}(r^*) e^{-(\lambda_n^2)^{(2)} \bar{x}} \end{aligned} \quad (\text{II.I.24})$$

$$\begin{aligned} \theta_{01}^{(2)}(\bar{x}) = & (\theta_{01}^{(2)} - \theta_{m1}^{(2)})_{fd} + \frac{4r^*}{1 + r^*} \bar{x} \\ & + \sum_{n=1}^{\infty} (C_n)_1^{(2)} R_n^{(2)}(1) e^{-(\lambda_n^2)^{(2)} \bar{x}} \end{aligned} \quad (\text{II.I.25})$$

$$\theta_{m1}^{(2)}(\bar{x}) = \left(\frac{4r^*}{1 + r^*} \right) \bar{x} \quad (\text{II.I.26})$$

$$\Phi_{11}^{(2)}(\bar{x}) = 1.0 \quad (\text{II.I.27})$$

$$\Phi_{01}^{(2)}(\bar{x}) = 0.0 \quad (\text{II.I.28})$$

$$\text{Nu}_{11}^{(2)}(\bar{x}) = \frac{1.0}{\theta_{11}^{(2)}(\bar{x}) - \theta_{m1}^{(2)}(\bar{x})} \quad (\text{II.I.29})$$

$$\begin{aligned} \theta_o^{(2)}(\bar{r}, \bar{x}) = & \frac{1}{(1 + r^*) M(1 - r^*)^2} \left\{ \frac{(1 - B)}{2} (\bar{r}^2 - 1) \right. \\ & - \frac{(\bar{r}^4 - 1)}{8} + \frac{B\bar{r}^2}{2} \ln \bar{r} - \frac{(r^*)^2}{2} [(r^*)^2 - B] \ln \bar{r} \Big\} \\ & - (\theta_{oo}^{(2)} - \theta_{mo}^{(2)})_{fd} + \frac{4}{(1 + r^*)} \bar{x} \\ & + \sum_{n=1}^{\infty} (C_n)_o^{(2)} R_n^{(2)}(\bar{r}) e^{-(\lambda_n^2)^{(2)}\bar{x}} \end{aligned} \quad (\text{II.I.30})$$

$$\begin{aligned} \theta_{oo}^{(2)}(\bar{x}) = & (\theta_{oo}^{(2)} - \theta_{mo}^{(2)})_{fd} + \frac{4\bar{x}}{(1 + r^*)} \\ & + \sum_{n=1}^{\infty} (C_n)_o^{(2)} R_n^{(2)}(1) e^{-(\lambda_n^2)^{(2)}\bar{x}} \end{aligned} \quad (\text{II.I.31})$$

$$\begin{aligned} \theta_{1o}^{(2)}(\bar{x}) = & (\theta_{1o}^{(2)} - \theta_{mo}^{(2)})_{fd} + \frac{4\bar{x}}{(1 + r^*)} \\ = & \sum_{n=1}^{\infty} (C_n)_o^{(2)} R_n^{(2)}(r^*) e^{-(\lambda_n^2)^{(2)}\bar{x}} \end{aligned} \quad (\text{II.I.32})$$

$$\theta_{mo}^{(2)}(\bar{x}) = \frac{4\bar{x}}{(1 + r^*)} \quad (\text{II.I.33})$$

$$\Phi_{oo}^{(2)}(\bar{x}) = 1.0 \quad (\text{II.I.34})$$

$$\Phi_{1o}^{(2)}(\bar{x}) = 0.0 \quad (\text{II.I.35})$$

$$Nu_{oo}^{(2)} = \frac{1.0}{\theta_{oo}^{(2)}(\bar{x}) - \theta_{mo}^{(2)}(\bar{x})} \quad (II.I.36)$$

3. The third kind

$$\theta_1^{(3)}(\bar{r}, \bar{x}) = 1 + \sum_{n=0}^{\infty} (C_n)_1^{(3)} (R_n(\bar{r}))_1^{(3)} e^{-(\lambda_n^2)_1^{(3)} \bar{x}} \quad (II.I.37)$$

$$\begin{aligned} \Phi_{11}^{(3)}(\bar{x}) = & - \sum_{n=0}^{\infty} 2(1 - r^*) (C_n)_1^{(3)} \left\{ \frac{d[(R_n(\bar{r}))_1^{(3)}]}{d\bar{r}} \right\}_{\bar{r}=r^*} \\ & e^{-(\lambda_n^2)_1^{(3)} \bar{x}} \end{aligned} \quad \dots (II.I.38)$$

$$\Phi_{o1}^{(3)}(\bar{x}) = 0.0 \quad (II.I.39)$$

$$\theta_{o1}^{(3)}(\bar{x}) = 1 + \sum_{n=0}^{\infty} (C_n)_1^{(3)} (R_n(1))_1^{(3)} e^{-(\lambda_n^2)_1^{(3)} \bar{x}} \quad (II.I.40)$$

$$\theta_{11}^{(3)}(\bar{x}) = 1.0 \quad (II.I.41)$$

$$\begin{aligned} \theta_{m1}^{(3)}(\bar{x}) = & 1 + \frac{4r^*}{1 + r^*} \sum_{n=0}^{\infty} 2(1 - r^*) (C_n)_1^{(3)} \\ & \left\{ \frac{d[(R_n(\bar{r}))_1^{(3)}]}{d\bar{r}} \right\}_{\bar{r}=r^*} \frac{e^{-(\lambda_n^2)_1^{(3)} \bar{x}}}{(\lambda_n^2)_1^{(3)}} \end{aligned} \quad (II.I.42)$$

$$Nu_{11}^{(3)}(\bar{x}) = \frac{\Phi_{11}^{(3)}(\bar{x})}{1 - \theta_{m1}^{(3)}(\bar{x})} \quad (II.I.43)$$

For this case the limiting value of the Nusselt number as \bar{x} becomes large is of considerable interest and was not apparent from the asymptotic analysis of section II.D. If we write out the series expressions appearing in (II.I.41), and notice that as $x \rightarrow \infty$ only the leading

terms of these series make any contribution, we obtain

$$Nu_{11}^{(3)} \big|_{fd} = \frac{1 + r^*}{4r^*} (\lambda_1^2)_1^{(3)} \quad (II.I.44)$$

$$\theta_o^{(3)}(\bar{r}, \bar{x}) = 1 + \sum_{n=0}^{\infty} (c_n)_o^{(3)} (R_n(\bar{r}))_o^{(3)} e^{-(\lambda_n^2)_o^{(3)} \bar{x}} \dots (II.I.45)$$

$$\theta_{oo}^{(3)}(\bar{x}) = 1.0 \quad (II.I.46)$$

$$\theta_{1o}^{(3)}(\bar{x}) = 1 + \sum_{n=0}^{\infty} (c_n)_o^{(3)} (R_n(r^*))_o^{(3)} e^{-(\lambda_n^2)_o^{(3)} \bar{x}} \quad (II.I.47)$$

$$\phi_{oo}^{(3)}(\bar{x}) = \sum_{n=0}^{\infty} 2(1 - r^*) (c_n)_o^{(3)} \left\{ \frac{d[(R_n(\bar{r}))_o^{(3)}]}{d\bar{r}} \right\}_{\bar{r}=1} e^{-(\lambda_n^2)_o^{(3)} \bar{x}} \quad (II.I.48)$$

$$\phi_{1o}^{(3)}(\bar{x}) = 0.0 \quad (II.I.49)$$

$$\theta_{mo}^{(3)}(\bar{x}) = 1 - \frac{4}{(1 + r^*)} \sum_{n=0}^{\infty} 2(1 - r^*) (c_n)_o^{(3)} \left\{ \frac{d[(R_n(\bar{r}))_o^{(3)}]}{d\bar{r}} \right\}_{\bar{r}=1} \frac{e^{-(\lambda_n^2)_o^{(3)} \bar{x}}}{(\lambda_n^2)_o^{(3)}} \quad (II.I.50)$$

$$Nu_{oo}^{(3)}(\bar{x}) = \frac{\phi_{oo}^{(3)}(x)}{1 - \theta_{mo}^{(3)}(\bar{x})} \quad (II.I.51)$$

$$Nu_{oo}^{(3)} \big|_{fd} = \frac{1 + r^*}{4} (\lambda_1^2)_o^{(3)} \quad (II.I.52)$$

The solution of the third kind, when the temperature step

is applied at the outer wall is the extension of the classical Graetz problem and reduces to it at $r^* = 0$.

4. The fourth kind

$$\theta_1^{(4)}(\bar{r}, \bar{x}) = \frac{-r^*}{2(1-r^*)} \ln \bar{r} + \sum_{n=0}^{\infty} (C_n)_1^{(4)} (R_n(\bar{r}))_1^{(4)} e^{-(\lambda_n^2)_1^{(4)} \bar{x}} \quad (\text{II.I.53})$$

$$\theta_{11}^{(4)}(\bar{x}) = \theta_{11}^{(4)}_{fd} + \sum_{n=0}^{\infty} (C_n)_1^{(4)} (R_n(r^*))_1^{(4)} e^{-(\lambda_n^2)_1^{(4)} \bar{x}} \quad \dots (\text{II.I.54})$$

$$\theta_{o1}^{(4)}(\bar{x}) = 0.0 \quad (\text{II.I.55})$$

$$\Phi_{11}^{(4)}(\bar{x}) = 1.0 \quad (\text{II.I.56})$$

$$\Phi_{o1}^{(4)}(\bar{x}) = \Phi_{o1}^{(4)}_{fd} + \sum_{n=0}^{\infty} 2(1-r^*) (C_n)_1^{(4)} \left\{ \frac{d[(R_n(\bar{r}))_1^{(4)}]}{d\bar{r}} \right\}_{\bar{r}=1} e^{-(\lambda_n^2)_1^{(4)} \bar{x}} \quad (\text{II.I.57})$$

$$\theta_{m1}^{(4)}(\bar{x}) = \theta_{m1}^{(4)}_{fd} - \frac{4}{1+r^*} \sum_{n=0}^{\infty} 2(1-r^*) (C_n)_1^{(4)} \left\{ \frac{d[(R_n(\bar{r}))_1^{(4)}]}{d\bar{r}} \right\}_{\bar{r}=1} \frac{e^{-(\lambda_n^2)_1^{(4)} \bar{x}}}{(\lambda_n^2)_1^{(4)}} \quad (\text{II.I.58})$$

$$Nu_{11}^{(4)} = \frac{1.0}{\theta_{11}^{(4)}(\bar{x}) - \theta_{m1}^{(4)}(\bar{x})} \quad (\text{II.I.59})$$

$$Nu_{o1}^{(4)} = \frac{\Phi_{o1}^{(4)}(\bar{x})}{-\theta_{m1}^{(4)}(\bar{x})} \quad (\text{II.I.60})$$

$$\theta_o^{(4)}(\bar{r}, \bar{x}) = \frac{1}{2(1 - r^*)} \ln \left(\frac{\bar{r}}{r^*} \right) + \sum_{n=0}^{\infty} (C_n)_o^{(4)} (R_n(\bar{r}))_o^{(4)} e^{-(\lambda_n^2)_o^{(4)} \bar{x}} \quad (\text{II.I.61})$$

$$\theta_{oo}^{(4)}(\bar{x}) = \theta_{oo}^{(4)} \Big|_{fd} + \sum_{n=0}^{\infty} (C_n)_o^{(4)} (R_n(1))_o^{(4)} e^{-(\lambda_n^2)_o^{(4)} \bar{x}} \quad (\text{II.I.62})$$

$$\theta_{1o}^{(4)}(\bar{x}) = 0.0 \quad (\text{II.I.63})$$

$$\Phi_{oo}^{(4)}(\bar{x}) = 1.0 \quad (\text{II.I.64})$$

$$\Phi_{1o}^{(4)}(\bar{x}) = \Phi_{1o}^{(4)} \Big|_{fd} - \sum_{n=0}^{\infty} 2(1 - r^*) (C_n)_o^{(4)} \left\{ \frac{d \left[(R_n(\bar{r}))_o^{(4)} \right]}{d\bar{r}} \right\}_{\bar{r}=r^*} e^{-(\lambda_n^2)_o^{(4)} \bar{x}} \quad (\text{II.I.65})$$

$$\theta_{mo}^{(4)}(\bar{x}) = \theta_{mo}^{(4)} \Big|_{fd} + \frac{4r^*}{(1 + r^*)} \sum_{n=0}^{\infty} 2(1 - r^*) (C_n)_o^{(4)} \left\{ \frac{d \left[(R_n(\bar{r}))_o^{(4)} \right]}{d\bar{r}} \right\}_{\bar{r}=r^*} \frac{e^{-(\lambda_n^2)_o^{(4)} \bar{x}}}{(\lambda_n^2)_o^{(4)}} \quad (\text{II.I.66})$$

$$Nu_{oo}^{(1)}(\bar{x}) = \frac{1.0}{\theta_{oo}^{(4)}(\bar{x}) - \theta_{mo}^{(4)}(\bar{x})} \quad (\text{II.I.67})$$

$$Nu_{1o}^{(4)}(\bar{x}) = \frac{\Phi_{1o}^{(4)}(\bar{x})}{-\theta_{mo}^{(4)}(\bar{x})} \quad (\text{II.I.68})$$

The values calculated for the various geometries are presented in tables II.I.1 to II.I.8 and figures II.I.1 to II.I.12.

As is indicated by the preceding formulas, the values of interest at any axial station, \bar{x} , are obtained by adding or subtracting the series of the eigenfunctions to the fully established or terminal values. In all the cases where $\bar{x} \geq 1.0$ the terminal values have (or very nearly have) been obtained. As \bar{x} diminishes the series represents a progressively greater part of the local value. Since the series contains an exponential term, $e^{-\lambda_n^2 \bar{x}}$, the larger values of \bar{x} receive only the contribution of the first few terms, which are known very precisely from the machine calculation. For values of $\bar{x} \leq 0.01$, however, the higher terms (those beyond $n = 3$ or 4 in the present case) have begun to contribute. These terms are obtained from the graphical method described in section II.G and from the asymptotic (large λ) solutions. While the machine calculation easily provides 5 or 6 significant figures, the terms beyond the third or fourth are known only to 1 or 2 percent and, accordingly, the level of confidence in the values of the fundamental solutions diminishes with \bar{x} .

Those quantities which start from zero at $\bar{x} = 0$ and increase to their terminal values somewhere downstream are particularly affected by this uncertainty since, for small values of \bar{x} , the absolute values of these quantities are provided by the differences of nearly equal quantities and the uncertainty in the series represents a large fraction of the residual values.

An effort is made, in the tables, to represent the confidence in the recorded values by the number of significant figures retained. Fortunately the physical nature of the problem provides some internal checks on the

accuracy, i.e. for small \bar{x} $\phi_{11}^{(1)}$ approaches $\phi_{11}^{(3)}$, $\theta_{11}^{(2)}$ approaches $\theta_{11}^{(4)}$, etc. From these considerations it appears that the values of the series used for the wall values at $\bar{x} = 10^{-4}$ are within ± 1 percent of the actual or correct values. At this value of \bar{x} , $\phi_{11}^{(1)}$ and $\phi_{11}^{(3)}$ are reliable to ± 1 percent, and $\theta_{11}^{(2)}$ and $\theta_{11}^{(4)}$ are (because they have diminished in absolute value) reliable to ± 5 percent.

The opposite wall values (e.g. $\theta_{01}^{(2)}$) diminish rather rapidly and in all the cases for $\bar{x} \leq 0.01$ they are substantially zero (less than 0.1 percent of terminal value).

For very small values of \bar{x} the Leveque approximations provide a good estimate for the applicable quantities. For all cases where the non-zero boundary condition is at the outer wall, and for the inner wall heated cases with $r^* \geq 0.5$, the Leveque solution agrees well with the computation at $\bar{x} = 10^{-4}$. For small values of r^* , when the heating is at the inner wall it appears that the approximate solution will not become valid until \bar{x} is very small. For $r^* = 0.02$, $\bar{x} \leq 10^{-6}$ seems to be required, but for $r^* \geq 0.05$, $\bar{x} \leq 10^{-5}$ appears adequate.

This difficulty arises from the neglect of the curvature term in equation (II.E.5). For small values of r^* the depth of penetration of the temperature signal must be very small before this is justified.

The graphical representation of the fundamental solutions provides a very convenient method of superposition to construct the more complicated boundary conditions. Examples of this are presented in appendix G.

THE FUNDAMENTAL SOLUTIONS OF THE FIRST KIND TEMPERATURE STEP AT THE INNER WALL														
r^*	\bar{x}	$\phi_{11}^{(1)}$	ϕ_{01}	$\theta_{m1}^{(1)}$	$Nu_{11}^{(1)}$	$Nu_{01}^{(1)}$	r^*	\bar{x}	$\phi_{11}^{(1)}$	ϕ_{01}	$\theta_{m1}^{(1)}$	$Nu_{11}^{(1)}$	$Nu_{01}^{(1)}$	
0.02	0.0001	78.5	-	0.0011	78.6	-	0.25	1.0	7.8173	-0.78173	0.25256	10.459	3.0953	
	0.00015	72.3	-	0.0014	72.4	-		∞	7.8173	-0.78173	0.25256	10.459	3.0953	
	0.00025	65.4	-	0.0019	65.5	-		0.0001	31.9	-	0.0038	32.1	-	
	0.0005	57.5	-	0.0031	57.7	-		0.00015	28.2	-	0.0050	28.3	-	
	0.001	50.87	-	0.00523	51.2	-		0.00025	24.1	-	0.0071	24.2	-	
	0.0015	47.51	-	0.00715	47.85	-		0.0005	19.5	-	0.0113	19.7	-	
	0.0025	43.77	-	0.01070	44.20	-		0.001	15.84	-	0.0183	16.1	-	
	0.005	39.28	-	0.01877	40.03	-		0.0015	14.07	-	0.0242	14.42	-	
	0.01	35.475	-0.00143	0.03332	36.70	0.0430		0.0025	12.14	-	0.0346	12.57	-	
	0.015	33.495	-0.0125	0.04670	35.136	0.2678		0.005	9.978	-	0.0564	10.57	-	
	0.025	31.207	-0.06959	0.07048	33.574	0.9873		0.01	8.2381	-0.00763	0.0923	9.0756	0.0827	
	0.05	28.381	-0.24089	0.11297	31.996	2.1323		0.015	7.3765	-0.0505	0.12296	8.4106	0.1103	
	0.1	26.124	-0.41628	0.15149	30.788	2.7478		0.025	6.4213	-0.2242	0.17352	7.7695	0.1293	
	0.15	25.399	-0.47357	0.16398	30.381	2.8873		0.05	5.3148	-0.63984	0.25334	7.1182	0.2526	
	0.25	25.087	-0.49814	0.16934	30.202	2.8873		0.1	4.5666	-0.97446	0.31231	6.6406	3.1202	
0.05	0.5	25.051	-0.50101	0.16997	30.181	2.9477	0.5	0.15	4.3859	-1.0559	0.32662	6.5133	3.2329	
	1.0	25.051	-0.50102	0.16997	30.181	2.9477		0.25	4.3315	-1.0805	0.33093	6.4739	3.2650	
	∞	25.051	-0.50102	0.16997	30.181	2.9477		0.5	4.3281	-1.0820	0.33120	6.4714	3.2670	
	0.0001	52.0	-	0.0014	52.1	-		1.0	4.3281	-1.0820	0.33120	6.4714	3.2670	
	0.00015	47.0	-	0.0018	47.1	-		∞	4.3281	-1.0820	0.33120	6.4714	3.2670	
	0.00025	41.6	-	0.0027	41.70	-		0.5	28.3	-	0.0058	28.5	-	
	0.0005	35.4	-	0.0045	35.6	-		0.00015	24.8	-	0.0076	25.0	-	
	0.001	30.44	-	0.0076	30.67	-		0.00025	21.0	-	0.0106	21.2	-	
	0.0015	27.95	-	0.01036	28.24	-		0.0005	16.7	-	0.0168	17.0	-	
	0.0025	25.19	-	0.01539	25.59	-		0.001	13.34	-	0.0266	13.70	-	
	0.005	22.03	-	0.02652	22.63	-		0.0015	11.70	-	0.0349	12.12	-	
	0.01	19.397	-0.00247	0.04606	20.334	0.0536		0.0025	9.916	-	0.0492	10.43	-	
	0.015	18.052	-0.0198	0.06366	19.279	0.311		0.005	7.930	-	0.0784	8.605	-	
	0.025	16.521	-0.1018	0.09426	18.241	1.080		0.01	6.3406	-0.0116	0.1251	7.2476	0.0928	
	0.1	0.05	14.671	-0.32906	0.14681	17.195		2.2414	1.0	0.01	5.596	-0.0751	0.16406	6.6496
0.1		13.269	-0.54371	0.19140	16.409	2.8408	0.015	4.6975		-0.3212	0.22672	6.0747	0.477	
0.15		12.857	-0.60751	0.20457	16.164	2.9697	0.025	3.7131		-0.88454	0.28575	5.4811	2.7423	
0.25		12.700	-0.63191	0.20961	16.068	3.0147	0.05	3.0728		-0.13156	0.35014	5.0385	3.3723	
0.5		12.685	-0.63423	0.21009	16.058	3.0189	0.1	2.9279		-0.14139	0.40548	4.9249	3.4869	
1.0		12.685	-0.63424	0.21009	16.058	3.0189	0.15	2.8876		-0.14412	0.40975	4.8922	3.5173	
∞		12.685	-0.63424	0.21009	16.058	3.0189	0.25	2.8854		-0.14427	0.40999	4.8904	3.5189	
0.0001		40.4	-	0.0022	40.4	-	0.5	2.8854		-0.14427	0.40999	4.8904	3.5189	
0.00015		36.0	-	0.0028	36.1	-	∞	2.8854		-0.14427	0.40999	4.8904	3.5189	
0.00025		31.4	-	0.0041	31.5	-	1.0	0.0025		19.1	-	0.0145	19.4	
0.0005		26.1	-	0.0066	26.3	-	0.0025	15.64		-	0.0660	16.248	-	
0.001		21.95	-	0.0110	22.19	-	0.01	12.421		-0.0170	0.16248	12.591	0.105	
0.0015		19.19	-	0.0147	20.18	-	0.015	10.515		-0.1084	0.21032	10.154	0.5154	
0.0025		17.62	-	0.0215	18.01	-	0.025	8.6875		-0.4571	0.28586	9.7004	1.5990	
0.005		15.04	-	0.0362	15.60	-	0.05	7.6163		-1.2423	0.39926	8.3066	3.1115	
0.15	0.01	12.918	-0.0030309	0.0613	13.762	0.0641	0.5	0.075	6.3574	-1.6427	0.45261	6.5970	3.6294	
	0.015	11.851	-0.029231	0.0835	12.931	0.350		0.10	5.2161	-1.8319	0.47770	6.3066	3.8348	
	0.025	10.651	-0.14091	0.1212	12.121	1.162		0.125	4.2791	-1.9309	0.48951	6.0728	3.9241	
	0.05	9.2272	-0.43067	0.1838	11.305	2.3429		0.150	3.6372	-1.9628	0.49507	5.9346	3.9647	
	0.1	8.1989	-0.68601	0.23388	10.702	2.9332		0.250	3.0018	-1.9982	0.50000	5.8000	4.0000	
	0.15	7.9209	-0.75573	0.24748	10.526	3.0537		∞	2.0000	-2.0000	0.50000	5.8000	4.0000	
	0.25	7.8249	-0.77981	0.25218	10.464	3.0923		1.0	0.0025	19.1	-	0.0145	19.4	4.0000
	0.5	7.8173	-0.78173	0.25256	10.459	3.0953		0.0025	15.64	-	0.0660	16.248	-	
	0.0001	40.4	-	0.0022	40.4	-		0.01	12.421	-0.0170	0.16248	12.591	0.105	
	0.00015	36.0	-	0.0028	36.1	-		0.015	10.515	-0.1084	0.21032	10.154	0.5154	
	0.00025	31.4	-	0.0041	31.5	-		0.025	8.6875	-0.4571	0.28586	9.7004	1.5990	
	0.0005	26.1	-	0.0066	26.3	-		0.05	7.6163	-1.2423	0.39926	8.3066	3.1115	
	0.001	21.95	-	0.0110	22.19	-		0.075	6.3574	-1.6427	0.45261	6.5970	3.6294	
	0.0015	19.19	-	0.0147	20.18	-		0.10	5.2161	-1.8319	0.47770	6.3066	3.8348	
	0.0025	17.62	-	0.0215	18.01	-		0.125	4.2791	-1.9309	0.48951	6.0728	3.9241	

TABLE II.I.1

THE FUNDAMENTAL SOLUTIONS OF THE FIRST KIND
TEMPERATURE STEP AT THE OUTER WALL

r^*	\bar{x}	$\phi_{oo}(1)$	$\phi_{1o}(1)$	$\theta_{mo}(1)$	$Nu_{oo}(1)$	$Nu_{1o}(1)$	r^*	\bar{x}	$\phi_{oo}(1)$	$\phi_{1o}(1)$	$\theta_{mo}(1)$	$Nu_{oo}(1)$	$Nu_{1o}(1)$
0.02	0.0001	23.0	-	0.015	23.3	-	0.25	0.0001	3.3450	-0.2909	0.3117	4.8595	0.9334
	0.00015	19.9	-	0.019	20.3	-		0.00015	2.5719	-1.4080	0.4148	4.3949	3.3943
	0.00025	16.6	-	0.026	17.0	-		0.05	1.6696	-4.3061	0.51485	3.9270	7.4907
	0.0005	12.9	-	0.040	13.4	-		0.1	1.0219	-6.8599	0.70058	3.4130	9.7917
	0.001	9.961	-	0.062	10.6	-		0.15	0.84697	-7.58725	0.73472	3.1927	10.280
	0.0015	8.538	-	0.080	9.281	-		0.25	0.78654	-7.77981	0.74651	3.1028	10.440
	0.0025	6.996	-	0.110	7.862	-		0.5	0.78174	-7.8173	0.74744	3.0953	10.459
	0.005	5.270	-	0.169	6.341	-		∞	0.78173	-7.8173	0.74744	3.0953	10.459
	0.01	3.8806	-0.146	0.2566	5.2201	0.467			24.1	-	0.011	24.4	-
	0.015	3.1941	-0.6992	0.32524	4.7337	2.150		0.0001	20.9	-	0.015	21.3	-
	0.025	2.4341	-3.5457	0.43244	4.2888	8.1993		0.00015	17.5	-	0.021	17.9	-
	0.05	1.5372	-12.085	0.60536	3.8952	19.963		0.00025	13.7	-	0.034	14.1	-
	0.1	0.8463	-20.827	0.75731	3.4390	27.501		0.0005	10.61	-	0.053	11.20	-
	0.15	6.0908	-23.683	0.80647	3.1473	29.365		0.001	9.124	-	0.068	9.793	-
	0.25	5.1236	-24.907	0.82756	2.9478	30.097		0.0015	7.514	-	0.095	1.300	-
	0.5	5.0106	-25.050	0.83002	2.9477	30.181		0.0025	5.717	-	0.144	6.698	-
	1.0	5.0102	-25.051	0.83003	2.9477	30.181		0.005	4.2772	-0.0292	0.225	5.5171	0.1301
	∞	5.0102	-25.051	0.83003	2.9477	30.181		0.01	3.5684	-0.2007	0.2866	5.0019	0.7004
0.05	0.0001	23.3	-	0.014	23.6	-		0.015	2.7863	-0.89618	0.38271	4.5138	2.3417
	0.00015	20.2	-	0.018	20.5	-		0.025	1.8847	-2.5590	0.52830	3.9956	4.8438
	0.00025	16.8	-	0.025	17.2	-		0.05	1.2761	-3.8977	0.63474	3.4936	6.1407
	0.0005	13.1	-	0.039	13.6	-		0.1	1.1291	-4.2237	0.66054	3.3261	6.3943
	0.001	10.1	-	0.060	10.8	-		0.15	1.0848	-4.3219	0.66832	3.2706	6.4669
	0.0015	8.668	-	0.078	9.403	-		0.25	1.0820	-4.3281	0.66880	3.2670	6.4714
	0.0025	7.103	-	0.108	7.962	-		0.5	1.0820	-4.3281	0.66880	3.2670	6.4714
	0.005	5.355	-	0.1669	6.420	-		∞	1.0820	-4.3281	0.66880	3.2670	6.4714
	0.01	3.9515	-0.0419	0.2525	5.2861	0.166			25.0	-	0.098	25.2	-
	0.015	3.2583	-0.3887	0.3204	4.7944	1.213		0.0001	21.7	-	0.013	22.0	-
	0.025	2.4912	-2.0299	0.42617	4.3414	4.7632		0.00015	18.1	-	0.018	18.5	-
	0.05	1.5901	-6.5777	0.59338	3.9106	11.085		0.00025	14.2	-	0.029	14.6	-
	0.1	0.91511	-10.873	0.73191	3.4135	14.856		0.0005	11.08	-	0.045	11.6	-
	0.15	0.71716	-12.150	0.77279	3.1563	15.722		0.001	9.564	-	0.059	10.16	-
	0.25	0.64447	-12.638	0.78842	3.0317	16.030		0.0015	7.919	-	0.082	8.627	-
	0.5	0.63425	-12.685	0.78991	3.0389	16.058		0.0025	6.080	-	0.128	6.978	-
	1.0	0.63424	-12.685	0.78991	3.0389	16.058		0.005	4.6214	-0.0322	0.198	5.7600	0.117
	∞	0.63424	-12.685	0.78991	3.0389	16.058		0.01	3.9025	-0.4501	0.2530	5.2285	0.5920
0.1	0.0001	23.6	-	0.013	23.9	-		0.015	3.1088	-0.64244	0.34078	4.7160	1.8352
	0.00015	20.4	-	0.017	20.8	-		0.025	2.2037	-1.7691	0.47143	4.1692	3.7525
	0.00025	17.0	-	0.024	17.5	-		0.05	1.6150	-2.6113	0.56310	3.6964	4.6729
	0.0005	13.3	-	0.037	13.8	-		0.01	1.4818	-2.8277	0.58390	3.5612	4.8428
	0.001	10.27	-	0.058	10.9	-		0.15	1.4447	-2.8824	0.58970	3.5211	4.8880
	0.0015	8.808	-	0.076	9.53	-		0.25	1.4427	-2.8854	0.59001	3.5189	4.8904
	0.0025	7.227	-	0.104	8.070	-		0.5	1.4427	-2.8854	0.59001	3.5189	4.8904
	0.005	5.461	-	0.16	6.508	-		∞	1.4427	-2.8854	0.59001	3.5189	4.8904
	0.01	4.041	-0.0409	0.2453	5.3534	0.154			25.0	-	0.098	25.2	-

TABLE II.1.2

THE FUNDAMENTAL SOLUTIONS OF THE SECOND KIND
INNER WALL HEATED

r^*	\bar{x}	$(\theta_{11} - \theta_{ml})_{ml}$	$(\theta_{01} - \theta_{ml})_{ml}$	θ_{ml}	Nu_{11}	r^*	\bar{x}	$(\theta_{11} - \theta_{ml})_{ml}$	$(\theta_{01} - \theta_{ml})_{ml}$	θ_{ml}	Nu_{11}
0.02	0.0001	0.0109	-0.0578431	0.0578431	91.9	0.25	0.50	0.083992	-0.011622	0.18181	11.905
	0.00015	0.0121	-0.0411765	0.0411765	82.7		1.00	0.083992	-0.011622	0.36363	11.905
	0.00025	0.0137	-0.0419608	0.0419608	73.2		∞	0.083992	-0.011622	∞	11.905
	0.0005	0.0159	-0.0439216	0.0439216	62.9						
	0.001	0.0182	-0.0478431	0.0478431	54.8						
	0.0015	0.0196	-0.0411765	0.0411765	50.9		0.0001	0.0253	-0.0480000	0.048000	39.5
	0.0025	0.02145	-0.0319608	0.0319608	46.63		0.00015	0.0291	-0.0312000	0.031200	34.4
	0.005	0.02389	-0.0339216	0.0339216	41.86		0.00025	0.0344	-0.0320000	0.032000	29.1
	0.010	0.02652	-0.0378431	0.0378431	38.093		0.0005	0.0429	-0.0340000	0.034000	23.3
	0.015	0.027534	-0.0011765	0.0011765	36.319		0.0010	0.0530	-0.0380000	0.038000	18.9
	0.025	0.028938	-0.0017265	0.0017265	34.556		0.0015	0.05863	-0.0012000	0.001200	16.77
	0.05	0.030188	-0.0023548	0.0023548	33.126		0.0025	0.06887	-0.0020000	0.002000	14.52
	0.10	0.030554	-0.0025470	0.0025470	32.729		0.0050	0.08280	-0.0039660	0.003966	12.08
	0.15	0.030575	-0.025581	0.025581	32.705		0.010	0.097798	-0.0079365	0.007936	10.2251
	0.25	0.030576	-0.0025589	0.019607	32.705		0.025	0.106554	-0.011639	0.011639	9.3848
	0.50	0.030576	-0.0025589	0.039215	32.705		0.05	0.116623	-0.017318	0.017318	8.5746
	1.0	0.030576	-0.0025589	0.078431	32.705		0.10	0.125964	-0.023475	0.023475	7.9287
	∞			∞			0.15	0.128963	-0.025395	0.025395	7.7541
							0.25	0.128974	-0.025520	0.025520	7.535
							0.50	0.128974	-0.025520	0.025520	7.535
							∞	0.128974	-0.025520	∞	7.535
0.05	0.0001	0.0172	-0.0419047	0.0419047	58.0	0.5	0.0001	0.0289	-0.031333	0.031333	34.6
	0.00015	0.0193	-0.0428571	0.0428571	51.9		0.00015	0.0331	-0.031333	0.031333	30.3
	0.00025	0.0220	-0.0447019	0.0447019	45.5		0.00025	0.0391	-0.033333	0.033333	25.6
	0.00050	0.0259	-0.0495238	0.0495238	38.6		0.0005	0.0490	-0.036667	0.036667	20.4
	0.0010	0.0301	-0.0419047	0.0419047	33.2		0.0010	0.0611	-0.031333	0.031333	16.4
	0.0015	0.03277	-0.0328571	0.0328571	30.52		0.0015	0.0693	-0.0220000	0.022000	14.4
	0.0025	0.03626	-0.0347619	0.0347619	27.58		0.0025	0.0809	-0.023333	0.023333	12.37
	0.0050	0.04132	-0.0395238	0.0395238	24.20		0.0050	0.0987	-0.026667	0.026667	10.13
	0.0100	0.046466	-0.0018993	0.0018993	21.521		0.010	0.11858	-0.013281	0.013281	8.433
	0.015	0.049314	-0.0027891	0.0027891	20.278		0.015	0.13041	-0.019437	0.019437	7.667
	0.025	0.052465	-0.0041662	0.0041662	19.061		0.025	0.14427	-0.038881	0.038881	6.931
	0.050	0.055273	-0.0055521	0.0055521	18.090		0.05	0.15741	-0.039220	0.039220	6.353
	0.10	0.056095	-0.0061010	0.0061010	17.827		0.10	0.16151	-0.042531	0.042531	6.192
	0.15	0.056141	-0.0061270	0.028571	17.812		0.15	0.16176	-0.042750	0.042750	6.182
	0.25	0.056144	-0.0061284	0.04761	17.811		0.25	0.16179	-0.042750	0.042750	6.181
	0.50	0.056144	-0.0061284	0.09523	17.811		0.50	0.16179	-0.042750	0.042750	6.181
	1.0	0.056144	-0.0061284	0.19047	17.811		∞	0.16179	-0.042750	∞	6.181
0.10	0.0001	0.0207	-0.0436363	0.0436363	48.3	1.0	0.0001	0.0425	-0.0005	0.0005	23.5
	0.00015	0.0235	-0.0454545	0.0454545	42.6		0.00015	0.04893	-0.005	0.005	11.2
	0.00025	0.0273	-0.0490909	0.0490909	36.7		0.00025	0.0893	-0.013352	0.013352	7.4895
	0.0005	0.0331	-0.0418181	0.0418181	30.2		0.0005	0.13352	-0.029147	0.029147	6.7732
	0.0010	0.0399	-0.0336363	0.0336363	25.1		0.0010	0.14764	-0.043309	0.043309	6.0857
	0.0015	0.0447	-0.0354545	0.0354545	22.64		0.0015	0.16432	-0.058882	0.058882	5.5160
	0.0025	0.04999	-0.0390909	0.0390909	20.01		0.0025	0.18031	-0.062906	0.062906	5.4248
	0.0050	0.05842	-0.0018180	0.0018180	17.12		0.0050	0.18562	-0.064196	0.064196	5.3874
	0.010	0.067108	-0.0036247	0.0036247	14.902		0.010	0.18571	-0.064286	0.064286	5.3847
	0.015	0.072001	-0.0053157	0.0053157	13.888		0.015	0.18571	-0.064286	0.064286	5.3847
	0.025	0.077494	-0.0079186	0.0079186	12.904		0.025	0.18571	-0.064286	0.064286	5.3847
	0.05	0.082452	-0.010719	0.010719	12.128		0.05	0.18571	-0.064286	0.064286	5.3847
	0.10	0.083900	-0.011562	0.036363	11.918		0.10	0.18571	-0.064286	0.064286	5.3847
	0.15	0.083988	-0.011618	0.054545	11.906		0.15	0.18571	-0.064286	0.064286	5.3847
	0.25	0.083992	-0.011622	0.090909	11.905		0.25	0.18571	-0.064286	0.064286	5.3847

TABLE II.1.3

THE FUNDAMENTAL SOLUTIONS OF THE SECOND KIND

OUTER WALL HEATED

r^*	\bar{x}	$(\theta_{00}^{(2)} - \theta_{10}^{(2)})$	$(\theta_{10}^{(2)} - \theta_{20}^{(2)})$	$\theta_{20}^{(2)}$	$Nu_{\infty}^{(2)}$	r^*	\bar{x}	$(\theta_{00}^{(2)} - \theta_{10}^{(2)})$	$(\theta_{10}^{(2)} - \theta_{20}^{(2)})$	$\theta_{20}^{(2)}$	$Nu_{\infty}^{(2)}$
0.02	0.0001	0.0341	-0.0339215	0.0339215	29.3	0.25	0.0001	0.0331	-0.0332000	0.0332000	30.2
	0.00015	0.0393	-0.0358823	0.0358823	25.4		0.00015	0.0381	-0.0348000	0.0348000	26.2
	0.00025	0.0470	-0.0398039	0.0398039	21.3		0.00025	0.0458	-0.0380000	0.0380000	22.0
	0.0005	0.0597	-0.0419607	0.0419607	16.8		0.00050	0.0575	-0.0416000	0.0416000	17.4
	0.001	0.07560	-0.0439215	0.0439215	13.2		0.0010	0.07248	-0.0432000	0.0432000	13.80
	0.0015	0.0856	-0.0458823	0.0458823	11.55		0.0015	0.08281	-0.0448000	0.0448000	12.08
	0.0025	0.1022	-0.0498039	0.0498039	9.784		0.0025	0.09760	-0.0480000	0.0480000	10.25
	0.005	0.1266	-0.0519078	0.0519078	7.898		0.0050	0.1208	-0.0516000	0.0516000	8.275
	0.010	0.15381	-0.0539094	0.0539094	6.5017		0.010	0.14700	-0.053883	0.053883	6.8025
	0.015	0.16999	-0.057546	0.057546	5.8828		0.015	0.16272	-0.056690	0.056690	6.1455
	0.025	0.18868	-0.06325	0.06325	5.2999		0.025	0.18110	-0.064040	0.064040	5.5217
	0.05	0.20595	-0.11773	0.11773	4.8579		0.050	0.19832	-0.094040	0.160000	5.0422
	0.10	0.21092	-0.12735	0.12735	4.7412		0.10	0.20354	-0.10172	0.320000	4.9128
	0.15	0.21121	-0.12791	0.12791	4.7346		0.15	0.20386	-0.10218	0.480000	4.9052
	0.25	0.21123	-0.12794	0.12794	4.7342		0.25	0.20388	-0.10231	0.800000	4.9047
	0.50	0.21123	-0.12794	0.12794	4.7342		0.50	0.20388	-0.10230	1.600000	4.9047
	1.00	0.21123	-0.12794	0.12794	4.7342		1.00	0.20388	-0.10230	3.200000	4.9047
	∞	0.21123	-0.12794	0.12794	4.7342		∞	0.20388	-0.10230	∞	4.9047
0.05	0.0001	0.0337	-0.0338095	0.0338095	29.7	0.5	0.0001	0.0325	-0.032666	0.032666	30.8
	0.00015	0.0389	-0.0357142	0.0357142	25.7		0.00015	0.0373	-0.0340000	0.0340000	26.8
	0.00025	0.0465	-0.0395238	0.0395238	21.5		0.00025	0.0443	-0.036666	0.036666	22.6
	0.00050	0.0591	-0.0419047	0.0419047	16.9		0.0005	0.0560	-0.0413333	0.0413333	17.9
	0.0010	0.0748	-0.0438095	0.0438095	13.4		0.001	0.07039	-0.042666	0.042666	14.21
	0.0015	0.0856	-0.0457142	0.0457142	11.7		0.0015	0.08033	-0.0440000	0.0440000	12.45
	0.0025	0.1011	-0.0495238	0.0495238	9.895		0.0025	0.09457	-0.046666	0.046666	10.57
	0.005	0.1252	-0.0519037	0.0519037	7.991		0.005	0.1170	-0.0513333	0.0513333	9.547
	0.010	0.15203	-0.0537987	0.0537987	6.5776		0.010	0.14232	-0.056561	0.056561	7.0265
	0.015	0.16803	-0.0575782	0.0575782	5.9514		0.015	0.15762	-0.063873	0.063873	6.3445
	0.025	0.18650	-0.063323	0.063323	5.3617		0.025	0.17565	-0.074763	0.074763	5.6031
	0.050	0.20344	-0.11304	0.11304	4.9155		0.050	0.19282	-0.08440	0.13333	5.1861
	0.10	0.20867	-0.12254	0.12254	4.7988		0.10	0.19818	-0.085060	0.26667	5.0458
	0.15	0.20867	-0.12257	0.12257	4.7919		0.15	0.19855	-0.085490	0.40000	5.0371
	0.25	0.20868	-0.12257	0.12257	4.7919		0.25	0.19855	-0.085510	0.66667	5.0365
	0.50	0.20868	-0.12257	0.12257	4.7919		0.50	0.19855	-0.085510	1.33333	5.0365
	1.00	0.20868	-0.12257	0.12257	4.7919		1.00	0.19855	-0.085510	2.66667	5.0365
	∞	0.20868	-0.12257	0.12257	4.7919		∞	0.19855	-0.085510	∞	5.0365
0.1	0.0001	0.0334	-0.0336363	0.0336363	29.9	0.1	0.0001	0.0334	-0.0336363	0.0336363	29.9
	0.00015	0.0386	-0.0354545	0.0354545	25.9		0.00015	0.0386	-0.0354545	0.0354545	25.9
	0.00025	0.0461	-0.0390909	0.0390909	21.7		0.00025	0.0461	-0.0390909	0.0390909	21.7
	0.0005	0.0586	-0.0418181	0.0418181	17.1		0.0005	0.0586	-0.0418181	0.0418181	17.1
	0.001	0.07406	-0.0436363	0.0436363	13.50		0.001	0.07406	-0.0436363	0.0436363	13.50
	0.0015	0.08470	-0.0454545	0.0454545	11.81		0.0015	0.08470	-0.0454545	0.0454545	11.81
	0.0025	0.09991	-0.0490909	0.0490909	10.01		0.0025	0.09991	-0.0490909	0.0490909	10.01
	0.005	0.1237	-0.051818	0.051818	8.083		0.005	0.1237	-0.051818	0.051818	8.083
	0.010	0.15034	-0.0536247	0.0536247	6.6517		0.010	0.15034	-0.0536247	0.0536247	6.6517
	0.015	0.16622	-0.0553158	0.0553158	6.0160		0.015	0.16622	-0.0553158	0.0553158	6.0160
	0.025	0.18333	-0.0600000	0.0600000	5.3333		0.025	0.18333	-0.0600000	0.0600000	5.3333
	0.050	0.20000	-0.0666667	0.0666667	4.5000		0.050	0.20000	-0.0666667	0.0666667	4.5000
	0.100	0.21667	-0.0714286	0.0714286	3.7500		0.100	0.21667	-0.0714286	0.0714286	3.7500
	0.200	0.23333	-0.0761905	0.0761905	3.0000		0.200	0.23333	-0.0761905	0.0761905	3.0000
	0.500	0.26667	-0.0833333	0.0833333	2.0000		0.500	0.26667	-0.0833333	0.0833333	2.0000
	1.000	0.28571	-0.0882353	0.0882353	1.5000		1.000	0.28571	-0.0882353	0.0882353	1.5000
	∞	0.28571	-0.0882353	0.0882353	1.5000		∞	0.28571	-0.0882353	0.0882353	1.5000

TABLE II.1.4

THE FUNDAMENTAL SOLUTIONS OF THE THIRD KIND
TEMPERATURE STEP AT THE INNER WALL

r^*	\bar{x}	$\phi_{ii}^{(3)}$	$\theta_{oi}^{(3)}$	$\theta_{mi}^{(3)}$	$Nu_{ii}^{(3)}$	r^*	\bar{x}	$\phi_{ii}^{(3)}$	$\theta_{oi}^{(3)}$	$\theta_{mi}^{(3)}$	$Nu_{ii}^{(3)}$
0.02	0.0001	78.0	-	0.001	78.4	0.25	0.0001	31.9	-	0.0038	32.0
	0.00015	71.9	-	0.0014	72.3	0.5	0.00015	28.1	-	0.0050	28.2
	0.00025	65.1	-	0.0019	65.5	1.0	0.00025	24.0	-	0.0071	24.2
	0.0005	57.3	-	0.0031	57.7	∞	0.0005	19.4	-	0.0113	19.7
	0.001	50.71	-	0.0052	51.2		0.001	15.82	-	0.0183	16.11
	0.0015	47.35	-	0.0071	47.92		0.0015	14.05	-	0.0242	14.40
	0.0025	43.62	-	0.0105	44.28		0.0025	12.13	-	0.0346	12.56
	0.005	39.19	-	0.0186	40.12		0.005	9.976	-	0.0564	10.47
	0.01	35.394	-	0.0331	36.775		0.01	8.2382	-	0.0923	9.0758
	0.015	33.412	0.0116	0.0470	35.209		0.015	7.3766	0.03575	0.12336	8.4147
	0.025	31.122	0.0129	0.0739	33.690		0.025	6.4209	0.00507	0.17815	7.8126
	0.05	28.207	0.01019	0.13407	32.574		0.05	5.2488	0.03177	0.29346	7.4289
	0.1	24.666	0.057292	0.23740	32.345		0.1	3.8763	0.14493	0.47417	7.3708
	0.15	21.723	0.16699	0.32824	32.338		0.15	2.8861	0.36106	0.68844	7.3708
	0.25	16.857	0.28613	0.47872	32.337		0.25	1.6024	0.52418	0.78288	7.3708
	0.5	8.9413	0.43053	0.72350	32.337		0.5	0.36844	0.93959	0.95028	7.3708
	1.0	2.5157	0.91501	0.92220	32.337		1.0	0.019212	0.99683	0.99739	7.3708
	∞	0.0	1.0000	1.0000			∞	0.0	1.0000	1.0000	7.3708
0.05	0.0001	51.5	-	0.0012	51.5	0.5	0.0001	28.2	-	0.0057	28.4
	0.00015	46.6	-	0.0015	46.6		0.00015	24.7	-	0.0075	24.9
	0.00025	41.2	-	0.0023	41.3		0.00025	20.9	-	0.0105	21.1
	0.0005	35.2	-	0.0041	35.3		0.0005	16.7	-	0.0166	17.0
	0.001	30.30	-	0.0072	30.5		0.001	13.32	-	0.0265	13.68
	0.0015	27.87	-	0.0099	28.15		0.0015	11.68	-	0.0347	12.10
	0.0025	25.16	-	0.0149	25.55		0.0025	9.909	-	0.0490	10.42
	0.005	22.03	-	0.0261	22.62		0.005	7.929	-	0.0782	8.602
	0.01	19.405	0.03195	0.04562	20.332		0.01	6.3407	0.03871	0.1250	7.2465
	0.015	18.060	0.00204	0.06341	19.282		0.015	5.5987	0.00729	0.1644	6.6527
	0.025	16.528	0.01488	0.09620	18.288		0.025	4.6968	0.04351	0.2322	6.1172
	0.05	14.605	0.078007	0.16980	17.592		0.05	3.6492	0.18808	0.3692	5.7851
	0.1	12.273	0.21677	0.29722	17.464		0.1	2.4675	0.44405	0.57004	5.7382
	0.15	10.391	0.33670	0.40489	17.461		0.15	1.6829	0.62075	0.70671	5.7382
	0.25	7.4510	0.52437	0.57326	17.460		0.25	0.78305	0.82354	0.86354	5.7382
	0.5	3.2443	0.79290	0.81419	17.460		0.5	0.11564	0.97394	0.97985	5.7382
	1.0	0.61508	0.96074	0.96477	17.460		1.0	0.0025220	0.99943	0.99956	5.7382
	∞	0.0	1.0000	1.0000			∞	0.0	1.0000	1.0000	5.7382
0.1	0.0001	40.4	-	0.0021	40.4	1.00	0.0001	8.64	-	0.0660	9.25
	0.00015	36.1	-	0.0028	36.2		0.00015	5.242	0.00119	0.1625	8.259
	0.00025	31.4	-	0.0040	31.5		0.00025	4.5014	0.00982	0.21093	7.4047
	0.0005	26.1	-	0.0065	26.3		0.0005	3.6868	0.05685	0.29193	6.2068
	0.001	21.94	-	0.0109	22.2		0.001	2.7028	0.23561	0.44867	5.2023
	0.0015	19.88	-	0.0146	20.2		0.0015	2.1021	0.39817	0.56800	4.8660
	0.0025	17.61	-	0.0214	18.00		0.0025	1.2914	0.6297	0.73433	4.8609
	0.005	15.04	-	0.0361	15.60		0.005	0.8308	0.89014	0.92119	4.8608
	0.01	12.920	0.03320	0.0612	13.76		0.01	0.44405	0.99033	1.0000	4.8608
	0.015	11.852	0.00301	0.0837	12.94		0.015	0.2708	-	-	-
	0.025	10.652	0.02049	0.1244	12.165		0.025	0.1625	-	-	-
	0.05	9.1600	0.1012	0.2136	11.648		0.05	0.03371	-	-	-
	0.1	7.3855	0.26918	0.36295	11.562		0.1	0.0	-	-	-
	0.15	5.9683	0.40768	0.49372	11.560		0.15	0.0	-	-	-

TABLE II.1.5

THE FUNDAMENTAL SOLUTIONS OF THE THIRD KIND
TEMPERATURE STEP AT THE OUTER WALL

r^*	\bar{x}	$\theta_{10}^{(3)}$	$\phi_{00}^{(3)}$	$\theta_{mo}^{(3)}$	$Nu_{00}^{(3)}$	r^*	\bar{x}	$\theta_{10}^{(3)}$	$\phi_{00}^{(3)}$	$\theta_{mo}^{(3)}$	$Nu_{00}^{(3)}$
0.02	0.0001	-	23.2	0.013	23.5	0.25	0.0001	0.0139	3.3450	0.3120	4.8616
	0.00015	-	20.1	0.017	20.5		0.00015	0.0840	2.5716	0.41803	4.4188
	0.00025	-	16.8	0.024	17.2		0.00025	0.3369	1.6427	0.60416	4.1499
	0.0005	-	13.1	0.038	13.6		0.0005	0.8400	0.76967	0.81292	4.1141
	0.001	-	10.1	0.061	10.8		0.001	0.95041	0.36427	0.91145	4.1135
	0.0015	-	8.638	0.079	9.379		0.0015	0.96648	0.08162	0.98016	4.1135
	0.0025	-	7.049	0.109	7.914		0.0025	0.99920	0.0019396	0.99953	4.1135
	0.005	-	5.280	0.16	6.350		0.005	1.0000	0.051095	1.0000	4.1135
	0.01	0.00118	3.8810	0.2562	5.2174		0.01	1.0000	0.0	1.0000	4.1135
	0.015	0.0126	3.1941	0.3249	4.7316		0.015	-	24.2	0.012	24.5
	0.025	0.08227	2.4341	0.43369	4.2982		0.025	-	21.0	0.015	21.3
	0.05	0.34276	1.5241	0.62191	4.0312		0.05	-	17.5	0.021	17.9
	0.1	0.69722	0.68994	0.82751	3.9940		0.1	-	13.7	0.034	14.2
	0.15	0.86161	0.31481	0.92117	3.9934		0.15	-	10.6	0.053	11.2
	0.25	0.97109	0.06575	0.98353	3.9934		0.25	-	9.144	0.068	9.814
	0.5	0.99942	0.001311	0.99967	3.9934		0.5	-	7.524	0.095	8.311
	1.0	1.0	0.0652124	1.0000	3.9934		1.0	-	5.718	0.147	6.700
	∞	1.0	0.0	1.0000	3.9934		∞	0.00159	4.2773	0.248	5.5176
0.05	0.0001	-	23.4	0.013	23.7	0.5	0.0001	0.0135	3.5684	0.2871	5.0051
	0.00015	-	20.3	0.017	20.7		0.00015	0.0785	2.7859	0.38738	4.5475
	0.00025	-	16.9	0.024	17.4		0.00025	0.31286	1.8451	0.56785	4.2695
	0.0005	-	13.2	0.038	13.7		0.0005	0.84888	0.92805	0.78074	4.2327
	0.001	-	10.20	0.060	10.9		0.001	0.92159	0.47144	0.88860	4.2321
	0.0015	-	8.734	0.078	9.670		0.0015	0.95395	0.12170	0.97125	4.2321
	0.0025	-	7.139	0.108	8.000		0.0025	0.99844	0.004120	0.99903	4.2321
	0.005	-	5.362	0.166	6.428		0.005	1.0000	0.084722	1.0000	4.2321
	0.01	0.00140	3.9517	0.2525	5.2868		0.01	0.001467	4.6214	0.198	5.7615
	0.015	0.01354	3.2584	0.3206	4.7961		0.015	0.0135	3.9013	0.2543	5.2316
	0.025	0.08435	2.4911	0.42858	4.3594		0.025	0.069332	3.1083	0.3466	4.7571
	0.05	0.34310	1.5705	0.61631	4.0930		0.05	0.27967	2.1536	0.51803	4.4681
	0.1	0.89444	0.71766	0.82311	4.0570		0.1	0.59887	1.1814	0.73330	4.4299
	0.15	0.95888	0.33133	0.91832	4.0565		0.15	0.77776	0.65443	0.85225	4.4293
	0.25	0.96991	0.07066	0.98258	4.0565		0.25	0.93179	0.20086	0.95465	4.4293
	0.5	0.99937	0.001484	0.99963	4.0565		0.5	0.99644	0.010483	0.99763	4.4293
	1.0	1.0000	0.065542	1.0000	4.0565		1.0	0.99999	0.0428553	0.99999	4.4293
	∞	1.0000	0.0	1.0000	4.0565		∞	1.0000	0.0	1.0000	4.4293
0.1	0.0001	-	23.7	0.013	24.0		0.0001	0.0135	24.9	0.010	25.1
	0.00015	-	20.5	0.017	20.9		0.00015	0.0840	21.6	0.013	21.9
	0.00025	-	17.1	0.023	17.5		0.00025	0.3369	18.1	0.018	18.5
	0.0005	-	13.3	0.037	13.9		0.0005	0.8400	14.2	0.029	14.6
	0.001	-	10.33	0.058	11.00		0.001	0.95041	11.1	0.045	11.6
	0.0015	-	8.854	0.075	9.575		0.0015	0.96648	9.564	0.059	10.17
	0.0025	-	7.251	0.104	8.095		0.0025	0.99920	7.920	0.082	8.629
	0.005	-	5.465	0.161	6.513		0.005	1.0000	6.086	0.128	6.980
	0.01	0.00153	4.0442	0.2453	5.3590		0.01	0.001467	4.6214	0.198	5.7615

TABLE II.1.6

THE FUNDAMENTAL SOLUTIONS OF THE FOURTH KIND
INNER WALL HEATED

r^*	\bar{x}	$\theta_{11}^{(4)}$	$\phi_{01}^{(4)}$	$\theta_{ml}^{(4)}$	$Nu_{11}^{(4)}$	$Nu_{01}^{(4)}$	r^*	\bar{x}	$\theta_{11}^{(4)}$	$\phi_{01}^{(4)}$	$\theta_{ml}^{(4)}$	$Nu_{11}^{(4)}$	$Nu_{01}^{(4)}$
0.02	0.0001	0.0103	-	0.0478481	97.3	-	0.25	0.0001	0.0247	-	0.0480000	40.6	-
	0.00015	0.0116	-	0.0411765	86.5	-		0.00015	0.0285	-	0.0312000	35.2	-
	0.00025	0.0133	-	0.0419608	75.6	-		0.00025	0.0340	-	0.0320000	29.6	-
	0.0005	0.0156	-	0.0439216	64.1	-		0.0005	0.0423	-	0.0340000	23.6	-
	0.001	0.0181	-	0.0478431	55.4	-		0.001	0.0535	-	0.0380000	19.0	-
	0.0015	0.0196	-	0.0411765	51.2	-		0.0015	0.06067	-	0.0412000	16.81	-
	0.0025	0.02159	-	0.0419608	46.75	-		0.0025	0.07031	-	0.0440000	14.53	-
	0.005	0.02427	-	0.0439216	41.88	-		0.005	0.08679	-	0.0480000	12.08	-
	0.01	0.027035	-	0.0478431	38.096	-		0.01	0.10580	-	0.0520000	10.225	-
	0.015	0.028710	-	0.0411765	36.318	0.0302		0.015	0.11855	-	0.0560000	9.3824	0.0497
	0.025	0.03090	-	0.0419608	34.515	0.05419		0.025	0.13662	-	0.0600000	8.5481	0.282
	0.05	0.03406	-	0.0439216	32.692	1.9751		0.05	0.16543	-	0.0640000	7.7093	0.9989
	0.1	0.037256	-	0.0478431	31.262	2.8468		0.1	0.19783	-	0.0680000	7.0400	2.9082
	0.15	0.038702	-	0.0411765	30.665	2.8287		0.15	0.21417	-	0.0720000	6.7483	3.1128
	0.25	0.039664	-	0.0419608	30.281	2.9249		0.25	0.22669	-	0.0760000	6.5407	3.2314
	0.5	0.039914	-	0.0439216	30.183	2.9472		0.5	0.23090	-	0.0780000	6.4737	3.2658
	1.0	0.039919	-	0.0478431	30.181	2.9477		1.0	0.23105	-	0.0780000	6.4714	3.2670
	∞	0.039919	-	0.0478431	30.181	2.9477		∞	0.23105	-	0.0780000	6.4714	3.2670
0.05	0.0001	0.0160	-	0.0419047	62.4	-	0.5	0.0001	0.0289	-	0.031333	34.9	-
	0.00015	0.0181	-	0.0428511	55.2	-		0.00015	0.0331	-	0.0320000	30.4	-
	0.00025	0.0210	-	0.0447019	47.8	-		0.00025	0.0393	-	0.0333333	25.7	-
	0.0005	0.0251	-	0.0495238	39.9	-		0.0005	0.0496	-	0.0366667	20.5	-
	0.001	0.0298	-	0.0419047	33.8	-		0.001	0.0623	-	0.0413333	16.41	-
	0.0015	0.03268	-	0.0428511	30.87	-		0.0015	0.0712	-	0.0420000	14.46	-
	0.0025	0.03658	-	0.0447019	27.70	-		0.0025	0.0842	-	0.0433333	12.38	-
	0.005	0.04253	-	0.0495238	24.21	-		0.005	0.1054	-	0.0466667	10.13	-
	0.01	0.048370	-	0.0419047	21.522	0.0365		0.01	0.13191	-	0.0513333	8.4373	0.0545
	0.015	0.052171	-	0.0428511	20.276	0.237		0.015	0.15041	-	0.0520000	7.6890	0.3012
	0.025	0.057227	-	0.0447019	19.028	0.9028		0.025	0.17760	-	0.0533333	6.9087	1.0550
	0.05	0.064672	-	0.0495238	17.776	2.0335		0.05	0.22329	-	0.0566667	6.1393	2.3150
	0.1	0.072327	-	0.0419047	16.798	2.7134		0.1	0.27845	-	0.060403	5.5052	3.0931
	0.15	0.075830	-	0.0428511	16.392	2.8970		0.15	0.30884	-	0.063007	5.2129	3.3237
	0.25	0.078194	-	0.0447019	16.128	2.9940		0.25	0.33499	-	0.11700	4.9850	3.4667
	0.5	0.078822	-	0.0495238	16.060	3.0189		0.5	0.34597	-	0.13439	4.8952	3.5183
	1.0	0.078835	-	0.0419047	16.058	3.0189		1.0	0.34657	-	0.14169	4.8904	3.5189
	∞	0.078835	-	0.0419047	16.058	3.0189		∞	0.34657	-	0.14209	4.8904	3.5189
0.1	0.0001	0.0195	-	0.0436363	51.5	-	1.0	0.00025	0.0430	-	0.0005	23.5	-
	0.00015	0.0224	-	0.0454545	44.7	-		0.00015	0.04943	-	0.0050	11.2	-
	0.00025	0.0265	-	0.0490909	37.8	-		0.00025	0.05943	-	0.02000	7.4895	0.0601
	0.0005	0.0328	-	0.0418181	30.7	-		0.0005	0.07734	-	0.02995	6.7709	0.3287
	0.001	0.0399	-	0.0436363	25.3	-		0.001	0.10432	-	0.03995	6.0613	1.1583
	0.0015	0.04455	-	0.0454545	22.72	-		0.0015	0.12794	-	0.04944	5.3410	2.5578
	0.0025	0.05023	-	0.0490909	20.03	-		0.0025	0.15934	-	0.05944	4.9719	3.1567
	0.005	0.06023	-	0.0418181	17.12	0.0413		0.005	0.19794	-	0.06944	4.5459	3.6227
	0.01	0.070740	-	0.0436363	14.302	0.256		0.01	0.23786	-	0.07944	4.1478	3.9144
	0.015	0.077457	-	0.0454545	13.886	0.9422		0.015	0.27379	-	0.08944	4.0125	4.0060
	0.025	0.086584	-	0.0490909	12.875	2.0934		0.025	0.32379	-	0.09944	4.0125	4.0060
	0.05	0.10038	-	0.0418181	11.863	2.7777		0.05	0.37379	-	0.10944	4.0125	4.0060
	0.1	0.11494	-	0.0436363	11.072	2.9662		0.1	0.42379	-	0.11944	4.0125	4.0060
	0.15	0.12178	-	0.0454545	10.740	3.0692		0.15	0.47379	-	0.12944	4.0125	4.0060
	0.25	0.12854	-	0.0490909	10.523	3.0692		0.25	0.52379	-	0.13944	4.0125	4.0060

TABLE II.1.

THE FUNDAMENTAL SOLUTIONS OF THE FOURTH KIND
OUTER WALL HEATED

r^*	\bar{x}	$\theta_{oo}^{(4)}$	$\phi_{10}^{(4)}$	$\theta_{mo}^{(4)}$	$Nu_{oo}^{(4)}$	$Nu_{10}^{(4)}$	r^*	\bar{x}	$\theta_{oo}^{(4)}$	$\phi_{10}^{(4)}$	$\theta_{mo}^{(4)}$	$Nu_{oo}^{(4)}$	$Nu_{10}^{(4)}$
0.02	0.0001	0.0375	-	0.0339215	33.2	-	0.25	0.0001	0.0336	-	0.033000	30.0	-
	0.0015	0.0428	-	0.0358823	28.5	-		0.0015	0.0387	-	0.0348000	26.1	-
	0.0025	0.0503	-	0.0398039	23.7	-		0.0025	0.0463	-	0.0380000	22.0	-
	0.005	0.0634	-	0.0019607	18.4	-		0.005	0.0592	-	0.0016000	17.4	-
	0.001	0.08053	-	0.0039215	14.37	-		0.001	0.0787	-	0.0032000	13.8	-
	0.0015	0.09315	-	0.0058823	12.46	-		0.0015	0.0877	-	0.0048000	12.1	-
	0.0025	0.1123	-	0.0098039	10.47	-		0.0025	0.1056	-	0.008000	10.24	-
	0.005	0.1463	-	0.019078	8.357	-		0.005	0.1369	-	0.016000	8.27	-
	0.01	0.19302	-	0.039215	6.1302	-		0.01	0.17901	-	0.031985	6.8016	-
	0.015	0.2682	-0.216	0.058823	5.4399	3.28		0.015	0.21073	-0.0201	0.047948	6.1434	0.419
	0.025	0.28674	-0.663	0.098039	4.9375	6.34		0.025	0.26110	-0.1269	0.079418	5.5040	1.598
	0.05	0.40173	-3.013	0.196078	4.9375	15.128		0.05	0.35746	-0.5796	0.15253	4.8796	3.800
	0.1	0.59342	-8.482	0.37264	4.5294	22.761		0.1	0.50278	-1.4441	0.27133	4.3205	5.3224
	0.15	0.76051	-13.423	0.52557	4.2563	25.540		0.15	0.61039	-2.0966	0.35987	3.9917	5.8260
	0.25	1.0373	-21.617	0.77896	3.8713	27.751		0.25	0.75019	-3.9446	0.47491	3.6327	6.2002
	0.5	1.4874	-34.945	1.1911	3.3748	29.338		0.5	0.88435	-3.7583	0.58532	3.3441	6.4210
	1.0	1.8529	-45.764	1.5257	3.0565	29.995		1.0	0.92211	-4.0000	0.61639	3.2709	6.4689
	∞	1.9959	-50.000	1.6567	2.9477	30.1808		∞	0.92420	-	0.61810	3.26700	6.4714
0.05	0.0001	0.0366	-	0.0338095	27.2	-	0.5	0.0001	0.0322	-	0.0326666	31.2	-
	0.0015	0.0416	-	0.037142	24.0	-		0.0015	0.0371	-	0.0340000	27.1	-
	0.0025	0.0493	-	0.0395238	20.4	-		0.0025	0.0446	-	0.0366666	22.7	-
	0.005	0.0622	-	0.0019047	16.4	-		0.005	0.0570	-	0.0013333	17.9	-
	0.001	0.0794	-	0.0038095	13.1	-		0.001	0.0729	-	0.0026666	14.2	-
	0.0015	0.0918	-	0.0057142	11.5	-		0.0015	0.0843	-	0.0040000	12.4	-
	0.0025	0.1108	-	0.0095238	9.817	-		0.0025	0.1012	-	0.0066666	10.56	-
	0.005	0.1442	-	0.019047	7.950	-		0.005	0.1303	-	0.0133333	8.539	-
	0.01	0.19013	-	0.037505	6.5520	-		0.01	0.16899	-	0.026545	7.0205	-
	0.015	0.22517	-0.029	0.056547	5.9302	0.513		0.015	0.19762	-0.0146	0.039833	6.3378	0.365
	0.025	0.28175	-0.286	0.094381	5.3371	3.03		0.025	0.24232	-0.0869	0.065884	5.6679	1.320
	0.05	0.39346	-1.549	0.18544	4.8071	8.355		0.05	0.32516	-0.3761	0.12496	4.9950	3.010
	0.1	0.57605	-4.3262	0.34771	4.3793	12.442		0.1	0.44255	-0.8881	0.21518	4.3931	4.1272
	0.15	0.72938	-6.7263	0.48524	4.0960	13.862		0.15	0.52221	-1.2415	0.27678	4.0744	4.4855
	0.25	0.96911	-10.482	0.70032	3.7204	14.967		0.25	0.61361	-1.6471	0.34746	3.7572	4.7403
	0.5	1.3121	-15.856	1.0081	3.2889	15.728		0.5	0.68140	-1.9459	0.39883	3.5522	4.8711
	1.0	1.5265	-19.214	1.2005	3.0666	16.006		1.0	0.69289	-1.9989	0.40877	3.5196	4.8900
	∞	1.5767	-20.000	1.2455	3.0189	16.058		∞	0.69315	-2.0000	0.40897	3.5189	4.8901
0.1	0.0001	0.0355	-	0.0336363	28.3	-		0.0001	0.0322	-	0.0326666	31.2	-
	0.0015	0.0405	-	0.0354545	24.9	-		0.0015	0.0371	-	0.0340000	27.1	-
	0.0025	0.0482	-	0.039009	21.1	-		0.0025	0.0446	-	0.0366666	22.7	-
	0.005	0.0611	-	0.0018181	16.8	-		0.005	0.0570	-	0.0013333	17.9	-
	0.001	0.0782	-	0.0036363	13.4	-		0.001	0.0729	-	0.0026666	14.2	-
	0.0015	0.0904	-	0.0054545	11.8	-		0.0015	0.0843	-	0.0040000	12.4	-
	0.0025	0.1091	-	0.009009	9.984	-		0.0025	0.1012	-	0.0066666	10.56	-
	0.005	0.1419	-	0.018181	8.074	-		0.005	0.1303	-	0.0133333	8.539	-
	0.01	0.18672	-	0.036256	6.6462	-		0.01	0.16899	-	0.026545	7.0205	-

TABLE II.1.E

THE FUNDAMENTAL SOLUTIONS OF THE FIRST KIND

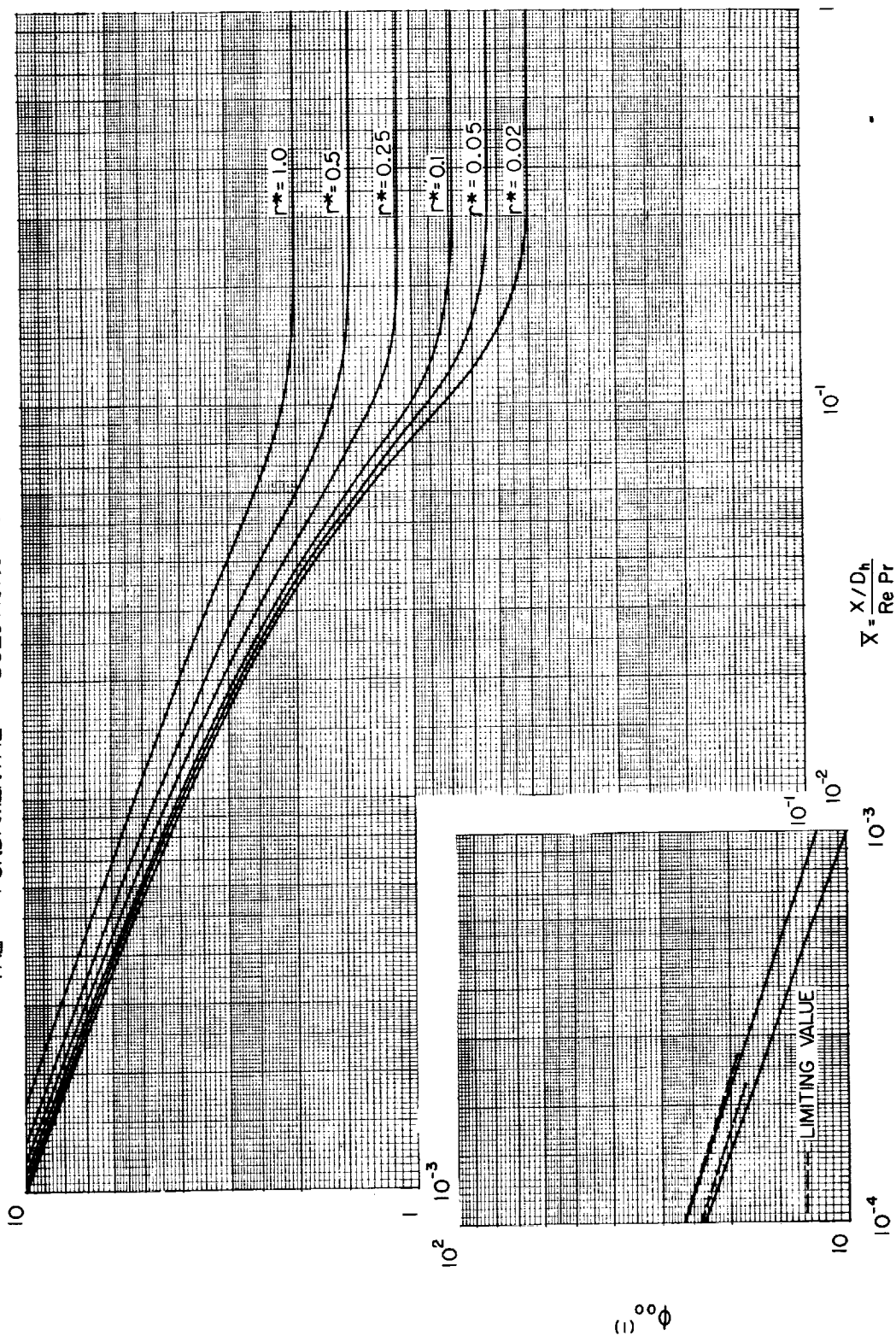


FIGURE II.1.2

THE FUNDAMENTAL SOLUTIONS OF THE FIRST KIND

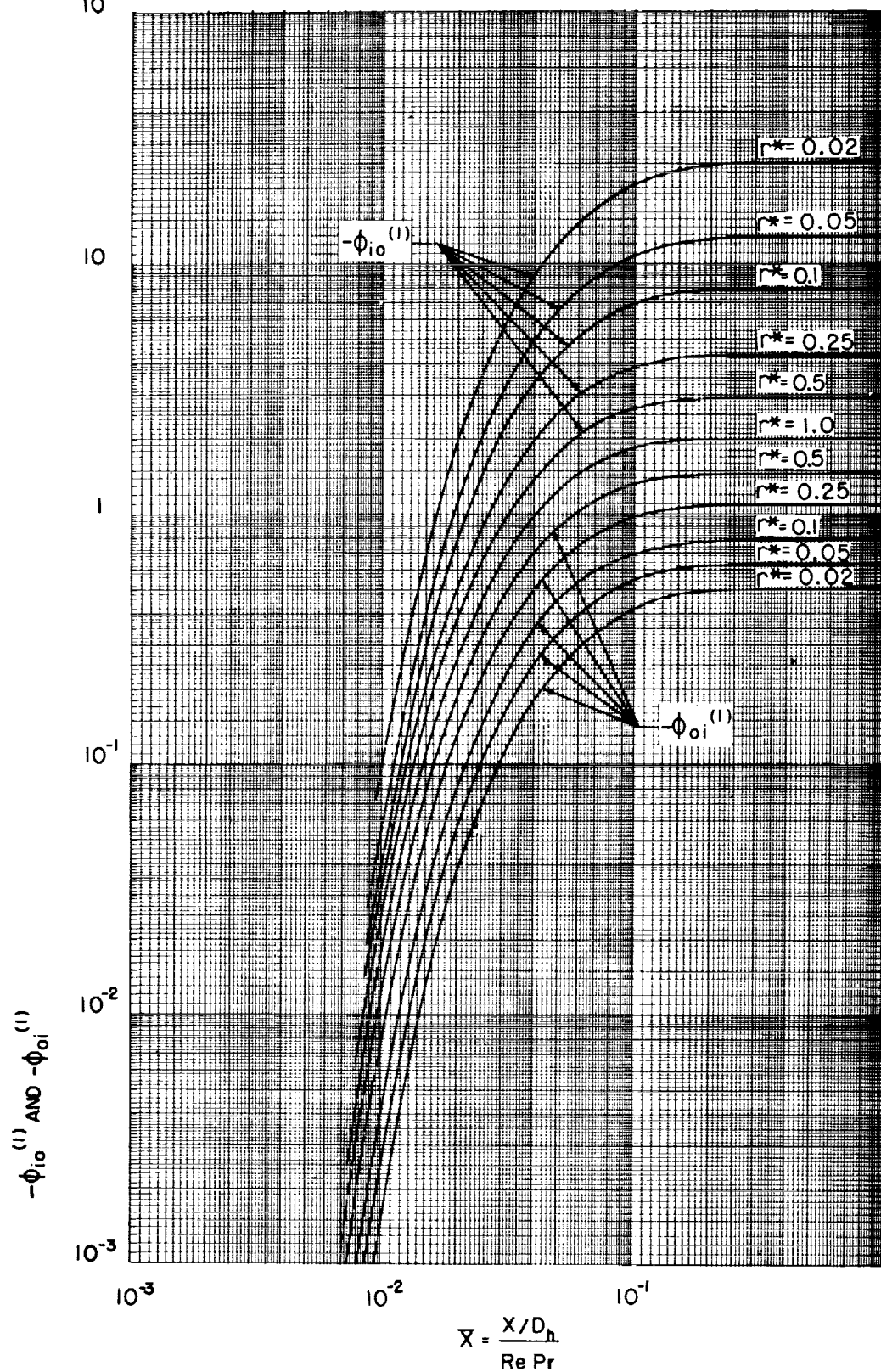


FIGURE II.1.3

THE FUNDAMENTAL SOLUTIONS OF THE FIRST KIND

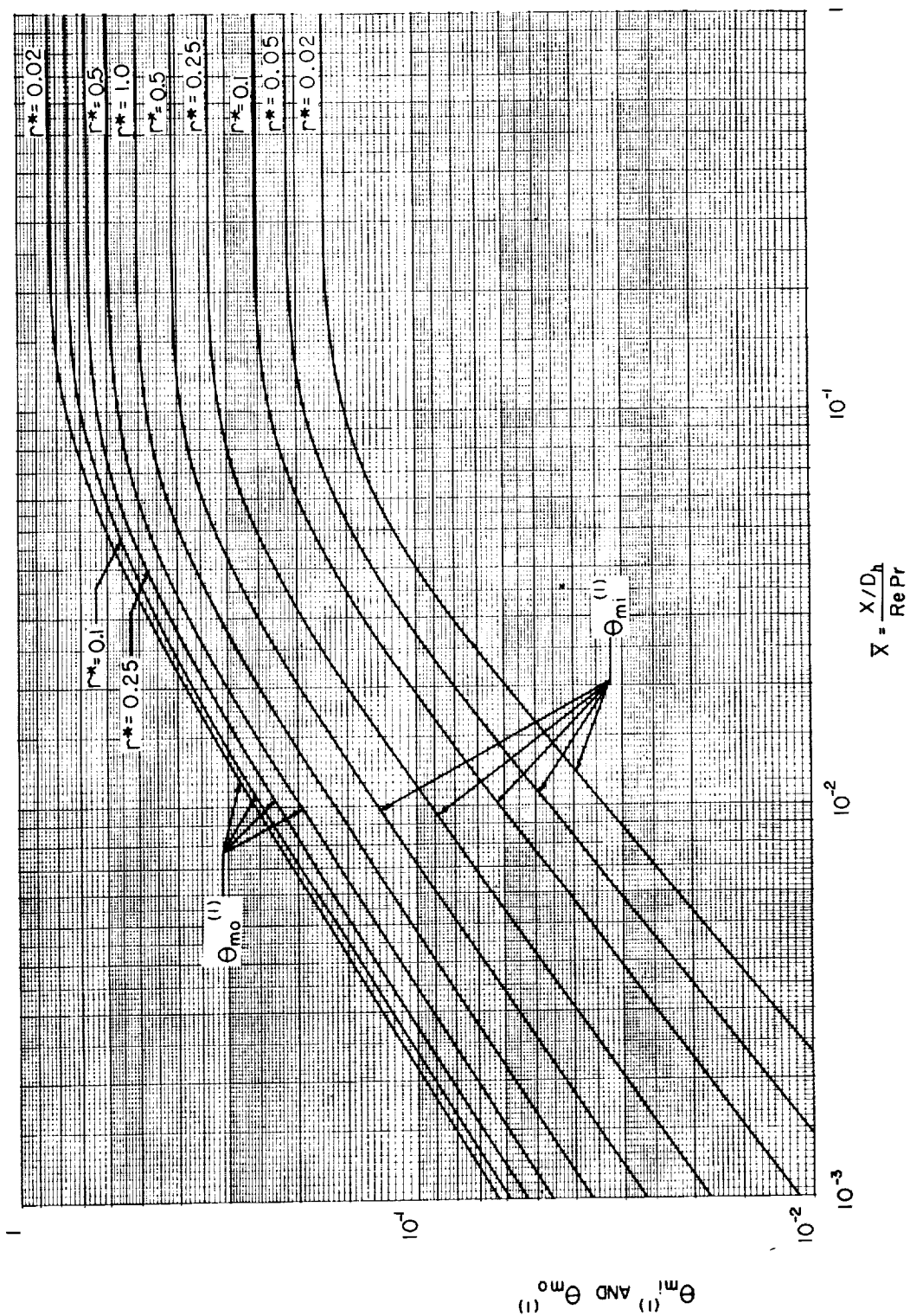


FIGURE II.I.4

THE FUNDAMENTAL SOLUTIONS OF THE SECOND KIND

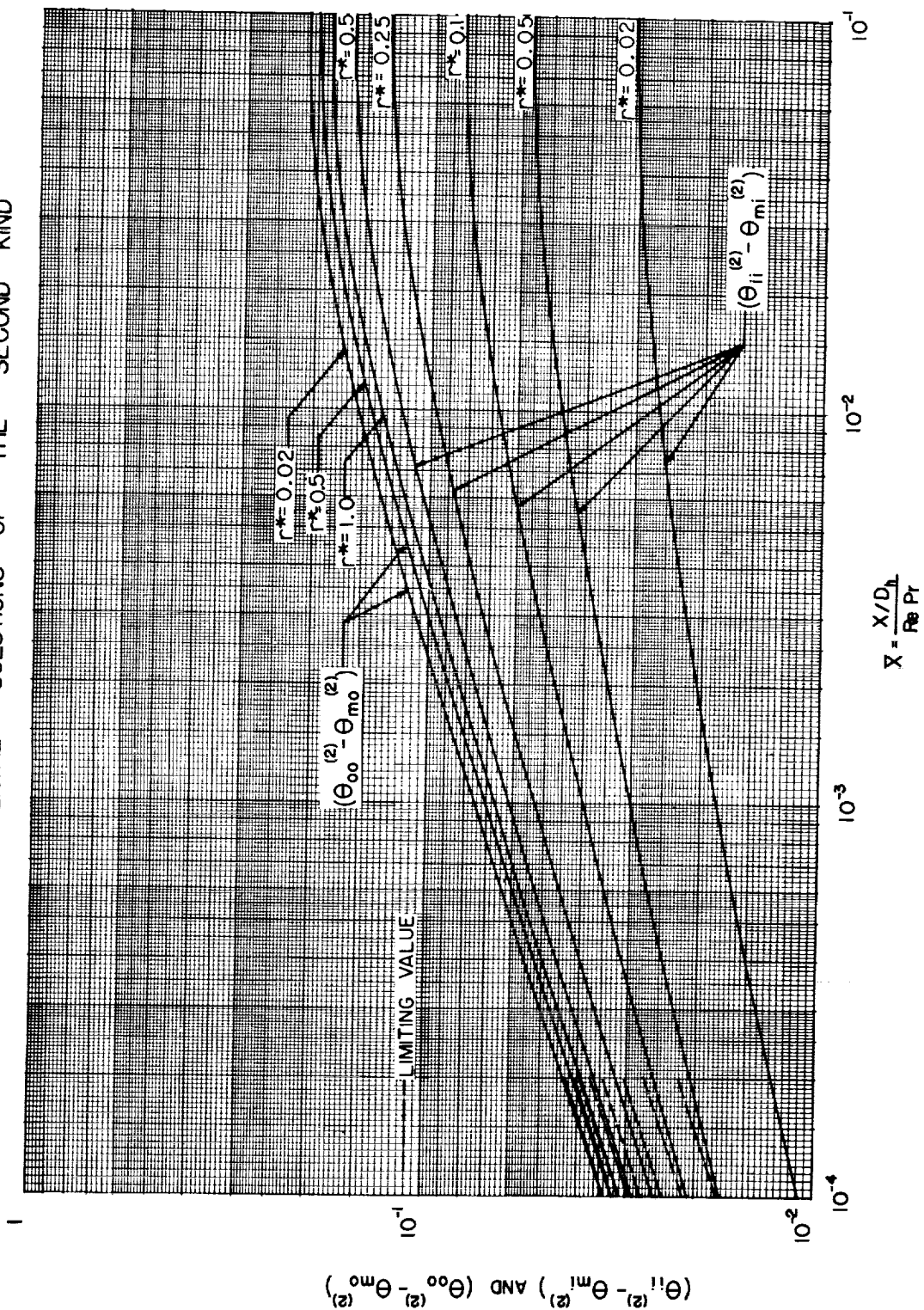


FIGURE II.1.5

THE FUNDAMENTAL SOLUTIONS OF THE SECOND KIND

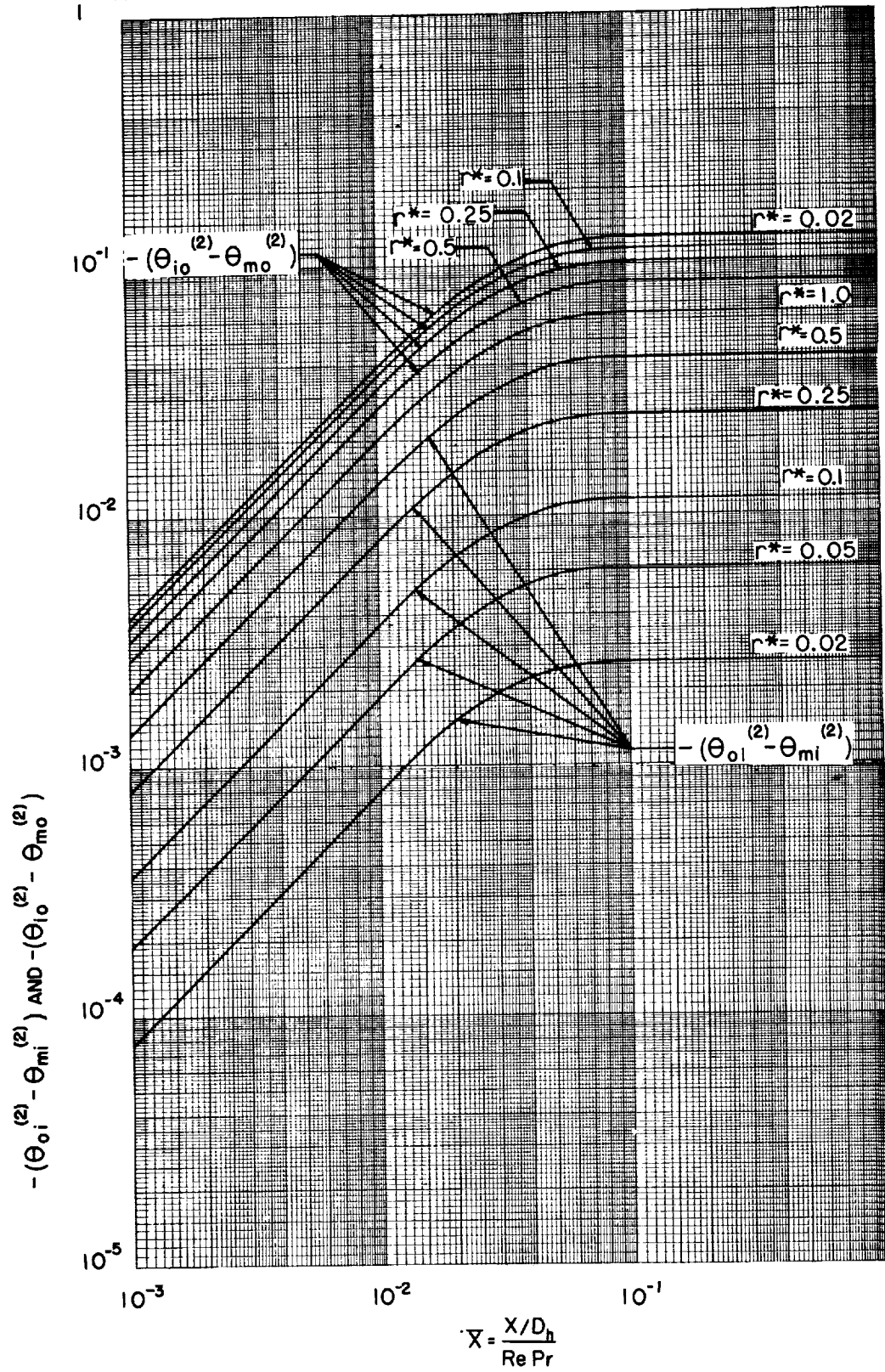


FIGURE II.I.6

THE FUNDAMENTAL SOLUTIONS OF THE THIRD KIND

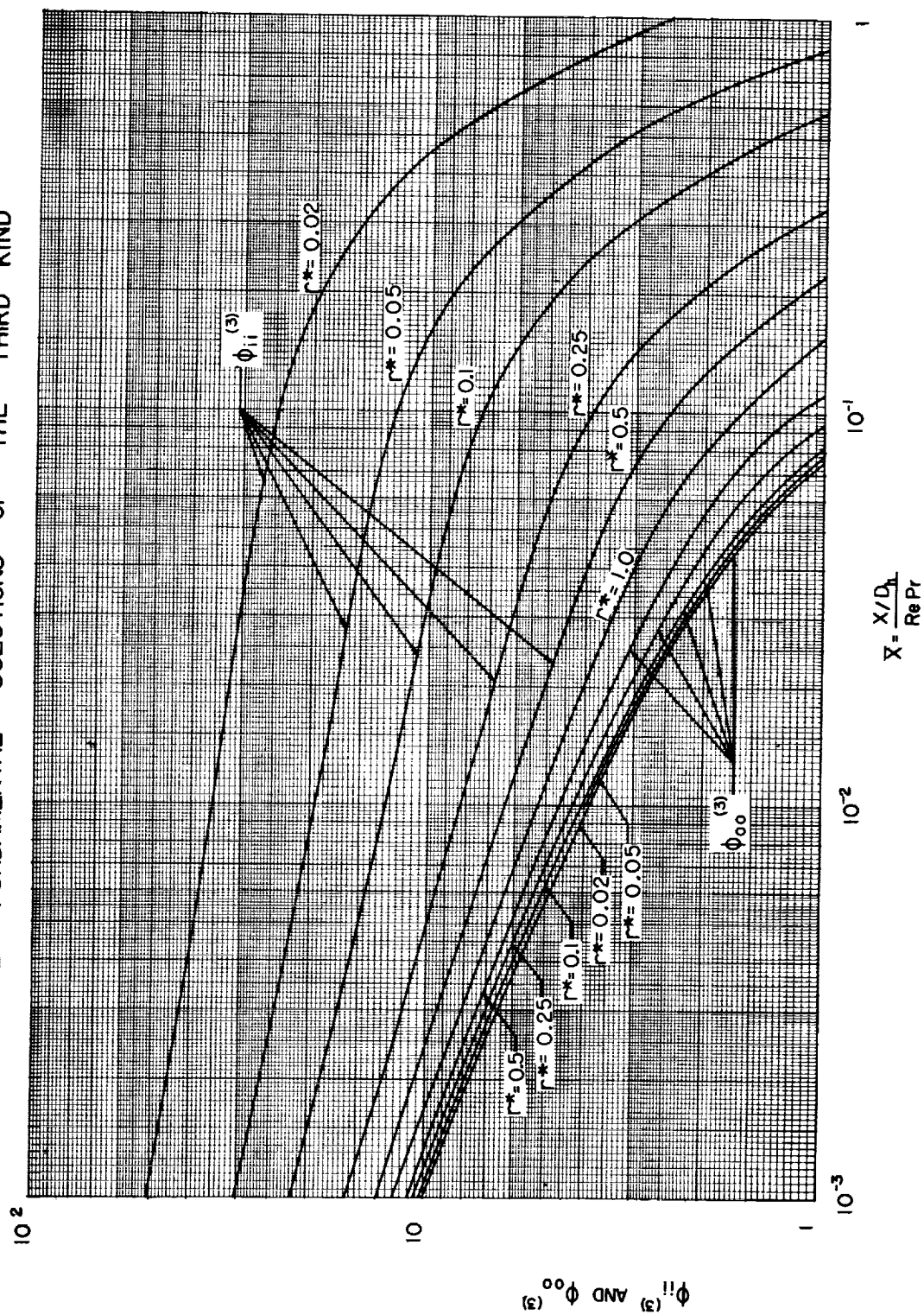


FIGURE II.1.7

THE FUNDAMENTAL SOLUTIONS OF THE THIRD KIND

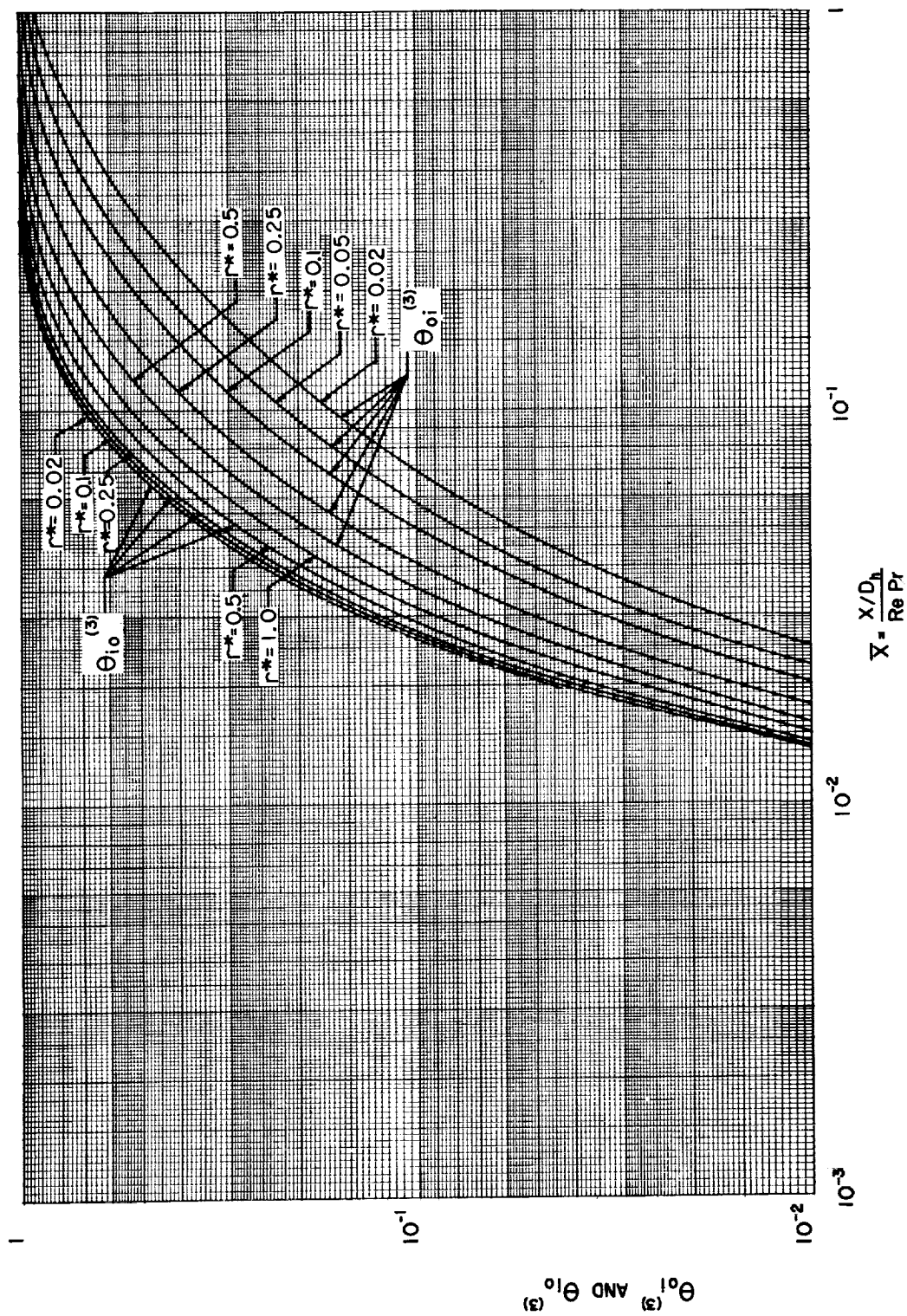


FIGURE II.1.8

THE FUNDAMENTAL SOLUTIONS OF THE THIRD KIND

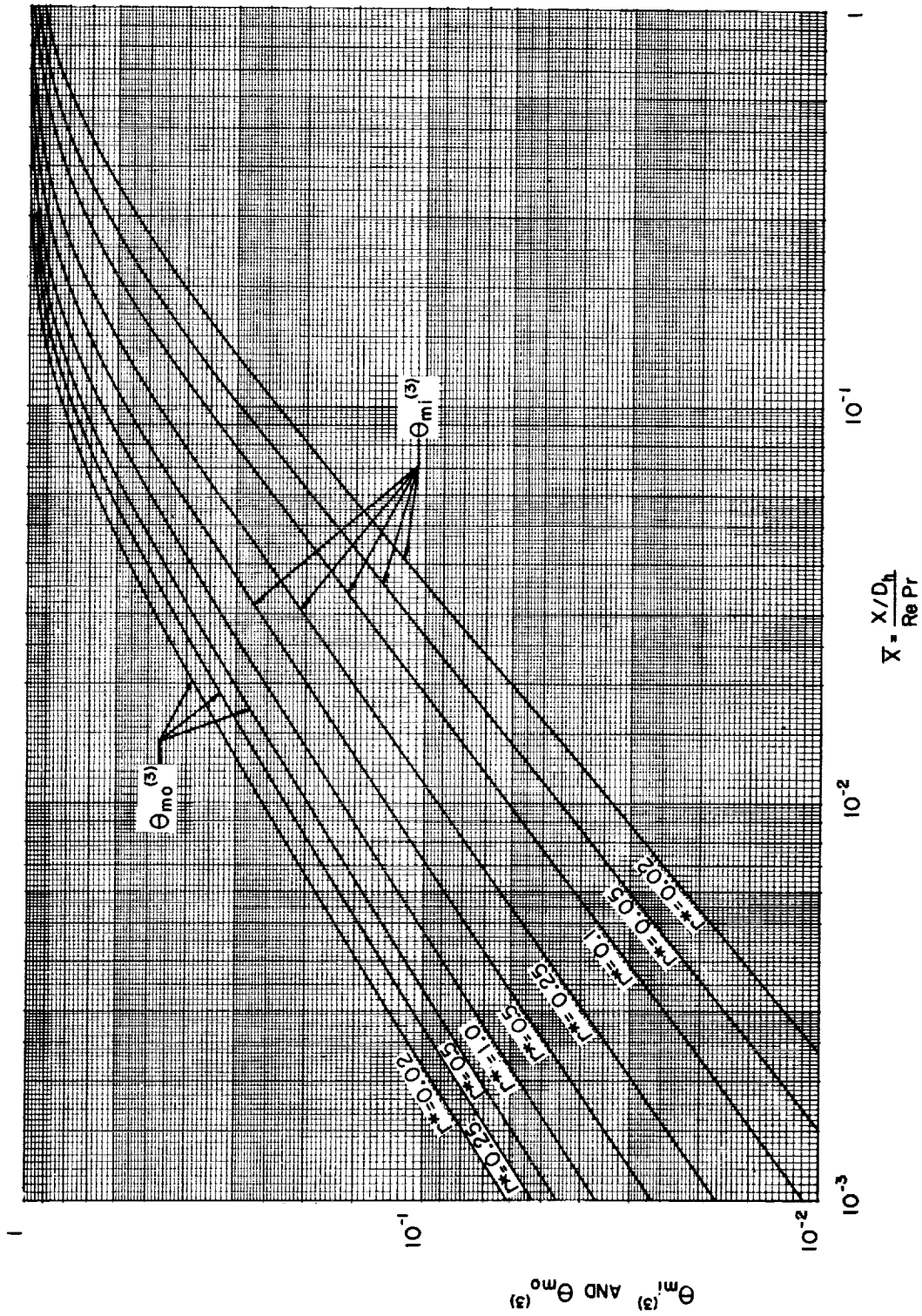


FIGURE II.1.9

THE FUNDAMENTAL SOLUTIONS OF THE FOURTH KIND

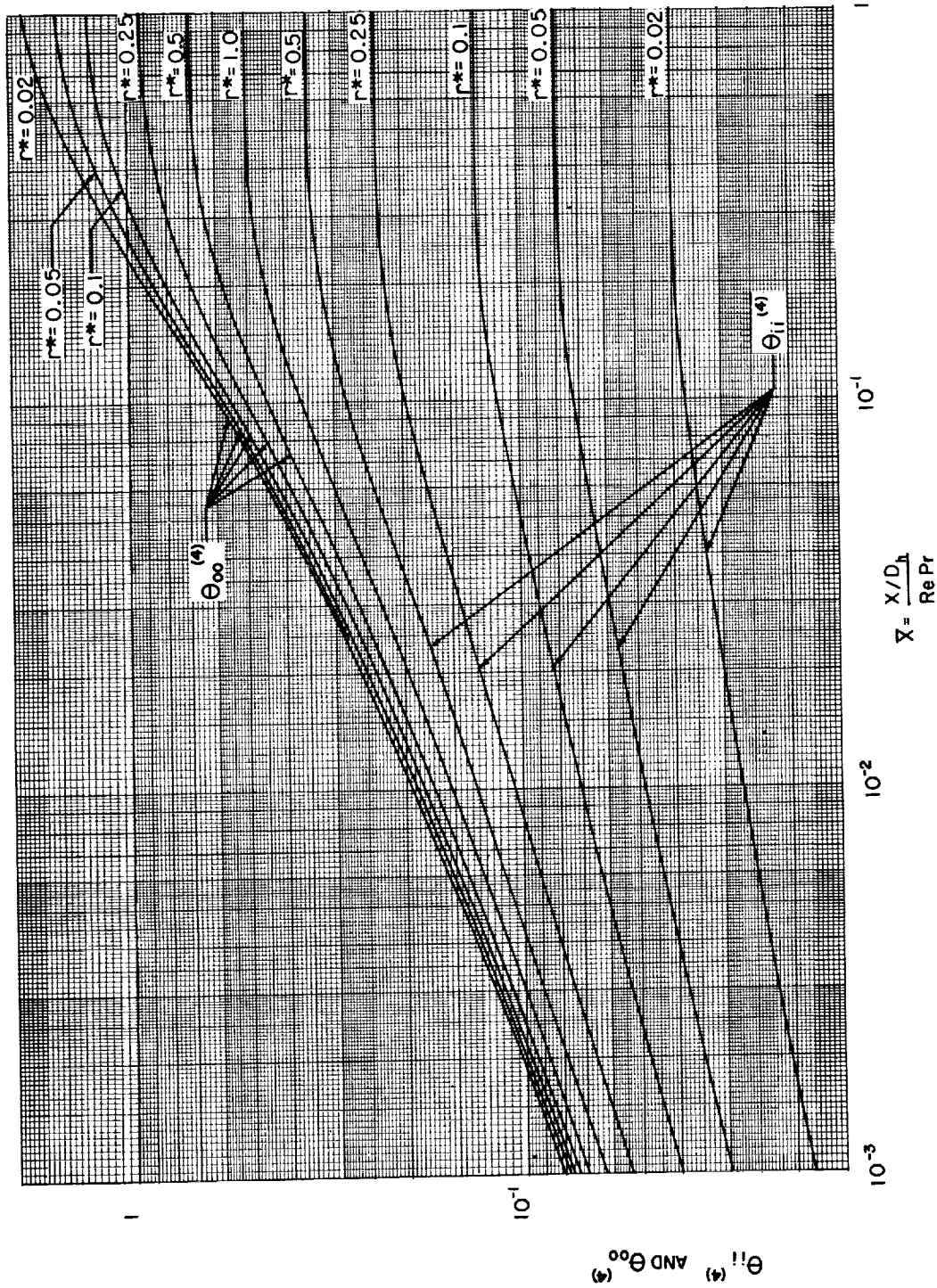


FIGURE II.I.10

THE FUNDAMENTAL SOLUTIONS OF THE FOURTH KIND

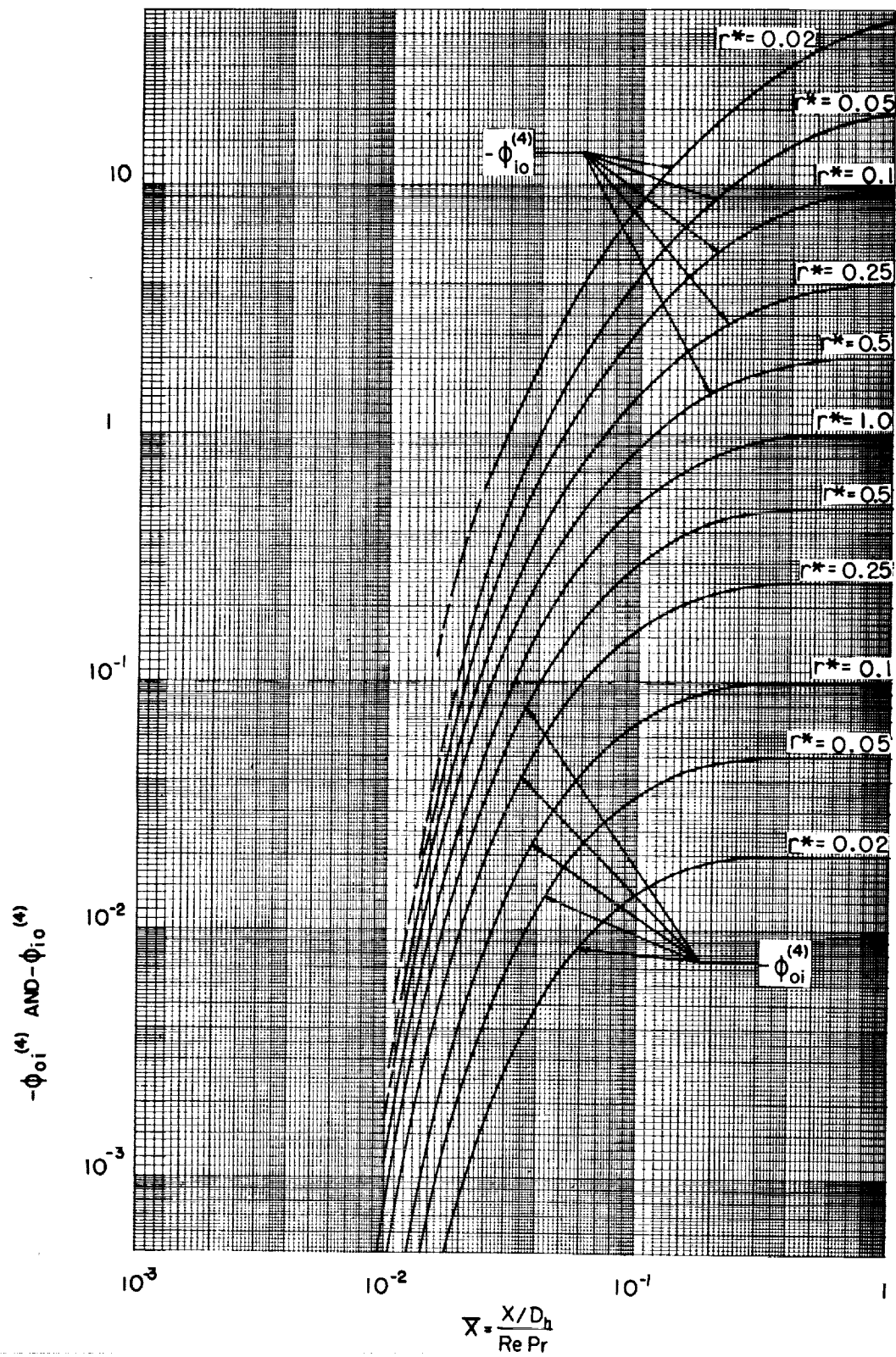


FIGURE II.I.11

THE FUNDAMENTAL SOLUTIONS OF THE FOURTH KIND

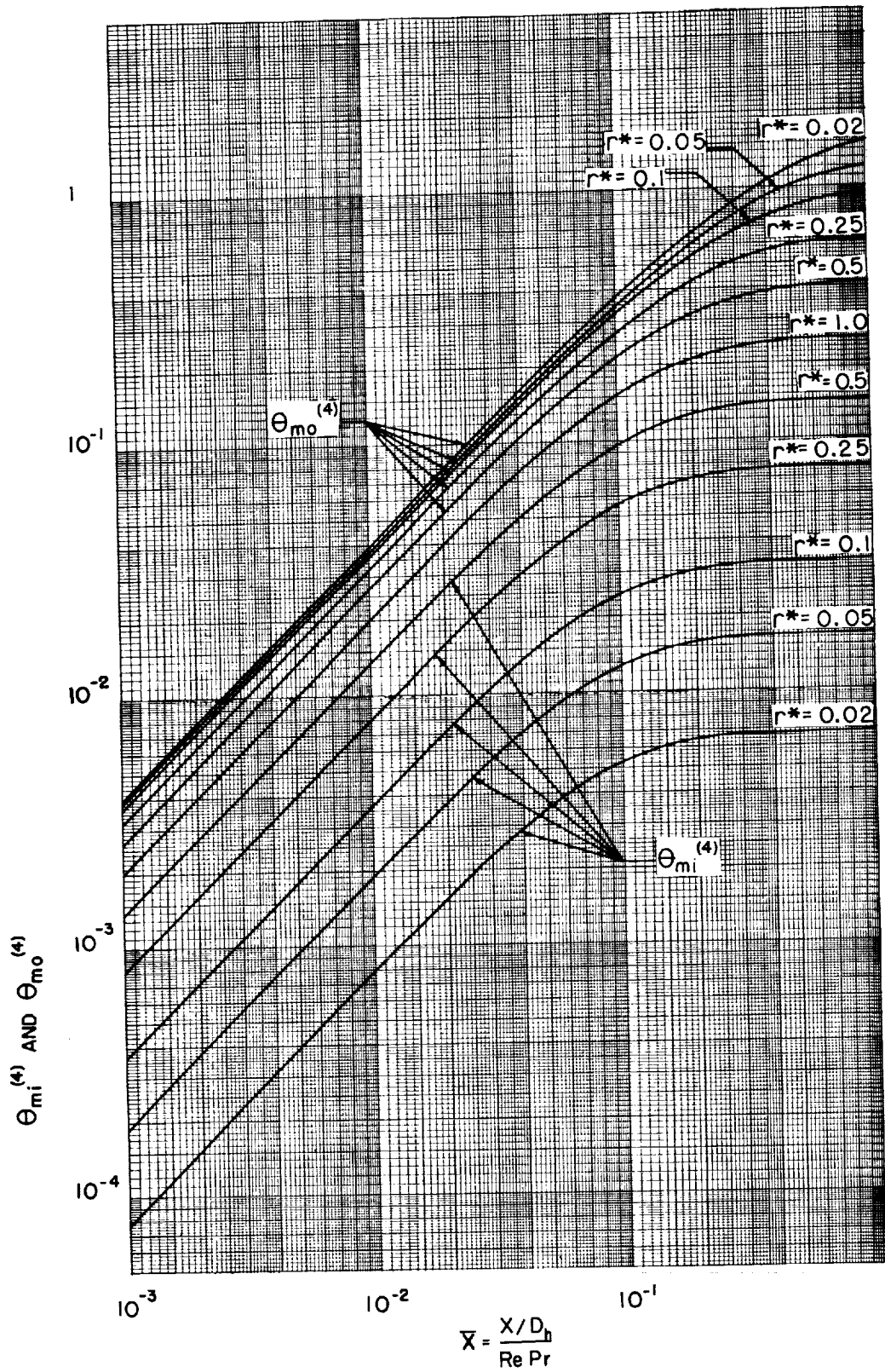


FIGURE II.1.12

III. EXPERIMENTAL WORK

III. A. Description of Apparatus.

The apparatus for the present investigation consists of a positive pressure system using air as the working fluid. The boundary walls of the annular passage are inconel tubing which themselves form the resistance heating elements. Electrical power is supplied by a two channel regulated AC power supply, each channel having 1 KVA capacity at 200 amperes maximum current. Figure III. A.2 is a diagram of the power supply circuit including the principal instrumentation.

The test section is 6 feet long, although in practice only 4 feet of this is heated. In this series of tests the initial 2 feet was used as a "starting" length to allow the velocity profile to develop. Two sizes of outer tube are used with inside diameters of approximately 1.96 and 1.00 inches. These, together with core tubes with outside diameters of approximately 0.375 and 0.500 inches, provide four radius ratios of 0.191, 0.256, 0.376, and 0.501.

Considerable care was taken to secure close tolerance inconel tubing. The specifications on the tubing are:

a. 2 inch outer tube;

I.D., 1.96 inches \pm 0.0025.

wall thickness, 0.020 inches \pm 0.001,

ovality, \pm 0.010 inches,

straightness, \pm 0.010 inches/foot;

b. 1 inch outer tube, 0.375 and 0.500 inch core tubes;

I.D. or O.D., specified values \pm 0.001 inches,

wall thickness, 0.020 inches \pm 0.001,

ovality, \pm 0.002 inches,

straightness \pm 0.002 inches/foot.

Inconel was selected because of its high specific resistivity ($98.1\mu\Omega$ - cm) which enables the use of relatively low heating currents.

In view of the close tolerance on the wall thickness (the pieces actually used have variations of wall thickness of less than ± 0.0003 inches) electrical heating provides essentially constant heat flux at the walls. Accordingly, the experimental apparatus provides values for the fundamental solutions of the second kind (and superpositions thereof) directly.

The assembled test section is mounted, vertically, on an 8 foot piece of aluminum channel 6 inches wide. The outer tube is supported in three lucite holders, two at the extreme ends of the tube and one at the point of the electrical connection to the heated tube. The core tube is held by two aluminum holders mounted 8 inches beyond the ends of the outer tube. To minimize eccentricity the holders were clamped together and bored simultaneously. While clamped, two aligning holes were drilled and reamed through all of the pieces. During the assembly on the channel these aligning holes were brought into line with a transit equipped with a traversing rack. Machined brass plugs with a central hole made with a #67 (0.032 inches) drill were pressed into the aligning holes. These holes were readily distinguished by the transit during the assembly, accordingly, it is felt that the axial misalignment of the holders is less than ± 0.015 inches.

A positioning bracket that contains the center tube fits into a bored recess in the end holders and bears against an "O" ring. A teflon plug fits over the tube and bears against it and the inside of a tapered hole in the positioning bracket effecting a seal and centering the tube with respect to the bracket. When installed, the core tube is put in tension to straighten any residual bow.

Four brass aligning spheres were made each having a diameter 0.010 inches less than the annular gap provided by the four geometries. During the running of the tests the concentricity is periodically checked by lowering the

appropriate sphere into the test section from the top. This insures that the axial misalignment will be less than 4% of the smallest gap width under all conditions.

The air enters at the lower end of the channel which is sealed to provide a plenum chamber 6 inches on a side.

To facilitate the right angle turn made by the flow a set of sheet metal turning vanes is mounted inside the plenum chamber. The entrance is a wooden nozzle with the converging wall profile a quadrant of an ellipse. The upstream face of the nozzle seals against an "O" ring in the top wall of the plenum. The joint between the nozzle and the tube section was carefully filled, sanded, and varnished to provide a continuous wall surface and to avoid tripping the boundary layer during the laminar flow runs. Details of the assembly are shown in Fig. III.A.3.

Just upstream of the nozzle, three screens are placed to reduce the turbulence level entering the test section and promote even distribution of the air flow. With both the inner and the outer tubes removed, a hot film anemometer (Ref.17) was used to measure the turbulence intensity at the center of the exit plane of the nozzle having the 1.96 inch throat. The results are as follows:

Condition	Velocity-ft/sec	Turbulence Intensity- $u'/U, \%$
No screens	50	6.9
One fine screen	23	1.3
	64	3.2
Three screens	10	0.30
	46	0.37
	79	0.58

The velocity profile at the nozzle exit plane was surveyed with a Pitot-static probe to insure that no serious maldistribution of flow resulted from the rather short radius turning of the air stream. The results of a survey are shown in Fig. III.A.1. These profiles were measured along a diameter of the nozzle exit normal to the mounting channel (i.e. along a radius of the curved streamlines) as the skewness of the flow is greatest along that line.

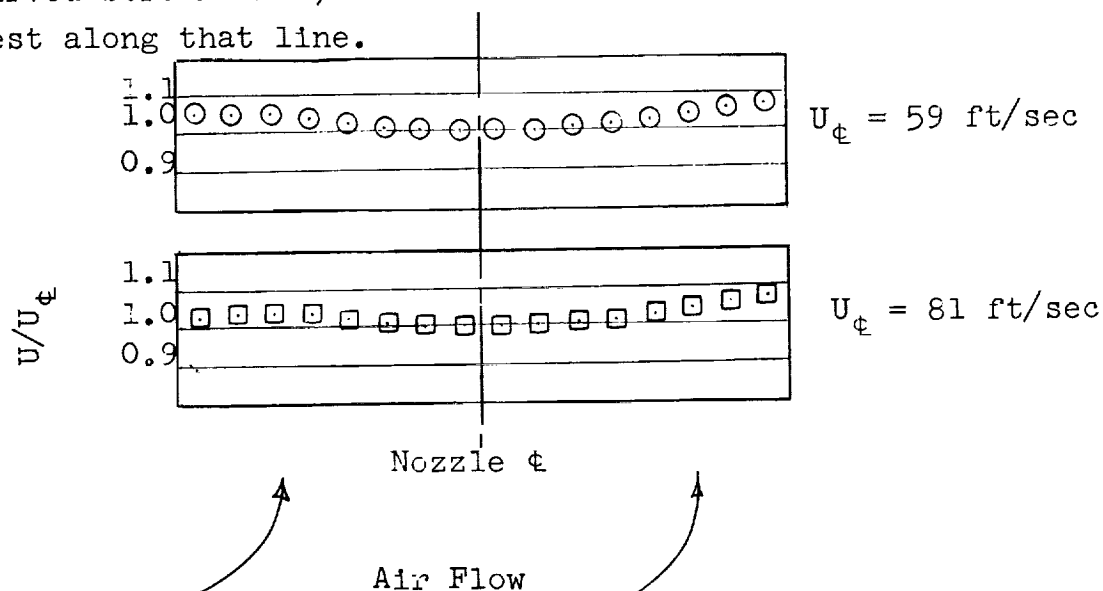


FIG. III.A.1

The air is supplied to the test section by a centrifugal blower producing a maximum static head of 30 inches of water. The air supply is shared with the companion apparatus, the parallel plane channel as described by McCuen¹¹. The air is metered by flat plate orifices. Either of two parallel metering sections is used, the sizes are as follows:

<u>Duct diameter</u>	<u>Orifice diameter</u>	<u>$\beta = d/D$</u>
6.367	4.225	0.664
6.367	1.910	0.300
1.498	0.824	0.550
1.498	0.375	0.250

A diagram of the metering system is shown in Fig. III.A.4. System static pressure is measured by a 30 inch vertical water manometer, differential pressure by one of three parallel manometers, a 16 inch vertical water manometer, or inclined oil manometers having ranges of 1 and 5 inches of water. The differential manometers were adjusted by comparison with a micro-manometer and the entire metering system was run in series with portable laboratory nozzle tanks whose calibration is regarded as well established. The total range of air flow which can be measured is from 1 to 750 cfm with a probable uncertainty of about $\pm 1\%$.

The power generated in the test section is determined by an ammeter in series with and a voltmeter across the resistive load. The ammeter used is a Weston model 901, the voltmeter a Hewlett-Packard model 400H, VTVM. A switching arrangement is used to permit the use of only one ammeter and one voltmeter even when both tubes are heated (see Fig. III.A.2).

The fluid mean temperature is determined as a function of axial position by adding the temperature rise due to the energy input to the inlet temperature. The inlet temperature is measured by thermocouples fastened to the turning vanes just upstream of the nozzle entrance.

At the outer wall, temperatures are measured by iron-constantan thermocouples spot welded directly to the outer surface of the tube. When the outer tube is heated a correction is made for the deviation of the outer surface temperature from that of the inner (see appendix A.). Power is supplied to the outer tube through OFHC copper rings soft-soldered to the outside surface. Thermocouple locations together with the positions of the current rings are shown in Fig. III.A.5.

In the core tube, thermocouples are placed as shown in Fig. III.A.6. When installed, the core tubes are positioned so that the thermocouples approximately oppose those on

the outer tube. In the heated section the couples are positioned in peripheral grooves in a hollow plastic insert which slips smoothly inside the core tube. The leads run down the center of this tube and out through a hollow copper tube which is soldered to the inside of the inconel tube and serves as a current bus. In the unheated section the couples are similarly positioned but the leads are in axial grooves milled in the outer surface of the plastic insert. Details of the center tube construction are shown in Fig. III.A.7. A similar correction for the temperature drop through the wall of the heated core tube is made. At the unheated end the plastic tube bearing the thermocouples is removable to facilitate the installation of the center tube.

The thermocouples were made from 30 gage, glass insulated, iron-constantan wire. Samples of the wire were calibrated against NBS thermometers. The maximum deviation from the standard tables¹⁴ was $\pm 0.25^{\circ}\text{F}$ throughout the range of interest.

The distribution of the thermocouple emf's to the potentiometer is through a multiple selector switch arrangement as shown in Fig. III.A.8. The thermocouple leads at the test section are connected through MS type multi-pin connectors to copper extension leads from the switch console. The metal housing of the connector tends to iso-thermalize the junctions to the copper. Details of the thermocouple circuit are shown in Fig. III.A.9.

The outside of the outer tube is wrapped with about two inches of Fiberglas, then the entire assembly, including the mounting channel is again wrapped with about one inch of Fiberglas. The heat leak through the insulating blanket is determined by removing the core tube and allowing the system to come to equilibrium with no air flow. To minimize internal free convection the tube is stuffed with Fiberglas. The analysis for the heat loss is presented in appendix B con-

sidering the conduction loss down the current leads. This heat loss is actually only of significance when the outer tube is heated.

The principal experimental interest is in the situation where only one of the boundary walls is heated. To minimize radiation interchange between the two surfaces a duplicate set of unheated tubes is provided in which the surface bounding the flow is nickel plated and polished. The derivation of the radiation interchange factors for the various geometries and the method of correction of the data for this loss are presented in appendix C.

Additional details of the construction and operation of the apparatus are given by Leung²⁷.

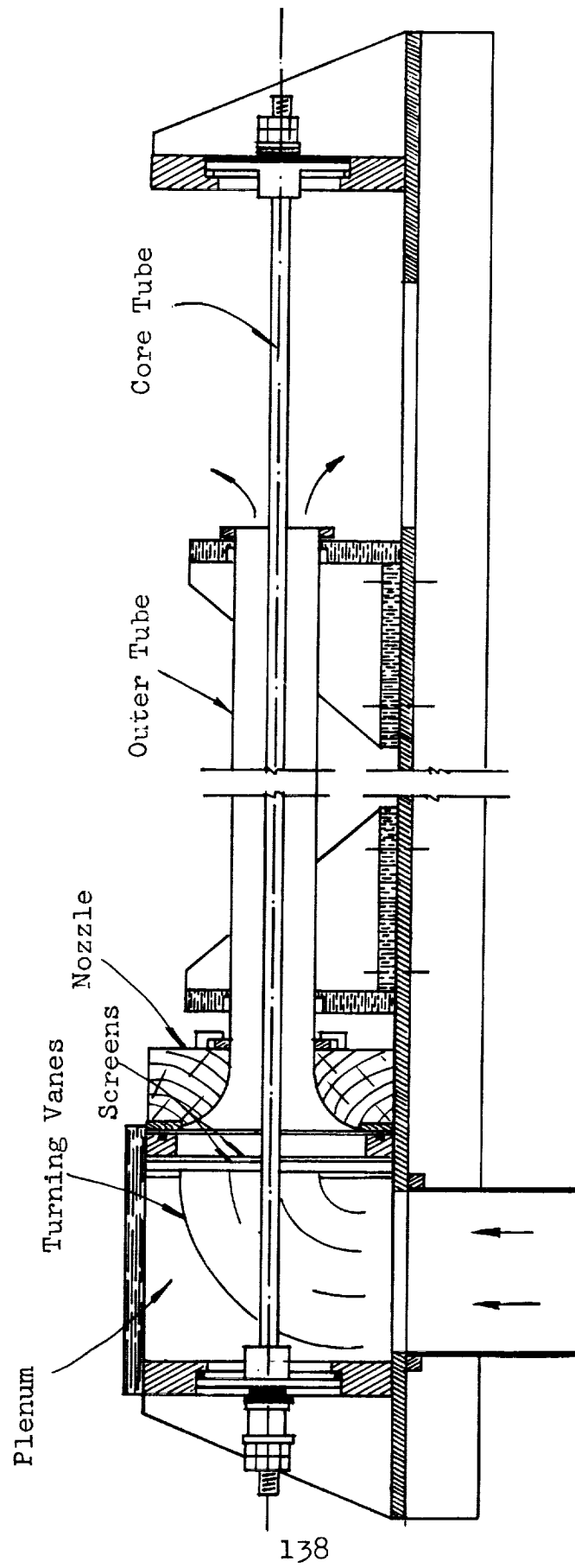


FIG. III.A.3 - Assembly Details

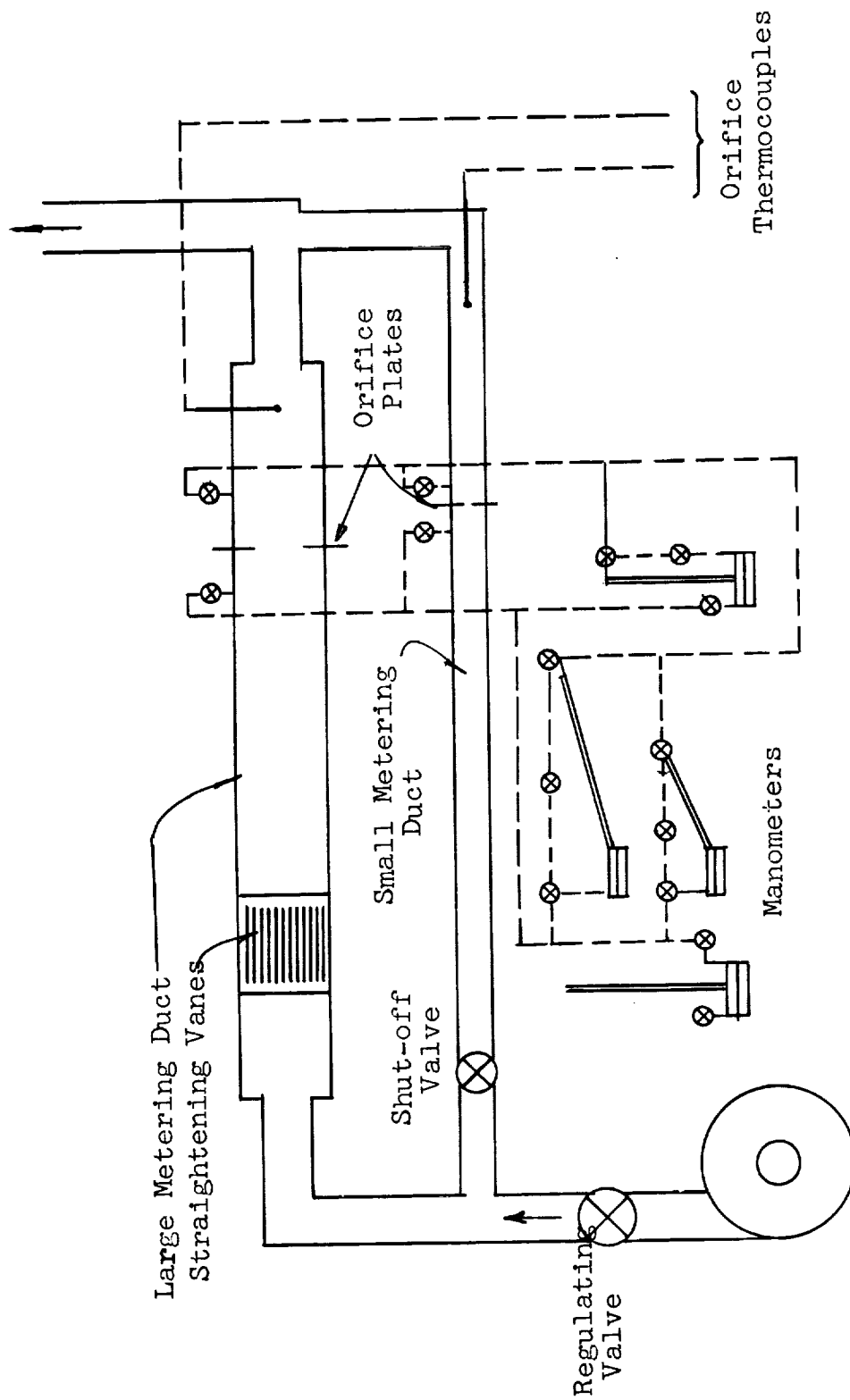


FIG. III.A.4 - Air Metering System

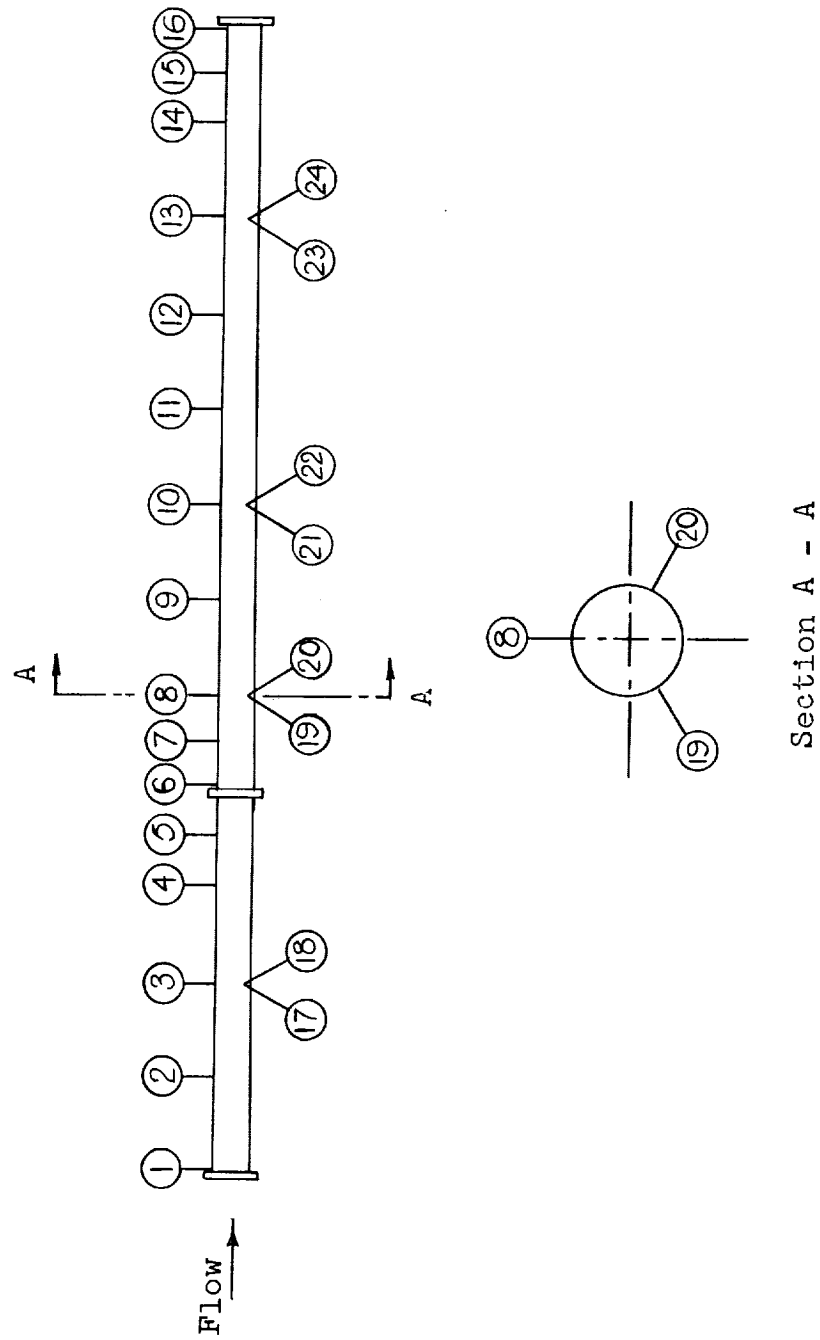


FIG. III.A.5 - Outer Tube Thermocouple Locations

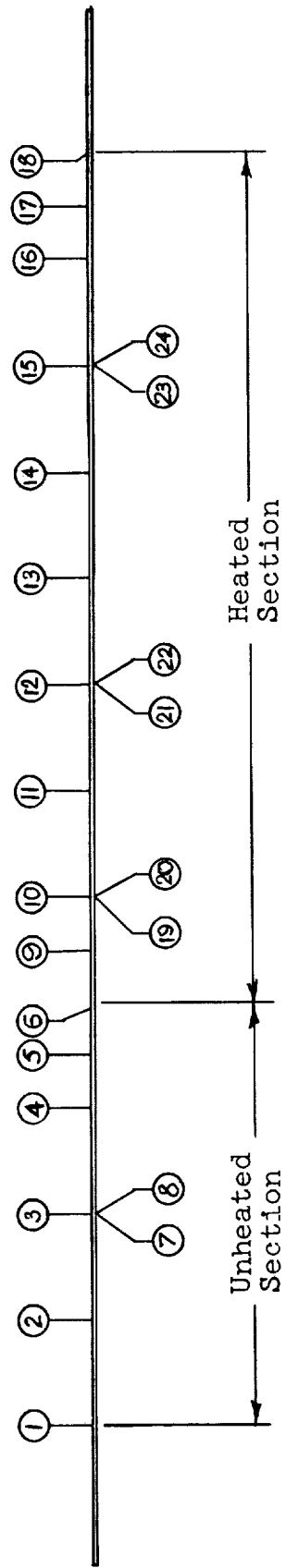


FIG. III.A.6 - Core Tube Thermocouple Locations

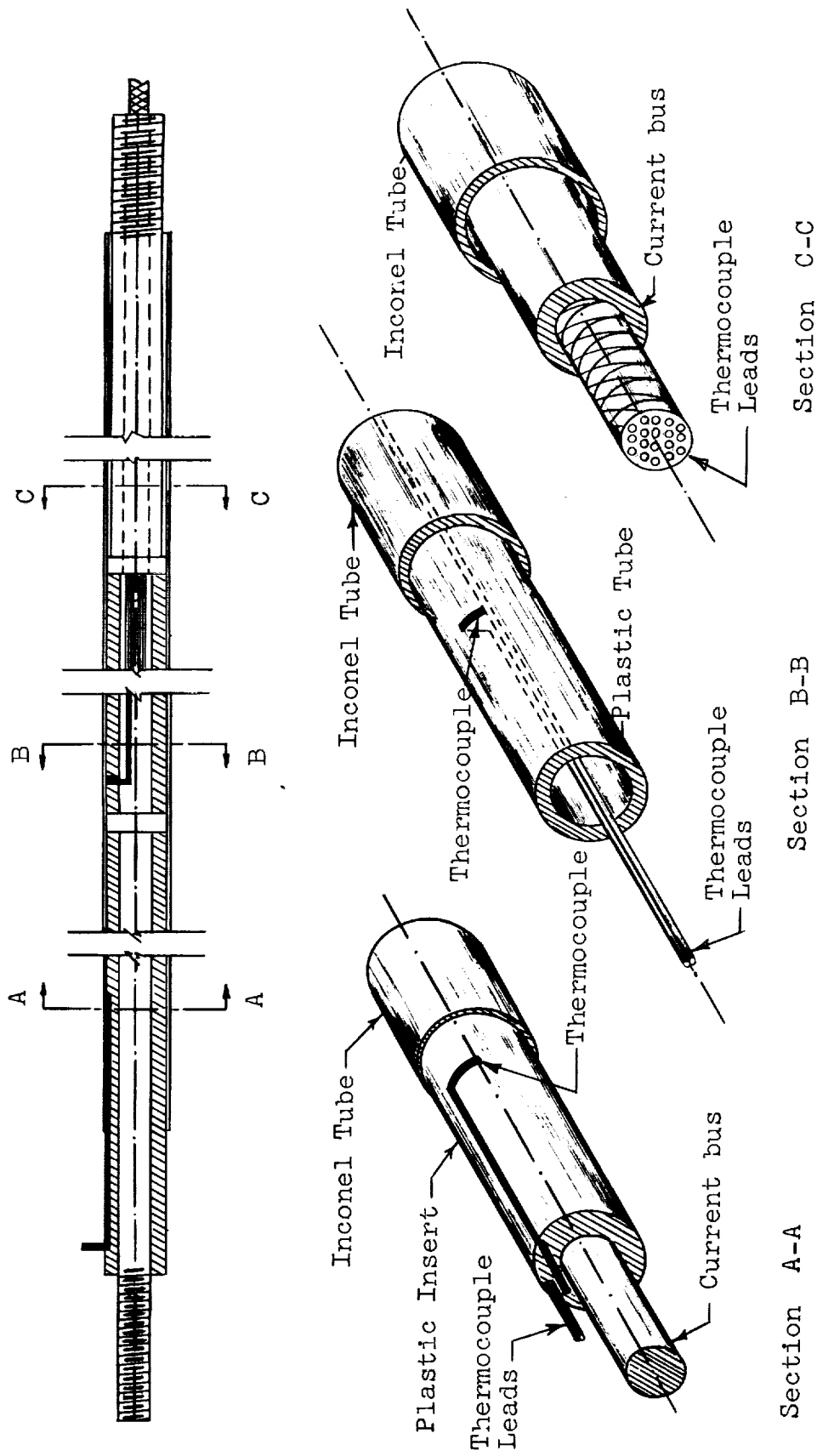


FIG. III.A.7 - Core Tube Construction

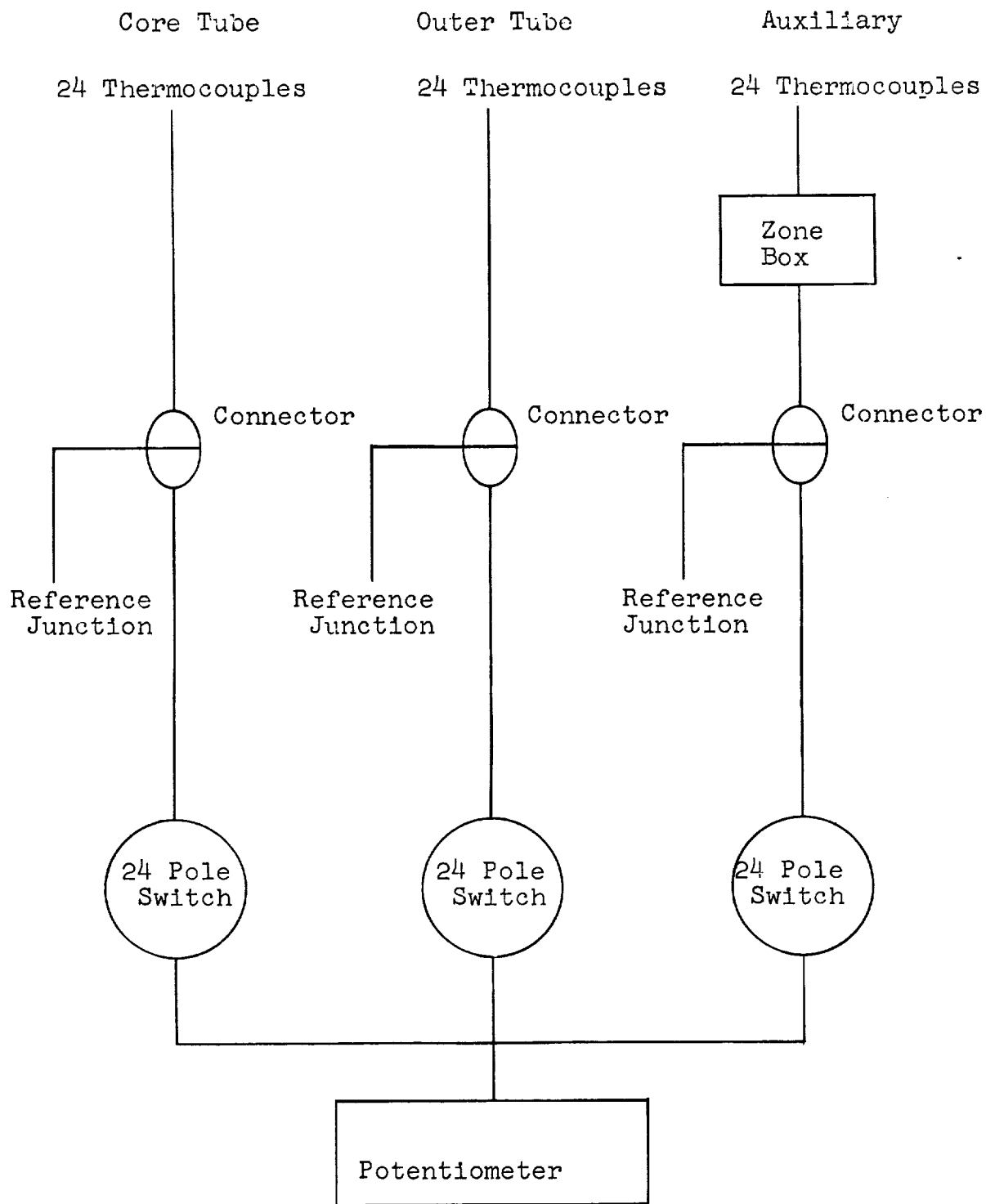


FIG. III.A.8 - Thermocouple Selector System

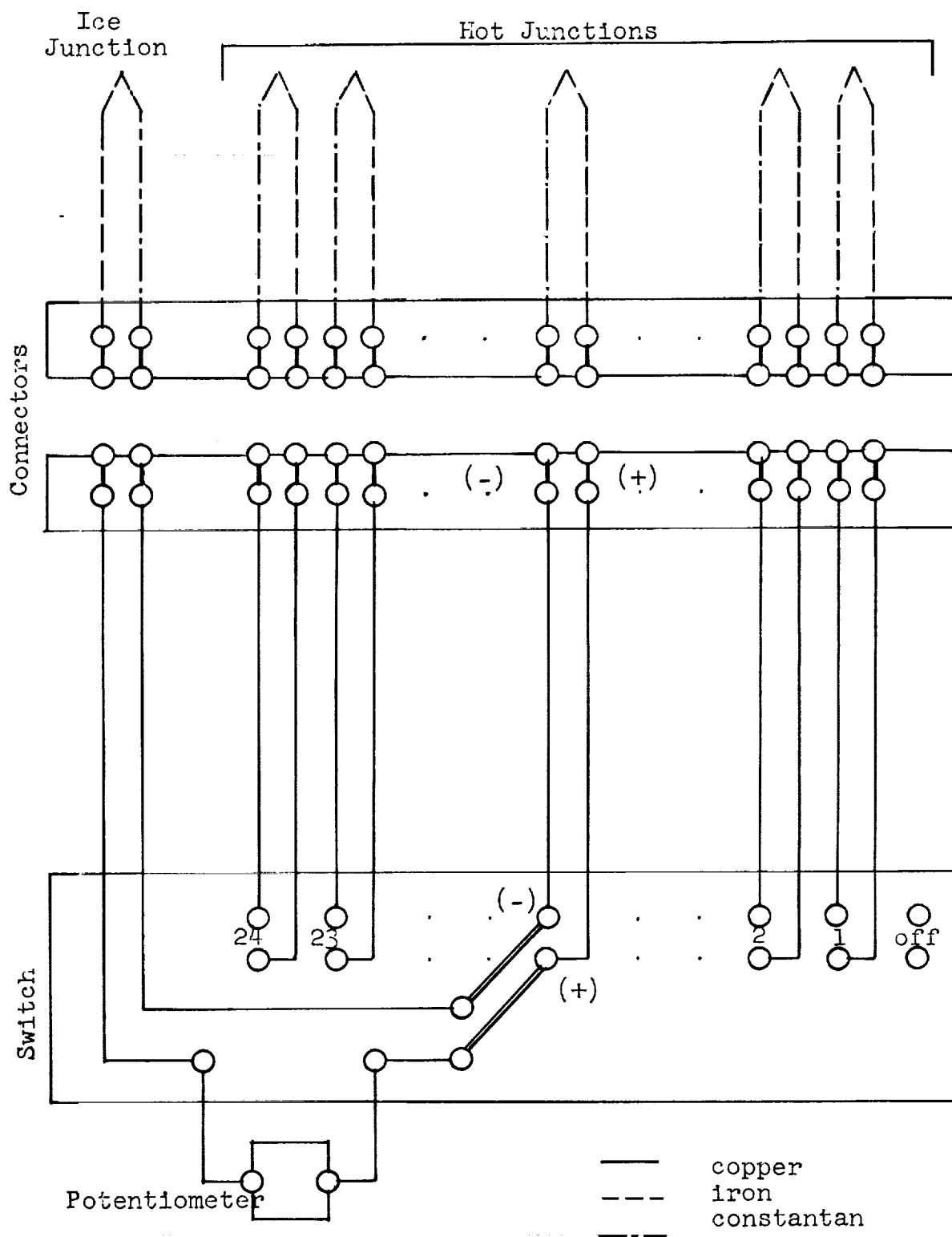


FIG. III.A.9 - Thermocouple Circuit

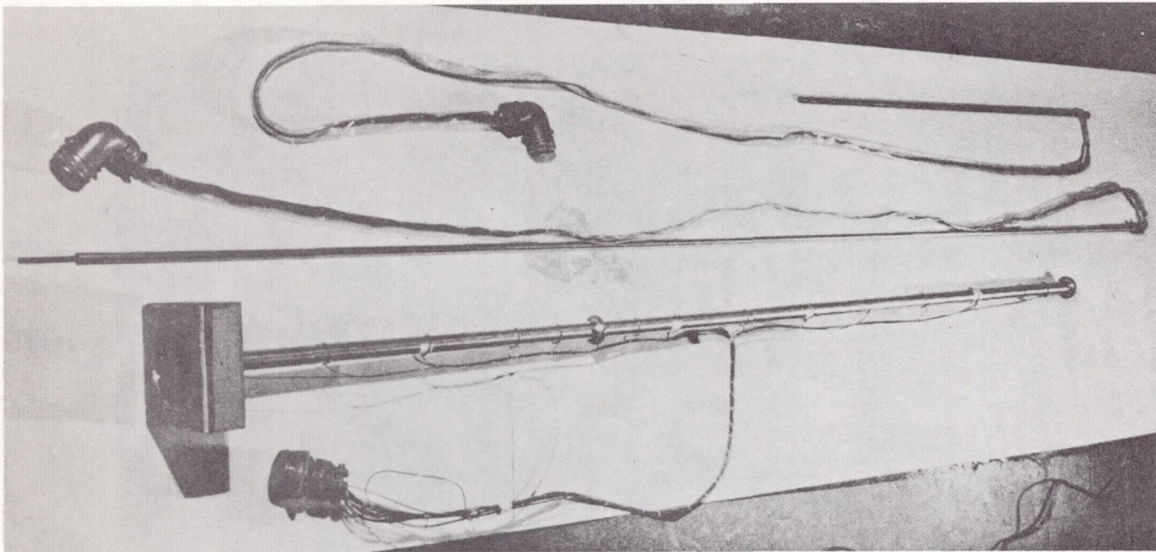


FIG. III.A.10 Inconel Tubes Used in the
Test Section

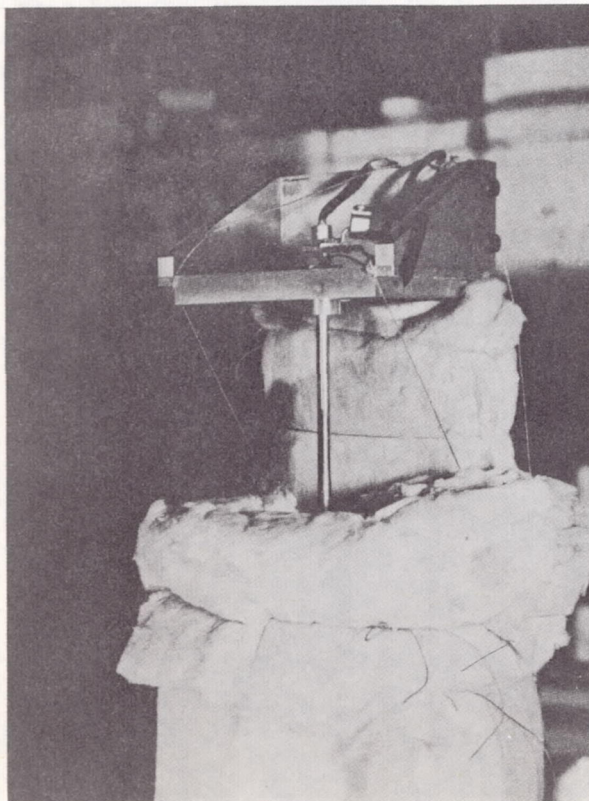


FIG. III.A.11
Test Assembly,
Exit End

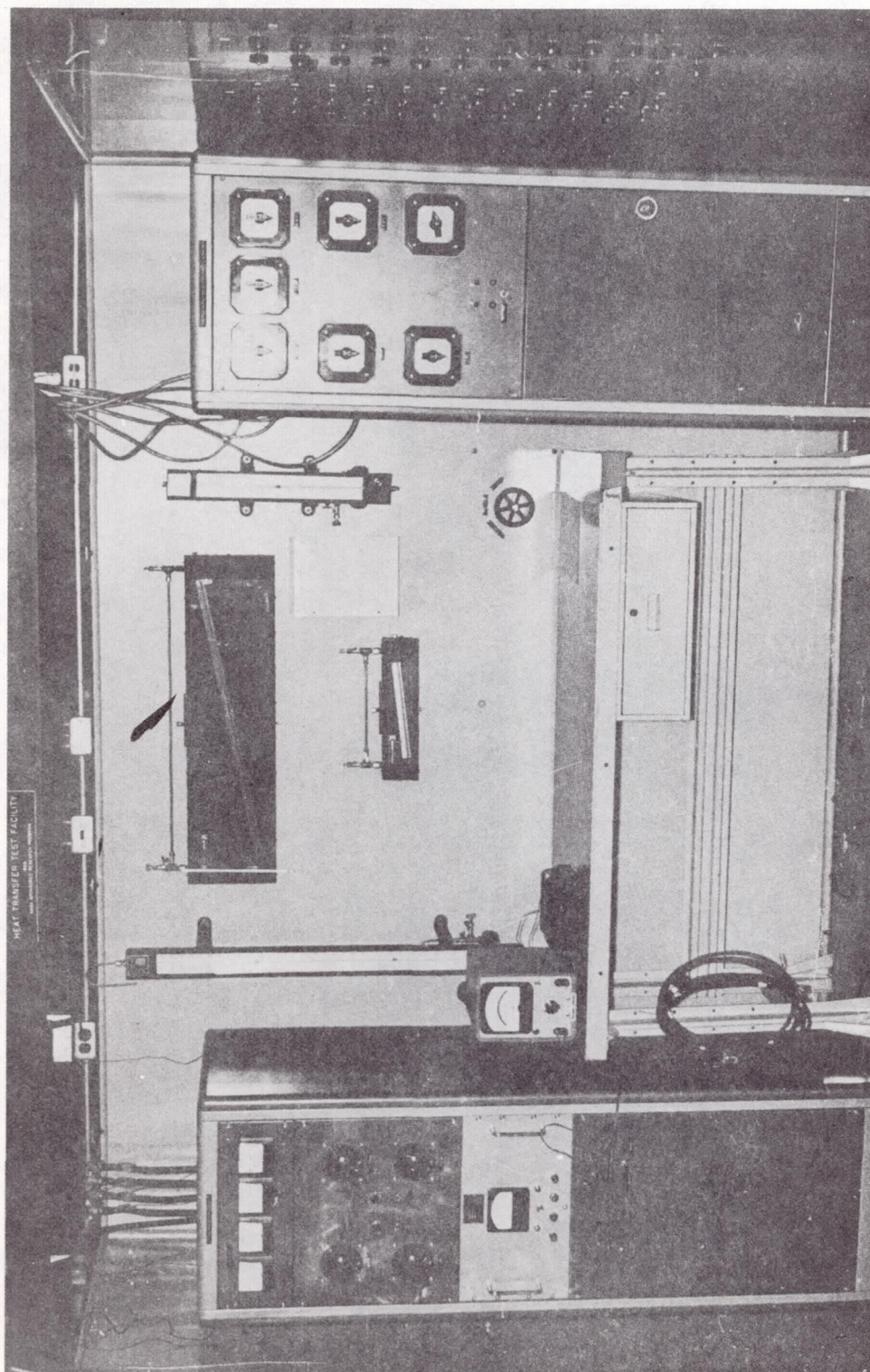


FIG. III.A.12 Power Supply and Instrumentation

III. B. Comparison of Experimental and Theoretical Values

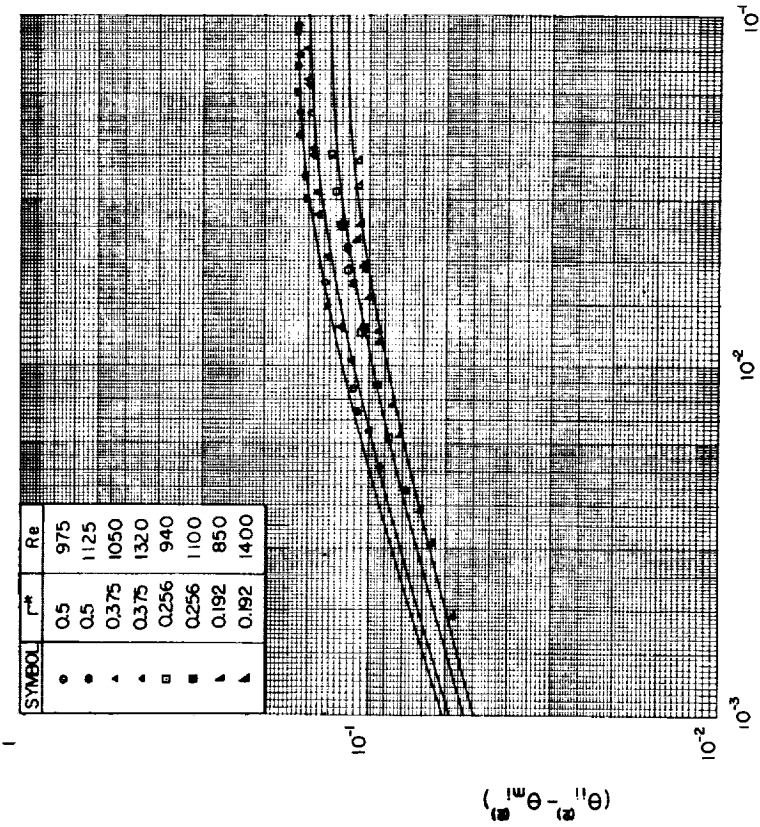
All of the geometries were run in laminar flow with the inner wall only heated. These results, together with the theoretical predictions, are shown in Fig. III.B.1. It is felt (see Appendix D) that these data have a probable uncertainty of ± 5.1 per cent. All of the data are within this interval of the theoretical value and most of the points are considerably better. The tendency of the data to lie somewhat low at the first station (small \bar{x}) may be due to an insufficient hydrodynamic entry length or to axial conduction in the tube wall.

When the outer wall is heated the variation of the fundamental solutions with r^* is much less pronounced. Accordingly, since the heat loss through the insulation in laminar flow was a significant fraction of the heat input only the smaller outer tube (1.0 inches I.D.) was run in this condition.

The results are shown in Fig. III.B.2 for $r^* = 0.376$. The probable uncertainty in this data is ± 7.3 per cent. Again all of the data lie well within this interval. It should be pointed out that the data for the outer wall heated do not really represent a constant heat flux situation but because of the dependence of the heat leakage on the tube wall temperature the heat flux declines about 10 per cent over the range of axial stations at which $(\theta_{oo}^2 - \theta_{mo}^2)$ was evaluated. The general good agreement of the data with the theory suggests that if the axial heat flux variation is not too severe the local wall-to-mean temperature difference can be estimated from the constant flux solution without serious error.

The apparatus is so designed as to allow operation with simultaneous heating from both walls of the annulus. Data from this mode of operation are taken as examples of superposition of the fundamental solutions and are presented in appendix G.

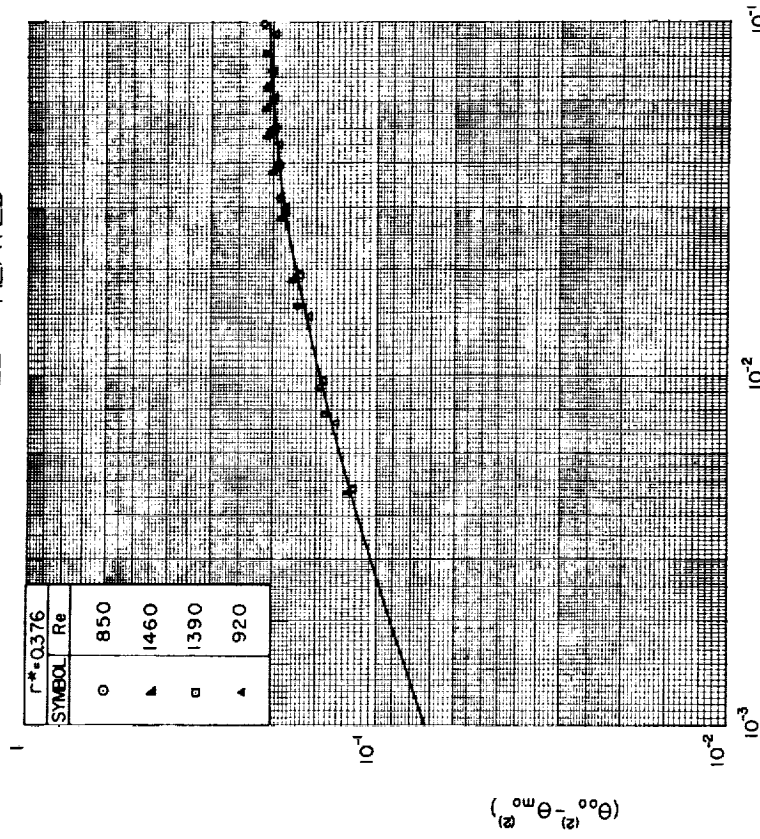
INNER WALL HEATED



$$x = \frac{x/D_h}{Re Pr}$$

FIGURE III.B.1

OUTER WALL HEATED



$$x = \frac{x/D_h}{Re Pr}$$

FIGURE III.B.2

APPENDIX A

CORRECTION FOR THE TUBE WALL TEMPERATURE DUE TO INTERNAL GENERATION

As described in Section III A, the thermocouples for measuring the tube wall temperature are in contact with the heated walls only on the side away from the flow boundary (i.e., on the outside of the outer tube and the inside of the core tube). For the case where the wall is heated some difference between the inner and outer surface temperatures can occur.

Consider a section of the tube as shown in Fig. A.1.

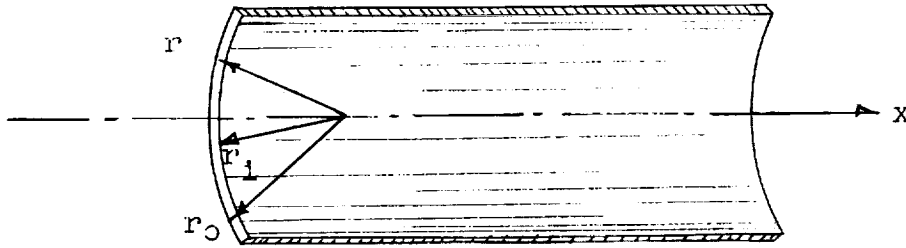


FIG. A.1

If we neglect temperature variation in the x-direction*, the equation of the temperature distribution in the tube wall is

$$r \frac{\partial^2 t}{\partial r^2} + \frac{\partial t}{\partial r} + \frac{rq'''}{k} = 0 \quad (\text{A.1})$$

The general solution to (A.1) is given by

$$t = \frac{-q'''}{4k} r^2 + G \ln r + H \quad (\text{A.2})$$

where G and H are arbitrary constants

*This same result is obtained if $\frac{\partial^2 t}{\partial x^2} = 0$, i.e., fully established flow with constant wall heat flux.

For the heating of the outer tube we have the boundary conditions

$$\frac{\partial t}{\partial r} = 0 \text{ at } r = r_o \text{ and } t = t_1 \text{ at } r = r_1.$$

Using these we can determine G and H. Then, evaluating (A.2) at $r = r_o$ yields

$$(t_o - t_1) = \Delta t_c = \frac{q'''}{2k} \left[r_o^2 \ln \frac{r_o}{r_1} - \frac{(r_o^2 - r_1^2)}{2} \right] \quad (A.3)$$

A somewhat more useful form of (A.3) for the experimental work is

$$\Delta t_c = \frac{1}{2\pi k} \left(\frac{q}{L} \right) \left[\frac{r_o^2}{(r_o^2 - r_1^2)} \ln \frac{r_o}{r_1} - \frac{1}{2} \right] \quad (A.4)$$

where (q/L) is the energy input per unit length of tube (BTU/hr.-ft.).

When the core tube is heated the boundary conditions are

$$\frac{\partial t}{\partial r} = 0 \text{ at } r = r_1 \text{ and } t = t_o \text{ at } r = r_o.$$

The application of these conditions yields the appropriate values of G and H in (A.2) and we have

$$(t_1 - t_o) = \Delta t_c = \frac{q'''}{2k} \left[\frac{(r_o^2 - r_1^2)}{2} - r_1^2 \ln \frac{r_o}{r_1} \right] \quad (A.5)$$

Alternatively

$$\Delta t_c = \frac{1}{2\pi k} \left(\frac{q}{L} \right) \left[\frac{1}{2} - \frac{r_1^2}{(r_o^2 - r_1^2)} \ln \frac{r_o}{r_1} \right] \quad (A.6)$$

For the geometries used in the experiments, the evaluation of (A.4) and (A.6) yields the following correction formulas:

1. Outer heated

A. Inside diameter of outer tube 1.96 inches

$$\Delta t_c = 1.838 \times 10^{-4} (q/L) \quad (A.7)$$

B. Inside diameter of outer tube 1.00 inches

$$\Delta t_c = 2.665 \times 10^{-4} (q/L) \quad (A.8)$$

2. Core tube heated

A. Outside diameter of core tube 0.50 inches

$$\Delta t_c = 7.54 \times 10^{-4} (q/L) \quad (A.9)$$

B. Outside diameter of core tube 0.376 inches

$$\Delta t_c = 9.91 \times 10^{-4} (q/L) \quad (A.10)$$

In each case the wall temperature is given by

$$t_{\text{wall}} = t_{\text{measured}} - \Delta t_c \quad (A.11)$$

It should be pointed out that for the laminar flow work presented here these corrections are entirely negligible, the range of (q/L) is between 10 and 50 BTU/hr.-ft.

APPENDIX B

HEAT LEAK DETERMINATION FOR THE OUTER TUBE

When the outer tube is heated the temperature difference between the wall and the surrounding ambient air causes some heat leak through the insulating blanket. For laminar flow, when the fluid film coefficient is relatively small, a significant fraction of the total energy generated passes out through the insulation or is conducted down the power lead which is connected to the copper ring at the start of the heated section. This loss affects the experimental data in two ways, by altering the energy supplied to the fluid prior to any axial station at which we desire to compute the film coefficient, and by altering the local wall heat flux on which that film coefficient is based.

To evaluate this loss, the insulated outer tube was stuffed with Fiberglas strips and, with the power on, allowed to come to equilibrium with the surrounding air. The power level was adjusted so that the temperature assumed by the tube was nearly equal to that which it would experience while running. The axial temperature distribution was generally dome-shaped as shown in Fig. B.2, dropping off at the ends where the leads are connected and rising to a maximum in the center. The dip in the center results from the presence of a fourth Lucite holder which is not actually contacting the tube in this series of tests.

For analysis, the system is idealized as shown in Fig. B.1.

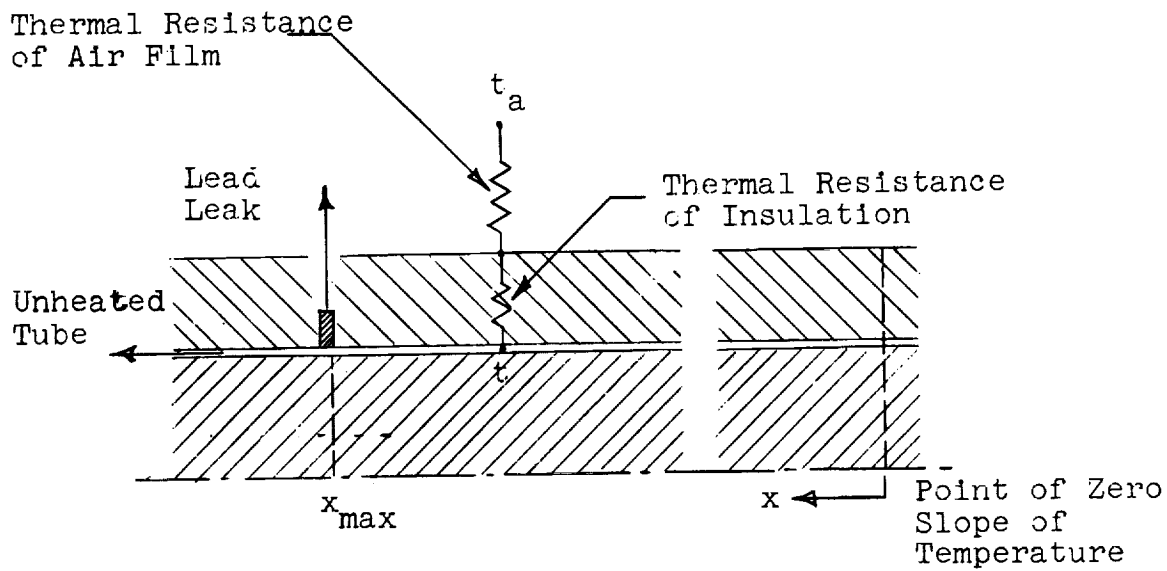


FIG. B.1

The temperature at any axial station is considered to be constant. (The results of Appendix A indicate that this is a good assumption.) The resistance of the insulating blanket and the free convection film resistance are lumped and considered to be a constant with length, that is, the heat flux going out through the insulation is assumed to be expressed by

$$q''_{ins} = h_L (t - t_a) \quad (B.1)$$

where the loss coefficient h_L is independent of temperature and axial position. The heat leak out the current lead and that into the unheated section of the tube are lumped and assumed to be

$$q_{lead} = K_L (t_L - t_a) \quad (B.2)$$

where t_L is the temperature at the connection of the lead to the tube.

If we let $\bar{t} = t - t_a$, the equation of the axial temperature distribution is

$$\frac{\partial^2 \bar{t}}{\partial x^2} - \frac{h_L C_t}{k A_c} \bar{t} + \frac{q'''}{k} = 0 \quad (B.3)$$

where C_t = circumference of the tube,

A_c = cross section area of the tube.

The general solution to (B.3) is

$$\bar{t} = G \sinh(mx) + H \cosh(mx) + \frac{q''' A_c}{h_L C_t} \quad (B.4)$$

where $m^2 = \frac{h_L C_t}{k A_c}$.

If we take $x = 0$ when $\frac{\partial \bar{t}}{\partial x} = 0$, then G must be zero and we have

$$\bar{t} = H \cosh(mx) + \frac{q''' A_c}{h_L C_t} \quad (B.5)$$

By fitting (B.5) to the experimental curve at two points, h_L and H can be evaluated. We have the boundary condition that when $x = x_{\max}$

$$-k A_c \frac{\partial \bar{t}}{\partial x} = K_L \bar{t}. \quad (B.6)$$

To obtain the lead leak constant, we differentiate (B.5) and substitute in (B.6), yielding

$$K_L = -H \sinh(mx_{\max}) \cdot \frac{m K A_c}{(\bar{t})_{x = x_{\max}}}. \quad (B.7)$$

Typical values obtained for h_L and K_L are as follows:

<u>Tube</u>	$\frac{h_L}{}$	$\frac{K_L}{}$
1.96 "	0.204 BTU/hr-ft ² - °F	0.0493 BTU/hr-°F
1.00 "	0.284	0.0381

A comparison of the temperature distribution computed from (B.5) and the measured distribution is given in Fig. B.2. The value of \bar{t} from (B.5) is forced to fit the experimental data at the start of the heated region and at the point of zero slope.

When the core tube is heated the temperature of the outer wall is not greatly different from the ambient, but when the outer wall is heated \bar{t} is about 50°F. For this condition the heat leak can be as much as 30% of the total energy input.

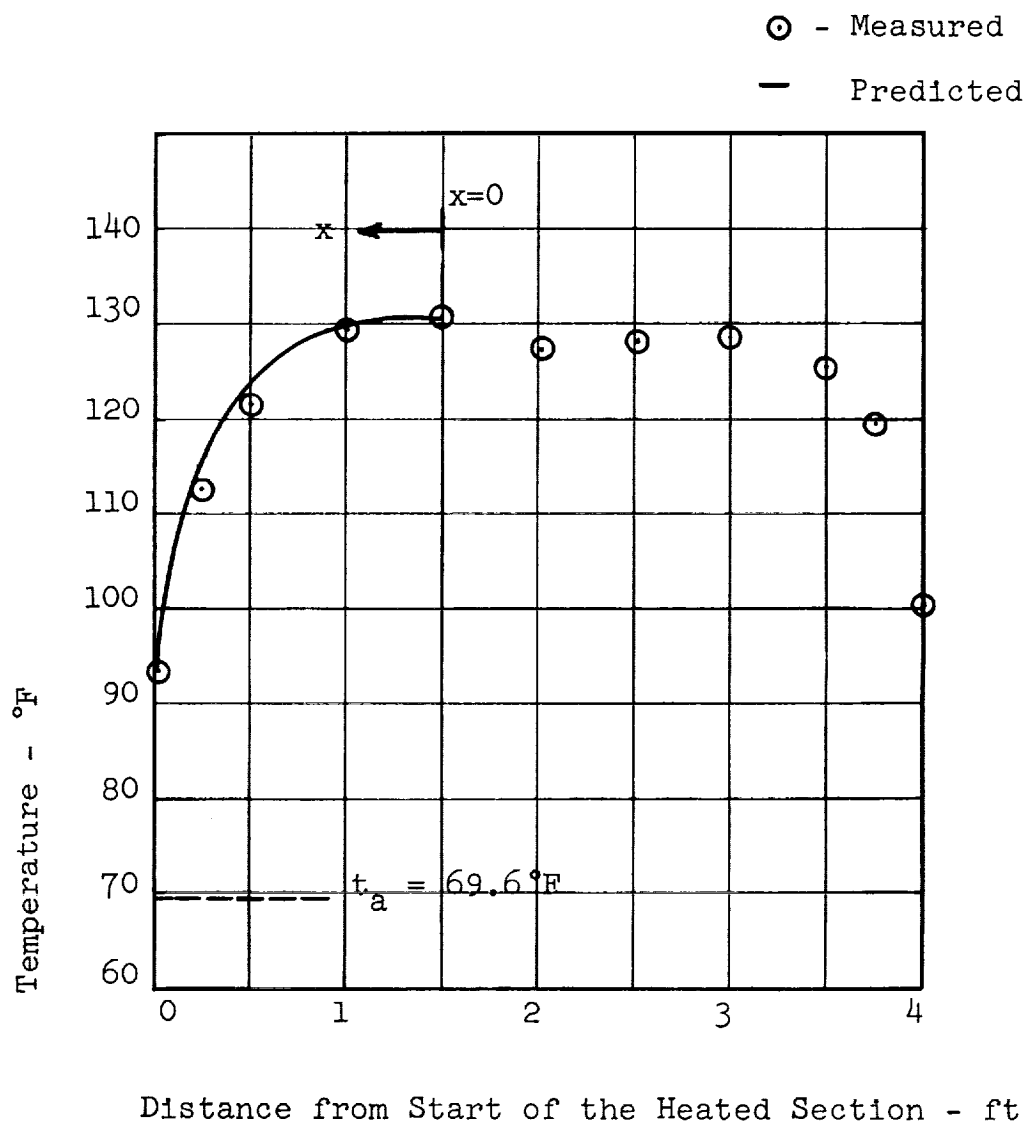


FIG. B.2

APPENDIX C

THE EFFECT OF RADIATION INTERCHANGE BETWEEN THE TWO SURFACES

If the inner and outer surfaces are each at a constant but different temperature, the net heat exchange due to radiation is given by

$$q_r = \frac{A_1}{\frac{1}{\epsilon_1} + \frac{A_1}{A_o} \left(\frac{1}{\epsilon_o} - 1 \right)} \sigma (T_1^4 - T_o^4) \quad (C.1)$$

where the subscript i refers to the inner wall surface, o to the outer.

During the tests, the axial temperature gradient is quite shallow, so that the constant temperature assumption is not a serious handicap except very near the start of the heated length. The value of the emissivity of inconel was assumed to be 0.35*, of the nickel-plated surface 0.1. Then, if we write (C.1) as

$$q''_{ri} = \frac{q_r}{A_1} = F_e \sigma (T_1^4 - T_o^4) \quad (C.2)$$

we can evaluate

$$F_e = \frac{1}{\frac{1}{\epsilon_1} + \frac{A_1}{A_o} \left(\frac{1}{\epsilon_o} - 1 \right)} \quad (C.3)$$

for the various geometries.

Note that the heat flux calculated from (C.2) is that at the inner wall, the flux at the outer wall is given by

*This is the value given by McAdams²⁶ for a clean, well-polished surface, after repeated heating and cooling.

$$q''_{ro} = r^* q''_{ri} \quad (C.4)$$

r^*	Heated wall	F_e
0.192	outer	0.0965
	inner	0.218
0.256	outer	0.0953
	inner	0.1932
0.376	outer	0.0933
	inner	0.160
0.501	outer	0.0915
	inner	0.1352

The objective of the adiabatic wall tests is to determine one of the fundamental solutions directly. The effect of this radiation loss on this determination is shown by the superposition example of I.B.

1. Inner wall heated

The experiment measures t_1 and determines t_m , but from (I.B.17) and (I.B.18) we get that*

$$(t_1 - t_m) = \frac{D_h}{k} [q_1''(\theta_{1i} - \theta_{m1}) + q_o''(\theta_{1o} - \theta_{mo})] \quad (C.5)$$

It is $(\theta_{1i} - \theta_{m1})$ that we seek. Here $q_o'' = r^* q_{ri}'' - q_L''$ and $q_1'' = q''_{\text{measured}} - q_{ri}''$.

$$(\theta_{1i} - \theta_{m1}) = \frac{(t_1 - t_m)}{q_1'' D_h/k} - \frac{r^* q_{ri}''}{q_1''} (\theta_{1o} - \theta_{mo}) \quad (C.6)$$

In laminar flow the temperature profile develops rather slowly, and for most of the range of axial distance covered

*The experiment deals only with fundamental solutions of the second kind, the superscript (2) has been omitted for brevity.

in the experiment, θ_{1o} is nearly zero. For the purposes of the correction to the experimental data it is assumed to be so. Note that this is making the correction to the mean temperature due to heating at the outer wall, but assuming that the heat supplied at the outer wall does not affect the inner wall temperature

2. Outer wall heated

In an analogous manner, (I.B.17) and (I.B.19) can be combined to give

$$(\theta_{oo} - \theta_{mo}) = \frac{(t_o - t_m)}{q_o'' D_h / k} + \frac{q_{r1}''}{q_o''} (\theta_{oi} - \theta_{mi}) \quad (C.7)$$

where $q_o'' = q''_{\text{measured}} + r * q_{r1}'' - q_L''$.

Equation (C.7) is used to correct the outer wall heated data in the same manner as (C.6), i.e., θ_{oi} is assumed to be zero.

For laminar flow, inner wall heated (the worst case) the heat transfer due to radiation can be as great ~~as~~ 10% of the total heat transferred.

APPENDIX D

EXPERIMENTAL UNCERTAINTY

The experimental uncertainty in the fundamental solutions, $\theta - \theta_m$, and the position parameter \bar{x} , can be estimated using the method described by Kline and McClintock⁷.

1. Uncertainty in \bar{x}

The defining equation is*

$$\bar{x} = \frac{x/D_h}{\text{RePr}} \quad (\text{D.1})$$

The uncertainty in D_h is negligible. The axial position of the thermocouples is easily accurate to $\pm 1/16$ inch. This is only $\pm 2\%$ of the first station evaluated, and becomes negligible as x grows larger. The uncertainty in Prandtl number is about $\pm 2.5\%$. The Reynolds number is evaluated from

$$\text{Re} = \left(\frac{w}{A_c}\right) \frac{D_h}{\mu}. \quad (\text{D.2})$$

The determination of the flow rate, w , is subject to the manometer error and the uncertainty of the orifice coefficient. The orifice coefficient should be reliable to $\pm 0.5\%$ (see Ref. 23). Even though the pressure differentials are small (0.5 inch) the manometer uncertainty is of the order of $\pm 1\%$ or $\pm 0.5\%$ when entered as the square root. The uncertainty of the density of air is about $\pm 1\%$. These combine to create a probable uncertainty in the flow rate of $\pm 1.2\%$. The viscosity of air is known to $\pm 1.5\%$, hence the probable uncertainty in Reynolds number is $\pm 1.7\%$. The uncertainty in \bar{x} becomes $\pm 3.6\%$ at the first station, declining to $\pm 3.0\%$ down the tube.

*Note that $x = 0$ corresponds to the start of the heated section.

2. Uncertainty in $\theta - \theta_m$

The computing equations for $\theta - \theta_m$ are (C.6) and (C.7).

a. Heating at the inner wall

During the tests, $t_i - t_m$ was set at approximately 30°F. The uncertainty in t_i is probably $\pm 0.5^\circ$. t_m is computed by adding the temperature rise due to heating to the inlet temperature. This temperature rise reaches a maximum of 20°. The ammeter and the voltmeter used for the power measurements have operating uncertainties of $\pm 0.75\%$ and $\pm 2\%$ respectively. The variation in wall thickness is $\pm 0.75\%$. The uncertainty in power measurement is then $\pm 2.3\%$, and the uncertainty in t_m about $\pm 1^\circ$. The relative uncertainty in $t_i - t_m$ becomes about $\pm 3.5\%$. The radiation loss is about 6% of the total input; if this estimate is off by $\pm 25\%$, the error in q_i'' is $\pm 1.5\%$. The correction term in (C.6) is, at its maximum, only about 3% of the first term, so a $\pm 50\%$ error here means only $\pm 1.5\%$. The thermal conductivity of air is probably reliable to $\pm 2\%$. The combination of these effects produces a total probable uncertainty in $\theta_{ii} - \theta_{mi}$ of $\pm 5.1\%$.

b. Heating at the outer wall

The same considerations apply to $\theta_{oo} - \theta_{mo}$, except that the heat leak through the insulating blanket is 20% to 30% of the total input. It is felt that the estimate of heat leak is good to $\pm 10\%$, hence the uncertainty in wall heat flux becomes $\pm 3.8\%$. This makes the uncertainty in $t_o - t_m$ $\pm 5.6\%$, and the probable uncertainty in $\theta_{oo} - \theta_{mo}$ $\pm 7.3\%$.

A summary of the uncertainties is given below. These uncertainties in all cases are based on 20 to 1 odds.

<u>Item</u>	<u>Core tube heated</u>	<u>Outer tube heated</u>
Thermal conductivity	$\pm 2.0\%$	$\pm 2.0\%$
Viscosity	$\pm 1.5\%$	$\pm 1.5\%$
Prandtl number	$\pm 2.5\%$	$\pm 2.5\%$
Flow rate	$\pm 1.2\%$	$\pm 1.2\%$
Re	$\pm 1.9\%$	$\pm 1.9\%$
\bar{x}	$\pm 3\%$ to $\pm 3.6\%$	± 3.0 to $\pm 3.6\%$
Heat flux	$\pm 2.8\%$	$\pm 3.8\%$
$\theta - \theta_m$	$\pm 5.1\%$	$\pm 7.3\%$

APPENDIX E

DETAILS OF THE NUMERICAL SOLUTION

The method of Berry and de Prima¹ is a convergent iteration scheme for finding the proper eigenvalues for a Sturm-Liouville equation. For the case at hand, this equation is given by (II.F.2). Actually, (II.F.2) represents a system of equations since two different boundary conditions are applied for each of the fundamental cases, and all the conditions are repeated for each value of radius ratio considered.

For each step of the iteration we seek a solution to (II.F.2) subject to (II.H.1). The requirement that this solution satisfy the boundary condition only at $\bar{r} = r^*$, creates an initial value problem. With $\lambda = (\lambda_n^2)_k$ a value is chosen for $R_n(r^*)$ or $R'_n(r^*)$ (note that only one of these is non-zero for any given case) and a numerical integration of II.F.2 is performed from $r^* \leq \bar{r} \leq 1$. In general, the solution so generated will not be normalized, that is

$$\int_{r^*}^1 w(\bar{r}) [R_n(\bar{r})]^2 d\bar{r} \neq 1$$

Since Eq. (II.F.2) is linear, it follows that

$$(R_n(\bar{r}))_k = K_n R_n(\bar{r}) \quad (\text{E.1})$$

where

$$K_n^2 = \frac{1}{\int_{r^*}^1 w(\bar{r}) [R_n(\bar{r})]^2 d\bar{r}} \quad (\text{E.2})$$

will be the desired solution satisfying (II.H.1). Equation (II.H.2) supplies the $(k + 1)$ st approximation to λ_n^2 and the iteration procedure continues. The values given by the

asymptotic expressions (see Section II.G) are used as the first approximations to λ_n^2 in all cases. The correction supplied by (II.H.2) is very strong; after the third iteration, the residual, given by $(R_n(1))_k (R'_n(1))_k$, is less than ± 0.0005 which is used as the convergence criterion for λ_n^2 .

The actual numerical integration is performed using a three-point predictor-corrector method due to Hamming²⁴. To illustrate the method, refer to Fig. E.1.

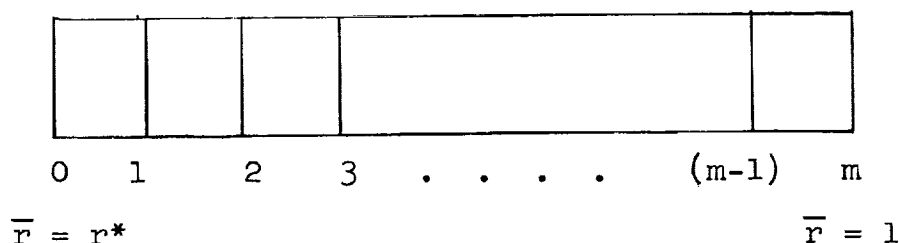


FIG. E.1

The interval $r^* \leq \bar{r} \leq 1$ is divided into equal increments $\Delta\bar{r}$. The station $\bar{r} = r^*$ is numbered 0, $r = r^* + \Delta\bar{r}$ is numbered 1, etc., up to $\bar{r} = 1$, which is station m. Omitting the iterative index, subscript k, let the value of nth eigenfunction at station p, $p = 0, 1, 2, \dots, m$, be denoted $R_n(p)$ and the derivatives by the prime notation $R'_n(p)$ and $R''_n(p)$. After the scheme is started, we predict the derivative at the $p + 1$ station by

$$R'_n(p + 1) = R'_n(p - 3) + \frac{4}{3}(\Delta\bar{r})[2R''_n(p) + 2R''_n(p - 2) - R''_n(p - 1)] \quad (E.3)$$

Using this we can calculate

$$R_n(p + 1) = \frac{1}{8} \left\{ 9R_n(p) - R_n(p - 2) + 3(\Delta\bar{r})[R'_n(p + 1) + 2R'_n(p) - R'_n(p - 1)] \right\} \quad (E.4)$$

The value of $R_n''(p + 1)$ can be calculated from the differential equation and the corrector (E.4) applied to both $R_n'(p + 1)$ and $R_n(p + 1)$. These next better values are then used to recalculate $R_n''(p + 1)$ and (E.4) applied again to settle the values of $R_n'(p + 1)$ and $R_n(p + 1)$. The scheme goes as follows:

- (1) Compute $R_n'(p + 1)$ from (E.3)
- (2) Compute $R_n(p + 1)$ from (E.4)
- (3) Compute $R_n''(p + 1)$ from (II.F.2)
- (4) Compute $R_n'(p + 1)$ from (E.4) (adding another prime to every term)
- (5) Compute $R_n(p + 1)$ from (E.4)
- (6) Repeat steps 3, 4, and 5.

Equation (E.3) is the predictor used with the Milne²⁵ method.

Considerable care is used in starting the procedure and an iteration is performed to correct the first station values by

$$R_n(1) = R_n(0) + \frac{(\Delta r)}{12} [5R_n'(0) + 8R_n'(1) - R_n'(2)] \quad (E.5)$$

After the integration is complete, the norm of the eigenfunction

$$\int_{r^*}^1 w(\bar{r}) [R_n(\bar{r})]^2 d\bar{r}$$

is calculated using Simpson's rule. When the iteration scheme has satisfied the criterion for closure, the eigenconstants are calculated from (II.F.7), again using Simpson's rule for the integration.

To provide a validity check on the method, the first six eigenvalues for the circular tube with constant wall heat flux (the fundamental solutions of the second kind for $r^* = 0$) were calculated. Table E.1 is a comparison of these values with those published by Siegel, Sparrow, and

Hallman²⁰. These integrations were performed using 250 divisions of the interval.

λ_n		
n	Siegel, et al	Present Values
1	7.16654	7.16654
2	12.9508	12.9508
3	18.6638	18.6636
4	24.3530	24.3532
5	30.0317	30.0317
6	35.7040	35.7030

The machine program is written in the Burroughs' version of ALGOL. The following symbols are used in the program.

<u>Quantity</u>	<u>Machine Symbol</u>
λ_n	L
λ_n^2	LL
Weight function, $w(\bar{r})$	W(I)
Position index, p	I
$R_n(p)$	R(I)
$R'_n(p)$	RP(I)
$R''_n(p)$	RDP(I)
$\Delta \bar{r}$	DEL
K_n^2	C

```

COMMENT  LAMINAR EIGENVALUES FOR THE ANNULUS;
INTEGER  N,I;
ARRAY RBR(340),W(340),G(340),R(340), RBRSQ(340), RBRHF(340),
      LNR(340), FRI(340) , FRO(340), RP(340),RDP(340);
INPUT VALUES(L,RO,RPO,DEL,EPS1,EPS2,THETAI,THETA0,RSTAR,K);
OUTPUT ANSWR (L,LL,RO,RPO,CI,CO,RSTAR,FOR I=(1,1,N);((C*0.5).
                                                    R(I))),

NOTE (L), CHEK1 (R(N),PR(N)), CEK2 (NORM);
FORMAT FRMT(B5,*L*,X12.8,B2,*LL*,X12.7,B2,*RO*,X12.8,B2,*RPO*,
      X12.8,B2,*CI*,F15.8,B2,*CO*,F15.8,B2,*RSTAR*,X6.3,W2,125
      (8X14.10,W2)), FRMT2 (*THIS INTERMEDIATE L IS*,X14.7,W2);
FORMAT FRMT3(*R(N)*,X15.10,*RNP*,X15.10,W0),
FRMT4(*NORM*,X15.10,W0);
PROCEDURE CONST(M,K,DEL,W(),F(),R();C);
BEGIN INTEGER I,M; C=0.0; FOR I=(1,2,M-2); C=C+DEL(4W(I).F(I).
      R(I)+2W(I+1).F(I+1).R(I+1))/3; C=(C+4DEL.W(M-1).F(M-1).
      R(M-1)) (K*0.5)/3;
RETURN END;
COMMENCE..READ (;;VALUES);
DR=1.0;
IF (DR NEQ RSTAR); BEGIN DR=RSTAR;
LGRS=LOG(RSTAR); B=((RSTAR*2)-1)/LGRS;
EN=1/(2(1+(RSTAR*2)-B)((1-RSTAR)*2));
M=(1-RSTAR)/DEL; N=FIX(M);
FOR I=(1,1,N-1); BEGIN
RBR(I)=RSTAR+I.DEL;
RBRSW(I)=RBR(I).RBR(I);
RBRHF(I)=SQRT(RBR(I));
LNR(I)=LOG(RBR+I));
W(I)=EN(RBR(I)-(RBR+I)*3)+B.RBR(I)LNR(I));
FRI(I)=(-4RSTAR.EN/(1+RSTAR))(((1-B)/4)(RBR(I)*2-LNR(I))-(RBR
      (I)*4)/16+B(RBR(I)*2LNR(I)/4-(RSTAR*2)(1+(RSTAR*2)-B)
      /4+(1+LGRS)/4-(RSTAR*4)/16)-THETAI;

```

```

FRO(I)=(-4EN/(1+RSTAR))*(((1-B)/4)*(RBR(I)*2-1)-(RBR(I)*4-1)/16
      +B(RBR(I)*2)LNR(I)/4-(RSTAR*2)*(RSTAR*2-B)LNR(I)/4)-THETA0
END END;W(N)=0.0; RBR(N)=1.0; RBRSQ(N)=1.0; RBRHF(N)=1.0;
INF..LL=L.L;
FOR I=(1,1,N); G(I)=LL.W(I);
RDPO=0.0; RP(1)=0.0; R(1)=RO;
FOR P=1.0,2.0; BEGIN
RDP(1)=- (RP(1)+G(1).R(1))/RBR(1);
RP(1)=DEL(RDPO+RDP(1))/2;
R(1)=RO+DEL(RPO+RP(1))/2-(DEL*2)*(RDP(1)-RDPO)/12 END;
RP(2)=R/(1)=DEL(3RDP(1)-RDPO)/2;
R(2)=RO+(RPO+4RP(1)+RP(2))DEL/3;
FOR P=1.0,2.0; BEGIN
RDP(2)=- (RP(2)+G(2).R(2))/RBR(2);
RP(1)=(5RDPO+8RDP(1)-RDP(2))DEL/12+RPO;
R(1)=(5RPO+8RP(1)-RP(2))DEL/12+RO;
RDP(1)=- (RP(1)+G(1).R(1))/RBR(1);
RP(2)=RPO+(RDPO+4RDP(1)+RDP(2))DEL/3;
R(2)=R(1)+DEL(RP(2)+RP(1))/2-(DEL*2)*(RDP(2)-RDP(1))/12 END;
RP(3)=RP(2)+DEL(3RDP(2)-RDP(2)-RDP(1))/2;
R(3)=(9R(2)-RO+3DEL.(RP(3)+2RP(2)-RP(1)))/8;
FOR P=1.0,2.0; BEGIN
RDP(3)=1(RP(3)+G(3).R(3))/RBR(3);
RP(3)=(9RP(2)-RPO+3DEL.(RDP(3)+2RDP(2)-RDP(1)))/8;
R(3)=(9R(2)-RO+3DEL.(RP(3)+2RP(2)-RP(1)))/8 END;
RP(4)=RPO+(4.0)DEL.((2.0)(RDP(3)+RDP(1))-RDP(2))/3.0;
R(4)=(9R(3)-R(1)+3DEL.(RP(4)+2RP(3)-RP(2)))/8;
FOR P=1.0,2.0; BEGIN
RDP(4)=- (RP(4)+G(4).R(4))/RBR(4);
RP(4)=(9RP(3)-RP(1)+3DEL.(RDP(4)+2RDP(3)-RDP(2)))/8;
R(4)=(9R(3)-R(1)+3DEL.(RP(4)+2RP(3)-RP(2)))/8 END;
FOR I=(4,1,N-1); BEGIN
RP(I+1)=RP(I-3)+(1.3333333)DEL.((2.0)(RDP(I)+RDP(I-2))-RDP(I-1));
R(I+1)=(9R(I)-R(I-2)+3DEL.(RP(I+1)+2RP(I)-RP(I-1)))/8;

```



```

FOR P=1.0,2.0; BEGIN
RDP(I+1)=- (RP(I+1)+G(I+1).R(I+1))/RBR(I+1);
RP(I+1)=(9RP(I)-RP(I-2)+3DEL.(RDP(I+1)+2RDP(I)-RDP(I-1)))/8;
R(I+1)=(9R(I)-R(I-2)+3DEL.RP(I+1)+2RP(I)-RP(I-1))/8 END END;
WRITE (;;CHEK1,FRMT3);
NORM=0.0;
FOR I=(1,2,N-1); NORM=NORM+DEL(4W(I)(R(I).R(I))+2W(I+1)(R(I+1)
    ).R(I+1)))/3;
WRITE (;;CEK2,FRMT4);
C=1/NORM
IF ((ABS(C.R(N).RP(N))) GEQ EPS3); GO RECORD;
CONST (N,C,DEL,W(),FRI(),R());CI);
CONST (N,C,DEL,W(),FRO(),,R());CO);
WRITE (;;ANSWR,FRMT); GO COMMENCE;
RECORD..WRITE (;;NOTE,FRMT2);
L=SQRT(LL+C.R(N).RP(N));
GO INF;
FINISH;

```

APPENDIX F

DERIVATION OF THE EXPANSION COEFFICIENTS

In order to establish completely the solution to the energy equation it was necessary to expand the initial condition on $\bar{\theta}_j^{(k)}$ as an infinite series of the eigenfunctions (II.F.6) with the expansion coefficients, C_n , given by (II.F.7). For computational purposes, particularly to establish the asymptotic values of the C_n , it was necessary to provide a more convenient form for the integrals appearing in (II.F.7).

We desire to evaluate the integral

$$\int_{r^*}^1 w(\bar{r}) R_n^2(\bar{r}) d\bar{r} \quad (F.1)$$

which is the norm of the eigenfunction. Let us write Eq.(II.F.2) as

$$\frac{d}{d\bar{r}} \left(\bar{r} \frac{dR_n}{d\bar{r}} \right) + \lambda^2 w(\bar{r}) R_n = 0 \quad (F.2)$$

Taking $\frac{\partial}{\partial \lambda}$ of the above we have

$$\frac{\partial}{\partial \lambda} \left[\frac{\partial}{\partial \bar{r}} \left(\bar{r} \frac{\partial R_n}{\partial \bar{r}} \right) \right] + 2\lambda w(\bar{r}) R_n + \lambda^2 w(\bar{r}) \frac{\partial R_n}{\partial \lambda} = 0$$

Since the order of partial differentiation may be reversed this may be written as

$$\frac{\partial}{\partial \bar{r}} \left[\bar{r} \frac{\partial}{\partial \bar{r}} \left(\frac{\partial R_n}{\partial \lambda} \right) \right] + 2\lambda w(\bar{r}) R_n + \lambda^2 w(\bar{r}) \frac{\partial R_n}{\partial \lambda} = 0 \quad (F.3)$$

If we multiply (F.3) by R_n and integrate between r^* and 1, we have

$$\begin{aligned} \int_{r^*}^1 R_n \frac{\partial}{\partial \bar{r}} \left[\bar{r} \frac{\partial}{\partial \bar{r}} \left(\frac{\partial R_n}{\partial \lambda} \right) \right] d\bar{r} + 2\lambda \int_{r^*}^1 w(\bar{r}) R_n^2 d\bar{r} \\ + \lambda^2 \int_{r^*}^1 w(\bar{r}) \left(\frac{\partial R_n}{\partial \lambda} \right) R_n d\bar{r} = 0 \end{aligned} \quad (F.4)$$

Integrating by parts twice we can get

$$\begin{aligned} 2\lambda \int_{r^*}^1 w(\bar{r}) R_n^2 d\bar{r} = - \left[\bar{r} R_n(\bar{r}) \frac{\partial}{\partial \bar{r}} \left(\frac{\partial R_n}{\partial \lambda} \right) \right]_{r^*}^1 \\ + \left[\left(\frac{\partial R_n}{\partial \lambda} \right) \bar{r} \left(\frac{\partial R_n}{\partial \bar{r}} \right) \right]_{r^*}^1 - \int_{r^*}^1 \left(\frac{\partial R_n}{\partial \lambda} \right) \left[\frac{\partial}{\partial \bar{r}} \left(\bar{r} \frac{\partial R_n}{\partial \bar{r}} \right) \right. \\ \left. + \lambda^2 w(\bar{r}) R_n \right] d\bar{r} = 0 \end{aligned} \quad (F.5)$$

If $\lambda = \lambda_n$ the integral on the right hand side of (F.5) vanishes and we have*

$$\begin{aligned} \int_{r^*}^1 w(\bar{r}) R_n^2 d\bar{r} = \frac{1}{2\lambda_n} \left\{ - \left[\bar{r} R_n(\bar{r}) \frac{\partial}{\partial \bar{r}} \left(\frac{\partial R_n}{\partial \lambda_n} \right) \right]_{r^*}^1 \right. \\ \left. + \left[\left(\frac{\partial R_n}{\partial \lambda_n} \right) \bar{r} \left(\frac{\partial R_n}{\partial \bar{r}} \right) \right]_{r^*}^1 \right\} \end{aligned} \quad (F.6)$$

* there the derivative $\partial R_n / \partial \lambda_n$ is used to indicate $(\partial R_n / \partial \lambda)_{\lambda=\lambda_n}$.

For the various fundamental cases certain of the terms in (F.6) will vanish by virtue of the boundary conditions but for each specific case the value of the norm may be readily obtained.

The numerator of (II.F.7) has the form

$$\int_{r^*}^1 w(\bar{r}) F_j^{(k)}(\bar{r}) R_n(\bar{r}) d\bar{r} \quad (F.7)$$

where $F_j^{(k)}(\bar{r}) = \bar{\theta}_j^{(k)}(\bar{r}, 0)$. To evaluate this, multiply (F.2) by $F(r)$ and integrate by parts. Then

$$\begin{aligned} \int_{r^*}^1 F_j^{(k)}(\bar{r}) w(\bar{r}) R_n(\bar{r}) d\bar{r} = & - \frac{1}{\lambda_n^2} \left\{ \left[F_j^{(k)}(\bar{r}) \left(\bar{r} \frac{\partial R_n}{\partial \bar{r}} \right) \right]_{r^*}^1 \right. \\ & \left. - \int_{r^*}^1 \left(\bar{r} \frac{\partial R_n}{\partial \bar{r}} \right) \left(\frac{dF_j^{(k)}}{d\bar{r}} \right) d\bar{r} \right\} \end{aligned} \quad (F.8)$$

Let us consider (F.8) for each of the initial conditions developed in section II.D.

For the first case

$$\bar{\theta}_1^{(1)}(\bar{r}, 0) = F_1^{(1)}(\bar{r}) = - \frac{\ln \bar{r}}{\ln r^*}, \text{ then}$$

$$\frac{dF_1^{(1)}(\bar{r})}{d\bar{r}} = - \frac{1}{\bar{r} \ln r^*} \quad \text{so that}$$

$$\int_{r^*}^1 F_1^{(1)}(\bar{r}) w(\bar{r}) R_n(\bar{r}) d\bar{r} = - \frac{1}{\lambda_n^2} r^* \left(\frac{\partial R_n}{\partial \bar{r}} \right)_{\bar{r}=r^*} \quad (F.9)$$

Given that $F_0^{(1)}(\bar{r}) = \frac{\ln \bar{r}}{\ln r^*} - 1$ we obtain in an analogous manner

$$\int_{r^*}^1 F_0^{(1)}(\bar{r}) w(\bar{r}) R_n(\bar{r}) d\bar{r} = \frac{1}{\lambda_n^2} \left(\frac{\partial R_n}{\partial \bar{r}} \right)_{\bar{r}=1} \quad (F.10)$$

For case 2, the first term on the right hand side of (F.8) vanishes by virtue of the boundary conditions and we have

$$\int_{r^*}^1 F_j^{(2)}(\bar{r}) w(\bar{r}) R_n(\bar{r}) d\bar{r} = \frac{1}{\lambda_n^2} \int_{r^*}^1 \bar{r} \left(\frac{\partial R_n}{\partial \bar{r}} \right) \left(\frac{dF_j^{(2)}}{d\bar{r}} \right) d\bar{r}$$

Integrating by parts yields

$$\begin{aligned} \int_{r^*}^1 F_j^{(2)}(\bar{r}) w(\bar{r}) R_n(\bar{r}) d\bar{r} &= \frac{1}{\lambda_n^2} \left[\bar{r} \left(\frac{dF_j^{(2)}}{d\bar{r}} \right) R_n(\bar{r}) \right]_{r^*}^1 \\ &\quad - \frac{1}{\lambda_n^2} \int_{r^*}^1 R_n(\bar{r}) \frac{d}{d\bar{r}} \left(\bar{r} \frac{dF_j^{(2)}}{d\bar{r}} \right) d\bar{r} \end{aligned}$$

Recall that $F_j^{(2)}(\bar{r}) = -\theta_j^{(2)}(\bar{r})_{fd}$ and

$$\frac{d}{d\bar{r}} \left(\bar{r} \frac{d\theta_j^{(2)}(\bar{r})_{fd}}{d\bar{r}} \right) = \left(\frac{\partial \theta_j^{(2)}}{\partial \bar{x}} \right) w(\bar{r})$$

so that we have

$$\int_{r^*}^1 F_j^{(2)}(\bar{r}) w(\bar{r}) R_n(\bar{r}) d\bar{r} = \frac{1}{\lambda_n^2} \left[\bar{r} \left(\frac{dF_j^{(2)}}{d\bar{r}} \right) R_n(\bar{r}) \right]_{r^*}^1$$

$$+ \frac{1}{\lambda_n^2} \int_{r^*}^1 \left(\frac{\partial \theta_{mj}^{(2)}}{\partial \bar{x}} \right) w(\bar{r}) R_n(\bar{r}) d\bar{r}$$

Further

$$w(\bar{r}) R_n(\bar{r}) = - \frac{1}{\lambda_n^2} \frac{\partial}{\partial \bar{r}} \left(\bar{r} \frac{\partial R_n}{\partial \bar{r}} \right)$$

so that

$$\int_{r^*}^1 F_j^{(2)}(\bar{r}) w(\bar{r}) R_n(\bar{r}) d\bar{r} = + \frac{1}{\lambda_n^2} \left[\bar{r} \left(\frac{dF_j^{(2)}}{d\bar{r}} \right) R_n(\bar{r}) \right]_{r^*}^1$$

$$- \frac{1}{\lambda_n^4} \left(\frac{\partial \theta_{mj}^{(2)}}{\partial \bar{x}} \right) \left[\bar{r} \frac{\partial R_n}{\partial \bar{r}} \right]_{r^*}^1$$

The second term on the right vanishes and

$$\frac{dF_j^{(2)}}{d\bar{r}} = \pm \frac{1}{2(1-r^*)} \quad \text{at } \bar{r} = r_j, \text{ and zero on the opposite wall.}$$

Hence

$$\int_{r^*}^1 F_1^{(2)}(\bar{r}) w(\bar{r}) R_n(\bar{r}) d\bar{r} = - \frac{r^* R_n(r^*)}{\lambda_n^2 2(1-r^*)} \quad (\text{F.11})$$

and

$$\int_{r^*}^1 F_0^{(2)}(\bar{r}) w(\bar{r}) R_n(\bar{r}) d\bar{r} = - \frac{R_n(1)}{\lambda_n^2 2(1-r^*)} \quad (F.12)$$

For the third kind $F_j^{(3)}(\bar{r}) = -1$, then $\frac{dF_j^{(3)}}{d\bar{r}} = 0$
and we have immediately

$$\int_{r^*}^1 F_1^{(3)}(\bar{r}) w(\bar{r}) R_n(\bar{r}) d\bar{r} = - \frac{r^*}{\lambda_n^2} \left(\frac{\partial R_n}{\partial \bar{r}} \right)_{\bar{r}=r^*} \quad (F.13)$$

and

$$\int_{r^*}^1 F_0^{(3)}(\bar{r}) w(\bar{r}) R_n(\bar{r}) d\bar{r} = \frac{1}{\lambda_n^2} \left(\frac{\partial R_n}{\partial \bar{r}} \right)_{\bar{r}=1} \quad (F.14)$$

For the fourth kind

$$F_1^{(4)}(\bar{r}) = \frac{r^*}{2(1-r^*)} \ln \bar{r}$$

and

$$F_0^{(4)}(\bar{r}) = - \frac{1}{2(1-r^*)} \ln \frac{\bar{r}}{r^*}$$

so that (see case 1)

$$\int_{r^*}^1 F_1^{(4)}(\bar{r}) w(\bar{r}) R_n(\bar{r}) d\bar{r} = - \frac{r^* R_n(r^*)}{\lambda_n^2 2(1-r^*)} \quad (\text{F.15})$$

and

$$\int_{r^*}^1 F_0^{(4)}(\bar{r}) w(\bar{r}) R_n(\bar{r}) d\bar{r} = - \frac{R_n(1)}{\lambda_n^2 2(1-r^*)} \quad (\text{F.16})$$

APPENDIX G EXAMPLES OF SUPERPOSITION OF THE FUNDAMENTAL SOLUTIONS

The graphs of the fundamental solutions, Figs.II.I.1 to II.I.12, are particularly convenient for rapid calculations involving superposition of the elementary boundary conditions. To illustrate this computation let us consider some specific examples.

1. Heat flux specified on one wall, temperature on the other

Assume that the heat flux on the inner wall is as shown in Fig. G.1, while the outer wall is held at 212°F. The fluid is air which enters at 70°F with a Reynolds Number of 1428. The outer tube is 4 inches in inside diameter, the core tube 1 inch in outside diameter. The tubes are 150 inches long. We seek the temperature at the inner wall, the fluid mean temperature, and the heat flux at the outer wall as functions of axial position. The pertinent physical constants are:

$$r^* = 0.25$$

$$D_h = 0.25 \text{ ft}$$

$$\text{RePr} = 1000.$$

This problem will require the superposition of cases 3 and 4. Let us approximate the cosine distribution by the steps shown in G.1. If ξ_n is the value of \bar{x} at which the step of heat flux, q_n'' , is applied, we will have the following:

ξ_n	$q_{in}'' D_h/k$	- °F
0	10	
0.005	100	
0.015	90	
0.035	- 90	
0.045	-100	
0.050	- 10	

We can obtain the inner wall temperature from

$$t_1(\bar{x}) = 70 + 142 \theta_{10}^{(3)}(\bar{x}) + \Sigma(q_{in}'' D_h/k) \theta_{11}^{(4)}(\bar{x} - \xi_n) \dots \quad (G.1)$$

The summation is taken only of those steps for which $\bar{x} > \xi_n$. Similarly, the outer wall heat flux is given by

$$q_o''(\bar{x}) = \frac{k}{D_h} [142 \Phi_{oo}^{(3)}(\bar{x}) + \Sigma(q_{in}'' \frac{D_h}{k}) \Phi_{o1}^{(4)}(\bar{x} - \xi_n)] \quad (G.2)$$

and the mean temperature by

$$t_m(\bar{x}) = 70 + 142 \theta_{mo}^{(3)}(\bar{x}) + \Sigma(q_{in}'' \frac{D_h}{k}) \theta_{m1}^{(4)}(\bar{x} - \xi_n) \quad (G.3)$$

These values are shown in Figs. G.2 and G.3. Examples of the calculation are as follows.

$$\begin{aligned} 1.) \quad \bar{x} &= 0.01 \\ t_1 &= 70 + (142)(0) + (10)(0.106) + (100)(0.0868) \\ t_1 &= 79.7^\circ\text{F} \\ q_o'' &= [0.0146/0.25] [(142)(4.28) - (10)(0.0004) - (100)(0)] \\ q_o'' &= 609 \text{ Btu/hr ft}^2 \\ t_m &= 70 + (142)(0.225) + (10)(0.008) + (100)(0.004) \\ t_m &= 102.4^\circ\text{F} \end{aligned}$$

$$2.) \quad \bar{x} = 0.05$$

$$t_1 = 70 + (142)(0.313) + (10)(0.165) + (100)(0.161) \\ + (90)(0.149) - (90)(0.119) - (100)(0.87)$$

$$t_1 = 126.3^\circ\text{F}$$

$$q_o'' = [0.0146/0.25][(142)(1.85) - (10)(0.0782) - (100) \\ (0.0670) - (90)(0.0420) + (90)(0.0034) + (100)(0)]$$

$$q_o'' = 251 \text{ Btu/hr ft}^2$$

$$t_m = 70 + (142)(0.568) + (10)(0.035) + (100)(0.0328) \\ + (90)(0.0265) - (90)(0.012) - (100)(0.004)$$

$$t_m = 155.2^\circ\text{F.}$$

Notice that in this example, even though heating is taking place at the inner wall, the inner wall temperature is below the mean temperature. This is due to the strong influence of the hot outer wall.

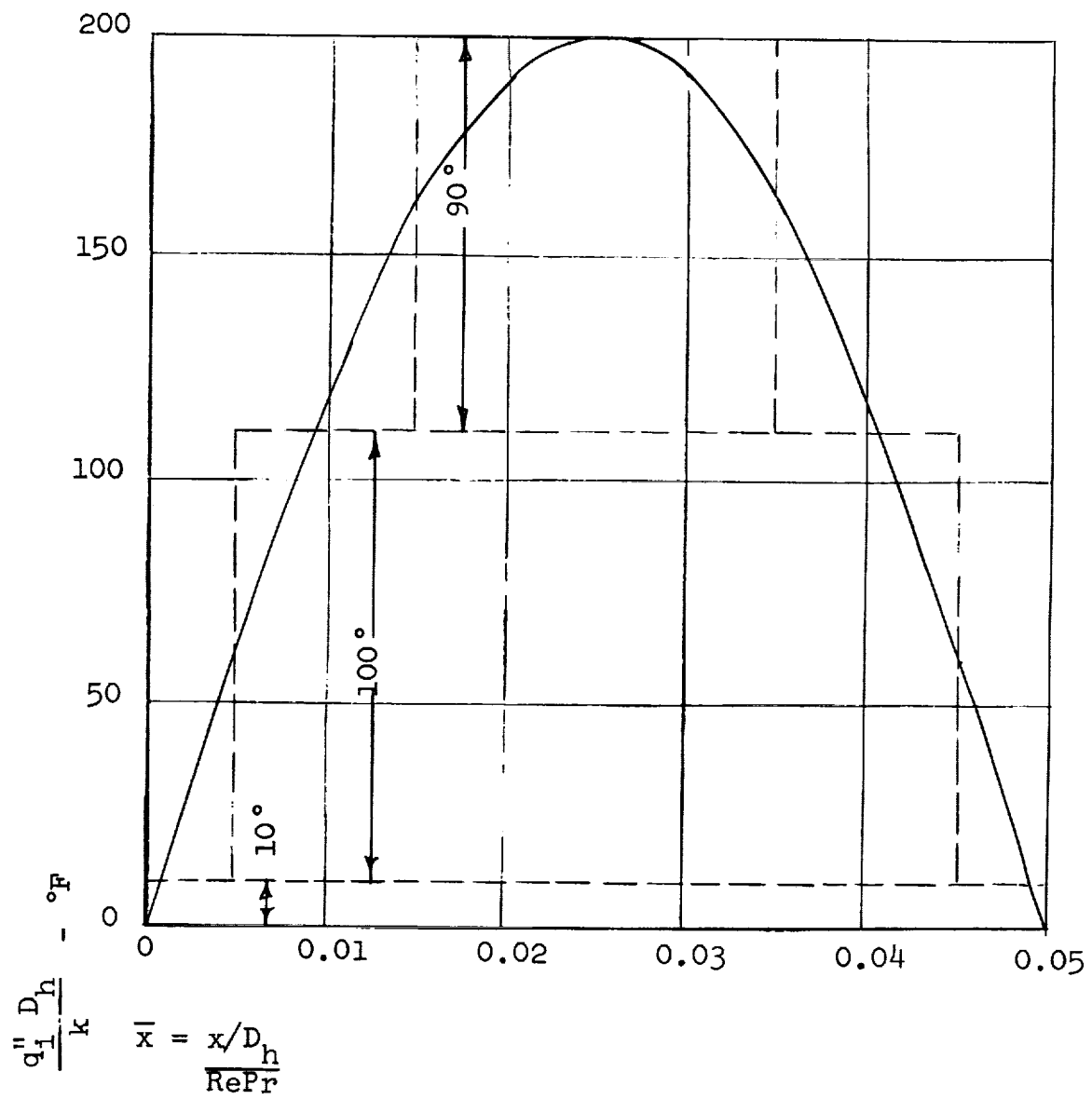


FIG. G.1

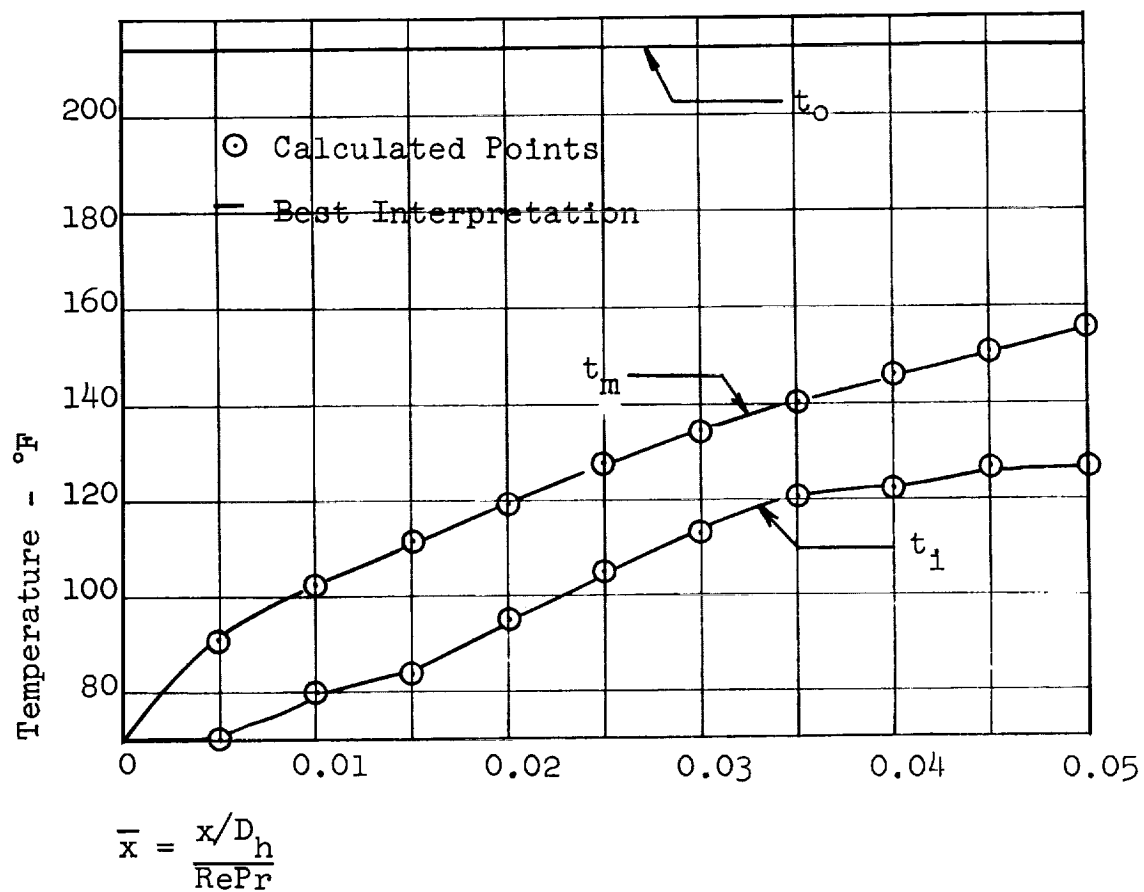


FIG. G.2

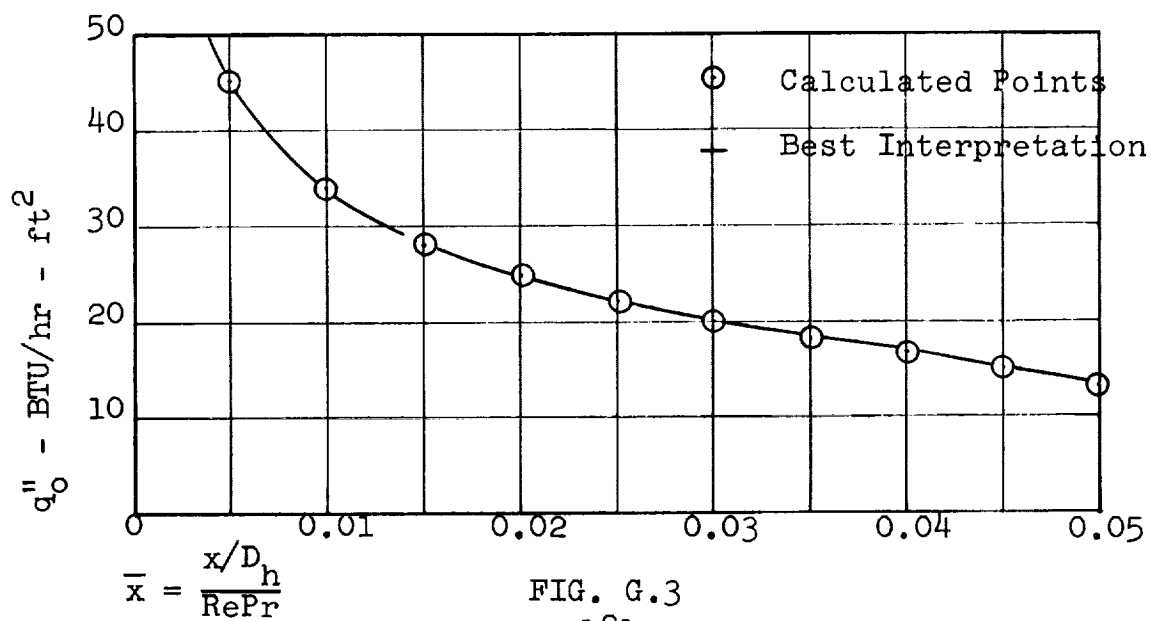


FIG. G.3

2. Heat flux specified on both walls

This is a situation which could be set up experimentally. The inner wall heat flux is essentially constant at an arbitrary level but the flux at the outer wall decreases with \bar{x} since the heat loss through the insulation increases with the wall temperature.

The radius ratio is 0.376. The values of the fundamental solutions are given in Figs. G.8 and G.9. These values were taken from cross plots made up from Tables II.I.5 and II.I.6.

The results of two asymmetrically heated runs are shown in Figs. G.4 through G.7. In run G.1 the wall heat fluxes were approximately equal, in run G.2 the heat flux at the inner wall was approximately twice that at the outer wall. The actual wall fluxes as they were measured (corrected for radiation interchange and heat leak) are shown in Figs. G.4 and G.6 together with the approximate distributions chosen to represent them. A comparison of the actual and predicted temperatures is shown in Figs. G.5 and G.7.

For run G.1, the fluid mean temperature is computed from

$$t_m(\bar{x}) = 75.7 + 178 \theta_{m1}^{(2)}(\bar{x}) + \sum_n (q_o'' D_h/k)_n \theta_{mo}^{(2)}(\bar{x} - \xi_n) \quad (G.4)$$

where ξ_n is the value of \bar{x} for which the n -th step of heat flux is applied. Similarly

$$t_1(\bar{x}) = t_m(\bar{x}) + 178[\theta_{i1}^{(2)}(\bar{x}) - \theta_{m1}^{(2)}(\bar{x})] \\ + \sum_n (q_o'' D_h/k)_n [\theta_{io}^{(2)}(\bar{x} - \xi_n) - \theta_{mo}^{(2)}(\bar{x} - \xi_n)] \quad (G.5)$$

and

$$\begin{aligned}
 t_o(\bar{x}) = t_m(\bar{x}) + \sum_n (q_o'' D_h/k)_n [\theta_{oo}^{(2)}(\bar{x} - \xi_n) - \theta_{mo}^{(2)}(\bar{x} - \xi_n)] \\
 + 178[\theta_{o1}^{(2)}(\bar{x}) - \theta_{m1}^{(2)}(\bar{x})]
 \end{aligned} \tag{G.6}$$

The summations include only those steps for which $\bar{x} > \xi_n$.

For run G.2 the mean temperature is given by

$$\begin{aligned}
 t_m(\bar{x}) = 82 + \sum_n (q_1'' D_h/k)_n \theta_{m1}^{(2)}(\bar{x} - \xi_{n1}) \\
 + \sum_n (q_o'' D_h/k)_n \theta_{mo}^{(2)}(\bar{x} - \xi_{no})
 \end{aligned} \tag{G.7}$$

The wall temperatures are given by

$$\begin{aligned}
 t_1(\bar{x}) = t_m(\bar{x}) + \sum_n (q_1'' D_h/k)_n [\theta_{11}^{(2)}(\bar{x} - \xi_{n1}) - \theta_{m1}^{(2)}(\bar{x} - \xi_{n1})] \\
 + \sum_n (q_o'' D_h/k)_n [\theta_{1o}^{(2)}(\bar{x} - \xi_{no}) - \theta_{mo}^{(2)}(\bar{x} - \xi_{no})] \\
 \dots \tag{G.8}
 \end{aligned}$$

$$\begin{aligned}
 t_o(\bar{x}) = t_m(\bar{x}) + \sum_n (q_o'' D_h/k)_n [\theta_{oo}^{(2)}(\bar{x} - \xi_{no}) - \theta_{mo}^{(2)}(\bar{x} - \xi_{no})] \\
 + \sum_n (q_1'' D_h/k)_n [\theta_{o1}^{(2)}(\bar{x} - \xi_{n1}) - \theta_{m1}^{(2)}(\bar{x} - \xi_{n1})] \\
 \dots \tag{G.9}
 \end{aligned}$$

As an example of the calculation take the location $\bar{x} = 0.07$.

$$t_m = 82 + 200(0.075) - 13(0.0109) + 105(0.204) - 15(0.102)$$

$$t_m = 116.7^\circ\text{F}$$

$$t_1 = 116.7 + 200(0.147) - 13(0.112) - 105(0.091) + 15(0.0759)$$

$$t_1 = 136.2^\circ\text{F}$$

$$t_o = 116.7 + 105(0.202) - 15(0.190) - 200(0.0335) + 13(0.011)$$

$$t_o = 128.4^\circ\text{F}$$

Notice that the terms for which $\xi_n > \bar{x}$ are all zero.

As a comparison the wall temperatures in run G.1 were computed assuming the wall fluxes were both constant at their average values. This prediction is shown as the dashed line in Fig. G.5. While this prediction represents the wall temperatures less well than the multi-step approximation, it is still reasonable since the actual axial variation of the heat flux is not severe. Notice that the constant flux prediction deviates from the measured values most on the outer wall, near the step, where the actual wall flux is varying most rapidly.

The wall temperatures in run G.2 were computed assuming the heat fluxes to be those which were actually measured but that the wall-to-mean temperature differences were those given by the fully developed (large \bar{x}) solutions. This method provides an adequate prediction for the wall temperatures for $\bar{x} > 0.1$ but, again, the axial variation of flux is not very severe.

For the fundamental solutions of the second kind, the first significant eigenvalue is larger than for the other cases ($\lambda_0^{(2)} \equiv 0$), and, hence, fully developed conditions are achieved most rapidly for this case.

Run G.1 assumed flux

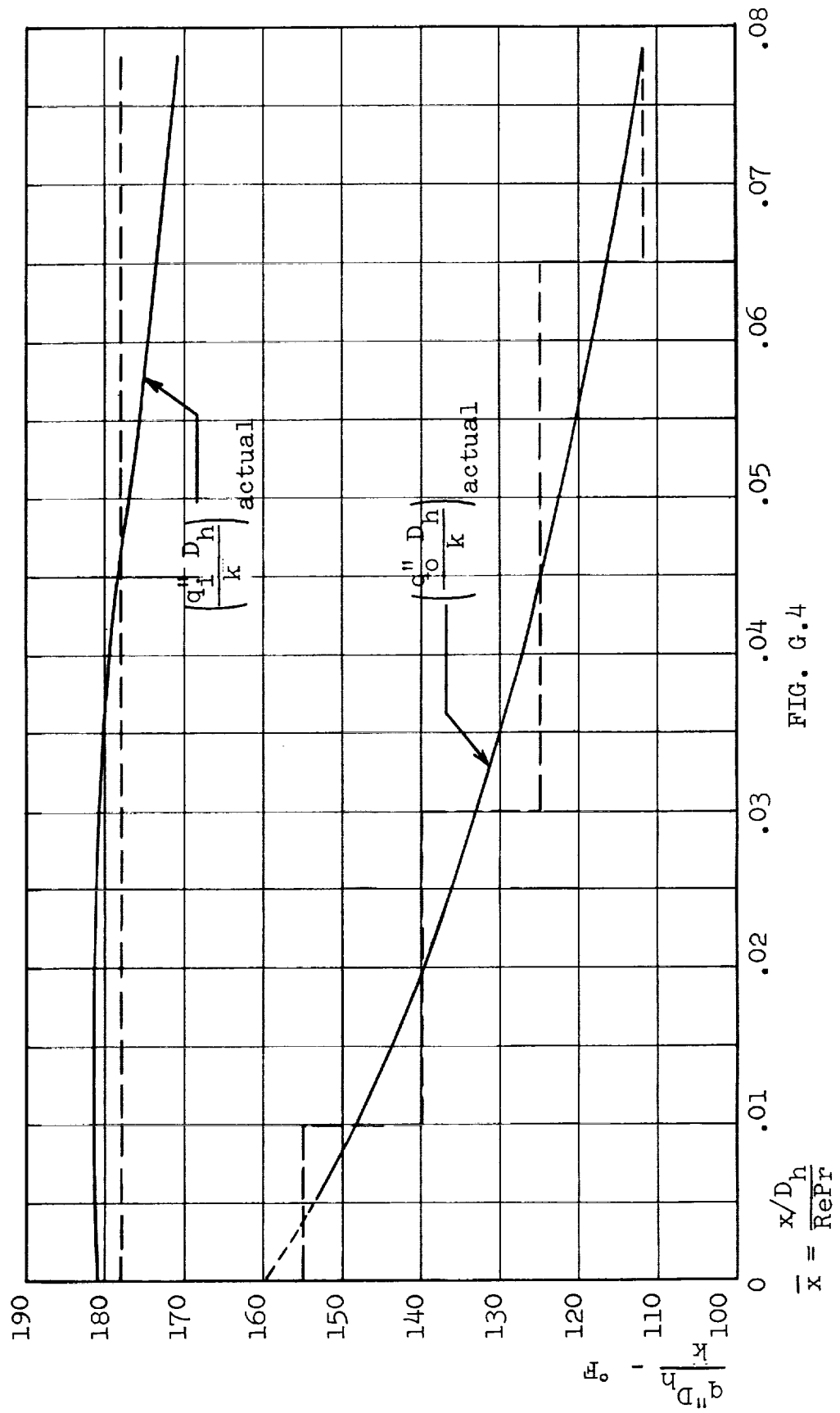


FIG. G.4

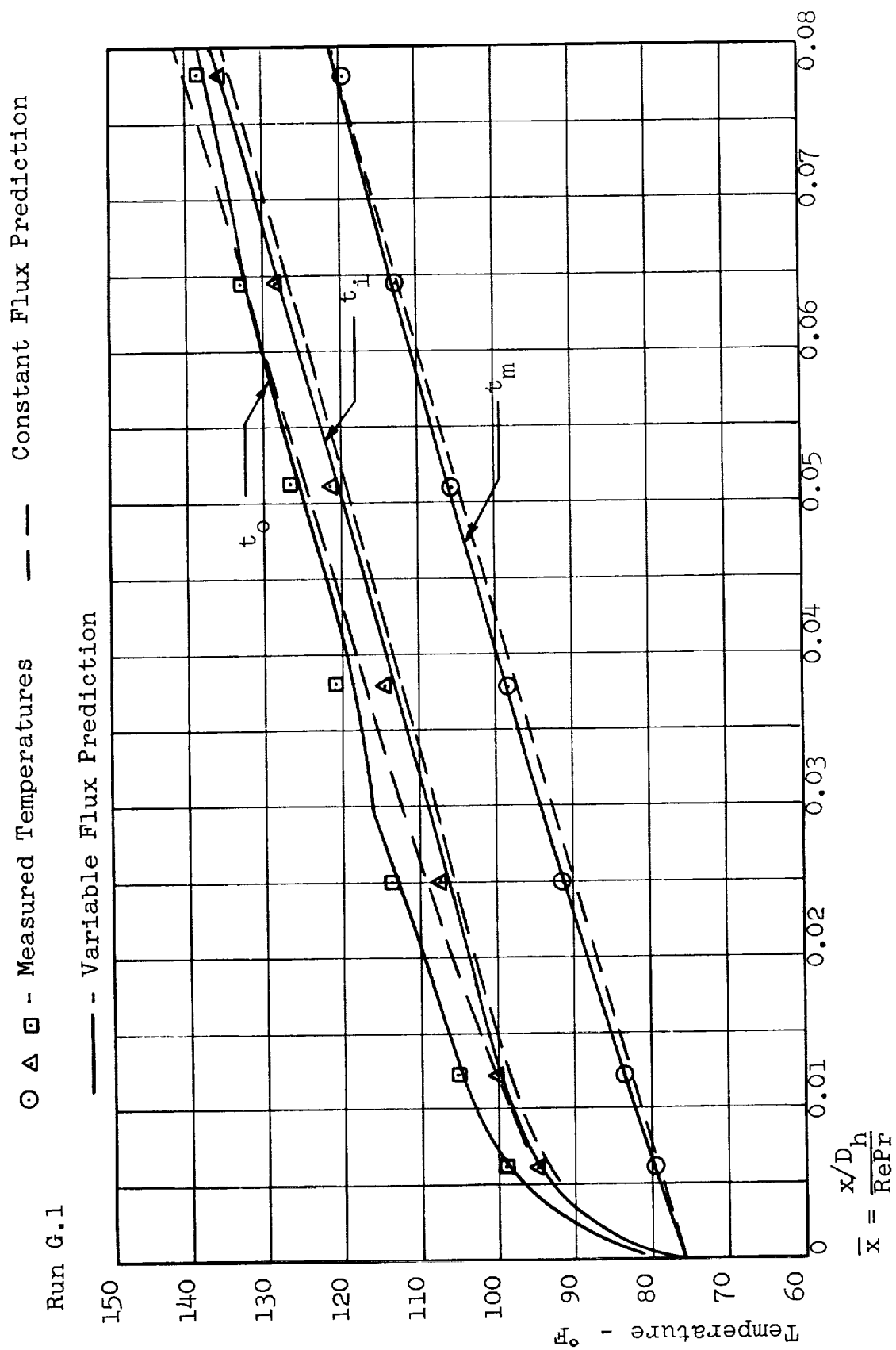


FIG. G.5

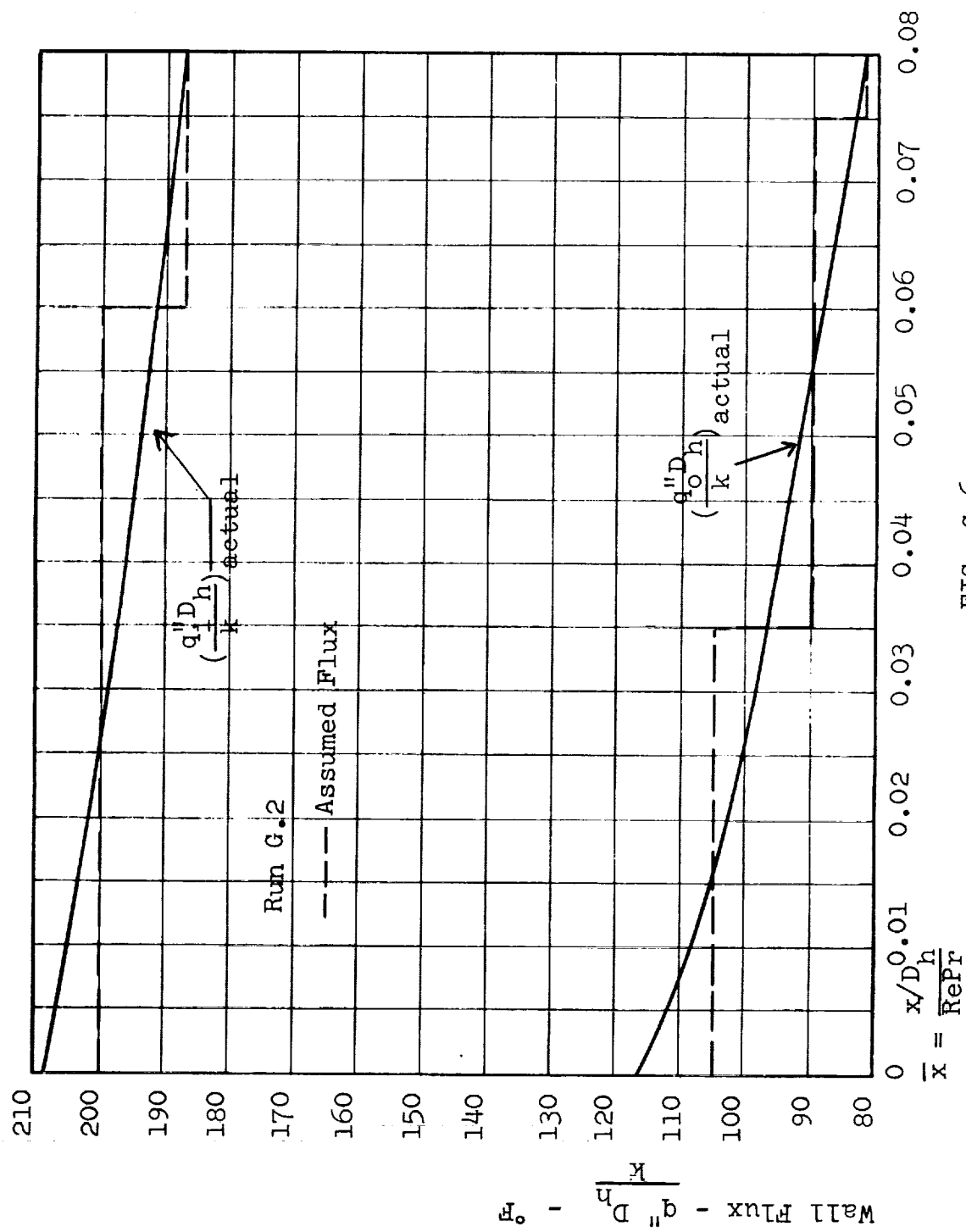


FIG. G.6

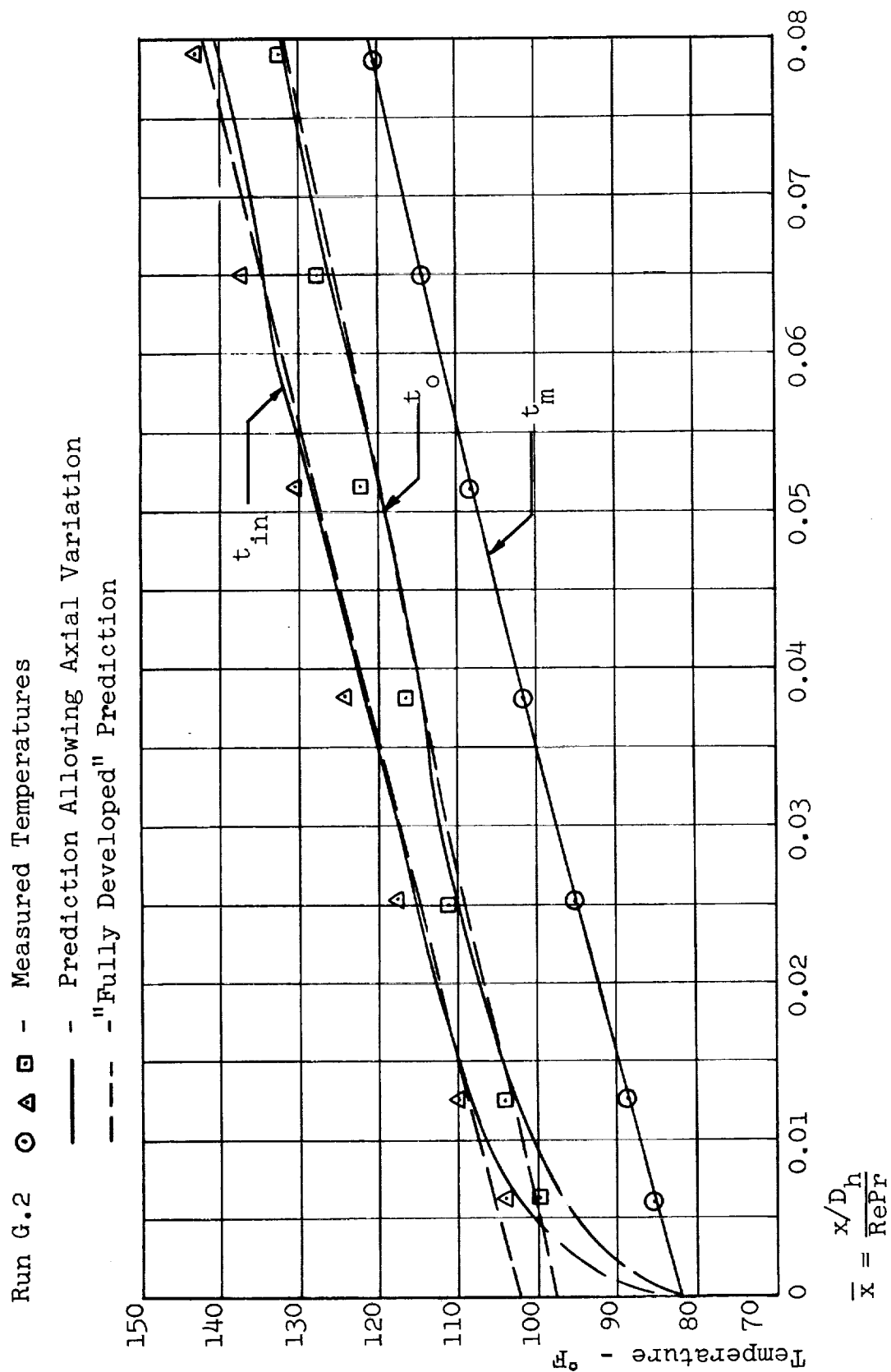


FIG. G.7

The Fundamental Solutions of the Second Kind

$$r^* = 0.375$$

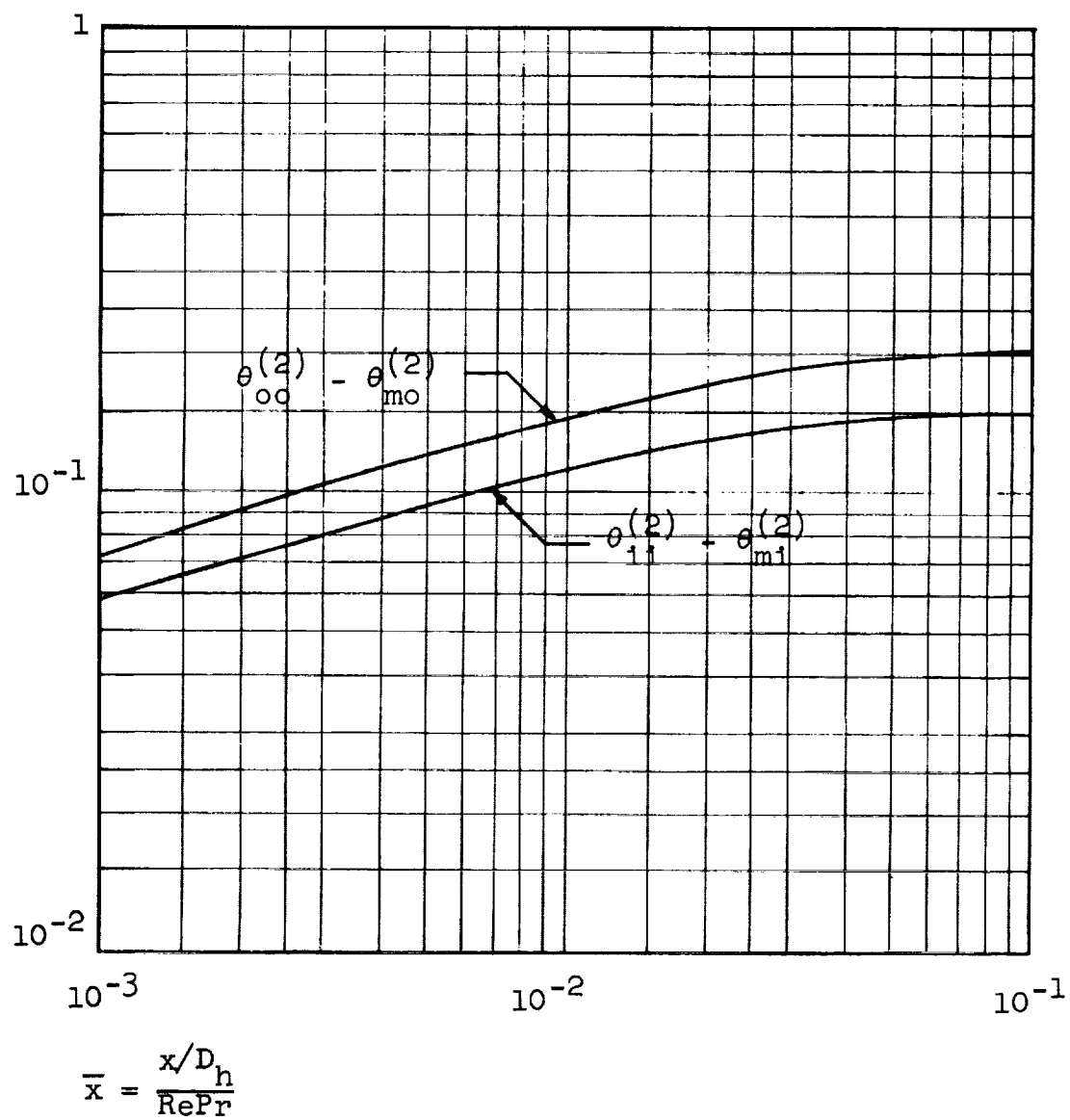
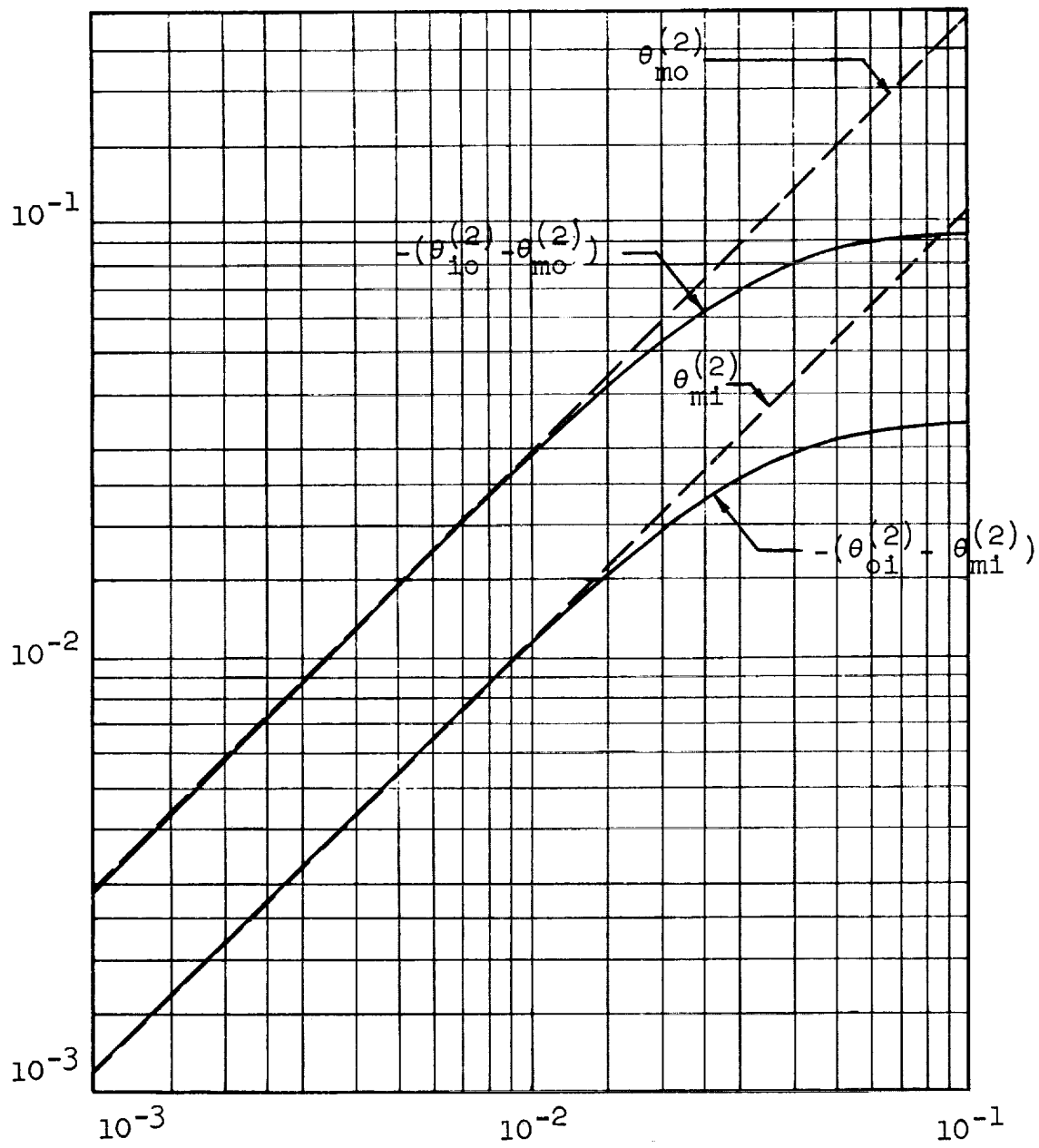


FIG. G.8

The Fundamental Solutions of the Second Kind
 $r^* = 0.375$



$$\bar{x} = \frac{x/D_h}{RePr}$$

FIG. G.9

REFERENCES

1. Berry, V. J. and de Prima, C. R., "An Iterative Method for the Solution of Eigenvalue Problems", Jour. Appl. Phys., vol.23, p.195,(1952).
2. Cess, R. D., and Schaffer, E. C., "Summary of Laminar Heat Transfer between Parallel Plates with Unsymmetrical Wall Temperatures", J. Aero.Sciences, p. 538, August (1959).
3. Cess, R. D., and Schaffer, E. C., "Laminar Heat Transfer between Parallel Plates with an Unsymmetrically Prescribed Heat Flux at the Walls", Applied Scientific Research, section A, vol.9, p.64,(1960).
4. Courant, R., and Hilbert, D., "Methods of Mathematical Physics", vol.1, Interscience Publishers, Inc., New York, (1953).
5. Graetz, L., "Ueber die Wärmeleitungsfähigkeit von Flüssigkeiten", Annalen der Physik und Chemie, vol.18, p.79, (1883).
6. Jakob, M., and Rees, K. A., "Heat Transfer to a Fluid in Laminar Flow through an Annular Space", Trans. A.I.Ch.E., vol. 37, p.619, (1941).
7. Kline, S. J., and Mc.Clintock, E. A., "The Description of Uncertainties in Single Sample Experiments", Mech. Eng., January 1953.
8. Lamb, H., "Hydrodynamics", Cambridge University Press, London, (1924).
9. Leveque, M. A., "Les Lois de la Transmission de Chaleur par Convection", Annales de Mines, vol. 13, p.201, April (1928).
10. Lipkis, R. P., Discussion on Reference 19, Trans. ASME, vol. 78, p.441(1956).
11. McCuen, P. A., "Heat Transfer with Laminar and Turbulent Flow between Parallel Planes with Constant and Variable Wall Temperature and Heat Flux", Ph.D. Dissertation, Stanford University, (1961).
12. Murakawa, K., "Heat Transmission in Laminar Flow through Pipes with Annular Space", Trans. Jap. Soc. Mech. Engrs., 88, (19), p.15, (1953).

13. Murakawa, K., "Analysis of Temperature Distribution of Nonisothermal Laminar Flow of Pipes with Annular Space", Trans. Jap. Soc. Mech. Engrs., 18, (67), p.43 (1952).
14. Reference Tables for Thermocouples, National Bureau of Standards Circular 561, April 27, (1955).
15. Purday, H. F. P., "Steamline Flow", Constable and Co. Ltd., London, (1949).
16. Reynolds, W. C., Kays, W. M., and Kline, S. J., "Heat Transfer in the Turbulent Incompressible Boundary Layer with Arbitrary Wall Temperatures and Heat Flux", NASA Memo 12-3-58w, (1958).
17. Runstadler, P. W., "Experimental Study of a Basic Flow Model in the Wall Layers of the Turbulent Boundary Layer", Ph.D. Dissertation, Stanford University, (1961).
18. Schenke, J., "A Problem of Heat Transfer in Laminar Flow between Parallel Plates", Applied Scientific Research, vol. 5, section A, p.241, (1955).
19. Sellars, J. R., Tribus, M., and Klein, J. S., "Heat Transfer to Laminar Flow in a Round Tube or Flat Conduit - the Graetz Problem extended", Trans. ASME, vol.78, p. 441, (1956).
20. Siegel, R., Sparrow, E. M., and Hallman, T. M., "Steady Laminar Heat Transfer in a Circular Tube with Prescribed Wall Heat Flux", Applied Scientific Research, vol. 7, section A., p.386, (1958).
21. Singh, S. N., "The Determination of Eigenfunctions of a Certain Sturm-Liouville Equation and its Application to Problems of Heat Transfer", Applied Scientific Research, vol. 7, section A., p.237 (1958).
22. Klein, J., and Tribus, M., "Forced Convection from Non-Isothermal Surfaces", ASME Paper 53-SA-46 (1953).
23. Flow Measurement, Chapter 4, Part 5, ASME Power Test Codes, Supplements on Instruments and Apparatus, (1959).
24. Hamming, R. W., "Stable Predictor-Corrector Methods for Ordinary Differential Equations", Jour. of ACM, vol. 6, No. 1, p. 37, (1959).

25. Milne, W. E., "Numerical Solution of Differential Equations", John Wiley and Sons, Inc., New York (1953).
26. McAdams, W. H., "Heat Transmission", Third Edition, McGraw-Hill, New York, (1954).
27. Leung, Y. W., Dissertation in Progress, Stanford University, (1961).